Titre: Title:	Impact de médias lestants et de polymères alternatifs sur la performance de la floculation lestée
Auteur: Author:	Mathieu Lapointe
Date:	2019
Type:	Mémoire ou thèse / Dissertation or Thesis
Référence: Citation:	Lapointe, M. (2019). Impact de médias lestants et de polymères alternatifs sur la performance de la floculation lestée [Thèse de doctorat, Polytechnique Montréal]. PolyPublie. https://publications.polymtl.ca/3727/

URL de PolyPublie: PolyPublie URL:	https://publications.polymtl.ca/3727/
Directeurs de recherche: Advisors:	Benoit Barbeau
Programme: Program:	Génies civil, géologique et des mines

UNIVERSITÉ DE MONTRÉAL

IMPACT DE MÉDIAS LESTANTS ET DE POLYMÈRES ALTERNATIFS SUR LA PEROFMRANCE DE LA FLOCULATION LESTÉE

MATHIEU LAPOINTE

DÉPARTEMENT DES GÉNIES CIVIL, GÉOLOGIQUE ET DES MINES

ÉCOLE POLYTECHNIQUE DE MONTRÉAL

THÈSE PRÉSENTÉE EN VUE DE L'OBTENTION

DU DIPLÔME DE PHILOSOPIAE DOCTOR

(GÉNIE CIVIL)

OCTOBRE 2018

UNIVERSITÉ DE MONTRÉAL

ÉCOLE POLYTECHNIQUE DE MONTRÉAL

Cette thèse intitulée:

IMPACT DE MÉDIAS LESTANTS ET DE POLYMÈRES ALTERNATIFS SUR LA PEROFMRANCE DE LA FLOCULATION LESTÉE

présentée par : LAPOINTE Mathieu

en vue de l'obtention du diplôme de : Philosophiae Doctor

a été dûment acceptée par le jury d'examen constitué de :

Mme PRÉVOST Michèle, Ph. D., présidente

M. BARBEAU Benoit, Ph. D., membre et directeur de recherche

M. DORNER Sarah, Ph. D., membre

M. MONETTE, Frédéric, Ph. D., membre externe

DÉDICACE

Je ne dédis pas ce document à ma famille. Celui que je leur dédierai un jour sera exempté des termes «turbidité» et «floculation». Je les remercie plutôt pour leur patience, leur compréhension, leur patience, leur support, leur patience et leur amour!

REMERCIEMENTS

Celles et ceux qui doivent être remercié(e)s l'ont déjà été (ou le seront bientôt)! Je remercie néanmoins par écrit dans cette thèse mon directeur de recherche : Benoit Barbeau. Il ne sait pas à quel point j'ai pu apprendre grâce à lui. Et pour une millième fois, je souhaite aussi remercier ma conjointe pour sa compréhension, sa patience et surtout, ses conseils. Elle m'a énormément soutenue. Elle non plus ne sait pas à quel point.

De façon plus protocolaire et formelle, je tiens à souligner cet environnement de recherche et d'apprentissage exceptionnel qu'est la Chaire industrielle CRSNG en eau potable. Cette équipe m'a aussi beaucoup appris!

RÉSUMÉ

La floculation lestée est largement utilisée en Amérique du Nord et en Europe lors du traitement des eaux potables, usées et industrielles. Sa popularité s'explique notamment par son efficacité d'enlèvement des flocs, sa compacité, sa facilité de mise en œuvre et sa robustesse vis-à-vis des variations de qualité de l'affluent. Cette technologie de traitement requiert l'utilisation d'un média lestant, ce dernier permettant d'augmenter la densité et la taille des flocs. Plusieurs types de médias peuvent être utilisés. Des technologies employant du sable de silice, de la magnétite, du charbon actif ou des boues de décantation comme médias lestants sont commercialisées depuis plus de 30 ans. Un floculant synthétique de poids moléculaire élevé (*viz*, le polyacrylamide) est indispensable à la floculation lestée. En plus de permettre la liaison entre les microflocs coagulés et le média lestant, il améliore la cinétique d'agrégation et augmente la résistance des flocs au cisaillement. Ce dernier atout est particulièrement important pour la floculation lestée durant laquelle des intensités de mélange considérables doivent être induites pour la suspension du média lestant.

Le monomère d'acrylamide relargué par le polyacrylamide est considéré comme potentiellement cancérigène pour l'humain tandis que plusieurs polymères synthétiques issus des effluents d'eaux usées municipales, incluant le polyacrylamide, posent également un risque sur les écosystèmes aquatiques récepteurs. En ce sens, plusieurs pays ont déjà fortement restreint (concentration maximale en Amérique du Nord : 1 mg/L) ou même complètement banni l'utilisation des polyacrylamides pour des applications en eau potable. Néanmoins, ces floculants synthétiques demeurent très performants à très faibles concentrations, très peu coûteux et peu sujets à la biodégradation une fois en solution. Sans polyacrylamide, plusieurs installations construites depuis les 30 dernières années en Amérique du Nord (et dans le monde) ne pourraient opérer à pleine capacité. Cette situation est en d'autant plus vrai pour des applications en eaux froides comme au Canada en raison des effets négatifs sur les performances de la floculation-décantation. Outre ses inconvénients sur la santé humaine et l'environnement, le polyacrylamide comporte également un enjeu lié à l'opération : le développement précoce de perte de charge dans un filtre granulaire.

En tant qu'alternative, des floculants à base de polysaccharides peuvent être employés. Ceux-ci nécessitent cependant des concentrations considérablement plus élevées et sont moins tolérants aux forces de cisaillement et de compression induites lors du mélange. Par exemple, des polymères à

base d'amidon sont déjà exploités pour la floculation lestée; les concentrations requises par rapport au polyacrylamide sont typiquement trois à cinq fois plus élevées et l'abattement de turbidité est moindre. Les installations de traitement sont soit confrontées au risque sur la santé et l'environnement lors de l'utilisation de polyacrylamide, soit au risque d'une mauvaise décantation et d'une exportation de microflocs vers les filtres granulaires lors de l'utilisation de polymère d'amidon.

Parallèlement au floculant, les propriétés du média lestant joue également un rôle de premier plan en ce qui concerne la performance de la floculation lestée. Toutefois, les propriétés que doit avoir un média lestant pour une application donnée (*e.g.*, eau potable peu chargée en turbidité vs eaux usées avec une teneur élevée en matières en suspension) sont peu connues. Les informations sur ce sujet sont rares dans la littérature scientifique et aucune approche systématique ou séquentielle n'est actuellement proposée quant à la sélection d'un média lestant et la concentration devant être utilisée. De plus, aucune étude ne compare ou ne décrit clairement l'impact de la taille et de la densité d'un média lestant.

L'objectif principal de cette thèse était d'évaluer et de comprendre l'influence du type de floculant et de média lestant sur la performance de la floculation lestée. Il était visé de 1) développer une méthode en laboratoire permettant de mesurer la densité, la taille et la forme des flocs lestés, 2) d'évaluer et d'améliorer la performance des polymères d'amidon activé comme alternative au polyacrylamide et 3) de mesurer les impacts différenciés de la densité, de la taille, de la composition chimique ainsi que de la surface disponible des médias lestants sur la vitesse de chute des flocs et sur l'abattement de turbidité.

Cette thèse fait dans un premier temps le tri des divers polymères synthétiques et naturels potentiellement applicables en floculation. Dans cette revue de littérature, les avantages et inconvénients de divers floculants sont présentés ainsi que leurs mécanismes d'adsorption/agrégation. Se basant sur les propriétés intrinsèques d'un floculant telles que le poids moléculaire et la densité de charge, cette revue permet notamment de confirmer le potentiel des polymères à base d'amidon en floculation lestée.

La première phase expérimentale de cette thèse a d'abord comparé les performances de l'amidon à celles du polyacrylamide. Une méthode en microscopie optique ainsi qu'une caméra a permis de mesurer la taille, la forme ainsi que la densité des flocs lestés. Tel qu'anticipé, les performances de

l'amidon ont été moindres en ce qui a trait à l'enlèvement de turbidité, à la taille des flocs formés et leur résistance au cisaillement. Cependant, les résultats ont démontré qu'en utilisant une combinaison de ces deux polymères, il est possible de remplacer la majeure partie du polyacrylamide utilisé par de l'amidon (jusqu'à 70 %) et ce, sans affecter l'enlèvement de turbidité, la cinétique d'agrégation et la résistance des flocs au cisaillement. Le remplacement complet du polyacrylamide par un polymère d'amidon anionique a également été possible lorsque ce dernier était opéré en conditions optimales de coagulation. L'écart de performance entre les floculants d'origine synthétique vs naturelle peut donc être considérablement réduit notamment lorsqu'un média lestant constitué majoritairement de SiO_2 (*i.e.*, sans autres oxydes divers) est utilisé et lorsqu'un temps de mélange plus long est utilisé lors de la maturation des flocs. Avec ces modifications, les concentrations d'amidon requises ont été significativement réduites (de 2,0 à 0,7 mg/L), tout en respectant les attentes en termes de turbidité à l'eau décantée (1 UTN).

Le deuxième volet de cette thèse a permis d'évaluer l'impact de médias lestants de densité (1240–5100 kg/m^3), de taille (40–300 µm), de forme et de composition chimique variables sur la vitesse de chute des flocs et sur l'enlèvement des particules. Les résultats ont démontré que l'utilisation de média lestant plus dense augmentait la densité des flocs, mais réduisait cependant leur taille. Cette diminution de taille a été essentiellement associée au gradient de vitesse plus élevé requis lors du mélange de médias lestants plus lourds. Conséquemment, malgré une vitesse de chute des flocs plus élevée, l'abattement peut être légèrement affecté lors de l'utilisation d'un média considérablement plus dense que le sable de silice (*e.g.*, la magnétite). Les meilleurs abattements de turbidité ont été mesurés lors de l'utilisation de l'anthracite (1450 kg/m^3) et pour un temps de décantation supérieur à une min. La présente étude décrit la sélection du média lestant comme étant un compromis entre la charge superficielle maximale applicable (avant d'observer la présence de flocs lestés dans les eaux décantées) et l'abattement de turbidité maximal obtenu lors de mélange à plus faible intensité. Cette thèse propose également une approche plus systématique lors de la sélection d'un média lestant, soit en fonction de la surface de média offerte (en m^2/L) plutôt qu'en termes de concentration massique de média (en g/L). Cette nouvelle approche est d'autant plus valable lors de la comparaison de médias lestants de densité et de taille différentes.

Il est anticipé que cette thèse puisse accompagner les municipalités, l'industrie ainsi que les chercheurs(euses) du milieu lors de la sélection et lors du développement de floculants et de médias lestants alternatifs. Les conclusions tirées rendent désormais la floculation lestée encore plus

modulable et robuste en offrant plus de flexibilité quant à la charge superficielle ciblée ou à l'enlèvement de particules souhaité. De plus, grâce à la méthode développée permettant l'évaluation de la densité des flocs lestés (environ 1400–1600 kg/m^3 lorsque le sable de silice est utilisé), un diagnostic plus précis quant au choix d'un floculant et d'un média lestant peut dorénavant être posé. Cette méthode permettrait aussi de modéliser et prédire l'enlèvement de flocs au sein d'un décanteur lamellaire.

En tout, cette thèse a permis de publier (cinq) et soumettre (deux) sept articles scientifiques dans les revues suivantes : *Advances in Colloid and Interface Science* (soumis), *Water Research* (trois publiés), *Journal of Environmental Engineering* (publié), *Journal - American Water Works Association* (soumis) et *Journal of Water Supply: Research and Technology-Aqua* (publié).

ABSTRACT

Ballasted flocculation, a process consisting in injecting micron-sized granular media to increase the specific gravity and size of flocs, is being increasingly used in the water treatment industry owing to its potential to achieve very high superficial design velocities. This offers the advantages of a more compact process (*i.e.*, smaller footprint), stable suspended solids removal performance, faster start-up, and important cost savings compared to conventional flocculation. Flocculation requires the use of synthetic polymers, mainly polyacrylamide, which are frequently used in water treatment to improve the performance of conventional clarification and ballasted flocculation, as they increase the floc resistance to shearing (the shearing being notably high in ballasted flocculation, around 165 s^{-1}). Polymer addition also improves the aggregation kinetics between the ballast media and the coagulated particles. However, synthetic polymers like polyacrylamide present some risks related to the presence of residual toxic monomers of acrylamide and to the ecotoxicity of the polyelectrolyte itself once released in the water bodies. Moreover, polyacrylamide may increase headloss in granular media filters. These phenomena occur due to the presence of unsettled microflocs that contain high molecular weight polymer chains. Therefore, many countries, particularly in Europe, have forbidden or restricted the use of synthetic polyelectrolytes such as polyacrylamide for drinking water applications. In North America, the dosage is limited to 1 mg/L.

Due to the aforementioned constraints, there is growing interest in eliminating or drastically reducing the use of synthetic polyelectrolytes. For over thirty years, many polysaccharide-based polymers have been promoted as economical, efficient, and eco-friendly flocculants. Moreover, such biosourced polymers may eliminate two of the drawbacks associated with synthetic polymers: monomer toxicity and granular filtration headloss. Although starch-based flocculants offer fairly good flocculation performance, the dosages required are higher than those for polyacrylamide. This is true even in ballasted flocculation applications, where the required starch dosages were shown to be 3–5 times higher than for synthetic polyacrylamide polymers. In addition, flocs produced with activated starch polymers are more fragile and more sensitive to shearing than flocs produced with polyacrylamide.

Ballast media characteristics also have a large effect on the performance of ballasted flocculation. However, no systematic approach has yet been proposed to compare and select an appropriate ballast medium with respect to its specific gravity and size.

The main objective of this study was to identify favorable conditions for the use of an activated starch polymer and alternative ballast media during ballasted flocculation. Specifically, this work involved: 1) development of a microscopic method for measuring floc density, size, and shape factor; 2) evaluation and improvement of the performance of starch polymers as an alternative to polyacrylamide; and 3) measurement of the individual impact of the ballast media size, density, shape, and chemical composition on the settling velocity distribution of the flocs and on turbidity removal.

The following hypotheses were proposed: 1) the floc settling velocity is strongly related to the ballast media incorporation level; 2) by simultaneously identifying the optimal mixing conditions and the appropriate ballast media characteristics (size and chemical composition), starch polymers can achieve the industrial standard in terms of settled water turbidity; and 3) the use of denser and larger ballast media will lead to flocs with a higher settling velocity, but lower ultimate turbidity removal.

A comprehensive overview of high molecular weight polymers for improving clarification was carried out. In this literature review, submitted to *Advances in Colloid and Interface Science*, the impacts of intrinsic flocculant characteristics, such as molecular weight, charge density, and spatial molecular configuration, were reviewed and explained. Synthetic vs. natural flocculants were also compared and the polymers' respective advantages and disadvantages were listed. The different functional groups involved during the initial polymer chain adsorption were also enumerated for each polymer of interest. Finally, floc monitoring techniques and polymer molecular weight and charge density analysis methods were reviewed and discussed.

The first experimental part of the study was dedicated to the comparison of starch and polyacrylamide. Floc size and density (typically around 1400–1600 kg/m^3 when ballasted with silica sand) were measured during flocculation by direct microscopic observations with a modified counting cell. A camera was installed on a square jar test beaker to evaluate the rate of floc aggregation. As anticipated, both turbidity removal and floc size were notably impacted when a starch-based flocculant was used rather than a conventional polyacrylamide. However, a dual

starch-polyacrylamide polymer system used during ballasted flocculation was able to significantly reduce the required polyacrylamide dosage (around 70% for surface water) without impacting floc size, aggregation kinetics, floc resistance to shearing or turbidity removal,.

Favorable conditions for the complete replacement of polyacrylamide with an anionic activated starch polymer during ballasted flocculation were identified, including: mixing intensity and time; coagulation pH; ballast size and chemical composition; and polymer charge density. Ultimately, under optimal coagulation conditions, only 0.7 mg of activated starch/L was required to reach the settled water turbidity objective of 1 NTU.

In the second part of the study, the impacts of the ballast media size (40–300 µm), specific gravity (1240–5100 kg/m^3), shape, and chemical composition on floc settling velocity distribution and turbidity removal were evaluated. It was determined that the final ballast media selection is a compromise between settled water quality and the maximum allowable superficial velocity. These experiments also revealed the advantages of operating ballasted flocculation with a media having a relatively low specific gravity; lower required velocity gradient for the suspension of lighter ballast media improved turbidity removal. On the other hand, using a denser ballast media led to higher floc specific gravities and settling velocity distributions, which could be an advantage in certain industrial applications when higher solids flux removals are needed.

A systematic approach was also proposed to compare and select an appropriate ballast medium with respect to its specific gravity and size. It was confirmed that flocculation performance was controlled by the surface area of the medium available for ballasted flocculation (expressed as m^2 of media/L rather than g of media/L). This concept was of importance when ballast media with significantly different densities and sizes were compared; identical mass-based concentrations of two media with different average diameters or densities had different particle concentrations and surface areas.

It is expected that the conclusions from this work will provide important information to municipalities, researchers, and the water treatment industry regarding the selection and/or development of alternative flocculants and ballast media. The information concerning alternative media performance will also increase process robustness and flexibility, notably in terms of applied superficial velocity and turbidity removal. The microscopic technique developed in this work can provide descriptive information concerning floc characteristics (*e.g.*, diameter, compactness,

density, and shape). Such information is essential to properly model (*i.e.*, predict the gravity separation) and optimize the process. This is of interest for any commercial ballasted flocculation process.

Finally, as a result of the work done in this project, seven articles were either published (five) or submitted (two): *Advances in Colloid and Interface Science* (submitted); *Water Research* (3 published); *Journal of Environmental Engineering* (published); *Journal - American Water Works Association* (submitted); and *Journal of Water Supply: Research and Technology-Aqua* (published).

TABLE DES MATIÈRES

LISTE DES TABLEAUX

LISTE DES FIGURES

LISTE DES SIGLES ET ABRÉVIATIONS

A	Ellipsoidal projected area
AA	Acrylic acid
AF4	Asymmetrical flow field–flow fractionation
Al	Aluminum
AM	Acrylamide
ANT	Anthracite
BDOC	Biological dissolved organic carbon
$CBOD_5$	5-day carbonaceous biochemical oxygen demand
BM	Ballast medium
C_D	Drag coefficient
CD	Charge density
CG	Crushed glass
CICEP	Chaire industrielle CRSNG en eau potable
CMC	Carboxymethyl cellulose
COD	Chemical oxygen demand
D_E	Equivalent diameter
DMAEMA	Diméthylaminoéthylméthacrylate
DOC	Dissolved organic carbon
DSC	Differential scanning calorimetry
FI	Flocculation index
FTIR	Fourier transform infrared spectroscopy
FW	Filtered water
g	Graft

G	Mean velocity gradient
GAC	Granular activated carbon
GS	Garnet sand
HAA	Haloacetic acids
IL	Ilmenite
K	Aggregate/floc permeability
l	Ellipse shortest dimension
L	Ellipse longest dimension
MALLS	Multiangle laser light scattering
Me(OH)x	Metal hydroxides
meq	Milliequivalents
MES	Matière en suspension
MI	Microsand incorporation
MS	Microsand or Magnetite sand
MVES	Matière volatile en suspension
MW	Molecular weight
NGSP	Natural-graft-synthetic polymer
NMR	Nuclear magnetic resonance
NOAEL	no-observed-adverse-effect level
NOM	Natural organic matter
NSF	National Sanitation Foundation
NTU	Nephelometric turbidity unit
OMS	Organisation mondiale de la Santé
PAA	Polyacrylic acid

PAC	Polyaluminium chloride
PAM	Polyacrylamide
PDA	Photometric dispersion analyzer
PDF	Probability density function
PEG	Polyethylene glycol
PDADMAC	Polydiallyldimethyl ammonium chloride
PIV	Particle image velocimetry
PSSA	Polystyrenic sulfonic acid
PVA	Polyvinyl alcohol
PVP	Polyvinyl pyrrolidone
PVPA	Polyvinyl phosphonic acid
PVSA	Polyvinyl sulfonic acid
PZC	Point of zero charge
r	Pearson coefficient
R	Aggregate/floc radius
Re	Reynolds number
RMS	Root-mean-square
SCV	Streaming current value
SD	Standard deviation
SEC	Size exclusion chromatography
SEM	Scanning electron microscopy
SG	Specific gravity
SM	Standard methods
SPO	Sous-produits de désinfection

SPO_4	Soluble phosphate
SS	Silica sand
SW	Settled water or surface water
TGA	Thermogravimetric analysis
THM	Trihalomethanes
TOC	Total organic carbon
TSS	Total suspended solids
UFC	Uniform formation conditions
UTN	Unité de turbidité néphélométrique
UVA_{254}	UV absorbance
V	Floc or microsand volume
Ve	Elution volume
VSS	Volatile suspended solids
WW	Wastewater
XRD	X-ray diffraction
α	Facteur d'efficacité de collisions
η	Intrinsic viscosity
θ	Floc shape factor
ρ_{MS}	Microsand relative density
ρ_{CFM}	Chemical floc matrix relative density
ρ_F	Apparent ballasted floc relative density

LISTE DES ANNEXES

CHAPITRE 1 INTRODUCTION

Les polymères organiques synthétiques ou naturels font partie des principaux protagonistes de l'efficacité de plusieurs technologies de traitement en environnement. La séparation due à l'effet de gravité, *i.e.* la décantation, fait partie de ces technologies nécessitant l'utilisation d'un polymère à titre de floculant. Ces polymères à haut poids moléculaire, couramment employés lors du traitement conventionnel, sont également déployés au sein d'une multitude de technologies brevetées : Actiflo®, DensaDeg®, BioMag™, CoMag™, SIROFLOC™ et Ultrapulsator®. Sans floculant efficace, ces décanteurs ne pourraient pas être opérés à pleine capacité (charge superficielle jusqu'à 85 m/h dans le cas de l'Actiflo®; MDDELCC (2018)) étant donné la faible taille et la faible densité des flocs formés. Considérant leur versatilité, leur stabilité, leur performance et leur faible coût, il est anticipé que le marché mondial des polymères utilisés en traitement des eaux croitra de plus de 20 % d'ici 2021. Selon le rapport *Flocculants: Technologies and Global Markets* (2017), les recettes annuelles mondiales du marché seront alors de près de 6 milliards de dollars.

Actuellement, plus de quatre millions de Québécois consomment de l'eau traitée par l'entremise d'un polymère synthétique (*e.g.*, polyacrylamide (PAM)). Or, il a été démontré que l'utilisation du PAM cause le relargage de monomères d'acrylamide lesquels sont classés probablement cancérigènes pour les humains (Rice, 2005). La contribution de l'eau potable à l'exposition au monomère d'acrylamide (concentration de l'ordre de 0,1–0,2 µg acrylamide/L, soit environ 0,2–0,4 µg/jour ou 0,003–0,006 µg/kg (masse corporelle)/jour considérant un poids de 70 kg) demeure toutefois marginale lorsqu'elle est comparée à d'autres vecteurs dans l'alimentation : teneur moyenne respective de 50 et 200 µg acrylamide/kg d'aliment pour le pain et le café (WHO, 2002). Ces deux aliments combinés peuvent contribuer jusqu'à 70 % de l'exposition totale au monomère (23–69 %; Parzefall (2008)). Burek et al. (1980) ainsi que Tyla et al. (2000) mentionnent que les signes cliniques observables pour divers cancers (*inter alia*, glandes surrénales, glande thyroïde, poumon, cerveau et système épidermique) associés à la présence d'acrylamide dans l'eau potable deviennent statistiquement significatifs chez les rats à partir d'une exposition quotidienne de plus de 2000 µg acrylamide/kg/jour. Pour une exposition de 90 jours, Burek et al. (1980) ont démontré que le *no-observed-adverse-effect level* (NOAEL) sur 344 rats était atteint pour une dose journalière inférieure à 200 µg acrylamide/kg/jour. Santé Canada et l'Organisation mondiale de la

Santé (OMS) affirment toutefois qu'il est pour l'instant difficile d'évaluer avec précision l'ampleur du risque pour la santé humaine. Considérant l'étude plus récente de Parzefall (2008), l'exposition totale moyenne serait de l'ordre de 1 µg acrylamide/kg/jour tandis qu'elle serait de plus 5 µg acrylamide/kg/jour pour 1 % des consommateurs. Considérant cette valeur moyenne de 1 µg acrylamide/kg/jour, l'eau potable contribuerait à moins de 0,6% de l'exposition au monomère d'acrylamide (considérant une dose de 0,4 mg PAM/L lors de la floculation).

Afin de réduire l'exposition en provenance des eaux de consommation, plusieurs pays tels que l'Espagne, le Japon, la Suisse, la France et l'Allemagne ont décidé de fortement restreindre (dose maximale : 0,2 mg/L) ou de bannir l'utilisation de floculant à base d'acrylamide. En Amérique du Nord, advenant l'interdiction du PAM, plusieurs installations construites depuis 30 ans ne pourraient opérer à pleine capacité, en particulier pour des applications en eaux froides comme au Canada. Le risque en lien avec le monomère d'acrylamide y est pour l'instant contrôlé en limitant les doses admissibles de PAM à 1 mg/L. Considérant une teneur de 0,05 % en monomère d'acrylamide dans le produit commercial, les concentrations théoriques maximales sont respectivement de 0,1 et 0,5 µg/L en Europe (EN-1407) et en Amérique du Nord (NSF/ANSI 60). En ce qui a trait à l'impact sur l'environnement et les milieux récepteurs, le risque du monomère d'acrylamide demeure faible puisqu'il est en partie (bio)dégradé (de 20 µg/L à 1 µg/L en moins de 24h pour des eaux extraites de boues déshydratées; Arimitu, Ikebukuro et Seto (1975)). Cependant, des études mentionnent que les polymères synthétiques cationiques à haut poids moléculaire, tels que le PAM, peuvent être nuisibles aux écosystèmes aquatiques récepteurs étant donné leur grande facilité à s'agréger à certains biocolloïdes et organismes aquatiques (Bolto & Gregory, 2007; Johnson, K. A. et al., 1986).

Outre les enjeux liés à la santé humaine et à la protection de l'environnement, les floculants à poids moléculaire élevé présentent également des enjeux liés à l'opération : 1) augmentation et développement précoce de pertes de charge lors de la filtration granulaire (Zhu, H., Smith, Zhou, & Stanley, 1996) et 2) difficulté de pompage liée à la viscosité de la solution mère du produit solubilisé. En comparaison au PAM, les polymères à base d'amidon peuvent considérablement ralentir le développement des pertes de charge en filtration granulaire ainsi que le colmatage membranaire (Ouellet, 2017a). Il est aussi connu, une fois en solution, que les polymères à base d'amidon présentent une viscosité beaucoup plus faible comparativement au PAM; il en résulte donc un pompage plus aisé de ces biopolymères. Toutefois, les polymères à base d'amidon ont des

poids moléculaires plus faibles et une structure plus ramifiée en comparaison au PAM. Dû à leur plus faible longueur effective pour le pontage, la littérature scientifique indique que les polymères à base d'amidon sont moins performants et requièrent des doses plus élevées par rapport au PAM conventionnel (Bolto & Gregory, 2007; Gaid & Sauvignet, 2011; Singh, Ram Prakash, Pal, Rana, & Ghorai, 2013). Il est également à considérer que les PAM sont issus de produits pétrochimiques et se (bio)dégradent plus lentement que les floculants biosourcés (El Halal et al., 2015). Considérant que les polymères d'amidon ne sont pas notablement plus onéreux que le PAM, la sélection finale du polymère utilisé en floculation lestée constitue un compromis entre l'efficacité d'agrégation des particules, le risque toxicologique lié à la présence de monomère et de sous-produits résiduels issus de la polymérisation, l'impact de son utilisation sur les écosystèmes aquatiques et la facilité d'opération.

Le type de floculant a assurément un impact direct sur la taille des flocs et par le fait même, la performance de la décantation. Toutefois, la densité des agrégats joue un rôle également notable sur l'abattement de particules et la robustesse des filières de décantation. La floculation lestée, notamment le procédé Actiflo®, est dorénavant une technologie mondialement commercialisée. Néanmoins, les impacts de la taille et de la composition chimique du sable sur la performance de la floculation sont peu connus. De plus, le rôle de la densité du média lestant et son taux d'incorporation dans la structure des flocs ne sont pas décrits dans la littérature actuelle. Certains auteurs ont par le passé étudié les performances de magnétite comme média lestant (Pavlova & Dobrevsky, 2005), mais aucune étude ne décrit clairement et objectivement l'impact de la densité du média lestant sur la vitesse de chute de flocs lestés et sur l'abattement de turbidité.

La présente thèse vise donc à comparer les performances du PAM à celles des floculants à base d'amidon et explore les impacts confondus et différenciés de la taille, de la densité, de la forme et de la composition chimique de divers médias lestants sur la performance de la floculation lestée pour des applications en eaux potables et usées.

Cette thèse se divise en onze chapitres. Sept articles y sont présentés, lesquels sont suivis d'une discussion et d'une conclusion. Une revue de littérature sur les divers floculants employés dans l'industrie ainsi que sur leurs mécanismes d'action est présentée au chapitre 2 (article 1; soumis dans *Advances in Colloid and Interface Science*). Une méthode développée durant cette thèse caractérisant les flocs lestés est ensuite présentée au chapitre 4 (article 2; publié dans *Water*

Research). Cette méthode permet notamment d'évaluer la taille, la forme et la densité d'un floc lesté et, par conséquent, de calculer sa vitesse de chute. Les comparaisons faites entre les polymères à base d'amidon et les PAM sont présentées au chapitre 5 (articles 3; publié dans *Journal of Water Supply: Research and Technology-Aqua*), au chapitre 6 (article 4; publié dans *Water Research*) et au chapitre 7 (article 5 : soumis dans *Journal - American Water Works Association*). Cette série de trois articles met de l'avant deux méthodes permettant de combler l'écart de performance entre l'amidon et le PAM : 1) en optimisant l'amidon et 2) en employant un système de polymères combinés (amidon + PAM). Finalement, l'impact de médias lestants alternatifs ayant des densités et des tailles variables est décrit au chapitre 8 (article 6; publié dans *Journal of Environmental Engineering*) et au chapitre 9 (article 7; publié dans *Water Research*). La Figure 1.1 synthétise les sept articles inclus dans la thèse. D'autre contributions (articles, conférences et rapports techniques) n'ayant pas été incluses dans cette présente thèse y sont égalemnt présentées.

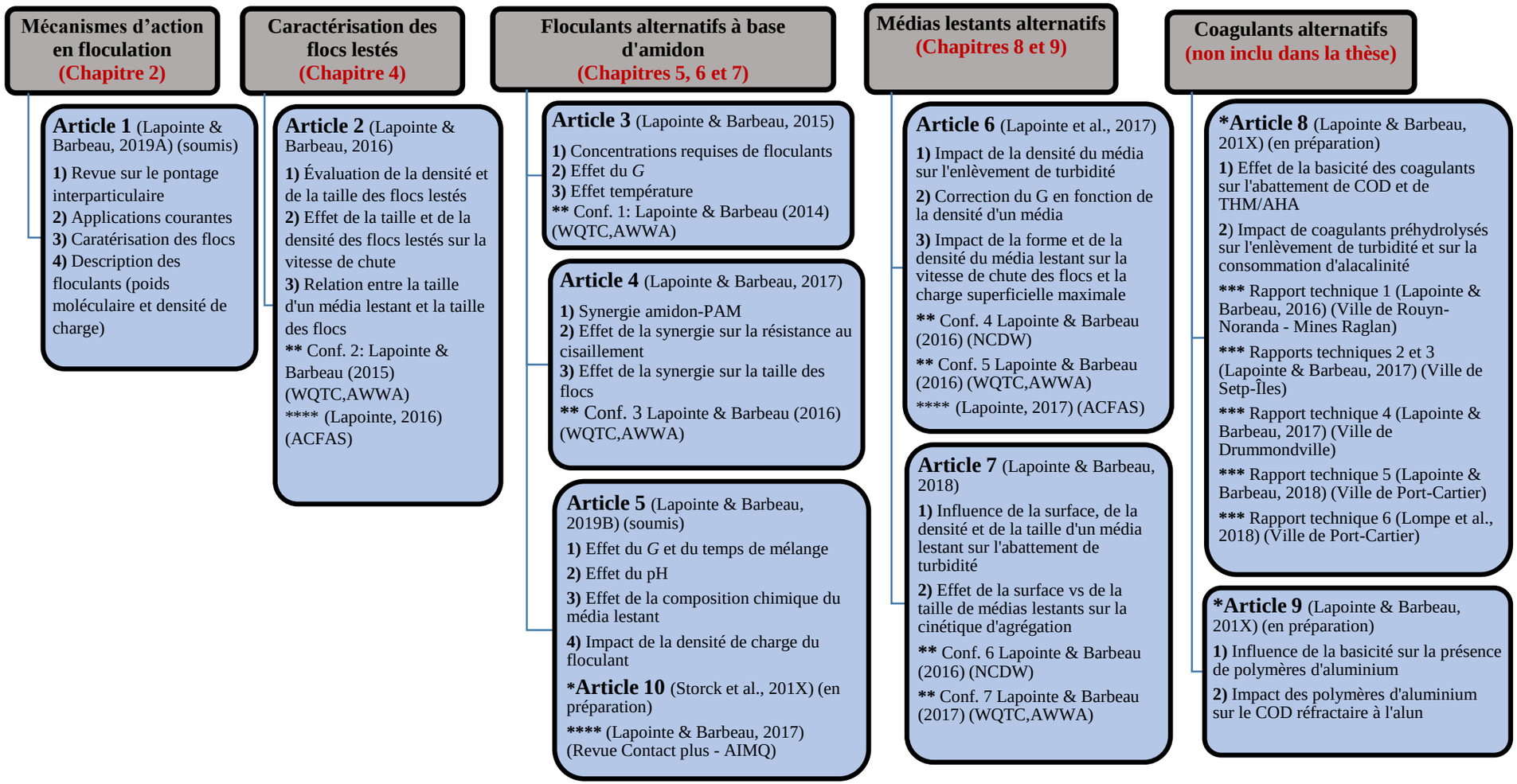

Figure 1.1 : Organigramme de la thèse

***Articles additionnels (3) non inclus dans la thèse**
****Conférences (7) avec comité de révision liées aux articles**
***** Rapports techniques (6) lié aux articles**
******Texte de vulgarisation (3)**

CHAPITRE 2 ARTICLE 1 – UNDERSTANDING THE ROLES OF SYNTHETIC VS. NATURAL POLYMERS TO IMPROVE CLARIFICATION THROUGH INTERPARTICLE BRIDGING: A REVIEW

Ce chapitre consiste en une revue de littérature (soumise dans *Advances in Colloid and Interface Science*) des mécanismes régissant la floculation et, plus particulièrement, l'agrégation par pontage interparticulaire. Divers floculants en développement ou conventionnellement utilisés dans l'industrie, qu'ils soient synthétiques, naturels ou copolymérisés, y sont présentés. Leurs principaux sites d'adsorption et groupements fonctionnels permettant leur attachement initial sur une surface (colloïde, macromolécule dissoute, média lestant à base d'oxyde de silice, *etc*.) y sont aussi synthétisés. Une fois adsorbée, la structure allongée d'un polymère organique peut lier deux (ou plusieurs) microflocs. En ce qui concerne les systèmes d'agrégations contrôlés par ce mécanisme, il est possible d'en estimer la performance, notamment via le poids moléculaire et la densité de charge du floculant en question. Étant donné leur importance respective en floculation, leur caractérisation doit être effectuée avec précision. Cette revue détaille donc les méthodes les plus utilisées, mais aussi les plus avancées, permettant l'évaluation du poids moléculaire et de la densité de charge d'un polymère. Les méthodes afin de mesurer la taille, la densité ainsi que la forme des flocs y sont également résumées.

Understanding the roles of synthetic vs. natural polymers to improve clarification through interparticle bridging: A review

Mathieu Lapointe[1]* *and Benoit Barbeau*[1]

[1] Industrial NSERC Chair on Drinking Water, Department of Civil, Geological and Mining Engineering, Polytechnique Montreal, Montreal, Quebec H3C 3A7, Canada

*Corresponding author e-mail: mathieu.lapointe@polymtl.ca

Abstract

Flocculation and settling performance (kinetic, robustness, upflow velocity, and overall solids removal) have been significantly improved over the past forty years due to the development of very high molecular weight polymers. Intrinsic flocculant characteristics such as the molecular weight, charge density, and spatial molecular configuration are of importance during water flocculation by interparticle bridging. In this review, synthetic vs. natural flocculants are compared and the polymers' respective advantages/disadvantages are listed. The different functional groups involved during initial polymer chain adsorption are also enumerated for each discussed polymer. A flocculant should principally be selected on the basis of its aggregation performance, solubility and ease of implementation, cost, stability, (bio)degradability, impact on downstream processes, commercial availability, and aquatic/human toxicity. It is generally the rule that organic synthetic polymers are associated with better solid removal than natural ones during clarification. On the other hand, natural polymers require higher dosage but offer other advantages such as higher biodegradability and lower toxicity. Given the different benefits offered by each type of flocculant, promising and alternative natural-*graft*-synthetic polymers are presented as a compromise in terms of flocculation effectiveness vs. biodegradation and toxicity. Some starch-*graft*-polyacrylamide and carboxymethyl cellulose-*graft*-polyacrylamide exhibit similar flocculation performance to conventional acrylamide-acrylic acid copolymers but are more biodegradable and less toxic due to the nature of their backbone. Finally, floc monitoring techniques as well as polymer molecular weight and charge density analysis methods are reviewed and discussed.

Keywords: *interparticle bridging flocculation; synthetic and natural flocculants; natural-graft-synthetic flocculants; aggregation monitoring; polymer molecular weight and charge density*

2.1 Introduction

Gravitational separation is a central technology in environmental engineering and water treatment. The extensive use of clarification is attributable to its cost/efficient solid/liquid separation performance (Sillanpää, Ncibi, Matilainen, & Vepsäläinen, 2018; Yang, R., Li, Huang, Yang, & Li, 2016). Aggregation rate, process robustness, and flow capacity have all been significantly improved over the past forty years due to the development of very high molecular weight (MW) flocculants and a deeper understanding of their aggregation mechanisms (Aguilar et al., 2005; Anthony, King, & Randall, 1975; Napper, 1983). Due to their low required dosages, their affordability, and the fact that they are relatively pH independent, these flocculants are considered amongst the most important chemicals used in the solid–liquid separation industry and, as a consequence, are still frequently studied (Biswal & Singh, 2004; Shaikh, S. M. R. et al., 2017). Such products are notably used for drinking water production and wastewater treatment since their use may reduce the required coagulant dosage (alum reduction of 67% in Bolto, Dixon, Eldridge et King (2001)) and, most notably, improve the floc size and settling velocity (Nasser et James (2006); Lapointe et Barbeau (2017)). The development of high-MW flocculants allows the operation of high-rate (30–85 m/h) settling processes (*e.g.*, Actiflo®, DensaDeg®, BioMag™, CoMag™, and SIROFLOC™) and the improvement of solids retention in sludge blanket clarifiers (*e.g.*, Ultrapulsator®). Polymers are also extensively used in paper and mining industry sedimentation processes or as selective flocculants for specific ore recovery (Ravishankar, Pradip, & Khosla, 1995). The worldwide flocculants market was estimated at USD $5.0 billion in 2016 and is expected to grow considerably to reach $6.8 billion by 2021. In 2021, the report *Flocculants: Technologies and Global Markets* estimates, the drinking and wastewater treatment industry will account for 66% of the market ($4.5 billion).

The term *flocculation* as used in this review will refer to the ability of a moderate-to-very-high-MW polymer (anionic, cationic, nonionic, or amphoteric) to accelerate and improve particulate matter agglomeration (*i.e.*, already destabilized solids) via an interparticle bridging mechanism. This mechanism enables the connection of two (or more) particles on a long polymer chain. Hence, this review is not dedicated to primary coagulation, where the coagulant is used to destabilize, adsorb, and precipitate/trap soluble or colloidal contaminants for example highly cationic polyelectrolytes such as polyDADMAC, used for turbidity removal. This article is, first, a

comprehensive overview of the different polymers used during flocculation that solicits adsorption-bridging mechanisms. Intrinsic flocculant characteristics such as the MW, charge density (CD) and spatial molecular configuration are detailed. Synthetic vs. natural flocculants are compared and their advantages/disadvantages are listed: challenges related to the polymerization method, implementation/solubility, solids removal performance, stability, cost, commercial availability, biodegradability, and aquatic/human toxicity are considered.

Second, complementing previous works on the subject (*e.g.*, Bolto (1995); Tripathy et De (2006); Bolto et Gregory (2007)), this review discusses natural-*graft*-synthetic polymers (referred hereafter as NGSP) as a promising alternative to synthetic polymers, the former being considered as a compromise between flocculation effectiveness and environmental impact/polymer toxicity. An ideal polymer dedicated to flocculation should be, depending on its application, inexpensive, pH independent, non-toxic, produced from a renewable material, and biodegradable, and should generate low headloss in granular media filters or, if used in conjunction with membrane processes, low fouling. If possible, polymer chains trapped in settled flocs should help sludge dewatering without compromising sludge reuse as agriculture fertilizer. Not all of these criteria are currently met while using synthetic polymers. For example, some of the best-performing synthetic high-MW polymers are toxic and considered only slowly biodegradable (Fielding, 1999; Rice, 2005; Sharma, Dhuldhoya, & Merchant, 2006). On the other hand, natural flocculants biodegrade faster and are non-toxic, but exhibit lower solids removal performance during clarification and/or require higher dosages (Bolto & Gregory, 2007; Lapointe & Barbeau, 2015). NGSP present simultaneously many advantages of synthetic and natural flocculants, but with only some of the drawbacks.

The most often employed and the most recent MW and CD polymer characterization techniques are also summarized. Additionally, the different polymer functional groups involved in initial polymer chain adsorption are enumerated for each discussed polymer. Finally, frequently used monitoring floc size, density, and shape techniques are presented and compared.

2.2 Aggregation mechanisms of high-molecular-weight polymers

For water flocculation systems principally involving bridging mechanisms, the aggregation rate and floc size stability are mostly controlled by the flocculant MW, its spatial conformation, the CD, and the presence of key functional groups allowing polymer chain adsorption onto flocs (Bolto

& Gregory, 2007; Gregory & Barany, 2011; Nasser & James, 2006). The aggregation of particles through a bridging structure can be described as a two-step pathway: 1) initial chain adsorption and bridging, followed by 2) floc maturation/reconfiguration. Before the interparticle connection occurs, the chain must be adsorbed onto a particle surface; hence, the global kinetic of flocculation in such a system is influenced by 1) the time required to complete the connection between two particles *i* and *j* via bridging and 2) the time needed to agglomerate a certain number *n* of those *i*,*j* connections to complete floc maturation. This section is an overview of this two-step pathway for different flocculant types (synthetic, natural, and NGSP) that identifies the main functional groups (*e.g.*, carboxyl groups) promoting polymer chains adsorption onto surfaces of particles such as silicates, metal oxides/hydroxides, organic colloids, and heavy metals.

2.2.1 Polymer chain adsorption

The very first step in interparticle bridging is the adsorption of a polymer segment onto a particle surface, which is made possible via electrostatic interaction, hydrogen bonding, or divalent cations binding (Bolto & Gregory, 2007). In the case of highly cationic polydiallyldimethyl ammonium chloride (PDADMAC) or highly cationic PAM used as primary coagulants, negatively charged natural organic matter (NOM) or colloids will adsorb through electrostatic interactions. Similarly, polyacrylic acid (PAA), polyvinyl sulfonic acid (PVSA), polyvinyl phosphonic acid (PVPA), or other polyelectrolytes with high anionic CD will preferably adsorb onto positively charged iron oxides (for pH under the oxide's point of zero charge (PZC)). However, in some systems, the polymer chain adsorption and interparticle connection are mainly due to hydrogen bonding. In the water industry, this situation is most prevalent when a nonionic or low-CD (<10%) PAM is used for the flocculation of coagulated particles with metal hydroxides ($Me(OH)_x$; Duan, Jinming et Gregory (2003)). In the case of a low CD, that is, when electrostatic interactions are not dominant, PAM chain adsorption will essentially occur through hydrogen bonding between $Me(OH)_x$ and PAM amide groups (Lee, L. T. & Somasundaran, 1989; Pefferkorn, 1999). More specifically, the C=O function of the amide behaves as a base, while metal hydroxides act as proton donors. In this reaction, the importance of the cationic hydroxide species rather than the neutral amorphous $Al(OH)_3$ was also mentioned by Lee, L. T. et Somasundaran (1989), as cationic species such $Al(OH)^{2+}$ and $Al(OH)_2^{+}$ promote the linkage between the base and the proton donor during hydrogen bonding.

Divalent cations such as Ca^{2+} are also expected, in some systems, to have an important impact during the aggregation of negatively charged colloids with anionic polyelectrolytes. It is likely that such ions, if present in sufficient concentration (around 40 mg Ca^{2+}/L), will act as a binding agent between anionic polyelectrolyte sites and negative particles, despite the anticipated electrostatic repulsion (Berg, Claesson, & Neuman, 1993; Bolto & Gregory, 2007). Therefore, the required time to adsorb a polymer chain is influenced by, among other factors, the ongoing adsorption pathway: 1) electrostatic interactions, 2) hydrogen bonding, and/or 3) divalent cation binding.

In some applications, those three adsorption pathways are simultaneously occurring—for instance, in the case of an anionic PAM onto positively charged iron oxide in the presence of a sufficient Ca^{2+} concentration. In this case, anionic carboxyl groups of PAM would interact with cationic patches present on ferric oxide particles (for pH under the PZC), while hydrogen bonding could also occur between the iron hydroxide groups and the C=O groups of PAM, and, finally, divalent cation binding would also be active, albeit to a lower extent. Different adsorption pathways are presented in Figure A- 1.

2.2.2 Interparticle bridging

Polymer MW is often used as an indicator to predict the performance of a flocculant. Higher MW translates into higher probability of available dangling polymer segments and hence also of interparticle bridging (Ruehrwein & Ward, 1952). However, a distinction must be made between the MW and the effective polymer chain length, the latter being notably influenced by the polymer structure (linear vs. ramified; Podzimek (1994)) and the water chemistry. As initially proposed by Napper (1983) and cited in Bolto et Gregory (2007), the nonionic root–mean–square end-to-end distance of a polymer chain can be estimated by 0.06 $MW^{1/2}$. Multiangle laser light scattering (MALLS) can also be used to evaluate the end-to-end distance by measuring the scattered intensity at angle θ as function of the incident light wavelength (Andersson, Wittgren, & Wahlund, 2003). Based on this equation, the root–mean–square end-to-end distance of a nonionic PAM with a high MW of 10^7 g/mol would be around 135 nm (see Figure 2.1). However, this end-to-end distance is likely to change after polymer adsorption onto particles, depending on the polymer chain configuration (flat or dangling; Gregory et Barany (2011)). As shown in Figure 2.1, this led to the concept of available chain segments for bridging (*loops* and *tails*) vs. unavailable chain portions already attached (train) onto particles (Napper, 1983).

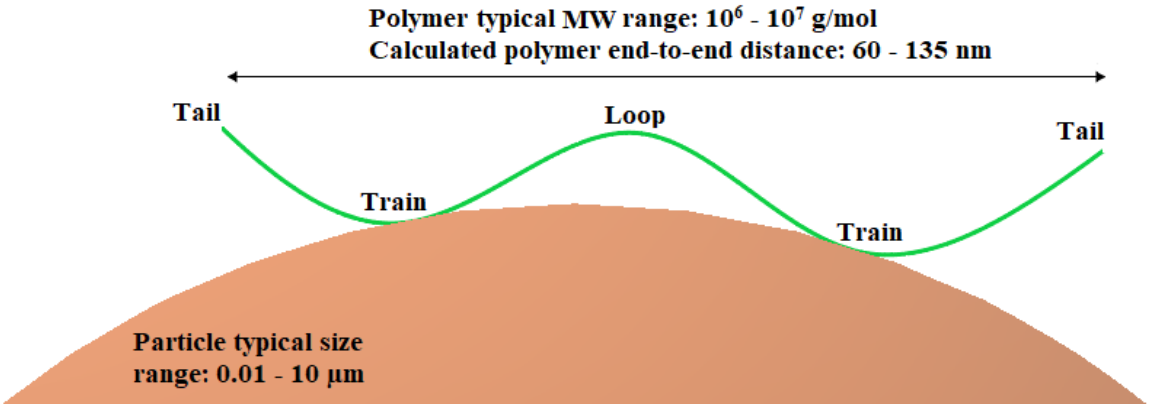

Figure 2.1: Theoretical polymer chain adsorption leading to available *tails* and *loop* segments as proposed by Napper (1983).

As an example, important electrostatic interactions between a cationic PAM with a high CD and negative colloids will theoretically lead to a flat polymer chain configuration on the surfaces. In this case, only a few *loops* and *tails* would be available and interparticle connections would be unlikely to occur (Yukselen & Gregory, 2004). Moreover, polymer chains can underdo reconfiguration during flocculation, since the functional groups (dictating the CD) and available site for hydrogen bonding are progressively consumed during aggregation. The configuration of the polymer chain on the surface is then in constant mutation until it reaches a final state.

Apart from the MW, the effective polymer chain length and the number of available dangling segments for bridging are intimately linked to the polymer CD. The chain extension is, among other factors, influenced by electrostatic repulsion of intramolecule segments (Bolto & Gregory, 2007). To improve interparticle bridging flocculation, the optimal CD will not be selected only based on electrostatic interaction with particles but also for its ability to maintain a certain polymer chain extension under a given background water chemistry (Bolto & Gregory, 2007). A typical example of intersegment repulsion would be the case of an anionic PAM with a low CD used for the flocculation of precipitated NOM with alum, during which bridging would theoretically occur through hydrogen bonding (between aluminum hydroxides and PAM amide groups; see section 2.2.1). In this case, negative–negative repulsion sites are attributable to the low anionic CD ensuring the chain extension. However, such behavior can be influenced by the ionic strength, segment repulsion being inversely proportional to the ion concentrations (Bolto & Gregory, 2007),

since dissolved salts have a tendency to stabilize the polymer charge. The evolution of the polymer chain configuration on the surface is of importance, since reconfiguration in a less favorable manner (flat configuration vs. dangling) is associated with floc size reduction (Gregory & Barany, 2011; Yukselen & Gregory, 2004). Industrial applications using high-MW PAM often attenuate the effect of reconfiguration by splitting the flocculant dosages, for example 50% at the beginning of the flocculation and 50% at mid-flocculation.

MW and the effective length of the polymer structure are also important factors controlling floc strength (Yukselen & Gregory, 2004), collision efficiency (Agarwal, Gupta, & Doraiswamy, 2009), and polymer adsorption kinetic (segment adsorption time being inversely proportional to MW; Gregory (1988)). After the polymer adopted is in its final state of adsorption onto the surface, it is then anticipated that floc maturation will occur—a period during which particle–polymer microflocs collide together to form larger aggregates. This system refers to the typical flocculation model in which aggregation rate is proportional to mixing intensity, particle concentration, and collision efficiency (Thomas, Judd, & Fawcett, 1999).

2.3 Flocculant molecular weight and charge density

Polymers are classified according to their CD (anionic, cationic, nonionic, or amphoteric) and MW (low, moderate, high, or very high). Depending on the type of particles to flocculate (*e.g.*, metal hydroxides/oxides coated with NOM, biocolloids, macromolecules, organic fibers, etc.), the water chemistry, the mixing time and intensity, and the geometry of the flocculation tank, a certain CD and MW must be selected in order to improve interparticle bridging and floc settleability. The impact of the polymer on downstream processes must also be considered in polymer selection. Irreversible membrane fouling, excessive granular filtration headloss (Zhu, H. et al., 1996) or ineffective sludge dewatering (Novak, Prendeville, & Sherrard, 1988) are potential consequences of inadequate flocculant selection. The rationale for the selection of an optimal CD and MW for each application has been already reported by other researchers (Bolto & Gregory, 2007; Nasser & James, 2006), highlighting the importance of accurately and precisely characterizing flocculants. Polymer structure (linear vs. branched) is also known to impact the effective length of the polymer chain and as a consequence, the effectiveness of flocculation via interparticle bridging mechanisms. This section presents some of the most common, as well as some more advanced, characterization techniques used by industry and researchers to properly determine flocculant CD and MW.

2.3.1 Molecular weight determination

In this section, different MW determination methods are discussed and recommended based on the polymer's spatial configuration. Linear homopolymer compared to highly branched synthetic-*g*-natural copolymers will have different interactions with the solvent and hence different morphology and extension behavior with different specific solvents. Methods using polymer standards as calibration are notably impacted by such polymer structure complexities.

Viscosity method

MW can be indirectly evaluated by viscosity analysis methods, which are typically employed for the characterization of commercial products (Bolto & Gregory, 2007). The intrinsic viscosity (η) is reported to be proportional to the flocculant MW, where log of MW is linearly proportional to log of η. As reported by Fevola, Hester et McCormick (2003), this linear proportionality is especially true for flocculants with a linear structure, such as homopolymerized PAM. However, the basic relation between viscosity and MW, as shown in Eq. 1c (where K and α are specific to each polymer–solvent system), does not take into account the polymer's spatial configuration (linear vs. branched). It is well known that for two polymers with the same MW, branched polymers exhibit a lower intrinsic viscosity compared to linear polymers (Tripathy & Singh, 2001). Hence, the MW of some highly branched flocculants may be underestimated by this method.

$$\eta = K\,MW^{\alpha} \quad \text{(Eq. 1)}$$

This equation was first developed by Flory et Fox (1951), who proposed values of K and α that would consider the spatial configuration of the polymer (*e.g.*, with the root–mean–square end-to-end distance or with the radius of gyration of the dissolved polymer chain) and the thermodynamic interaction of the solvent–polymer system. The Flory and Fox equation was also recently used by Yang, R. et al. (2016) to evaluate a chitosan-based flocculant, and by Grube, Leiske, Schubert et Nischang (2018); both studies reported a linear relation between η and the MW of polyethylene glycol (PEG MW between 2000 and 50,000 g/mol).

Size exclusion chromatography coupled with multiangle laser light scattering

Size exclusion chromatography (SEC), mostly gel permeation chromatography, is a common technique used to fraction the macromolecule population forming the flocculant. Contrary to the indirect viscosity calculation method, SEC provides information on flocculant MW distribution

and allows a finer product selection for a given application. During SEC, the elution volume (V_e) of a molecule will be correlated with its MW. The number-average MW_N ($\sum N_i M_i / \sum N_i$, where N_i is the number of molecules having a specific molecular weight M_i) and weight-average MW_W ($\sum W_i M_i$, where $W_i = N_i M_i / \sum N_i M_i$) can also be calculated, the latter being notably influenced by the presence of larger molecules (Meiczinger, Dencs, Marton, & Dencs, 2005). The polydispersity, an indicator of the MW distribution dispersion, is then calculated by the ratio of weight-average MW to number-average MW.

The earlier work of Grubisic, Rempp et Benoit (1967) revealed the complexity of calibrating MW vs. V_e for different macromolecular structures, since more branched polymers for the same MW have longer retention time in the column compared to homopolymerized linear polymers, indicating better penetration of branched structure into the chromatography column beads. Inadequate calibration was also illustrated by Wyatt (1997) who compared the MW of two polymers (linear vs. branched polyacrylate) as a function of V_e. Grubisic et al. (1967) developed a calibration equation considering the structural/configurational aspect of a macromolecule using its radius of gyration and its hydrodynamic volume. This technique was notably used by Järnström, Lason et Rigdahl (1995) to measure the MW of a branched cationic starch polymer using linear PEO as standard; the calibrated method yielded a MW of 4.8×10^5, as opposed to 1.1×10^5 before calibration. SEC has also been successfully used for the determination of high-MW starch polymers of 1.4×10^6–2.3×10^7 g/mol using dextran standards from 4.9×10^4 to 4×10^7 g/mol (Simsek, Ovando-Martínez, Whitney, & Bello-Pérez, 2012)).

In a more recent analytical advance (Grube et al., 2018), PEO and PEG (polyethylene glycol) MW were measured by coupling SEC (calibrated with polystyrene) with multiangle laser light scattering (MALLS; equipped with 532-nm laser). By considering the scatter intensity at angle θ, MALLS can also be used to determine MW without the use of a standard curve, as opposed to SEC for which MW estimates are determined with a calibration curve and where chromatographic conditions can induce errors (*e.g.*, inadequate polymer/solvent interaction and/or particles causing interference). MALLS has been used for a wide range of MWs—from a few hundred to more than 10^8 g/mol. SEC-MALLS is more accurate than hydrodynamic analysis using viscometry or SEC alone for MW higher than 10,000 g/mol, but may provide incorrect MW under this threshold. In this technique, MW is measured as a function of light intensity scattered by the polymer over a certain range of angles. The developed equations are presented in Wyatt (1997) and Andersson et

al. (2003). SEC-MALLS notably eases the adjustment of the V_e vs. MW relation for branched polymers by measuring the root–mean–square molecule radius as a function of V_e for a comparable linear polymer (Wyatt, 1997). It provides information not only on weight-average MW_W and MW distribution but also on the radius of gyration and molecule conformation (Andersson et al., 2003; Wittgren & Wahlund, 1997).

Light scattering techniques to measure the weight-averaged MW for each separated macromolecules population has been extensively used by other researchers for the characterization of high molecular MW polymers. SEC-MALLS was successfully used by Chen, M. H. et Wyatt (1999) to characterize high-MW amylopectin, guar gum and a cellulose-based polymer, by Roussy, Van Vooren, Dempsey et Guibal (2005) to select an optimal chitosan-based flocculant (MW: $4.5x10^4$–$3.1x10^5$ g/mol; degree of deacetylation: 78–95%) for bentonite suspension, and by Fevola et al. (2003) to measure the MW distribution and the polydispersity of PAM.

Asymmetrical flow field–flow fractionation with multiangle laser light scattering

Alternatively to SEC, Grube et al. (2018) used asymmetrical flow field–flow fractionation (AF4) as a fractionation method prior to subsequent MALLS analysis. As mentioned earlier, MALLS is used to measure the weight-average MW of different pre-fractionated slices of the macromolecule MW distribution. For this technology and inversely to SEC, smaller molecules will elute first as they typically have higher diffusion coefficients. Consequently, the macromolecules with higher molar mass will diffuse more slowly. Nevertheless, as mentioned in the previous section, care should be taken for the analysis of small polymer MW with SEC and AF4 coupled with MALLS (Grube et al., 2018), hydrodynamics analysis using viscometry being more appropriate for such low-MW polymers (*i.e.*, <10,000 g/mol).

Wittgren et Wahlund (1997) adequately characterize the MW polydispersion of pullulan (a polysaccharide polymer with a weight-average MW from $2x10^5$ to $2x10^6$) with an online AF4-MALLS in less than five minutes; AF4 has also been identified as a very rapid separation method (less than 4 min), by Contado et Wahlund (2006). SEC and AF4 were compared by Rolland-Sabaté, Guilois, Jaillais et Colonna (2011) by measuring the MW distribution of different starches with variable amylose/amylopectin ratios. Compared to SEC, those researchers established that AF4 enables better separation of the different branched macromolecules from amylopectin (MW of 1.0–$4.8x10^8$ g/mol), hence offering a better characterization of starch when AF4 was coupled with

MALLS. Additionally, AF4 may surpass SEC or other conventional chromatography methods for the characterization of very-high-MW flocculant, including some specific PAM, due to the separation challenges associated with polymer adhesion/diffusion in the SEC column (Leeman, Islam, & Haseltine, 2007; Messaud et al., 2009). Since the early 2000, many other researchers have successfully characterized branched or linear high MW using AF4-MALLS: cationic starch with a very high MW of $2.6x10^7$–$2.4x10^8$ g/mol (Modig, Nilsson, & Wahlund, 2006), PAM with a very high MW of $2.0x10^7$ g/mol (with $2.3x10^4$–$7.9x10^5$ g/mol pullulan standards and with $8x10^4$–$5.5x10^6$ g/mol PAM standards; Leeman et al. (2007)), and a branched xanthan gum polymer with MW of $3.2x10^6$ g/mol (Viebke & Williams, 2000).

Nuclear magnetic resonance spectroscopy

Nuclear magnetic resonance (NMR) spectroscopy is another method proposed by some researchers to evaluate molecular size. It was reported by Neufeld et Stalke (2015) to be a robust technique to evaluate low-MW molecules ($<10^3$ g/mol), and was also more recently applied by Monakhova, Diehl, Do, Schulze et Witzleben (2018) to measure low-MW heparin ($<10^5$ g/mol). Notably, due to its cost, this technique is not conventionally used for high-MW polymers compared to SEC and other light-scattering techniques (Vanier, El Halal, Dias, & da Rosa Zavareze, 2017). NMR has been more particularly used for polymers' structural characterization or for the evaluation of some functional groups present on their backbone (see next section).

2.3.2 Molecular composition and structure

The polymer's molecular structure and composition have an important impact on effective polymer chain length and hence the polymer's ability to bridge particles (Yu, Wei, Wang, Li, & Yang, 2018). NMR spectroscopy and Fourier transform infrared spectroscopy (FTIR) figure among the most frequently used methods to perform such characterization. FTIR and NMR spectra were used (i) by Yu, Wei et al. (2018) and by Zhu, Z., Li et Jin (2009) to characterize the molecular structure (linear vs. branched) of starch-*g*-polyacrylic acid flocculant, (ii) by Tripathy et Singh (2001) to confirm the presence of PAM on alginate, (iii) by Chen, Q. et al. (2016) to identify carbonyl groups onto polyacrylic acid (PAA) (FTIR; peak between 1726 and 1740 cm^{-1}) and (iv) by Gillies, Dy, Fréchet et Szoka (2005) to quantify phenolic groups onto PEO backbone (MW: $2.0x10^4$–$1.6x10^5$ g/mol). FTIR and NMR were also used by Singh, V., Tiwari, Tripathi et Sanghi (2004) to analyze the size of PAM chains grafted onto a guar gum backbone. Such analyses are also frequently

employed for the characterization of conventionally used flocculants for drinking water applications; as an example, NMR spectra were used to evaluate the presence of grafted PAM onto PAA (Liu, Z. & Rempel, 1997).

X-ray diffraction (XRD) is another technique frequently applied to characterize the morphology and the polymer's molecular structure. This technique is particularly used for the identification of grafted polymer sections onto variable backbones. Singh, V. et al. (2004) were able to identify the presence of grafted PAM chain by comparing the XRD spectra of pure guar gum vs. guar gum–*g*–PAM, a peak at 16°–17° revealing the presence of PAM. Based on the presence of a broader peak observed between 20° and 30° in the case of grafted guar gum, these authors also reported a crystallinity decrease vs. pure guar gum. A similar XRD crystallinity analysis (scatter angle (2θ) from 10° to 45°) was performed by Biswal et Singh (2004), and the presence of PAM onto a CMC backbone was confirmed. Those researchers reported considerably reduced crystallinity in the case of CMC-*g*-PAM (no apparent peak) compared to pure PAM, in which the crystalline peaks appeared in the 2θ range (21°–42°).

Other techniques, such as thermogravimetric analysis (TGA), scanning electron microscopy (SEM), and differential scanning calorimetry (DSC), can be used for polymer structure characterization, to identify some common functional groups (*e.g.*, carboxyl groups), or to evaluate the morphological aspect of the powder/granule form of the polymer (Biswal & Singh, 2004; Sen, Ghosh, Jha, & Pal, 2011; Tripathy & Singh, 2001; Vanier et al., 2012).

2.3.3 Charge density determination

Charge density (CD) is, similarly to MW, a key parameter for effective flocculation via interparticle bridging, since it plays an important role in polymer chain expansion (notably due to intramolecular repulsion between charged segments; Bolto et Gregory (2007)). CD is frequently expressed as milliequivalents per gram (meq/g) or in terms of percentage of mole charged. Based on the Bolto et Gregory (2007) classification, CD is considered either low (~10%), moderate (~25%) or high (50–100%).

Polyelectrolyte CD can be determined by potentiometric titration (with a strong acid or base) or by direct polyelectrolyte titration using an oppositely charged titrant. Titration with a polyelectrolyte of known CD (when the point of zero charge is reached; see Eq. 2) is a more readily implementable

method and can evaluate CD for lower polymer concentrations compared to potentiometric titration (Bratskaya, S., Golikov, Lutsenko, Nesterova, & Dudarchik, 2008). However, this method requires an adequate titrant selection in terms of MW and CD; the titrant must interact with the polyelectrolyte according to a 1:1 stoichiometry. Typically, low-MW titrants are used to promote this 1:1 stoichiometry. Challenges related to this method are mentioned in Chen, J., Heitmann et Hubbe (2003), who pointed out that the electrokinetic stabilization can be influenced by the salt concentration and an incomplete polyelectrolyte titrant complexation, uncomplexed titrant being caused by its partial entrapment into the polymer chain to be characterized or due to an excess of the titrant in question.

$$CD = \frac{C_t \times V_t}{M} \text{ , when the point of zero charge is reached} \qquad \text{(Eq. 2)}$$

Where:

CD is the charge density (meq/g)

V_t is the consumed titrant volume (L)

C_t is the titrant concentration (meq/L)

M is the mass of polyelectrolyte to be characterized (g)

Direct polyelectrolyte titration, among other methods, was used by Solberg et Wågberg (2003), with an anionic potassium polyvinylsulphate titrant of known CD and a colorimetric end-point detector (orthotoluidine blue was used as a color indicator) to measure cationic PAM CD (1.22 meq/g at pH 5.6; corresponding to approximately 10%). A procedure involving the use of polyvinylsulphate as a titrant was also detailed in Terayama (1952) and in Kam et Gregory (1999). Those authors mentioned the importance of the selected method of end-point detection: by visual inspection or spectrophotometric determination of color change of orthotoluidine blue indicator or using a streaming current detector to validate the charge neutralization. Wassmer, Schroeder et Horn (1991) used ionene bromide as a cationic titrant for anionic PAA and polyvinyl sulfate; eriochrome black T served as indicator for end-point detection. For PAA, the authors demonstrated the effectiveness of the method in the concentration range of 0.01–10 mg/L; this method is hence appropriate for municipal applications, in which the dosage range is typically between 0.1 and 0.5 mg/L (in the case acrylic acid–acrylamide copolymers or acrylamide homopolymers). Acrylamide-

based polymers are notably limited to maximal dosages of 1 mg/L for drinking water applications in North America and 0.2 mg/L in many European countries (Lapointe & Barbeau, 2017).

2.4 Monitoring of aggregates

Monitoring systems are essential for selecting an adequate flocculant type and dosage and are complementary to jar-test procedures, the latter only evaluating flocculation performance indirectly through fixed settling conditions. Being largely influenced by flocculant type and dosage and the application (*e.g.*, drinking water, wastewaters, or industrial/mining effluents), the floc's morphology and its resistance to shearing generally define the admissible and required methods for their characterization. As an example, some particles counting systems are incapable of analyzing large floc, while some pixelation methods are unable to define the solid–liquid interface of some nano- or micro-sized particles.

This section reviews and discusses the most current methods to directly measure or indirectly estimate (via an indicator) floc size, density, and shape. As many techniques present limitations, recent research efforts for the elaboration of adapted on-line, full-scale and non-intrusive monitoring systems are also presented in this section.

2.4.1 Intrusive methods

The techniques mentioned in this section require manipulation of the suspension before its characterization; through a collector, or by aspiration by pumping, or with a pipette. Such intrusive sampling methods induce mechanic/hydraulic shearing and compression stress onto floc structure just before size characterization.

Optical microscopy

Combined optical microscopy and image analysis (off-line and on-line monitoring systems) is commonly used for characterizing flocs in different process applications. With this technique, the aggregate entity can be distinguished by pixel gray-level variance. The precision is then influenced by the relative size of flocs in the picture vs. the resolution of the image. By determining if a pixel is linked to the floc pixel group, connected component labelling techniques, implemented by scanning each pixel of a digital image, can be used to increase the 2D physical frontiers of an aggregate (Kilander, Blomström, & Rasmuson, 2006). Microscopy combined with image analysis

techniques allow the characterization of a relatively broad floc size range: 500–4300 µm (Mas & Ghommidh, 2001) and as low as 5 µm for a kaolinite suspension flocculated with guar gum (Shen & Maa, 2016). Microscopic analysis has the advantage of simultaneously providing information on mean floc size, floc size distribution, and shape (by measuring the longest and shortest dimensions). Typically, the 2D projected surface area of the ellipsoidal floc is evaluated by image analysis and afterward converted into an equivalent diameter (assuming a spherical floc shape; Xiao, F., Lam, Li, Zhong et Zhang (2011). For the activated sludge process, Barbusiński et Kościelniak (1995) used a technique wherein 65 flocs measurements were required to characterize a log-normal distribution (100–900 µm). For ballasted flocculation of surface water, a similar procedure was presented in Lapointe et Barbeau (2016), where floc diameter (log-normal distribution; 100–800 µm), relative density (normal distribution; 1.2–1.7) and shape (gamma distribution; longest dimension/shortest dimension ratio from 1–2.5) were measured. Contrary to light-scattering techniques, the method presented in Lapointe et Barbeau (2016) allows evaluation of the ballasted floc's specific gravity by quantifying the amount of incorporated ballast media into the floc structure (40 flocs per analysis). With kaolin suspension destabilized by alum, Han, Kim et Kim (2006) also used this procedure for measurement of floc size in the range of 5–1000 µm (1000–1300 flocs per analysis). Despite increasing resolution over the past decades (*e.g.*, 2.2 um/pixel; Shen et Maa (2016)), such methods are limited by pixelation definition, involve sampling and/or pumping, during which floc breakage can occur, and are known to be time-consuming (Cheng, W. P., Kao, & Yu, 2008).

Built-in observation devices

Built-in particle count systems using light scattering or imaging processing are commercially available and can be easily operated for lab-scale applications. However, all those methods are also considered hydraulically intrusive and must be implemented carefully to avoid modifying the floc size distribution and structure. For example, installation of particle counters on settled waters is not recommended. Settling and physical blocking (in the case of larger and denser flocs) into the observation chamber is a limiting aspect of many particle count devices: 2–400 µm, Brightwell DPA 4100; (Karizmeh, Delatolla, & Narbaitz, 2014); <500 µm, µFLOC (Radhakrishnan et al., 2018); <1200 µm, Multisizer 3; <2000 µm, Mastersizer (Sperazza, Moore, & Hendrix, 2004). To

characterize bimodal floc size distributions, these apparatuses were able to accurately measure the size distribution of small particles unlikely to settle and were successfully coupled with microscopic observations or with particle image velocimetry (PIV) to take in charge the characterization of larger aggregates.

Flocculation index

The flocculation index (FI; Gregory (1985), is less time-consuming than microscopic measurements and can serve as an indicator of floc size and aggregation rate. FI, which is based on the variability of the light scatter, has been reported to be linearly proportional to the mean floc diameter (R^2=0.94; Li, T., Zhu, Wang, Yao et Tang (2007)). The suspension is vacuumed into a photometric dispersion analyzer (PDA), where the root–mean–square of the fluctuations of light transmitted through flowing aggregates is obtained. Depending on the intensity transmitted, some information about floc size can be extracted as a function of the root–mean–square intensity (Gregory & Nelson, 1986). FI is rather considered an indicator of the relative change of mean floc size and does not allow floc size distribution evaluation (Kilander et al., 2006). Additionally, this technique, similarly to sampling during observation by microscopy, requires aspiration by pumping, hence potentially causing floc aggregation/breakage deposition in the tubing. Finally, Ball, Carriere et Barbeau (2011) concluded that the FI was a less sensitive indicator than pixel-based microscopic measurements (Brightwell DPA4100) for direct filtration where floc size was small (lower than 30 µm). However, for large floc size and concentration, the counting cell of the particle counter (800 µm) was found to clog, and the technique was therefore not applicable to these conditions.

2.4.2 Non-intrusive methods

Particle image velocimetry

The PIV technique has been extensively used in recent years, since unlike optical microscopy it allows direct non-invasive floc size measurement and shape characterization (Bouyer, Coufort, Liné, & Do-Quang, 2005; Ren, Nan, Zhang, & Zheng, 2017). PIV requires a high-speed digital charge coupled device (CCD) camera (around 1 image per millisecond) combined with image processing software and a thin light sheet, the latter being among other techniques generated by a pulsed laser expanded into cylindrical and a spherical lenses (Xiao, Feng, Lam, & Li, 2013). The

flocs characterization area in the beaker is then defined by the planar sheet of light, a thinner one being favored to reduce the probability of particle/floc superposition. Many applications of PIV to identify the optimal coagulation/flocculation conditions for water treatment have been reported over the past twenty years. PIV was recently used by Ren et al. (2017) to measure floc size in a continuous reactor as a function of PAC (polyaluminium chloride) dosage (mean diameter between 60 and 80 µm). Bouyer et al. (2005) evaluated the floc size distributions (around 20–400 µm) of a coagulated bentonite suspension with alum as function of time and mixing intensity. Xiao, F. et al. (2011) used a similar system to compare the performance of alum vs. ferric chloride, *inter alia* by evaluating the impact of shearing on floc size.

Non-intrusive techniques such as PIV are particularly interesting for flocculation processes where large and fragile flocs are growing (Chakraborti, Atkinson, & Van Benschoten, 2000). PIV was employed by Zhong, Zhang, Xiao, Li et Cai (2011) for the *in situ* measurement of flocs with a d_{50} as high as 1700 µm. With a similar PIV configuration, very large activated sludge aggregates of 1265–3737 µm were also characterized by Xiao, Feng et al. (2013). Other non-intrusive commercially available devices and less expensive techniques also employ similar illuminating-camera systems. As an example, the FlocCAM^{TM}, using an illuminated beam rather than a sheet of light, was employed by Lapointe and Barbeau (Lapointe & Barbeau, 2017, 2018a) to characterize ballasted flocs with mean diameters in the range of 450–700 µm. For this system, the number of images per second is lower than for a high-speed CCD camera, and the built-in image processing software only allows mean floc diameter characterization.

Light-scattering methods

Non-invasive scattering techniques (light, X-ray, or neutron) have also been successfully used by many researchers in the last 20 years to pull out information about floc size and shape. Jung, Amal et Raper (1995) used small angle light scattering for micron-sized hematite. Similar methods were used by Herrington et Midmore (1993) and by Rattanakawin (2005) for kaolin suspension. Amal, Gazeau et Waite (1994) successfully characterized hematite during aggregation using small-angle X-ray. Among the three scattering methods mentioned above, due to its higher wavelength, light scattering was reported more suitable to characterize larger micron-sized flocs (Bushell, Yan, Woodfield, Raper, & Amal, 2002).

2.4.3 Settling velocity techniques

One of the conventionally employed protocols combines PIV with column-settling tests to extract floc size, density, or shape. By assuming particle sphericity, direct floc size distribution and settling velocity measured by PIV combined under Stokes's law enable calculation of the floc's effective mean density (Dyer & Manning, 1999). Inversely, if the aggregate density is known (*e.g.*, non-porous and inert silica particles such as silt or sand), information about the drag coefficient, permeability, and floc shape can be derived from the same equation. Such a procedure can also be applied to porous particles if the density is known. Johnson, C., Li et Logan (1996) compared the settling velocity of porous vs. impermeable material using a settling test. Xiao, Feng et al. (2013) combined PIV with settling assays to evaluate the impact of large activated sludge floc permeability by comparing the settling pattern with latex particles. Similar hydrodynamic investigation was made with a double settling column (Li, X.-y. & Yuan, 2002). Based on Stokes's Law, the settling tests revealed that permeable activated sludge flocs settled faster compared to the predicted spherical impermeable floc of the same density and size. Floc density and porosity are hardly quantifiable by image analysis, since the flocs formed during conventional clarification treatment are heterogeneously porous 3-D structures (Thomas et al., 1999). Hence, semi-empirical methods combining theoretical settling equations with PIV and settling tests are an effective way to estimate aggregate density.

2.5 Flocculant types

This section presents an overview of typical flocculating agents used in the water industry. Synthetic and natural polymers are compared in terms of weight-average MW, CD, and available functional groups. Flocculants' advantages and drawbacks are summarized in Tables 2.1 and 2.2; new alternative NGSP are also listed in Table 2.3. Some grafted flocculants mentioned in section 2.5.3 are typically manufactured and used as selective flocculants for specific colloids/macromolecules in the food, biomedical, and pharmaceutical industries; considering their high MW and their biodegradability, those flocculants can be identified as promising alternatives for the water treatment industry as well.

2.5.1 Synthetic flocculants

Synthetic polymers are frequently used in the water flocculation industry. Their structure can be modified for specific applications, and a large number a functional groups can be grafted to them (Lu, Y. et al., 2011; Zhu, G., Liu, & Bian, 2018). In general, their purity is greater, they have better stability, they are not prone to biodegradation, and their performance regarding particle bridging is better than that of natural polymers (Aguilar et al., 2005; Carter & Scheiner, 1991). Usually, the presence of negatively charged polymer segments is attributable to functional groups such as carboxylic or sulfonic acids (Shaikh, S. M. R. et al., 2017) while cationic CD can be attributed to the presence of positively charged quaternary ammonium groups (Bolto & Gregory, 2007; Shaikh, S. M. R. et al., 2017).

Polyacrylamide

Due to its low cost and high effectiveness, polyacrylamide (PAM; Figure 2.2) is extensively employed as a flocculating agent in the clarification industry (Bolto & Gregory, 2007; Nasser & James, 2006; Pefferkorn, 1999; Samoshina, Diaz, Becker, Nylander, & Lindman, 2003). Typically, PAM with low CD and high MW (<30% and $>10^6$ g/mol; see Table 2.1) is used to increase floc size and strength and to improve settling rates. One of its most frequent applications is to increase size of flocs produced from coagulation with a metal salt (*e.g.*, alum or PAC; Ahmad, Wong, Teng et Zuhairi (2008). Anionic high-MW PAM (Figure 2.2A) can be obtained through the polymerization and partial hydrolysis of acrylamide or prepared by copolymerization involving acrylic acid and acrylamide (Bolto & Gregory, 2007). Poly(acrylamide-co-acrylic acid), classified as an anionic PAM, is also extensively used in the industry, since it offers negatively charged segments, in distinction from nonionic acrylamide homopolymer (Pefferkorn (1999)). Negative sites on PAM chains are essentially attributable to the presence of weak carboxylic acid groups (Figure 2.2B) and theoretically influenced by pH. However, PAM CD generally remains stable (*i.e.*, for typical pH during clarification using metal salts, 5.5–7.5) despite pH variations, since carboxylic acids have pKa under 4.9 (Michaels & Morelos, 1955; Namazian & Halvani, 2006). Nevertheless, some authors report a decreasing anionic CD caused by the complexation of metal ions (*e.g.*, Fe^{3+} or Al^{3+}) onto anionic carboxyl groups (Henderson & Wheatley, 1987; Pefferkorn, 1999). Under alkaline conditions (pH >10), additional anionic sites could develop, since PAM undergoes hydrolysis (Lee, L. T. & Somasundaran, 1989), which is unlikely to occur under typical

water surface and municipal wastewater pH. In such conditions, if the pH is higher than the PZC, PAM adsorption can also occur through its NH_2 function onto negatively charged oxides. In the case of high-MW cationic PAM (Figure 2.2B), it can be manufactured by the polymerization of acrylamide with cationic copolymers such as dimethylaminoethylmethacrylate (DMAEMA) and DADMAC (Baade, Hunkeler, & Hamielec, 1989; Solberg & Wågberg, 2003).

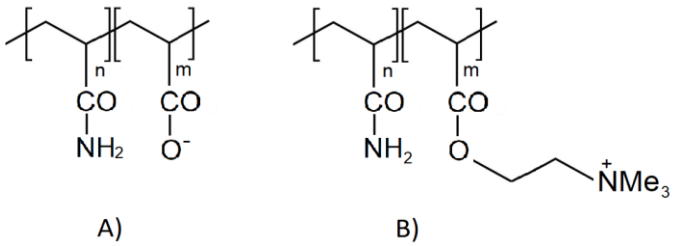

Figure 2.2: Anionic (A) vs. cationic polyacrylamide (PAM) (B).

In the case of PAM with low cationic CD, chain adsorption will also occur, depending on the CD level, via electrostatic interaction (*e.g.*, between cationic side-chain groups with a negatively charged silica particles) (Gregory & Barany, 2011; Samoshina et al., 2003; Shaikh, S. et al., 2018). As mentioned in section 2.2.1, amide groups of anionic or nonionic PAM are known to be well adsorbed through hydrogen bonding on silanol (Si-OH), aluminol (Al-OH), and other metal hydroxide groups presented at an inorganic particle surface (Lee, L., Rahbari, Lecourtier, & Chauveteau, 1991; Mpofu, Addai-Mensah, & Ralston, 2003).This adsorption pathway makes PAM an extensively used flocculant in drinking water flocculation, more notably when a metal salt is used as a coagulant. Many authors have already reported the advantages of PAM for conventional clarification (Aguilar et al., 2005), ballasted flocculation (Lapointe & Barbeau, 2016), and sludge dewatering applications (Mpofu, Addai-Mensah, & Ralston, 2004; Novak et al., 1988). The wastewater industry also uses such polyelectrolytes to improve floc size and strength as well as clarification rates (Ahmad et al., 2008).

The effectiveness of PAM as a flocculating agent is attributable to its high MW, its stability, and its flexibility in terms of possible CD. More specifically, its long linear structure, compared to branched polysaccharide-based polymers, considerably improves interparticle connections. However, PAM can, in some cases, undergo an important reconfiguration and adopt a less favorable and less expanded configuration at the particle surface, leading to floc size reduction as

function of aggregation time (Bolto & Gregory, 2007; Lapointe & Barbeau, 2017; Pefferkorn, 1999).

Polyacrylic acid

Polyacrylic acid (PAA; Figure 2.3) is prepared by the homopolymerization of acrylic acid (Tripathy & De, 2006) and can reach relatively high MW: as high as $4x10^6$ g/mol was reported by Das et Somasundaran (2004) and by Ravishankar et al. (1995). Similar to PAM, anionic sites on the PAA structure is also attributable to the presence of carboxylic groups negatively charged (pKa ~ 4.5) due to hydrogen dissociation from the carboxylic acids. In acidic conditions, this polyelectrolyte is considered nonionic; hence, the predominantly chain adsorption pathway would occur via hydrogen bonding, since the polymer chain–particle electrostatic interaction would then be limited. Wassmer et al. (1991) observed a considerable anionic CD decrease when the pH was reduced from 11 to 7.

Depending on pH, PAA can be used as a bridging agent for some positively charged oxides (Das & Somasundaran, 2003). It can also be employed as flocculant in a dual-polymer system. As mentioned in Gregory et Barany (2011), pDADMAC and PAA can be respectively used as primary coagulant and flocculant; and as mentioned in the previous section, acrylic acid groups and amide groups can also be copolymerized to form high MW with wide range of anionic CD (2%–50%; Tripathy et De (2006)). In this case, the copolymers would be typically classified as an anionic PAM.

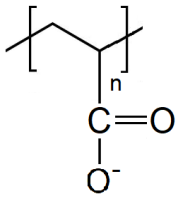

Figure 2.3: Polyacrylic acid (PAA).

PAA is one of the most used synthetic flocculants in the mineral industry due to its selective flocculant properties for different ores such as iron. The electrostatic interactions between an anionic PAA and positively charged iron oxide lead to large flocs despite relatively low PAA

dosages. This was reported by Ravishankar et al. (1995), where PAA was used for the aggregation of hematite at pH 6.2.

Polyethylene oxide

Polyethylene oxide (PEO; Figure 2.4) is an intrinsically uncharged (nonionic) polymer with a MW typically up to 10^6 g/mol, although a very high MW-PEO of $1.8x10^7$ g/mol was measured and confirmed by SEC-MALLS (Andersson et al. (2003)). It can be obtained by the catalytic polymerization of ethylene oxide (Tripathy, Pandey, Karmakar, Bhagat, & Singh, 1999), which leads to a relatively linear structure. Such a high-MW PEO is, however, susceptible to degradation caused by the presence of certain metal ions such as Fe^{3+} and Cr^{3+} (Tripathy & De, 2006). Such a nonionic polymer is expected to flocculate silica suspension by interparticle bridging, more notably through hydrogen bonding (Rubio & Kitchener, 1976) since no electrostatic attraction can come from an uncharged polymer chain. PEO chain adsorption can occur between ether oxygen and OH groups presented at the particle or oxide surface (silanol or aluminol groups) (Bolto & Gregory, 2007; Mpofu et al., 2003). Similarly to other polymers, PEO adsorption on different oxides is influenced by the PZC oxide and also considerably influenced by hydrogen bonding; optimum hydroxylation is required on the oxide surface (Koksal, Ramachandran, Somasundaran, & Maltesh, 1990).

PEO is used to flocculate clay suspension (Lapcik, Alince, & Van de Ven, 1995) and is frequently used in the mineral/mining industry, for flocculation and sludge dewatering of alumina, silica, and iron-based particles (Kumar, D., Jain, & Rai, 2018; Mpofu et al., 2003) and flotation of quartz particles (Gong et al., 2010). It is also used as a bridging agent in the pulp and paper industry (Van de Ven, Qasaimeh, & Paris, 2004). Polyvinyl alcohol (PVA) and polyvinyl pyrrolidone (PVP), also nonionic, have similar aggregation behaviors to PEO, namely, adsorption of non-polar polymer segments on more hydrophobic surfaces (Gregory & Barany, 2011).

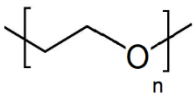

Figure 2.4: Polyethylene oxide (PEO).

Polyethylene imine

Polyethylene imine (PEI; Figure 2.5) can be polymerized using amines (≅ 1000–1400; Radhakrishnan et al. (2018)), as a linear or highly ramified structure (formed of primary, secondary, and tertiary amines). Its cationic CD varies as a function of pH: from 0% to 100% for respective pHs of 12 and 2 (Ong, Leong, & Chen, 2009). This polymer conserves a slightly cationic CD of 10% (*i.e.*, percent of amine groups that are still positively charged) even in very alkaline conditions (pH 10; Mészáros, Thompson, Bos et De Groot (2002); Suh, Paik et Hwang (1994)). In this study, the multiamine pKa range was from 9.7 to 10.7; therefore, this polyelectrolyte has the possibility to simultaneously conserve an expanded polymer chain configuration (due to intra-repulsive cationic forces in the branched polymer; Avadiar, Leong et Fourie (2014)) and to aggregate negatively charged colloids through electrostatic adsorption under a wide range of pHs. It has been shown that PEI is very efficient to flocculate negatively charged bentonite under a wide range of pHs (Öztekin, Alemdar, Güngör, & Erim, 2002); however, PEI typically has a smaller MW than PAM or PAA (only 7.5×10^5; Mészáros et al. (2002), and is thus instead classified as a moderate-MW polymer.

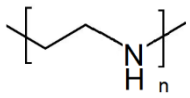

Figure 2.5: Polyethylene imine (PEI).

Polyvinyl alcohol

The linear structure of polyvinyl alcohol (PVA; Figure 2.6) is composed of copolymers of vinyl alcohol and vinyl acetate. However, the high density of hydroxyl groups on its structure can lead to a more cross-linked configuration (Miguez-Pacheco, Misra, & Boccaccini, 2014). This polymer is extensively used for the flocculation of many mineral oxides (Chibowski, Paszkiewicz, & Krupa, 2000; Duman, Tunç, & Çetinkaya, 2012; Sjöberg, Bergström, Larsson, & Sjöström, 1999) to improve settling effectiveness (Chang, Gupta, & Ryan, 1992). Similarly to PAM-kaolin systems (Besra, Sengupta, Roy, & Ay, 2003) and PAA-aluminum oxide systems (Santhiya, Subramanian, Natarajan, & Malghan, 1999), interparticle bridging behaviors in presence of nonionic PVA is

essentially due to hydrogen bonding, for example with silanol groups in the case of a silica surface. (Labidi & Djebaili, 2008; Pattanayek & Juvekar, 2002).

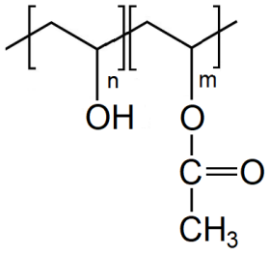

Figure 2.6: Polyvinyl alcohol (PVA) formed by the copolymerization of vinyl alcohol and vinyl acetate monomers.

Polyvinyl sulfonic acid and polystyrenic sulfonic acid

Polyvinyl sulfonic acid (PVSA; Figure 2.7A) can be prepared by polymerizing ethylene sulfonic acid, while polystyrenic sulfonic acid (PSSA; Figure 2.7B) can be prepared by sulfonation of polystyrene or polymerization of styrenic sulfonic monomer using acid or sodium salts (Tripathy & De, 2006). Sulfonic groups can be added onto a typical polymer backbone: PAM, PAA, or PEI. Polyelectrolytes with sulfonic acid groups are able to conserve their CD even at very low pH (Paneva et al., 2006; Tripathy & De, 2006; Wassmer et al., 1991), while anionic flocculant with carboxylic groups are subjected to CD decrease when pH is near or under 4.5. Such sulfonic flocculants are of interest for drinking water applications, notably when coagulation-flocculation must occur under acidic conditions, such as during enhanced coagulation with ferric salts at low pH of 4.5–5 to maximize humic substances removal (Volk et al., 2000).

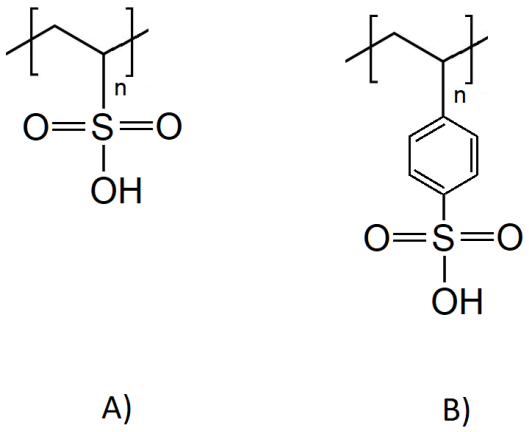

Figure 2.7: Polyvinyl sulfonic acid (PVSA) (A) and polystyrenic sulfonic acid (PSSA) (B).

Polyvinyl phosphonic acid

Due to their high anionic CD, polyvinyl phosphonic acids (PVPAs; Figure 2.8) are efficient when used as sequestering agents (Bolto, 1995) or for the removal of positively charged species such as iron oxides (Durmus et al., 2011). Similarly to the sulfonic groups mentioned in the previous section, phosphonic groups can be added to conventional polymers such as polyethylene (Molyneux, 2018). Moreover, the CD of PVPA is not influenced by pH, since the pK_1 of phosphonic groups is typically lower than 3 (Franz, 2001) and is only around 1–2 when naturally present on amylopectin (Järnström et al., 1995). Such anionic polyelectrolytes can also be used to adsorb positively charged compounds such as cationic proteins, biopolymers, or some colloids (Choi, Lee, Kim, Kim, & Lee, 2006).

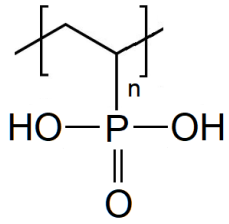

Figure 2.8: Polyvinyl phosphonic acid (PVPA).

2.5.2 Natural flocculants

Since the early 1990s, bio-sourced polymers have very often been proposed as an alternative to synthetic polymers (Kawamura, 1991; Wang, D., 2018). They offer a certain number of advantages over conventional polymers such as PAM or PAA: they are produced from renewable organic biomass, inexpensive, biodegradable, non-toxic, allow the reuse of sludge as agriculture fertilizer, and others. Bio-sourced polymers, also partially composed of ionizable groups such as carboxyl, have thus also been presented as economical and flexible alternatives to some synthetic polyelectrolytes (Sharma et al., 2006). Nonetheless, in many cases, higher dosages are required to reach equivalent performance with synthetic polymers (Bolto & Gregory, 2007; Lapointe & Barbeau, 2017; Singh, Ram Prakash et al., 2013) and their storage time is lower due to their instability and possible biodegradation (Tripathy & De, 2006).

Starch

Starch polymers are composed of two main glucose polymers: amylose and amylopectin. Depending on the amount of amylopectin (Figure 2.9B), starch adopts a more branched structure compared to other synthetic polymers such as PAM and PAA. Amylose (Figure 2.9A) is naturally of a lower molecular weight than amylopectin (10^4–$6x10^4$ g/mol) and presents a more linear structure (Buléon, Colonna, Planchot, & Ball, 1998); however, amylose with higher MW of 10^6 g/mol was reported in Vanier et al. (2017). Its levels can vary from 25%–95% depending on the starch's botanical origin (Masina et al., 2017; Pal, S., Mal, & Singh, 2005). Amylopectin typically offers a larger backbone of $5x10^4$–10^7 g/mol; also, larger molecules of 10^9 g/mol (see Table 2.2), corresponding to approximately 50,000 polymerized glucose units, were measured by Pérez, S., Baldwin et Gallant (2009). Hydroxyl is the only polar group available in the chain (*i.e.*, without carboxylate, phosphate and amino acid groups) and is expected to interact with $Me(OH)_x$ via hydrogen bonding (Laskowski, Liu, & O'Connor, 2007). However, a native starch polymer can acquire an anionic CD after a carboxymethylation procedure (Masina et al., 2017; Parovuori, Hamunen, Forssell, Autio, & Poutanen, 1995). During that process, hydroxyl groups are replaced by less polar, anionic carboxymethyl groups (Lawal et al., 2009). This carboxymethylation process can also be accomplished by the oxidation of starch with conventional oxidants such NaOCl (most

employed), O_3, and H_2O_2 (Vanier et al., 2017). A starch backbone can also be cationized when combined with trimethyl ammonium chloride (Pal, S. et al., 2005).

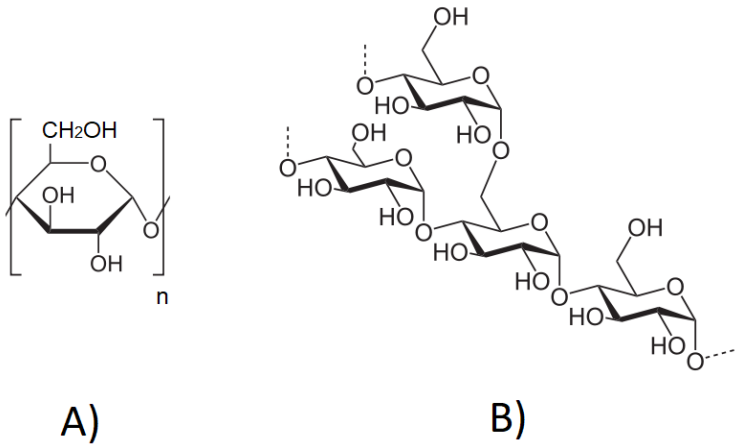

Figure 2.9: Amylose monomer (A) and amylopectin (B) branched structure.

When used as a flocculant, the anionic CD induced on the polymer structure is of importance in order to adopt and maintain an extended polymer chain configuration during aggregation (Bolto & Gregory, 2007). The MW is also an important factor allowing particle bridging. For this reason, the degree of oxidation must be adequately controlled to reach an adequate CD, but without causing partial depolymerization of amylopectin/amylose (Vanier et al., 2017). Starch reaction rate with hypochlorite is considerably influenced by pH, temperature, reaction time (Sánchez-Rivera et al., 2009; Sangseethong, Lertphanich, & Sriroth, 2009), and sodium hypochlorite concentration (Sánchez-Rivera, García-Suárez, Del Valle, Gutierrez-Meraz, & Bello-Pérez, 2005). The starch's origin (*e.g.*, potato, corn, rice) is also known to have an influence on the final oxidized polymer configuration and CD (Kuakpetoon & Wang, 2001). Under the same oxidation conditions (NaOCl, 0.8%-2% w/w), Kuakpetoon et Wang (2001) observed a higher carboxyl content when a potato-starch-based polymer was used than with rice- or corn-based polymers.

In general, starch requires higher dosage compared to synthetic polymers (*e.g.*, PAA or PAM): to achieve equivalent settled water turbidity, starch dosage must be 3–4 times higher than PAM (Gaid & Sauvignet, 2011). The same ratio was reported by Shogren, Randal L. (2009) when comparing a phosphorylated maize starch (3–4 ppm) with a polyacrylamide-co-acrylic acid (1 ppm) during kaolin aggregation, and a similar ratio of 4–5 was reported by Lapointe et Barbeau (2015) for 3–20-NTU surface waters. However, under more aggressive flocculation conditions, the ratio

starch/PAM dosage to reach similar performance regarding particle removal can be higher than 10 (Lapointe & Barbeau, 2017). This lower performance of starch is likely attributable to its lower MW, notably when compared to very-high-MW PAM. Nevertheless, other flocculation systems could employ simultaneously both polymer types, synthetic and natural, in a dual-polymer system. Synergistic effects have been gained by combining starch and PAM; a study by the present authors demonstrated that approximately 70% of PAM dosage can be replaced by starch without affecting turbidity removal (Lapointe & Barbeau, 2017).

Since the 1990s, many other applications of starch-based flocculants have been reported, including aggregation-flotation of iron-based particles for mining applications (Peres & Correa, 1996; Weissenborn, 1996) and settling improvement of anionic silica particles (Pal, S. et al., 2005). In this latter study, the authors reported an equivalent solids removal performance when compared with a synthetic commercial cationic PAM at equivalent dosage.

Chitosan/chitin

Chitosan (Figure 2.10B) is a polyaminosaccharide produced from partially deacetylated chitin (Figure 2.10A) (Bolto, 1995; Renault, Sancey, Badot, & Crini, 2009), the latter being extracted from the exoskeletons of shrimp, crab, and other shellfish (Jaafari, Ruiz, Elmaleh, Coma, & Benkhouja, 2004). Typically, the degree of *N*-acetylation of chitin from crab or shrimp shells is approximately 0.90–0.95 (Kurita, 2006), but the product can be fully deacetylated under alkaline conditions with sodium hydroxide (Domard & Rinaudo, 1983; Kurita, 2006). The degree of acetylation also influences the solubility; completely deacetylated chitosan is more soluble in acidic conditions (pH between 2 and 6.5), while highly acetylated chitin is more soluble in neutral and alkaline conditions (Seyfarth, Schliemann, Elsner, & Hipler, 2008)

After deacetylation and when used under acidic conditions (*i.e.*, reported pKa of 6.2–6.7; Kasaai, Arul et Charlet (2000)), cationic adsorption sites are carried by chitosan due to the protonation of its amino groups (Jaafari et al., 2004). Due to electrostatic affinity, chitosan is hence able to simultaneously remove dissolved organic carbon (DOC) and, with its moderate-to-high MW, increase floc size (Szyguła, Guibal, Palacín, Ruiz, & Sastre, 2009; Zeng, Wu, & Kennedy, 2008). Apart from cationic amino groups, chitosan chain adsorption leading to interparticle bridging can also occur through hydrogen bonds (Guibal & Roussy, 2007; No & Meyers, 2000; Renault et al.,

2009). Similar to cationic PAM, chitosan is able to aggregate anionic soluble compounds (through electrostatic affinities) and simultaneously flocculate particulate matter through interparticle bridging mechanisms. However, the protonation of amino groups (*i.e.*, the effective CD of the chitosan polymer chain) is influenced by pH (Bolto, 1995). Bagheri-Khoulenjani, Taghizadeh et Mirzadeh (2009) reported a linear relationship between CD and degree of deacetylation. The polymer's viscosity and solubility, the latter also influenced by MW, are likewise controlled by the level of deacetylation (Renault et al., 2009; Rinaudo, 2006).

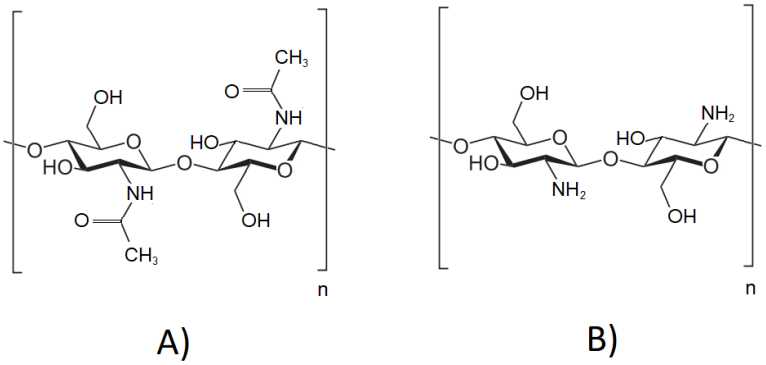

Figure 2.10: Chitin (A) and chitosan (B) structure.

Chitosan has been studied in the past for solid–liquid separation in drinking and wastewater applications: removal of kaolin and bentonite (Wang, S. et al., 2015), nitrate (Jaafari et al., 2004), metal ions (*e.g.*, Al^{3+}, Zn^{2+}, Cr^{3+}, Hg^{2+}, Pb^{2+}, and Ca^{2+}) (Bassi, Prasher, & Simpson, 2000; Zeng et al., 2008), and humic acid and algae (Bratskaya, S. Y., Avramenko, Sukhoverkhov, & Schwarz, 2002; Pérez, L., Salgueiro, Maceiras, Cancela, & Sánchez, 2016; Yang, Z. et al., 2014). It can also be used for sludge conditioning (Dongowski, 1990) and to improve clarification of pulp and paper industry effluent (Nicu, Bobu, Miranda, & Blanco, 2012). For some drinking water applications, it has been shown that chitosan combined with bentonite achieved similar NOM and turbidity removals to alum combined with polyacrylamide (Bolto, 1995).

Cellulose-based flocculant

Cellulose-based polymers are β-(1,4)-linked polysaccharides that are very similar to amylose composing starch polymers, the latter being a α-(1,4)-linked polysaccharides. This configuration allows starch to be more soluble in water. In contrast, cellulose is insoluble due to a series of

parallel glucose chain linkages caused by hydrogen bonding. However, carboxymethyl cellulose (CMC; Figure 2.11) is hydrosoluble and can be obtained by strictly controlled carboxymethylation of cellulose with sodium chloroacetate in alkaline conditions (Barba, Montané, Rinaudo, & Farriol, 2002).

According to Baar, Kulicke, Szablikowski et Kiesewetter (1994) and Heinze (1998), since the hydrogen atom in the cellulose hydroxyl group is replaced by a carboxymethyl substituent, CMC should be considered a negatively charged polyelectrolyte for pH higher than 4. CMC is hence an anionic soluble derivative from cellulose with attached carboxymethyl groups on the glucose monomer units (Gajdziok et al., 2015). CMC solubility depends on the degree of substitution and the etherification conditions (Barba et al., 2002). Generally, it is reported that increasing the degree of substitution increases solubility but also simultaneously degrades polymers (*i.e.*, MW is reduced). In Barba et al. (2002), respective CMC and MW of 328,700 g/mol and 277,900 g/mol were measured after increasing the degree of substitution from 0.95 to 2 (*i.e.*, after 1 etherification vs. 2). Alternatively, Kulicke, W.-M. et al. (1996) reported that sulfoethylated cellulose-based flocculant can reach relatively good solubility despite a low degree of substitution of 0.3, which limits the MW reduction.

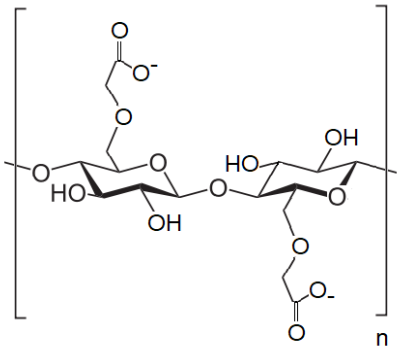

Figure 2.11: Carboxymethyl cellulose (CMC) structure.

CMC was reported effective when used as a selective flocculant for recovery of iron-based particles such as hematite (Kumar, D. et al., 2018; Praes, de Albuquerque, & Luz, 2013). Other similar polyelectrolytes, such as guar gum extracted from *Cyamopsis tetragonoloba* and linearly composed of β-(1,4)-linked mannose with branched (1,6)-linked glucose units at approximately every second mannose, are effective for alumina and iron particle aggregation (Jain, Tammishetti, Joshi, Kumar, & Rai, 2017). Xanthan gum, a microbial polysaccharide, is likewise promising for flocculation

applications because of its very high possible MW ($2x10^7$; García-Ochoa, Santos, Casas et Gómez (2000)).

Other polysaccharide-based flocculants

Other polysaccharide-based natural flocculants are currently used: pectin, pullulan, alginate, etc. Some of those biopolymers can be extracted from bacterial culture and present interesting properties for wastewater clarification: they are highly biodegradable, non-toxic, and compatible with existing biomass, and can be produced *in situ* and reach high MW ($>10^6$ g/mol). In optimal oxygenation conditions and temperature, a bioflocculant largely composed of polysaccharides (85%) with a MW of $1.8x10^6$ g/mol was obtained from a *Klebsiella* sp. culture (Shahadat et al., 2017). The chemical structure and the possible applications of polysaccharide-based flocculants have been discussed by many researchers (Cheng, K.-C., Demirci, & Catchmark, 2011; Ho, Norli, Alkarkhi, & Morad, 2009; Lee, K. Y. & Mooney, 2012; Salehizadeh, Yan, & Farnood, 2018). Their possible MW, CD, and some of their advantages and disadvantages are mentioned in Table 2.2. Similarly to starch and CMC, polysaccharide bio-based flocculants have good potential in aggregation system due to hydrogen bonding via hydroxyl groups and/or through electrostatic interactions (Yang, J.-S., Xie, & He, 2011), depending on the proportion of carboxymethyl groups.

2.5.3 Natural-*graft*-synthetic polymers

The literature shows that some combinations of synthetic and natural polymers, such as polysaccharide-*g*-PAM, offer better flocculation performance than synthetic or natural polymer used alone (Biswal & Singh, 2004; Rath, S. & Singh, 1997; Singh, Ram Prakash et al., 2000; Tripathy et al., 1999). Many advantages are gained from grafted/copolymerized synthetic-natural polyelectrolytes: they are more soluble, have higher MW than natural polysaccharides, feature adapted CD for selective flocculation, are more stable or more biodegradable, etc.

In many cases, such hybrid alternatives offering moderate biodegradability are expected to combine the advantages of natural and synthetic polymers (Yang, Z., Yang, Jiang, Cai, et al., 2013). However, preparation conditions, such as the MW of grafted polymer chains and the polymerization initiation conditions, can be critical for some flocculants and are discussed later in this section. With optimal preparation and polymerization conditions (*e.g.*, type of initiator and

concentration, pH, monomer concentration or initial MW of the grafted chain), grafted copolymers can reach relatively high MW (near 10^7 g/mole in some cases) and hence can be used as alternative bridging agents to improve gravitational separation. Current applications, new preparation methods, and chemical modifications of some increasingly used polysaccharide-*g*-synthetic polymers are presented in this section. Some examples of grafted polymers are also presented in Table 2.3, although many other combinations of NGSP are possible.

Starch-*graft*-acrylamide polymer

Grafting side-chains of acrylamide (or acrylamide-acrylic acid) onto a starch backbone is possible in the presence of a redox initiator such Ce^{+4} (Butler, Hogen-Esch, Meister, & Pledger Jr, 1983). Such ceric ions normally induce an oxidation reaction and radicals on the polymer backbone are formed. Cerium ions are the most common initiator for such type of copolymerization system and was elaborated by Mino et Kaizerman (1958). Butler et al. (1983) produced a starch-acrylamide (Figure 2.12; from Shogren, R. L., Willett et Biswas (2009)) water-soluble polymer with a MW as high as $5x10^6$. The same authors also reported a very high MW of $2x10^7$ achieved in optimal polymerization conditions.

Aggregation performance and turbidity removal were shown to be influenced by the size, not the amount, of the grafted PAM chain (Rath, S. K. & Singh, 1998). Those authors also confirmed that bridging mechanism was involved during aggregation via high-MW grafted PAM. In contrast, increasing the amount of PAM chain onto the amylopectin backbone could lead to an inappropriate CD and hence, to particles restabilization (kaolin resuspension). The starch-*g*-PAM polymer CD essentially depends on the amount of grafted PAM chain onto starch, the carboxymethylation conditions (if any), and the composition of PAM chain (*i.e.*, exclusively composed of acrylamide homopolymer or composed of copolymers of acrylamide and acrylic acid).

Some authors successfully copolymerized acrylamide with starch (amylopectin and/or amylose) for the aggregation of kaolin suspension. Rath, S. et Singh (1997) achieved an 80% turbidity removal with an amylopectin-*g*-PAM with a dosage lower than 0.1 mg/L. It was also reported by the same authors that amylopectin-*g*-PAM was more efficient than its analogue amylose-*g*-PAM, amylopectin typically having longer effective chain length and higher MW than amylose (Pal, S.

et al., 2005). Starch-acrylamide copolymers were also described as effective for hematite selective flocculation for mineral applications (Zhang et al., 2018).

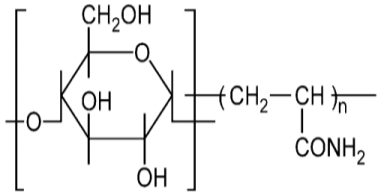

Figure 2.12: Starch-*g*-polyacrylamide structure.

Carboxymethyl cellulose-graft-acrylamide polymer

Copolymerization of acrylamide with carboxymethyl cellulose (Figure 2.13; from Yang, F., Li, He, Ren et Wang (2009)) is also possible by using a similar ceric-ion-initiated solution polymerization protocol, (Deshmukh, Sudhakar, & Singh, 1991) which allows for the formation of radicals by oxidative reactions (Okieimen, 2003). Okieimen (2003) reported that optimal polymerization conditions were obtained at 29°C, with a contact time of 30 min (between the ceric initiator and the cellulose backbone) and for a polymerization period of 120 min. Relatively high MW can be obtained by grafting PAM onto CMC: $3.22x10^6$ (Biswal & Singh, 2004). Yang, F. et al. (2009), with an ammonium persulphate/sodium sulfite redox system as an initiator and under optimal conditions (initiator concentrations: 300 mg/L; monomer concentrations: 20%; acrylamide/CMC ratio of 4; pH of 8) were able to produce CMC-*g*-PAM copolymers with a MW of $7.5x10^6$. For this study and for pH above 4, it is anticipated that CMC-*g*-PAM was negatively charged via anionic carboxymethyl and/or carboxyl groups.

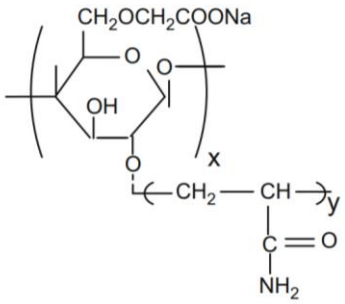

Figure 2.13: Carboxymethyl cellulose-*g*-polyacrylamide structure (CMC-*g*-PAM).

Among different polymer combinations (amylopectin-PAM, amylose-PAM or PVA-PAM), an hydroxyethyl cellulose-*g*-PAM was the most efficient for kaolin flocculation and exhibited the best sedimentation rate (Miyata, Sakata, & Senju, 1975). Its improved performance in comparison with other grafted polymers was attributable to its linear and extended cellulose backbone and its capacity to adsorb particles through interparticle bridging. Such polysaccharide-*g*-PAM flocculant was also successfully used for the textile industry as coagulant aid (Sanghi, Bhattacharya, & Singh, 2006). For the removal of silica in suspension, Biswal et Singh (2006) reported that very low dosage of a CMC-*g*-PAM (<0.3 mg/L) removed about 75%–80% of the initial turbidity. The same authors also reported successful applications of CMC-*g*-PAM having a MW of $2.8x10^6$ for kaolin and iron ore aggregation.

Starch-*graft*-polyacrylic acid polymer

Similarly to starch-*g*-polyacrylamide, a combination of starch and acrylic acid (Figure 2.14; from Zhu, Z. et al. (2009)) can be copolymerized with a ceric initiator. In the case of acrylic acid monomer, based on optimal polymerization conditions established by Athawale et Rathi (1999), a lower concentration of Ce^{4+} initiator was required compared to acrylamide monomer. Relatively high MWs of $3x10^6$ g/mol and higher were observed by Gugliemelli, Ollidene et Russell (1968).

Yu, Wei et al. (2018) reported producing a starch-*g*-PAA with ammonium persulfate as initiator (acrylic acid polymerization over 3 hours at 55°C) able to bridge particles due the to the presence of anionic carboxyl groups and hydrogen bonding. However, for the treatment of wastewaters from the textile industry, a starch-*g*-PAA offered sufficient aggregation performance, although it was less efficient than conventional acrylamide and acrylic acid copolymers (Jiraprasertkul, Nuisin, Jinsart, & Kiatkamjornwong, 2006). In the study of Jiraprasertkul et al. (2006), ammonium persulfate and tetramethylethylenediamine were used as initiator and coinitiator, respectively. The higher performance of acrylamide and acrylic copolymers can be partially be explained by hydrogen bonding interaction with the amide groups; nevertheless, Khalil et Aly (2002) reported smaller required dosages during flocculation for starch-*g*-PAA compared to carboxymethylated starch for pH between 6 and 8. By increasing the grafted percentage of PAA, and hence also increasing negative adsorption sites on the starch backbone, starch-*g*-PAA can be successfully used

to aggregate heavy metals such as Pb^{2+} and Cu^{2+} by an electrostatic interaction followed by bridging mechanisms (Güçlü et al., 2010; Keleş & Güçlü, 2006).

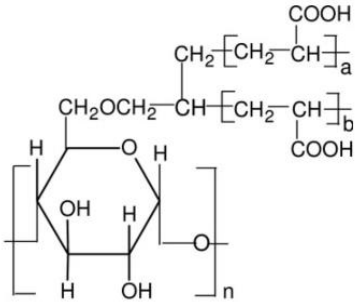

Figure 2.14: Starch-*g*-polyacrylic acid structure.

Other synthetic-*graft*-natural copolymers

Many other NGSP have been identified as promising alternative flocculants. Adhikary et Singh (2004) copolymerized a xanthan-*g*-PAM flocculant able to efficiently remove turbidity from an iron ore suspension. In combination with polyaluminium chloride (PAC), Wan, Li, Wang, Chen et Gu (2007) used a copolymerized guar gum–*g*–PAM of high MW ($6x10^6$ g/mol) to clarify high-turbidity wastewater (>4500 NTU; removal of 99%); the same authors reported turbidity removal of only 78% when guar gum was used in the same conditions. Laurienzo, Malinconico, Motta et Vicinanza (2005) successfully grafted alginate and polyethylene glycol (PEG). Their polymerization strategy allowed them to graft a significant amount of PEG, but the flocculant produced was only of low-to-moderate MW: $2x10^5$ g/mol. Higher MW was reported by Tripathy et Singh (2001); in their study, alginate was grafted with PAM rather than PEG, which allowed the formation of a higher MW: $1.4–2.5x10^6$ g/mol.

Finally, another type of copolymerized flocculant, a chitosan-*g*-PAM, was detailed in Yang, Z., Yang, Jiang, Cai, et al. (2013), the latter having the great advantage of offering anionic (via carboxyl groups on PAM) and cationic (via NH_3^+ groups on deacetylated chitosan) adsorption sites for the (selective) flocculation of surface waters or industrial waste waters (Song, H. et al., 2009). Such anionic-cationic flocculants would offer the possibility of adsorbing positively charged heavy metal on grafted PAM chains and simultaneously anionic NOM on the chitosan backbone. Yang, Z. et al. (2012) also found better turbidity removal in acidic and neutral pH condition with a

chitosan-*g*-PAM than in alum, PAM, or PAC used alone. Depending on the ratio of chitosan to acrylamide monomers, such flocculants can act as both primary coagulant and flocculant. Such dual functionality of starch-*g*-PAA used as flocculant for coagulated wastewater with PAC was also reported by Du, Q., Wang, Li et Yang (2018). This specific starch-*g*-PAA was used as a conventional flocculant acting via an interparticle bridging mechanism, and simultaneously as a calcium carbonate scale-inhibiter.

2.6 Synthetic, natural, or natural-*graft*-synthetic flocculant?

The following tables list the major advantages and drawbacks of different synthetic, natural, and natural-*g*-synthetic flocculants. It is assumed that only moderate-to-very-high-MW polymers are likely to improve aggregation via bridging mechanisms; hence, only flocculants with such characteristics are enumerated. The synthetic and natural MW flocculants listed in Tables 2.1 and 1.2 are also summarized in Figure 2.15 as a function of CD. In the case of neutral surface water coagulated with a metal salt, PAM, starch and PEO present adequate MW ($>10^6$ g/mol) and CD (<2 meq/g) for interparticle bridging flocculation (marked up in the yellow square). However, PEO is naturally nonionic and hence more likely to adopt non-extended chain conformation. Moreover, due to amide and carboxyl groups, PAM chains can be linked together by hydrogen bonding, which increases the number of attachment points compared to PEO (Botha et al., 2017). Consequently, due to its higher hydrophobicity compared to PAM, PEO is a more effective polymer for dewatering applications. Contrary to PAM and PEO, it must be mentioned that starch, largely composed of branched amylopectin, is expected to adopt a non-linear structure less favorable for interparticle bridging; in this case, polymer hydrodynamic size or root–mean–square end-to-end distance would be considered a complemental predictor of flocculant performance.

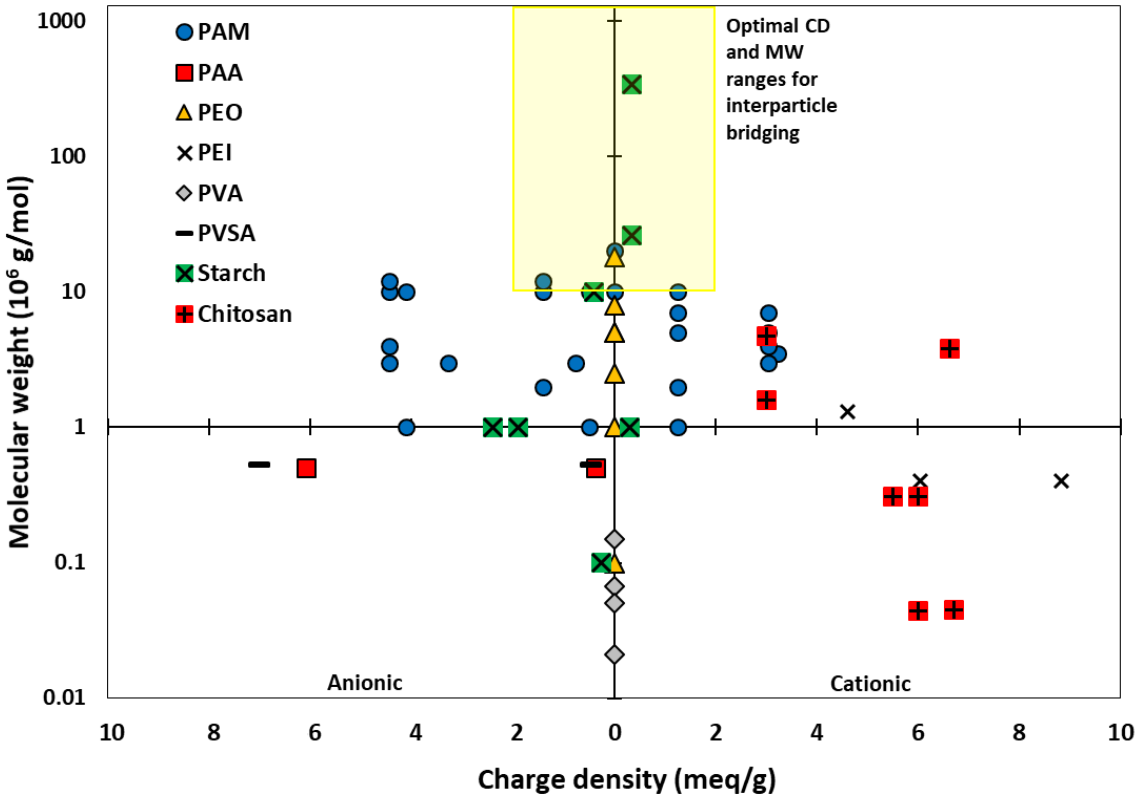

Figure 2.15: Variable molecular and charge density combinations for conventional synthetic and natural polymers, synthesized from Tables 2.1 and 2.2.

Table 2.1: Synthetic polymers characteristics and major advantages/disadvantages

	Studied molecular weight (g/mol)	Studied charge density (% or meq/g)	Advantages	Disadvantages
Polyacrylamide (PAM) or acrylamide-acrylic acid copolymers **Maximal MW:** **$2x10^7$ g/mol**	-Anionic: up to $3x10^6$ (Caskey & Primus, 1986) -Anionic: $3x10^6$–$1.2x10^7$ (Nasser & James, 2006) -Anionic: $1.2x10^7$ (Yang, Z. et al., 2012) Nonionic: 10^7–$2x10^7$ (Leeman et al., 2007) -Anionic: 10^6–10^7 (Lapointe & Barbeau, 2017) -Anionic: $2.3x10^5$–$6.2x10^6$ (Fevola et al., 2003) -Cationic: $3.5x10^6$ (Sableviciene, Klimaviciute, Bendoraitiene, & Zemaitaitis, 2005) -Cationic: $3x10^6$–$7x10^6$ (Nasser & James, 2006) -Cationic: 10^7 (Solberg & Wågberg, 2003) Anionic and cationic: more than $2x10^6$ (Samoshina et al., 2003) -Cationic: 1.7–$2.6x10^6$ (Fan, A., Turro, & Somasundaran, 2000) -Anionic: $1.2x10^7$ (Ovenden & Xiao, 2002) -Nonionic: $5x10^6$ (Tripathy et al., 1999) -Anionic: $5x10^6$ in case of acrylamide–acrylic acid copolymers (Shogren, Randal L., 2009)	-Anionic CD only influenced for pH <4.5 -Nonionic (Leeman et al., 2007) -Anionic: 5%–25% (Caskey & Primus, 1986) -Cationic: 38% (Sableviciene et al., 2005) -Anionic and Cationic: 10%–35% (Nasser & James, 2006) -Anionic: 3%–32% (Lapointe & Barbeau, 2017) -Cationic: 10% -Anionic and cationic: 10% (Samoshina et al., 2003; Solberg & Wågberg, 2003)	-Commercially available through a broad range of CD and MW. The CD is notably controlled by the amount of copolymerized acrylic acid monomers -Considered as the least expensive (very-) high-MW flocculant -Very stable mainly due to its low (bio)degradation (Satyanarayana & Chatterji, 1993) -Can reach very high MW (as high as $2x10^7$; Leeman et al. (2007)) -Very effective at low dosage (Lapointe & Barbeau, 2016, 2017) -Readily hydrosoluble -Composed of very stable amide groups in the case of anionic PAM (Bolto, 1995) -CD is not significantly influenced in neutral pH due to the presence of low-pKa functional groups (*e.g.*, carboxyl group pKa ≈ 4.5) (Namazian & Halvani, 2006; Owen, A. T., Fawell, Swift, & Farrow, 2002) -Long linear polymerized structure improving interparticle bridging (Bolto & Gregory, 2007; Nasser & James, 2006) -Can tolerate high shearing (G of $255s^{-1}$) before floc breakage (Lapointe, Brosseau, Comeau, & Barbeau, 2017) -Homogeneous CD distribution along the polymer chain -PAM chains or acrylamide monomers are not significant sources of disinfection by-products (Fielding, 1999) -Contrary to PEO or other synthetic polymers, hydrogen bonding via amide and carboxyl groups also occurs between two PAM chains (Botha et al., 2017)	-Possible pH and CD-dependent degradation of the ester links (Smith-Palmer, Campbell, Bowman, & Dewar, 1994) -Inducing cationic charge onto PAM can lead to a reduction of its MW (Krentz et al., 2006) -High-MW PAM can increase granular filter headloss (Zhu, H. et al., 1996) -Polymer toxicity (Fielding, 1999) -Monomer toxicity (Rice, 2005) -Composed of non-renewable material (Xing, Guo, Ngo, Cullum, & Listowski, 2010) -Dosage typically limited to 1 mg/L for drinking water application in North America and 0.2 mg/L in many European countries (Lapointe & Barbeau, 2017) -Some PAM of very high MW (>10^7) are hardly homogenized during solubilization/implementation -Sludge containing PAM is not allowed as agricultural fertilizer in some countries (*e.g.*, Germany; Krentz et al. (2006))
Polyacrylic acid (PAA) **Maximal MW:** **$4x10^6$ g/mol**	-Anionic: $2.5x10^5$ (Wiśniewska, M. et al., 2013) -Anionic: $2x10^3$–$4x10^6$ (Das & Somasundaran, 2003) -Anionic: 10^6 (Fan, A. et al., 2000) -Anionic: $2.5x10^5$–$4x10^6$ (Das & Somasundaran, 2004) -Anionic: 10^6–$4x10^6$ (Ravishankar et al., 1995) -Anionic: $3x10^6$–$3.5x10^6$ (Gugliemelli et al., 1968)	-Generally highly anionic due to the presence of carboxyl groups (typical pKa around 4.5–5) -Similar to other polymers with carboxyl groups, the CD is influenced by the pH (Wassmer et al., 1991) -Anionic: 2%–50% when polymerized with PAM (Tripathy & De, 2006)	-Very soluble at room temperature (Butler et al., 1983). -Very efficient in dual-polymer system (Fan, A. et al., 2000) for example, used in combination with cationic polyelectrolytes -Low degradation (Bolto, 1995) -Efficient for alumina-silica aggregation. Can be used as primary coagulant for some oxides when the aggregation pH is under the isoelectric point (Das & Somasundaran, 2003; Fan, A. et al., 2000) -Can be copolymerized with acrylamide monomer to offer a wide range of anionic CD (Tripathy & De, 2006) -Homogeneous CD distribution along the polymer chain	-Generally smaller than PAM -Can restabilize alumina–silica oxide particles under alkaline conditions (Das & Somasundaran, 2003; Wiśniewska, M. et al., 2013) -The CD mainly controlled by pH and drops near 0 for pH under 4.5–5 -CD decreases considerably in neutral–acidic conditions (Wassmer et al., 1991)
Polyethylene oxide (PEO) **Maximal MW:** **$1.8x10^7$ g/mol**	-Nonionic: $5x10^6$ (Tripathy & De, 2006) -Nonionic: $8x10^6$ (Yoon & Deng, 2004) -Nonionic: $1.8x10^7$ (Andersson et al., 2003) -Nonionic: $2.5x10^6$ (Mpofu et al., 2004) -Nonionic: 10^5–$5x10^6$ (Agarwal et al., 2009) -Nonionic: $5x10^6$ (Adachi & Wada, 2000) -Nonionic: 10^6–$8x10^6$ (Gong et al., 2010)	-Nonionic (Adachi & Wada, 2000; Mpofu et al., 2004)	-Very soluble (Tripathy & De, 2006) -MW can be easily estimated by intrinsic viscosity via a linear relation -Not considerably influenced by variation in ionic strength (Adachi & Wada, 2000) -High affinity with SiO_2 particles (Rubio & Kitchener, 1976) -Due to its higher hydrophobicity compared to PAM, PEO is more efficient for long term dewatering system and for sediments consolidation (Botha et al., 2017) -Similar to PAM, PEO is polymerized as long linear structures -Higher floc resistance to shearing compared to cationic or anionic PAM (clay suspension; Yoon et Deng (2004)) -Can reach very high MW (>10^7 g/mol; Andersson et al. (2003)) -Can be functionalized with carboxyl groups to improve the polymer chain adsorption (Botha et al., 2017)	-After solubilization, high-MW PEO can undergo auto-oxidative degradation and loss of viscosity caused by UV light, acidic conditions or by the presence of a certain metal ions, such as Fe^{3+} (Tripathy & De, 2006) -Nonionic polyelectrolyte, which can affect the polymer chain extension. Chain adsorption via electrostatic interactions is not possible -Floc resistance to shearing greatly influence by the PEO structure (Shaikh, S. M. R. et al., 2017) -In contrast with PAM, there is no amide groups available for hydrogen bonding (Botha et al., 2017)
Polyethylene imine (PEI) **Maximal MW:** **$1.8x10^6$ g/mol**	-Cationic: $7x10^4$–$1.8x10^6$ (Claesson, Paulson, Blomberg, & Burns, 1997; Gölander & Eriksson, 1987) -Cationic: $7.5x10^5$ (Avadiar et al., 2014) -Cationic: $1.3x10^6$ (Fuente et al., 2005) -Cationic: $7.5x10^5$ (Mészáros et al., 2002) -Cationic: $1.8x10^4$ (Lindquist & Stratton, 1976) -Cationic: $1.3x10^6$ (Cadotte et al., 2007) -Cationic: 10^5 (Tanaka, Ueoka, Takaki, Kataoka, & Saito, 1983) -Cationic: $6x10^5$–10^6 (Öztekin et al., 2002)	-Cationic: 26%–38% at 0.001 and 0.01 M NaCl, respectively (at pH 7; Ong et al. (2009)) -Cationic: 0%–100% for the respective pH of 12 and 2 (Ong et al., 2009) -Cationic: 0%–70% for the respective pH of 10.5 and 3 (Mészáros et al., 2002) -Cationic: 4.6 meq/g (Cadotte et al., 2007)	-Flocculation occurs through electrostatic (cationic polymer onto an anionic colloid) and bridging mechanisms (hydrogen bonding) even under alkaline conditions (up to pH 9; Lindquist et Stratton (1976) -Cationic CD was reported to be as high as 50% at pH 8–9 (Knox & Wan, 1996) and established at 10% at pH 10 (Mészáros et al., 2002) -Conserves a slightly cationic CD even under alkaline condition and can aggregate negatively charged colloids through electrostatic adsorption affinities under a wide range of pH (Ong et al., 2009) -Can also be used as primary coagulant due to its cationic CD	-Generally adopts a highly branched structure which affects the bridging mechanism (Tripathy & De, 2006) -Smaller MW (10^5; Tanaka et al. (1983)) than that of PAM (which can be as high as 10^7). -CD largely influenced by pH; CD inversely proportional to pH (Ong et al., 2009; Öztekin et al., 2002). -Cationic CD is considerably influenced by the ionic strength (Mészáros et al., 2002; Ong et al., 2009). The adsorption behaviors are hardly predictable.
Polyvinyl alcohol (PVA) **Maximal MW:** **$2.6x10^6$ g/mol**	-Nonionic: $7.7x10^5$–$2.6x10^6$ (Podzimek, 1994) -Nonionic: $6.7x10^4$ (Duman et al., 2012) -$5x10^4$ (Chibowski et al., 2000) -$2.1x10^4$ -$1.1x10^5$ (Chang et al., 1992)	-Nonionic (Duman et al., 2012; Sjöberg et al., 1999)	-Non-toxic (Duman et al., 2012) -Can destabilize clay particles despite a nonionic CD (Duman et al., 2012; Wiśniewska, Małgorzata, 2011) -Efficient for aluminum oxide flocculation (Chibowski et al., 2000) -Successfully applied to reduce sludge viscosity during hindered settling (Chang et al., 1992)	-PVA-silicate flocculation is considerably influenced by pH -Effective polymer length considerably influenced by its structure (ramified vs. linear; Podzimek (1994) -Typically low-to-moderate MW (10^4–10^6 g/mol) -Lower settling rates than higher polyelectrolytes such as PAM (Shaikh, S. M. R. et al., 2017)
Polyvinyl sulfonic acid (PVSA) and polystyrenic sulfonic acid (PSSA) **Maximal MW:** **$5.3x10^5$ g/mol**	-Anionic: $7x10^4$ (Duman et al., 2012) -Anionic: $5.3x10^5$ (Paneva et al., 2006)	-Anionic: Influenced by pH, 5%–75% (Bolto, 1995)	-Conserve their anionic CD even at low pH because of the low pKa of sulfonic acid groups (<3) (Tripathy & De, 2006) -Sulfonic groups can be grafted onto conventional high-MW acrylate or acrylamide polymers (Hoover & Butler, 1974) and on PEI (Molyneux, 2018)	-Typically of low-to-moderate MW (Paneva et al., 2006) -Crosslinking polymerization pattern or the formation of an insoluble gel can occur under inadequate sulfonating conditions (Tripathy & De, 2006) -Some sulfonic polymers can be instable (*e.g.*, instability of the sulfoethyl methacrylate monomer at the ester linkage (Bolto, 1995; Tripathy & De, 2006)
Poly (Vinyl Phosphonic Acid) (PVPA) **Maximal MW:** **$6.2x10^4$ g/mol**	-Anionic: $6.2x10^4$ (Bingöl, 2006)	-Anionic: Influenced by pH	-The CD of phosphonic polymers remains stable despite pH variation, even at very low pH (*e.g.,* 2) -Known to be non-toxic (Choi et al., 2006)	-Bridging mechanisms are affected by its low-to-moderate MW (Franz, 2001)

Table 2.2: Natural polymers characteristics and major advantages/disadvantages

	Studied molecular weight (g/mol)	Studied charge density (% or meq/g)	Advantages	Disadvantages
Starch (potato, maize, rice, wheat or cassava) **Maximal MW:** **$4x10^7$ g/mol** **$5.7x10^9$ g/mol (amylopectin)** **10^7 g/mol (amylose)**	-Cationic: $2.5–4x10^7$ (Bratskaya, Svetlana et al., 2005) -Anionic: 10^6 for amylose and as high as 10^8 for branched amylopectin (Zou et al., 2012) -Anionic: $1.5x10^5$ (Yu, Wei et al., 2018) -Anionic: $10^4–10^7$ (Salehizadeh et al., 2018) -Anionic: $10^6–10^7$ for linear amylose and $10^7–10^8$ for amylopectin (Weissenborn, 1996) -Anionic: $4.6x10^6–10^9$ for amylopectin (Shogren, Randal L., 2009) -$2.8x10^5$ for amylose and $7x10^7–5.7x10^9$ for amylopectin (Yoo & Jane, 2002) -Anionic: $<10^5$ at pH 5 and $>10^7$ at pH 7 (Meiczinger et al., 2005) -Cationic: $2.6x10^7–3.4x10^8$ (Modig et al., 2006) -Anionic: $1–4.8x10^8$ for amylopectin (Rolland-Sabaté et al., 2011) -Anionic: $5.8x10^5$ for starch and $8.7x10^5$ for a carboxymethylated starch (Sen et al., 2011)	-CD is typically controlled by the presence of carboxyl or phosphoryl groups -Anionic: 1.8 meq/g (Khalil & Aly, 2002) -Anionic: 0.065 meq/g due to the presence of carboxyl groups (Järnström et al., 1995) -Anionic: 0.4 meq/g at pH 8 and 0.2 meq/g at pH 10 for phosphorylated starch (Meiczinger et al., 2005) -Cationic: approximately 6% (Modig et al., 2006) -Anionic: 1.9 to 2.4 meq/g (Lapointe & Barbeau, 2015, 2017) -Anionic: 1.4% due to a carboxymethylation in presence of H_2O_2 (Parovuori et al., 1995) -Cationic: 0.3 meq/g	-Readily soluble (Levine, 1981) after carboxymethylation -Can reach very high MW ($>10^7$) when majorly composed of amylopectin (Pal, S. et al., 2005; Rolland-Sabaté et al., 2011; Zou et al., 2012) -Produced from renewable material -Non-toxic (Pal, S. et al., 2005; Tripathy & De, 2006) -Reduced granular filter clogging compared to conventional high-MW PAM used during flocculation (Zhu, H. et al., 1996) -CD can be modified by simple oxidation (*e.g.*, NaOCl, H_2O_2 or O_3; Vanier et al. (2017)) -No significant THM/AHA formation during chlorination (Lapointe & Barbeau, 2015) -Lower viscosity compared to PAM eases pumping -Affordable (Pal, S. et al., 2005; Sen, Kumar, Ghosh, & Pal, 2009) -CD is not significantly influenced by pH variations due to the presence of low pKa carboxyl groups (after carboxymethylation process) (Namazian & Halvani, 2006; Owen, A. T. et al., 2002) -Some starches can naturally contain phosphate groups on their amylopectin chains (Järnström et al., 1995), which confer stable and pH-independent anionic CD -Sludge containing starch can be oxidized on-site to increase biodegradability (El Halal et al., 2015)	-Normally requires carboxymethylation to induce anionic CD -Native starches are poorly soluble without carboxymethylation or phosphorylation (Shogren, Randal L., 2009) -The MW, aggregation effectiveness, and kinetic are influenced by the botanic starch source (*e.g.*, maize, potato, rice, wheat, cassava) and the ratio pf amylose to amylopectin (Krentz et al., 2006) -Easily degraded at the ether groups (Satyanarayana & Chatterji, 1993) -Limited storage time due to possible (bio)degradation -Typically, lower MW and smaller effective chain length compared to conventional synthetic PAM (Lapointe & Barbeau, 2017; Rath, S. & Singh, 1997) -Due to amylopectin chain, starch is a more branched structure than linearly acrylamide homopolymer. Its more ramified structure reduces its potential to connect aggregates via interparticle bridging (Lapointe & Barbeau, 2015) -Some starches' MW can be influenced by pH: from 10^7 to 10^6 for respective pH of 8 and 6 (Lee, J. H., Han, & Lim, 2009; Meiczinger et al., 2005) -Higher dosages are required compared to synthetic PAM (Lapointe & Barbeau, 2017; Singh, Ram Prakash et al., 2013) - MW is sensible to pH and temperature during the phosphorylation or carboxymethylation process (Dintzis & Fanta, 1996; Shogren, Randal L., 2009) -Heterogeneous distribution of the CD along the polymer chains. Amylopectin is susceptible to carry a higher content of negative charges (Järnström et al., 1995)
Chitosan/Chitin **Maximal MW:** **$4.7x10^6$ g/mol**	-$1.6x10^6–4.7x10^6$ (Huang, C., Chen, & Ruhsing Pan, 2000) -Cationic: $2.6x10^4–3.1x10^5$ (Guibal & Roussy, 2007) -Cationic: $2.2x10^4$ (Lee, M. et al., 2001) -Cationic: $4.6x10^5$ (Fan, W., Yan, Xu, & Ni, 2012) -Cationic: $5.0x10^5–2x10^6$ (Seyfarth et al., 2008) -Cationic: $10^4–1.5x10^5$ (Lavertu, Méthot, Tran-Khanh, & Buschmann, 2006) -$3.5x10^4–2.2x10^6$ (Kasaai et al., 2000) -Cationic: $4.4x10^4$ (Kamburova, Milkova, Petkanchin, & Radeva, 2008) -Cationic: $5.2x10^5$ (Wang, J.-P., Chen, Zhang, & Yu, 2008) -Cationic: $1.15x10^6$ (Laue & Hunkeler, 2006) -$8.3x10^5$ (Lu, Y. et al., 2011) -Cationic: $3.1x10^5$ (Yang, R. et al., 2016) -Cationic: $3.8x10^6$ (Wibowo, Velazquez, Savant, & Torres, 2007) -Cationic: $4.5x10^4–3.1x10^5$ (Roussy et al., 2005)	- CD is influenced by pH (amino groups pKa around 6.2–6.7; Kasaai et al. (2000)) - CD of chitosan is directly proportional to degree of deacetylation *i.e.*, amount of acetyl groups replaced by positively charged amino groups (Huang, C. et al., 2000) -Cationic: degree of deacetylation between 48% and 86% (corresponding to a CD between 3 and 6 meq/g; (Huang, C. et al., 2000; Yang, R. et al., 2016) -Cationic: 0–80% (Bolto, 1995) -Cationic: deacetylation of 85% (Kamburova et al., 2008) -Cationic: deacetylation of 73%–95% (Del Blanco, Rodriguez, Schulz, & Agullo, 1999) -Cationic: deacetylation of 90% (Guibal & Roussy, 2007) -Cationic: deacetylation of 94% (Wibowo et al., 2007) -Cationic: deacetylation of 78%–95% (Roussy et al., 2005)	-Can simultaneously be used as a primary coagulant and flocculant due to its cationic adsorption site and its high MW (No & Meyers, 2000; Zeng et al., 2008) -Low dosages are required when used as cationic polyelectrolytes removing anionic metal ions (Zeng et al., 2008) -Produced from renewable material: exoskeletons of shrimp, crab, and other shellfish (Jaafari et al., 2004) -Considered biodegradable (Bagheri-Khoulenjani et al., 2009; Jaafari et al., 2004) and non-toxic (Wang, J.-P. et al., 2008) -Biodegradable and the second most abundant biopolymer, after cellulose (Renault et al., 2009) -Reduced sludge toxicity compared to conventional synthetic polymer (Chi & Cheng, 2006; Divakaran & Pillai, 2001) -Linear relation between degree of deacetylation and CD (Yang, R. et al., 2016) -More efficient than PAM alone for the removal of kaolin under neutral–alkaline conditions due the presence of amino groups (for pH between 7 and 10; Wang, J.-P. et al. (2008))	-Compared to traditional synthetic polyelectrolytes, chitosan is more expensive (Zeng et al., 2008) -Its low-to-moderate MW and poor solubility in alkaline conditions limit applications (Lu, Y. et al., 2011) -CD and protonation of amino groups are influenced by pH (Bolto, 1995; Jaafari et al., 2004; Yang, R. et al., 2016). Cationic CD decreases as pH increases (Yang, Z. et al., 2012) -Alkaline conditions cause deprotonation of amino groups and decrease chitosan solubility (Rinaudo, 2006) -Similar to primary coagulant, overdosing chitosan used under acidic conditions can restabilize colloids -The quality and performance of commercial chitin is variable (Renault et al., 2009) -The level of deacetylation must be properly controlled to have appropriate solubility and viscosity (Kurita, 2006; Renault et al., 2009) -Must be used at pH under 6.5–6.9 (*i.e.*, under the apparent pKa of amino groups; Kurita (2006)) to (partially) conserve its cationic CD -Heterogeneous distribution of CD along the polymer chains -Solubility decreases as MW increases (Fan, W. et al., 2012; Renault et al., 2009) -Rapid degradation can occur, reducing MW (Bagheri-Khoulenjani et al., 2009)
Carboxymethyl cellulose (CMC) **Maximal MW:** **$2.1x10^6$ g/mol**	-Anionic: $2.1x10^5–2.1x10^6$ (Kulicke, W.-M. et al., 1996) -Anionic: $1.5x10^5–3.3x10^5$ (Barba et al., 2002) -Anionic: 10^5 (Baar et al., 1994) -Anionic: $2.5–7x10^5$ (Du, B. et al., 2009)	-CD can be influenced by low pH, (CMC pKa of 4.4; Song, J., Birbach et Hinestroza (2012)) -Considered anionic for pH higher than 4 (Baar et al., 1994; Heinze, 1998) -Anionic with degree of substitution of 0.7–1.2 (Du, B. et al., 2009)	-Most abundant biopolymer and biodegradable (Kumar, D. et al., 2018; Renault et al., 2009) -Unexpansive material (Nie, Liu, Zhan, & Guo, 2004) -Linear structure improving interparticle bridging -Can be used as a selective flocculant for some metal oxides (iron ore; Praes et al. (2013) -Non-toxic -Stable anionic CD for neutral pH	-Interparticle bridging limited by its MW of typically $<10^6$ (Yang, F. et al., 2009) -Flocculation performance influenced by pH (*e.g.*, for iron or silica oxides; Praes et al. (2013)) -Solubility is considerably influenced by the degree of substitution -CMC degradation is related to the increase of the degree of substitution, that is, anionic CD is inversely proportional to MW (MW reduction of 15% was observed by Barba et al. (2002))
Guar or xanthan gum **Maximal MW:** **$2x10^7$ g/mol**	-Anionic: $2x10^6–2x10^7$ (García-Ochoa et al., 2000) -Anionic: $1.2x10^6–1.8x10^6$ (Sutherland, 2001) Anionic: as high as $4.1x10^7$ when grafted with PAM (Ghorai, Sarkar, Panda, & Pal, 2013) Cationic: $6.6x10^5$ (Pal, Sagar, Mal, & Singh, 2007) -$3.2x10^6$ (Viebke & Williams, 2000) -Anionic: $2x10^6–2x10^7$ (Kumar, A., Rao, & Han, 2018)	-Anionic due to presence of grafted acetic and pyruvic acids (Şen et al., 2016) -Cationic (Pal, Sagar et al., 2007)	-Affordable (Sharma et al., 2006) -Biodegradable (Sharma et al., 2006) -Possibility of high MW between $2x10^6–2x10^7$ (García-Ochoa et al., 2000; Maier, Anderson, Karl, Magnuson, & Whistler, 1993) -Stable over a wide range of pH and temperature (Sutherland, 2001) -Unlike many anionic polysaccharides, it is soluble in its acid form at pH<3 (Sutherland, 2001) -Highly soluble even in cold water (García-Ochoa et al., 2000)	-Highly viscous even at low polymer concentrations (García-Ochoa et al., 2000) -Guar gum solubility can be drastically decreased in presence of divalent cations such as Ca2+ (García-Ochoa et al., 2000) -Guar gum from biomass growth is very sensible to the type and operation mode of bioreactor (batch vs. continuous) used during fermentation process, and to culture conditions (temperature, oxygen and nitrogen concentration) (Sánchez-Rivera et al., 2005) -Heterogeneous distribution of CD along polymer chains -Solutions have very high viscosity at low shearing (Viebke & Williams, 2000), which can lead to difficulties during pumping
Pectin **Maximal MW:** **$1.6x10^5$ g/mol**	-$1.6x10^5$ (Ho, Norli, Alkarkhi, & Morad, 2010) -Anionic: $5.7–6.7x10^4$ (Kamburova et al., 2008)	-Anionic (Kamburova et al., 2008)	-Efficient for kaolin suspension (Ho et al., 2010) -Linear structure (Salehizadeh et al., 2018)	-Typically low MW (<106) with limited interparticle connections
Pullulan **Maximal MW:** **$2x10^6$ g/mol**	-$4.5x10^4–6x10^5$ (Cheng, K.-C. et al., 2011) -Anionic: 10^6 (Shingel & Petrov, 2002) -$2x10^6$ (Lee, J.-H. et al., 2001) -$2x10^5–2x10^6$ (Wittgren & Wahlund, 1997)	-Nonionic (Cheng, K.-C. et al., 2011), but can be anionic with negative carboxyl groups (Shingel & Petrov, 2002)	-Very soluble and of low viscosity (Salehizadeh et al., 2018) -Linear structure (Salehizadeh et al., 2018) -Relatively low-MW dispersion compared to other polysaccharides (Wittgren & Wahlund, 1997) -Pullulan is notably produced from a starch solution	-Properties greatly influenced by fermentation cultivation conditions (Cheng, K.-C. et al., 2011) -Generally low-to-moderate MW ($<10^6$)
Alginate **Maximal MW:** **$4x10^5$ g/mol**	-Anionic: $3.2x10^4–4x10^5$ (Lee, K. Y. & Mooney, 2012) -Anionic: $1.1x10^5$ (Yang, J.-S. et al., 2011)	-Anionic, CD depending on carboxymethylation conditions	-Relatively low cost and low toxicity (Lee, K. Y. & Mooney, 2012) -MW can be considerably increased by grafting PAM ($2.5x10^6$; Tripathy, Karmakar et Singh (2001)) -Biodegradable and non-toxic (Salehizadeh et al., 2018)	-Low-to-moderate MW, subject to drastic decrease in presence of oxidants (Yang, J.-S. et al., 2011)

Table 2.3: Grafted synthetic-natural copolymers characteristics and major advantages/disadvantages

	Studied molecular weight (g/mol)	Studied charge density (% or meq/g)	Advantages	Disadvantages
Starch-*g*-polyacrylamide **Maximal MW:** **$6.9x10^7$ g/mol**	-Anionic: $3x10^5$–$2x10^7$ (Butler et al., 1983) -Anionic: $4.4x10^6$–$4.8x10^6$ in (Sen et al., 2011) -Cationic: $5x10^6$–$6.9x10^7$ (Krentz et al., 2006) -Anionic: higher than $3x10^6$ in the case of grafted PAM onto a central amylopectin structure (Miyata et al., 1975) -Anionic: $4.3x10^6$ and $4.8x10^6$ in a case of a carboxymethyled starch-*g*-PAM initiated with ceric ions or microwave, respectively (Sen et al., 2009)	-Anionic if PAM contains negative carboxyl groups or if starch has undergone carboxymethylation -Cationic, when combined to dimethyl diallyl ammonium chloride as cationic monomer (Cao, Zhang, Han, Feng, & Guo, 2012) -Anionic due to presence of carboxymethyl groups (Sen et al., 2011)	-Compromise between synthetic and natural polymers (Singh, Ram Prakash et al., 2000) -Can reach very high MW ($6.9x10^7$ g/mol; Krentz et al. (2006)) -Carboxymethyl starch-*g*-polyacrylamide can simultaneously remove turbidity and partially destruct cell wall of *E. coli* (Huang, M. et al., 2016) -Can acquire a wide range of CD depending on grafted PAM chain characteristics; offers possibility of intensive selective flocculation -Ecofriendly due to its high biodegradability (Sen et al., 2011)	-Optimal polymerization conditions (such as Ce^{4+} concentration, temperature, and time) depend on the type of monomer (*e.g.*, acrylamide vs. acrylic; Athawale et Rathi (1999)) -Relatively low solubility (Cao et al., 2012) -More expensive than conventional PAM -Possible ungrafting of PAM chains from starch backbone increases acrylamide discharge in the environment or in drinking water -Heterogeneous distribution of CD along polymer chains -Polymer solution starts degrading after only 48 hours (confirmed via intrinsic viscosity measurements (Sen et al., 2011))
Chitosan-*g*-polyacrylamide **Maximal MW:** **$4.8x10^6$ g/mol**	-Amphoteric: $3.1x10^6$ (Yang, Z. et al., 2012) -Cationic: $7x10^5$–$4.8x10^6$ (Laue & Hunkeler, 2006) -Cationic: higher than $8x10^5$ (Lu, Y. et al., 2011)	-Amphoteric: the global net CD depends on the ratio of deacetylated chitosan vs. acrylamide monomers -Considered as nonionic at its isoelectric point (5–7; Yang, Z. et al. (2012) -Cationic: 2.51–4.77 meq/g, CD obtained by grafting quaternary ammonium cationic monomers onto chitosan (Laue & Hunkeler, 2006)	-If amphoteric, it offers anionic (via carboxyl groups on PAM) and cationic (via NH3+ groups on deacetylated chitosan) adsorption sites for broader types of contaminants -Can simultaneously act as primary coagulant and flocculant, depending on the chitosan to acrylamide monomers ratio -In acidic and neutral pH, chitosan-*g*-PAM is more efficient than PAM, alum, or poly-aluminum chloride used alone for turbidity removal (Yang, Z. et al., 2012) -Lower dosages are required to remove turbidity by settling (kaolin suspension; Laue et Hunkeler (2006)	-Main aggregation mechanism (electrostatic interaction vs. bridging) is hardly predictable in neutral-transitional conditions -Less soluble than conventional acrylamide-acrylic acid copolymers -More expensive than PAM due to required preparation conditions (initiation with ceric ions followed by 3 hours of reaction at 30°C; Laue et Hunkeler (2006) -If amphoteric, heterogeneous distribution of anionic and cationic CD along polymer chains; the adsorption kinetic is harder to estimate by models
Carboxymethyl cellulose-*g*-polyacrylamide **Maximal MW:** **$7.5x10^6$ g/mol**	-Anionic: $2.1x10^6$–$3.2x10^6$ (Biswal & Singh, 2004) -Anionic: higher than $3x10^6$ in the case of PAM grafted onto a central amylopectin structure (Miyata et al., 1975) -Anionic: $7.5x10^6$ with an ammonium persulfate/sodium sulfite redox system as an initiator (Yang, F. et al., 2009) -Anionic: $3.1x10^6$ (Yang, Z., Yang, Jiang, Huang, et al., 2013) -Anionic: $1.3x10^6$–$3.2x10^6$ (Biswal & Singh, 2006)	-Anionic due to the carboxymethylation of cellulose and/or due to negative carboxyl groups on PAM (Yang, Z., Yang, Jiang, Huang, et al., 2013)	-Very efficient for kaolin suspension aggregation by providing the best sedimentation rate among other grafted copolymers such starch-PAM, and PVA-PAM (Miyata et al., 1975) -Low degradation compared to starch or CMC: reduction of viscosity was observed only after two weeks at 50°C (Okieimen, 2003) -Intrinsic viscosity is less temperature-dependent than PAM (20°C –50°C; Yang, F. et al. (2009))	-Under inappropriate conditions, low efficiency and frequency of grafting can be associated with ceric ion initiator (Okieimen, 2003) -Less stable compared to acrylamide homopolymers or acrylamide-acrylic acid copolymers -Performance largely depends on grafted PAM or MW (Okieimen, 2003) -Grafting level influenced by amount of initiator, acrylamide monomer concentration, and presence of cationic ions -Heterogeneous distribution of CD along polymer chains
Guar or xanthan gum–*g*–polyacrylamide **Maximal MW:** **$6x10^6$ g/mol**	-$3.1x10^6$ (Singh, R. P., Nayak, Biswal, Tripathy, & Banik, 2003) -Cationic: 2.5–$6x10^6$ (Wan et al., 2007)	-Cationic (Wan et al., 2007), but CD is influenced by pH -The CD is influenced by the acrylamide/xanthan or guar gum monomers ratio	-Can be polymerized at temperature as low as 10°C (Wan et al., 2007) -Cationic copolymers segment are efficient for heavy metal removal (Duan, Jiacai et al., 2010)	-Adsorption behaviors are influenced by pH (Wan et al., 2007) -Similar to primary coagulation, excess dosage can restabilize particles (Duan, Jiacai et al., 2010) -Heterogeneous distribution of CD along polymer chains
Starch-*g*-polyacrylic acid **Maximal MW:** **$3.6x10^6$ g/mol**	-Anionic: $3.6x10^6$ (Gugliemelli et al., 1968)	-Anionic: similar to PAA due the presence of negatively charged acrylate groups	-Lower concentration of Ce^{4+} initiator is required compared to acrylamide monomer (Athawale & Rathi, 1999) -Can simultaneously act as scale-inhibiter and flocculant (Du, Q. et al., 2018) -Flocculation requires smaller dosages than traditional carboxymethylated starch (Khalil & Aly, 2002) -Can electrostatically adsorb and flocculate heavy metal via interparticle bridging (*e.g.*, Pb_{2+} and Cu_{2+}; Keleş et Güçlü (2006) -Grafted PAA structure can adsorb ammonia (Chen, Q. et al., 2016)	-PAM has capacity to make more interparticle connections than starch-AA via hydrogen bonding and via amide groups (Jiraprasertkul et al., 2006) -Heavy cationic metal adsorption is highly influenced by pH (Güçlü et al., 2010) -Heterogeneous distribution of CD along polymer chains
Alginate-*g*-polyacrylamide **Maximal MW:** **$2.5x10^6$ g/mol**	-Anionic: 1.4–$2.5x10^6$ (Tripathy & Singh, 2001)	-Anionic: (Tripathy & Singh, 2000)	-Relatively high MW (>10^6)	-Subject to shear degradation and biodegradation (Tripathy & Singh, 2000, 2001)
Alginate-*g*-polyethylene glycol **Maximal MW:** **$2x10^5$ g/mol**	-Anionic: $2x10^5$ (Laurienzo et al., 2005)	-Anionic	-More stable than alginate due to hydrogen bonding between PEG and alginate monomer (Laurienzo et al., 2005)	-Low-to-moderate MW (<10^6) -Heterogeneous distribution of CD along polymer chains

2.7 Conclusion

This review has compared conventionally used synthetic vs. natural flocculants by listing their MW and CD and by describing their functional groups involved during interparticle bridging. Typical applications associated with each flocculant were also discussed. For drinking water applications where a hydrolyzed metal salt acts as primary coagulant, PAM and starch polymers are the most employed polymers for flocculation systems involving interparticle bridging due to their low CD, relatively high MW, low cost, and commercial availability. However, some promising natural-*g*-synthetic flocculants such as starch-*g*-PAM and CMC-*g*-PAM, if they could be produced at acceptable cost, would offer interesting options for the water industry considering their biodegradability, reduced toxicity, and relatively high MW. More research is needed regarding polymerization methods, to ensure better polymer chain stabilization and lower premature degradation once in solution.

Acknowledgment

The authors thank the Industrial-NSERC Chair in Drinking Water (Polytechnique Montreal) research program, which benefits from the financial support of the City of Montreal, Veolia Water Technologies Canada, the City of Laval, the City of Repentigny, the City of Longueuil, and the National Science and Engineering Research Council of Canada (NSERC).

CHAPITRE 3 OBJECTIFS, HYPOTHÈSES ET MÉTHODOLOGIE

3.1 Revue critique de la littérature antérieure

La floculation lestée est mondialement utilisée puisqu'elle figure parmi les méthodes de séparation les plus efficaces en termes d'abattement de matières particulaires (>90 %; Plum et al. (1998)), de robustesse et de charge superficielle opérable (validé jusqu'à 85 m/h; MDDELCC (2018)). Depuis plus de 35 ans, plusieurs chercheurs ont décrit la performance de la floculation lestée pour des applications en eau potable, notamment en mesurant l'abattement de turbidité en fonction de la charge superficielle appliquée : 82 % à plus de 15 m/h (échelle laboratoire; Sibony (1981)), 90 % à environ 35-40 m/h (échelle laboratoire; Desjardins, Koudjonou et Desjardins (2002), 98 % à 85 m/h (échelle pilote; Levecq, Breda, Ursel, Marteil et Sauvignet (2007). Ce type de technologie a également été utilisé pour des applications en eaux usées municipales : 85 % des MES à plus de 85 m/h (échelle pilote; Plum et al. (1998)) et 70 % de turbidité à 80 m/h (Imasuen, Judd, & Sauvignet, 2004).

Il est toutefois à mentionner que les performances évaluées en fonction à la charge superficielle sont aussi tributaires des types et des doses de coagulants et floculants sélectionnés. La littérature actuelle ne décrit que partiellement l'impact du mode opératoire (*e.g.*, intensité de mélange) sur la taille des flocs. La densité des flocs lestés est également un paramètre important pour la prédiction de leur vitesse de chute (Ghanem, Young, & Edwards, 2013). Or, aucune étude ne permet de quantifier la présence de média lestant incorporé au sein de la structure du floc sur sa densité apparente, rendant impossible la prédiction adéquate de la vitesse de chute des flocs lestés. Les études mentionnées précédemment évaluent indirectement la performance de la floculation lestée par des mesures d'abattement de particules en fonction d'un temps de décantation donné. Or, cette méthode indirecte ne permet pas de différencier les impacts de la floculation par rapport à ceux de la décantation obtenus pour un temps établi; une plus longue décantation pouvant entre autres masquer les effets d'un mauvais lestage *i.e.*, une mauvaise coagulation ou floculation. La caractérisation directe des flocs lestés proposé dans le cadre de cette thèse permettrait de mieux identifier les problèmes systémiques d'un traitement à l'étude.

Dans un autre ordre d'idée, les propriétés que doit avoir un média lestant sont peu connues. Elles dépendent d'une multitude de facteurs, dont la chimie de l'eau, les types et les concentrations de

coagulants et de polymères, l'abattement de matières en suspension recherché et la charge superficielle appliquée. Les médias lestants sont principalement définis par 1) leur taille, 2) leur densité, 3) leur composition chimique et 4) leur forme. Seulement quelques études en laboratoire ont évalué l'impact de la taille du média lestant sur l'enlèvement de turbidité. Sibony (1981) et De Dianous et Dernaucourt (1991) concluaient à cet effet que l'abattement de turbidité était inversement proportionnel à la taille du média lestant. Dans l'étude de Sibony (1981), la turbidité passe de 0,8 à 2,7 UTN lorsqu'un média lestant de 80-100 µm est utilisé plutôt qu'un média de 50-63 µm. Encore une fois, les auteurs quantifiaient les performances en fonction d'un temps de décantation prédéterminé (8 min et 3 min respectivement pour les études de Sibony (1981) et De Dianous et Dernaucourt (1991)), ne tenant pas compte de l'impact d'une éventuelle hausse de la charge superficielle. En ce qui concerne les trois autres facteurs (densité, composition chimique et taille), aucune étude n'a pour l'instant clairement évalué leur impact sur la performance de la floculation lestée. Néanmoins, les avantages de la magnétite (densité : 5100 kg/m^3) appliquée en floculation lestée (SIROFLOC^{TM}) ont été détaillés par Booker, Öcal et Priestley (1996), mais cette dernière étude ne compare par les performances de la magnétite par rapport à celles du sable de silice conventionnel (densité : 2650 kg/m^3). En ce qui concerne la forme du média lestant, aucune étude n'en détaille les effets. La littérature actuelle prévoit une pénalisation de la vitesse de chute des agrégats en fonction de l'irrégularité de leur forme par rapport à une sphère (théorie des dimensions fractales; Johnson, C. et al. (1996)). Pour des flocs non-lestés (densité de 1040-1100 kg/m^3), ces auteurs mentionnent notamment que le coefficient de trainée peut réduire de 10 % la vitesse de chute estimée pour des flocs sphériques par l'équation de Stokes. Néanmoins, l'impact de la forme des flocs lestés par rapport à celui de leur densité et de leur taille n'a jamais été quantifié.

L'utilisation des polymères d'amidon comme alternative au PAM lors de la floculation lestée est aussi un sujet peu couvert par la littérature scientifique. Selon Gaid et Sauvignet (2011), pour des abattements de turbidité similaires, les doses requises d'amidon sont de trois à cinq fois plus élevées comparativement au PAM. Cet écart de performance entre les floculants naturels et synthétiques a également été rapporté par Bolto et Gregory (2007). Cependant, aucune étude n'explique comment amoindrir cet écart. Il serait probable qu'une intensité adaptée, un temps de mélange plus long, des conditions de coagulation particulières (type d'hydroxydes et pH) ou une composition chimique du média lestant plus adaptée aux polymères d'amidon puissent améliorer leur performance. De

plus, l'influence de la densité de charge des deux types de polymères en floculation lestée n'est pas abordée dans la littérature. Or, il est connu en floculation conventionnelle qu'une densité de charge optimale peut être identifiée, cette dernière étant notamment influencée par la charge des particules coagulées, la force ionique et le pH. Il est anticipé que le PZC (*point of zero charge*) du média lestant joue aussi un rôle dans le cas de la floculation lestée. Le rôle du PZC par rapport à celui de la densité et de la taille d'un média lestant n'est pour l'instant pas connu. Finalement, les mécanismes régissant les interactions simultanées entre un polymère (à base d'acrylamide ou de polysaccharides), un média lestant et des hydroxydes métalliques (un coagulant) sont peu définis dans la littérature actuelle. Les mécanismes régissant le pontage entre ces floculants et divers types de colloïdes ont été décrits plus haut au chapitre 2.

3.2 Objectifs

L'objectif principal de cette thèse coniste à évaluer la performance de polymères à base d'amidon comme alternative au PAM ainsi que celle de médias lestants alternatifs au sable de silice lors de la floculation lestée.

Spécifiquement, la thèse vise à :

1) développer une méthode permettant de mesurer simultanément la densité de floc lestés, la taille des flocs lestés ainsi que leur forme,
2) évaluer et améliorer la performance des polymères d'amidon activé comme alternative au PAM en floculation lestée,
3) mesurer les impacts différenciés de la densité, de la taille, de la composition chimique ainsi que de la surface disponible des médias lestants sur l'abattement de turbidité et sur la vitesse de chute des flocs.

Ces trois sous-objectifs entrainent un certain nombre de questions en lien avec les interactions média lestant-polymère, le taux d'incorporation du média lestant dans la structure du floc et la concentration de particules résiduelles non-décantables.

1) Quel est le taux d'incorporation du média lestant au sein de la matrice chimique (floc) pour un système donné?

2) Quel est l'impact du facteur de forme d'un média intégré au floc ou du coefficient de trainée d'un floc (adéquatement) lesté sur sa vitesse de chute?

3) Pourquoi les abattements de particules sont-ils moindres lorsqu'un polymère à base d'amidon est utilisé plutôt qu'un PAM conventionnel? Comment serait-il possible d'améliorer les performances des polymères à base d'amidon utilisés en floculation lestée?

4) Quelles seraient les conditions d'opération et les propriétés idéales du média lestant afin de maximiser les performances de la floculation?

5) Les conditions de mélange doivent-elles être adaptées en fonction de la densité du média lestant?

Les objectifs spécifiques de cette thèse considèrent les hypothèses scientifiques originales suivantes :

Hypothèse 1 : La densité, la taille et le facteur de forme des flocs lestés peuvent être obtenus par une technique de comptage par microscopie optique. Cette hypothèse a été explorée au chapitre 4. Contrairement au logiciel de caractérisation, une méthode manuelle permettrait notamment de mieux scinder et caractériser la structure du média par rapport à celle du floc.

Hypothèse 2 : En raison de son poids moléculaire moins élevé et de sa structure plus ramifiée, l'amidon forme des flocs moins résistants au cisaillement que ceux formés par l'entremise du PAM. Cette hypothèse a été explorée au chapitre 5 et ensuite vérifiée aux chapitres 7 et 8. La structure plus ramifiée de l'amidon réduit sa longueur effective en vue d'une floculation par pontage interparticulaire.

Hypothèse 3 : Des médias lestants plus denses et plus volumineux doivent être maintenus en suspension avec une énergie de mélange plus élevée, laquelle est responsable de la désagrégation (érosion/fragmentation) partielle du floc. Cette hypothèse a été vérifiée aux chapitres 8 et 9. L'intensité de mélange durant la floculation lestée doit minimalement permettre la suspension du média lestant. Le cisaillement induit sur ce média doit donc combattre la force de gravité exercée, cette dernière étant influencée par la taille et la densité du média en question. Chaque média lestant requiert donc une intensité de mélange spécifique en vue d'un abattement de particules optimal.

3.3 Méthodologie

Cette section présente les types d'eau à l'étude ainsi que les divers coagulants, floculants et médias lestants utilisés. Le reste de la méthodologie se scinde en trois volets : 1) les modifications imputées à la procédure standard répliquant l'Actiflo® en laboratoire, 2) la caractérisation des flocs lestés et 3) les indicateurs de performance de la décantation. Concernant la procédure standard simulant l'Actiflo®, elle a été modifiée pour certains volets de cette thèse notamment lors de l'évaluation des conditions de mélange optimales pour les polymères d'amidon, ces derniers étant plus impactés que le PAM par le temps et l'intensité de mélange.

3.3.1 Caractéristiques des eaux

En tout, trois eaux de surface et les eaux usées municipales de la Ville de Repentigny ont été utilisées. Pour des applications en eau potable, les eaux du Fleuve Saint-Laurent (station de production d'eau potable Le Royer; Saint-Lambert), de la Rivière-des-Mille-Îles (station de Sainte-Rose; Laval) et de la Rivière-des-Prairies (stations de Pont-Viau et Chomedey; Laval) ont été sélectionnées. Les caractéristiques principales de ces eaux de surfaces sont présentées au Tableau 3.1. Des informations complémentaires sont également présentées au Tableau 8.2 (Repentigny et Sainte-Rose).

Tableau 3.1 : Caractéristiques des eaux à l'étude

Paramètre	*Fleuve St-Laurent*	*Riv.-des-Mille-Îles Riv.-des-Prairies*	*Eaux usées, Repentigny*
Turbidité (UTN)	2 - 5	5 - 70	90 - 160
pH	7,8 – 8,2	6,8 – 7,2	8,1 – 8,5
COD (mg C/L)	2,5 – 3,5	6,5 - 7,5	200 - 230 mg/L (DBO_5)
Abs. UV (cm^{-1})	0,045 - 0,060	0,240 - 0,265	N.D.
Alcalinité (mg CaCO3/L)	75 - 85	25 - 45	280 - 320

N.D. : non disponible

3.3.2 Coagulants, floculants et média lestants utilisés

De l'alun (*ALS*, *Kemira* : 4,3 % Al^{3+}), du sulfate ferrique (*PIX* 312, *Kemira* : 12.3% Fe^{3+}), du chlorure ferrique (*Hydrex* 3255, *Hydrex* : 13,5 % Fe^{3+}) et du polychlorure d'aluminium (*PAX XL6*;

basicité de 56 %, *Kemira*: 5,3 % Al^{3+}) ont été utilisés en tant que coagulant primaire. Les divers PAM et polymères d'amidon ainsi que leur poids moléculaire et leur densité de charge respectifs sont synthétisés au Tableau 3.2. Les PAM anioniques étudiés sont des poly(acrylamide-co-acrylate), le pourcentage relatif d'acrylate par rapport au monomère d'acrylamide dictant la densité de charge. Dans le cas des polymères d'amidon, ceux-ci ont subi une carboxyméthlylation (amidon activé) et similairement au PAM, les groupements carboxyles contrôlent leur densité de charge.

Tableau 3.2 : Poids moléculaire et densité de charge des floculants utilisés

Polymère Fournisseur	*Poids moléculaire, g/mol*	*Densité de charge, meq/g (% mol)*	*Classification, anionique ou cationique*
Superfloc A-100, Kemira	N.D. (~10^7)	1,03 (7%)	poly(acrylamide-co-acrylate) : anionique
Hydrex 3511, Hydrex	1,3-1,6 x 10^7	0,42 (3%)	poly(acrylamide-co-acrylate) : anionique
Hydrex 3551, Hydrex	1,3-1,6 x 10^7	2,41 (18%)	poly(acrylamide-co-acrylate) : anionique
Hydrex 3554, Hydrex	1,3-1,6 x 10^7	4,08 (32%)	poly(acrylamide-co-acrylate) : anionique
Hydrex 3613, Hydrex	1,3-1,6 x 10^7	1,20 (10%)	poly(acrylamide-co-diméthylaminoéthylméthacrylate quaternisé) : cationique
Hydrex 3841, Hydrex	2,0 x 10^6	1,89	Amidon : anionique, issu d'une carboxymethylation
Hydrex 3842, Hydrex	2,0 x 10^6	2,40	Amidon : anionique, issu d'une carboxymethylation
Hydrex 3807, Hydrex	N.D. (~10^6)	0,30	Amidon : cationique, issu d'une réaction avec un amine quaternaire

N.D. : non disponible

Le tableau 3.3 synthétise les propriétés des divers médias lestants testés. Le gradient de vitesse (*G*) optimal a été établi en laboratoire afin d'assurer la suspension du média lestant tout en maximisant l'abattement de turbidité, le *G* spécifique d'un média lestant étant donc proportionnel à sa densité et à sa taille. Les distributions granulométriques ne sont pas présentées dans cette section puisqu'elles étaient systématiquement modifiées à l'aide de tamis (45-300 µm), soit afin de

comparer les médias lestants sur une base de taille équivalente, soit dans le but de tester l'impact de la taille sur l'abattement de turbidité (la turbidité était mesurée en fonction de diverses tranches granulométriques de média). Les distributions granulométriques propres à chaque étude sont donc présentées dans les méthodologies spécifiques aux chapitres 4 à 9.

Tableau 3.3 : Propriété des médias lestants utilisés

Média lestant	*Densité*	*Ratio moyen L/l* [1]	*Dureté (Mohs)*	*G optimal* [2] *(s^{-1})*	*Point of zero charge (PZC)* [3]
Charbon actif en grain	1,24	1,72	2,0 - 3,0	100	2,5 -12,1 (from Norit ®) (Kosmulski, 2011)
Anthracite	1,45	1,61	2,2 - 3,0	100	7
Sable de silice	2,62	1,44	6,0 - 7,0	165	< 3 (Kim & Lawler, 2005; Kosmulski, 2011)
Verre broyé	2,58	2,05	5,5 - 7,0	165	< 3 (Kosmulski, 2011)
Ilménite	3,70	1,41	5,0 - 6,0	N.D.	4,5 - 7,2 (Kosmulski, 2006)
Sable de grenat	3,93	1,93	7,5 - 8,0	215	3.5 – 4 (Kosmulski, 2011)
Magnétite	5,08	1,36	5,5 - 6,5	255	6,5 - 6,7 (Kosmulski, 2011)

1 L,l :longueur et largeur du grain considérant une forme ellipsoïdale
2 Basé sur des mesures de turbidité
3 Obtenus entre 20-25°C

3.3.3 Floculation lestée à l'échelle laboratoire

Les protocoles simulant la floculation lestée à l'échelle laboratoire sont décrits dans cette section. Pour certains essais, la procédure standard répliquant le procédé Actiflo® était employée. Néanmoins, afin de tester les divers floculants et médias lestants sous des conditions plus contraignantes, les temps de floculation et de décantation ont été considérablement réduits lors de certains essais. Cette procédure permet notamment d'estimer les temps de contact minimaux; la compacité des unités de traitement étant également un enjeu important dans l'industrie.

La procédure présentée à la figure Figure 3.1 a été développée par *Veolia Water Technologies Canada* afin de reproduire les performances de l'Actifo® à pleine échelle. Elle consiste respectivement en une coagulation (*G*: 165–385 s^{-1}), une floculation (*G*: 165 s^{-1}) et une décantation de 2, 8 et 3 min :

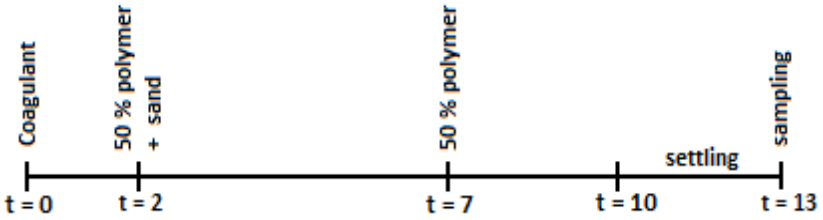

Figure 3.1 : Procédre standard répliquant l'Actiflo®, extraite de la section 5.2.

Cette procédure prévoit une injection du floculant en deux temps. Pour un polymère anionique, 50% de la dose est injectée au début de la floculation alors que l'autre 50% est injectée après 5 min de floculation (3 min dans le cas d'un polymère cationique). Cette séparation permet notamment la recroissance des flocs après leur bris ou la reconfiguration des chaines de polymères, tel qu'expliqué à la section 2.2.2 du chapitre 2 et présenté Figure A- 2 (en annexe).

Cette procédure proposant des temps d'injection ne prend pas en compte la densité de charge du floculant et des conditions de coagulation (*e.g.*, type d'hydroxydes et pH). Il a été observé que cette procédure ne pouvait être optimale et adaptée à tous les systèmes (*i.e.*, en fonction du coagulant, du polymère et du média lestant). Par exemple, la concentration de floculant, la taille et le nombre de grains lestants, le *G* et le poids moléculaire du floculant ont aussi un impact sur la cinétique d'agrégation. Conséquemment, afin d'identifier les conditions optimales pour chaque système évalué, divers temps de floculation (10 s à 8 min), de *G* (60 à 540 s^{-1}) et de temps de décantation (10 s à 4 min) ont été testés. Les effets du pH et de la densité de charge du floculant sont aussi décrits au chapitre 7.

3.3.4 Caractérisation des flocs lestés

La taille des flocs a été évaluée par microscopie optique (chapitre 4, section 4.2.4). Leur forme a été considérée comme étant ellipsoïdale et leur diamètre équivalent a été calculé à partir du volume de l'ellipse. Avec cette même méthode, le volume du média lestant pouvait être déterminé et la

densité du floc était ensuite calculée avec le ratio volume total des grains incorporés au floc/volume du floc. Le ratio longueur/largeur de l'ellipse pouvait également être calculé et inséré dans les équations de Stokes et de Newton afin de corriger la force de trainée.

3.3.5 Autres méthodes évaluant la performance de la floculation lestée

Cette section constitue une synthèse de tous les indicateurs de performance employés lors de cette thèse et présente aussi leur méthode de mesure respective. La turbidité et la taille des flocs servaient d'indicateurs principaux lors de la sélection de la concentration optimale de média lestant de même que des concentrations optimales de coagulant et de polymère. Les objectifs en termes d'abattement de turbidité sont identifiés dans chaque chapitre.

Tableau 3.4 : Indicateurs de performance de la floculation lestée

Indicateur	*Unité*	*Méthode*
Alcalinité	mg $CaCO_3$/L	SM 2320 B. (APHA, AWWA, & WEF, 2012), Titrateur électrométrique Mettler Toledo DL28
COD	mg C/L	Eau décantée et filtrée sur une membrane de 0,45 µm prélavée (PES Supor®-450 membrane; Pall) Sievers 5310c total organic carbon analyzer, GE Water, SM 5310 C. (APHA et al., 2012)
CODb	mg C/L	Eau décantée et filtrée sur une membrane de 0,45 µm prélavée (PES Supor®-450 membrane; Pall) Servais, Anzil et Ventresque (1989), (Sievers 5310c total organic carbon analyzer, GE Water)
Compte de particules	# part./mL	Compteur de particules, Brightwell Technologies, DPA-4100
Densité des flocs	-	Cellule de comptage (2 mm de profondeur, Model # 1801-G20) Caméra (Olympus DP70) Microscope optique (Olympus BX51) *Equivalent diameter method* (Lapointe & Barbeau, 2016)
Distribution de taille des flocs	µm	Cellule de comptage (2 mm de profondeur, Model # 1801-G20) Caméra (Olympus DP70) Microscope optique (Olympus BX51) *Equivalent diameter method* (Lapointe & Barbeau, 2016)
Diamètre moyen des flocs	µm	Caméra FlocCAM™, temps d'exposition de 1/1000 - 1/500 s (Lapointe & Barbeau, 2017, 2018a)

Tableau 3.4 : Indicateurs de performance de la floculation lestée (suite)

MES	mg/L	SM 2540 D. (APHA et al., 2012), filtrée sur une membrane de 0,45 µm prélavée (PES Supor®-450 membrane; Pall)
MVES	mg/L	SM 2540 E. (APHA et al., 2012), filtrée sur une membrane de 0,45 µm prélavée (PES Supor®-450 membrane; Pall)
SCV	-	Chemtrac® Systems, Inc. (ECA-2100, analyseur de charge)
SPO	µg THM/AHA/L	Méthode: Summers et al. (1996). Incubation pendant 24h à pH 8.0 et à 20oC avec une dose de Cl_2 suffisante afin de maintenir 1,0 mg Cl_2/L après 24h (*Uniform formation conditions*)
Turbidité	UTN	Turbidimètre, Hach 2100N, SM 2130 B. (APHA et al., 2012)
UVA_{254}	cm^{-1}	Eau décantée et filtrée sur une membrane de 0,45 µm prélavée (PES Supor®-450 membrane; Pall) (APHA et al., 2012)

CHAPITRE 4 ARTICLE 2 - CHARACTERIZATION OF BALLASTED FLOCS IN WATER TREATMENT USING MICROSCOPY

Cet article propose une méthode permettant de quantifier le pourcentage volumique du média lestant inclus dans la structure du floc. Elle a été publiée dans *Water Research* et permet dorénavant de calculer la densité moyenne d'un floc lesté ainsi que sa vitesse de chute. Cet article est donc présenté en amorce de cette thèse puisqu'il a été un outil incontournable venant en appui aux autres paramètres de suivi tels que la turbidité. Les impacts différenciés de la taille, de la densité et de la forme des agrégats formés sur la vitesse de chute y sont notamment mentionnés (diamètre > densité > forme). D'autres méthodes de caractérisation des flocs ainsi que leurs limites d'application ont également été présentées à la section 2.4.

Characterization of ballasted flocs in water treatment using microscopy

Mathieu Lapointe[1]** and Benoit Barbeau*[1]

[1] Industrial NSERC Chair on Drinking Water, Department of Civil, Geological and Mining Engineering, Polytechnique Montreal, Montreal, Quebec H3C 3A7, Canada

*Corresponding author e-mail: mathieu.lapointe@polymtl.ca

Abstract

Ballasted flocculation is widely used in the water industry for drinking water, municipal wastewater, storm water and industrial water treatment. This gravity-based physicochemical separation process involves the injection of a ballasting agent, typically microsand, to increase the floc density and size. However, the physical characteristics of the final ballasted flocs are still ill-defined. A microscopic method was specifically developed to characterize floc 1) density, 2) size and 3) shape factor. Using this information, probability density functions (PDF) of the floc settling velocity were calculated. The impacts of the mixing intensity, polymer dosage, microsand size and contact time during the floc maturation phase were assessed. No correlation was identified between the floc diameter, form and density PDF. The floc equivalent diameter mainly controls the settling velocity (r = 0.94), with the floc density (r = 0.26) and shape factor (r = 0.25) having lower impacts. A velocity gradient of 165 s^{-1} was optimal to maintain the microsand in suspension while simultaneously maximizing the floc diameter. An anionic high molecular weight polyacrylamide formed 1.5-fold larger aggregates compared with the starch-based polymer tested, but both polymers produced flocs of similar density (relative density = 1.53 ± 0.03). Generally, the floc mean settling velocity is a good predictor of the turbidity removal. An in-depth analysis of the floc characteristics indicates a correlation between the floc size and the largest microsand grain potentially embeddable in the floc structure.

Keywords:*Ballasted flocculation; Floc density; Floc size; Optical microscopy; Settling velocity*

4.1 Introduction

Ballasted flocculation is a separation process commonly used to remove particulate matter in diverse water treatment applications such as drinking water, storm water and industrial and municipal wastewater treatments. The process involves the injection of a ballasting agent, typically

microsand (MS), during flocculation to increase the floc density and diameter. Organic polymers with high molecular weight and low charge density are normally used as bridging agents between the flocs and MS (Desjardins et al., 2002).

Since the early 1980s, many researchers have investigated the performance of ballasted flocculation (Desjardins et al., 2002; Ghanem, A., Young, & Edwards, 2007; Lapointe & Barbeau, 2015; Plum et al., 1998; Sibony, 1981; Young & Edwards, 2000). The efficiency of separation and the quality of flocculation have only been assessed indirectly using measurements of particle counts or turbidity in settled waters. However, these techniques do not provide descriptive information concerning the floc characteristics (*e.g.*, diameter, compactness, density and shape). Such information is essential to properly model and optimize the process. This is of interest for any commercial ballasted flocculation process (*e.g.*, Actiflo®, Sirofloc® and CoMag®). Floc density, size and shape are essential parameters to determine the floc settling velocity, which is needed to predict the gravity separation (*i.e.*, particle removal). However, no study has yet evaluated the process by which the ballast media is incorporated into the flocs using experimental microscopy observations. Only theoretical predictions, based on Newton's and Stokes' laws, have been performed by Young et Edwards (2000).

Two important challenges must be addressed to control the efficiency of ballasted flocculation. First, the degree to which the ballast media is incorporated into the flocs will impact the ballast flocs settling velocity. Media incorporation in the floc increases both its size and density and hence the settling velocity (Ghanem et al., 2013). Second, the fraction of non-ballasted flocs will reduce the overall performance of the process, as this portion will have a low settling velocity and is therefore expected to be transported to the effluent. It is hypothesized that under suboptimal coagulation/flocculation conditions, poor incorporation of the ballasting media will control the performance, while under optimal coagulation conditions, the exportation of un-ballasted flocs controls the overall performance of the process.

Identifying optimal coagulation/flocculation conditions is challenging considering that many factors are expected to affect the quality of the ballasting by the media, including the agitation intensity, coagulant and polymer dosages, media ballast properties and concentrations, flocculation time, and temperature (Lapointe & Barbeau, 2015). We propose that a proper understanding of the ballasting process requires a better understanding of the quality of ballasting achieved under

variable operating conditions and that such an objective can be achieved by the use of microscopic floc characterization. The general objective of this study was to develop a technique to quantitatively evaluate the performance of floc ballasting by an external media. A standardized approach is first proposed to characterize ballasted flocs by density, size and shape. In a second step, this technique was used to study the performance of ballasted flocculation for (i) different ballasting media sizes and (ii) flocculation conditions (energy gradient, polymer type and dosage). The microscopy method has proven to be a sensitive technique for optimizing ballasted flocculation.

4.2 Materials and methods

4.2.1 Ballasting media characterization

The ballast media employed in this study was silica sand having a mean diameter of 140 µm and a size range of 45 to 300 µm. The impact of using a smaller diameter (a mean diameter of 80 µm and a grain size range of 45 to 140 µm) was also tested.

4.2.2 Floc formation

All experiments were conducted at the lab scale using either (i) surface waters from the Ste Rose water treatment plant, which is fed by the Mille-Îles River (Quebec, Canada), or (ii) municipal wastewaters from the Repentigny (Quebec, Canada) wastewater treatment plant. The Ste Rose waters exhibit a low alkalinity (40 mg $CaCO_3$/L), a neutral pH (7.0) and a moderate turbidity (5-10 NTU). The Repentigny wastewaters have a high alkalinity (150-200 mg $CaCO_3$/L), a neutral pH (7.5) and a high turbidity (90-150 NTU). Two-liter square beakers (B-Kers™, Phipps & Bird) were used to conduct jar tests at 21˚C. Velocity gradient (G) values were calculated using the Phipps & Bird chart as a function of the applied pale rotation speed. Alum ($Al_2(SO4)_3.14H_2O$) was used as a coagulant. Optimal dosages for turbidity removal (4.54 mg Al/L for the surface water and 8.18 mg Al/L for the wastewater) were identified through the following jar test procedure. Optimal coagulant dosage were also validated by streaming current measurements. Waters were flash-mixed for 2 min at 300 s^{-1}. After coagulation, the flocculant and microsand were injected according to the sequence described in Figure 4.1, which is derived from the work of Desjardins et al. (2002).Two alternative polymers were tested: Kemira A-100 (a low anionic and high molecular

weight polyacrylamide) and Hydrex 3842 (a low anionic and moderate molecular weight starch-based polymer). After flocculation, the waters were settled for 3 min. The settled water samples were collected 10 cm under the beaker surface. Turbidity measurements (Hach 2100N turbidimeter) were assessed following method 2130B from Standard Methods (2005).

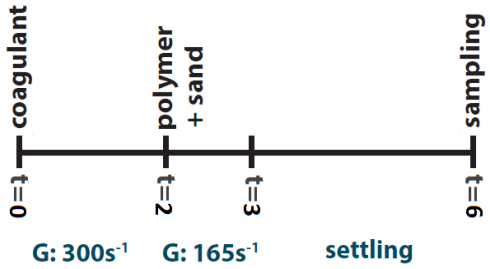

Figure 4.1: Lab-scale ballasted flocculation procedure.

4.2.3 Optical microscopy method for floc characterization

For this project, flocs could not be collected using a syringe or a peristaltic pump because settling was observed with both techniques. Samples were therefore collected during flocculation using a micropipette with a large opening (6 mm) to limit floc aggregation or breakage during sampling (Ghanem, A. et al., 2007). Samples were then placed in a modified Sedgewick Rafter counting cell (2 mm depth, Model # 1801-G20). A camera (Olympus DP70) connected to an optical microscope (Olympus BX51) was used to capture floc images (100X). The floc and microsand dimensions were assessed by an image processing software (DraftSight) with a calibrated scale. The counting cell was linearly scanned, and floc images (at least 40 flocs from 3 different sites on the cell) were captured to ensure an adequate representation of the floc distribution (procedure derived from Aguilar, Sáez, Lloréns, Soler et Ortuño (2003)). No dilution of the samples was necessary, as no floc coalescence was observed on the counting cell due to the low floc concentration and absence of mixing.

4.2.4 Calculation of floc density, diameter and shape

1) Floc diameters

Equivalent floc diameters (D_E) and microsand diameters were calculated from images obtained by microscopy considering an ellipsoidal shape. For each floc, the ellipsoidal projected area was

calculated with Equation 3.1. An equivalent diameter (D_E) was then calculated using Equation 3.2, which allows the floc size or microsand grain size calculation. A similar procedure was proposed by Johnson, C. et al. (1996).

Equation 3.1 $$A = \frac{L \cdot l \cdot \pi}{4}$$

where L: Ellipse longest dimension

l: Ellipse shortest dimension

A: Ellipsoidal projected area

Equation 3.2 $$D_E = \sqrt{\frac{4A}{\pi}} = \sqrt{L \cdot l}$$

2) Floc density

The ballasted floc density is directly linked to the fraction of the floc composed of microsand vs flocs originating from coagulated suspended solids (Equation 3.3).

Equation 3.3 $$\rho_F = \rho_{MS} \times MI + \rho_{CFM} \times (100\% - MI)$$

ρ_F: Apparent ballasted floc density

MI: Microsand incorporation (%)

ρ_{MS}: Microsand density = 2.65

ρ_{CFM}: Chemical floc matrix density (i.e., coagulant, polymer, coagulated NOM and trapped colloids) = 1.05 (Larue & Vorobiev, 2003)

Using microscopy data, the level of microsand incorporation (MI) into a chemical floc matrix can be calculated (cf. Equation 3.4) by calculating the ratio of the microsand volume with respect to the overall volume of the ballasted floc (sand + chemical matrix). As ballasted flocs can incorporate more than one microsand grain, the total volume of all *n* microsand grains is summed up.

Equation 3.4 $$MI\ (\%) = \frac{V_{microsand}}{V_{ballasted\ floc}} = \frac{\sum_{i=1}^{i=n} V_{MS,i}}{V_{floc}}$$

3) Floc shape factor

The *L/l* ratio (ellipse longest dimension/ellipse shortest dimension) was calculated to characterize the floc global geometry and evaluated the shape factor (θ). The θ parameter was derived from the Newton's equations by considering the floc as an ellipsoidal rather than a spherical particle. The shape factor is commonly used (Gorczyca & Ganczarczyk, 1996; Johnson, C. et al., 1996; Tambo & Watanabe, 1979) to lower the calculated theoretical settling velocity originating from flocs deviating from a perfect spherical geometry (Ghanem et al., 2013). For example, Ghanem et al. (2013) proposed a shape factor of 2.0 for their sand.

4.2.5 Calculation of settling velocities

The theoretical floc settling velocity can be calculated using Newton's law (as described by Johnson, C. et al. (1996)) in turbulent conditions or Stokes' law in laminar conditions (assuming that the drag coefficient is inversely proportional to the Reynolds number, i.e., $C_D = 24/Re$). In both cases, the equations require knowledge of the floc density, shape and diameter, which were obtained as described earlier. Non-ballasted floc settling velocities were calculated based on their measured sizes and on a theoretical relative density of 1.05, as mentioned in section *Floc shape factor*.

4.3 Results

4.3.1 Microscopy method repeatability

Flocs were formed using surface waters through the aforementioned jar test procedure. The repeatability of the proposed microscopy technique involved the full characterization of 80 ballasted flocs (40 flocs sampled twice during flocculation). The method repeatability was very good for evaluating floc size, relative density and shape, as these parameters had RSDs with mean values of 1.1%, 1.2% and 4.6%, respectively. The ellipsoidal procedure for the evaluation of the floc shape was compared to a conventional pixelation method. A difference lower than 4 %, in terms of equivalent floc projected area, was observed between both methods. Analyzing one sample requires approximately 2 hours of operator time.

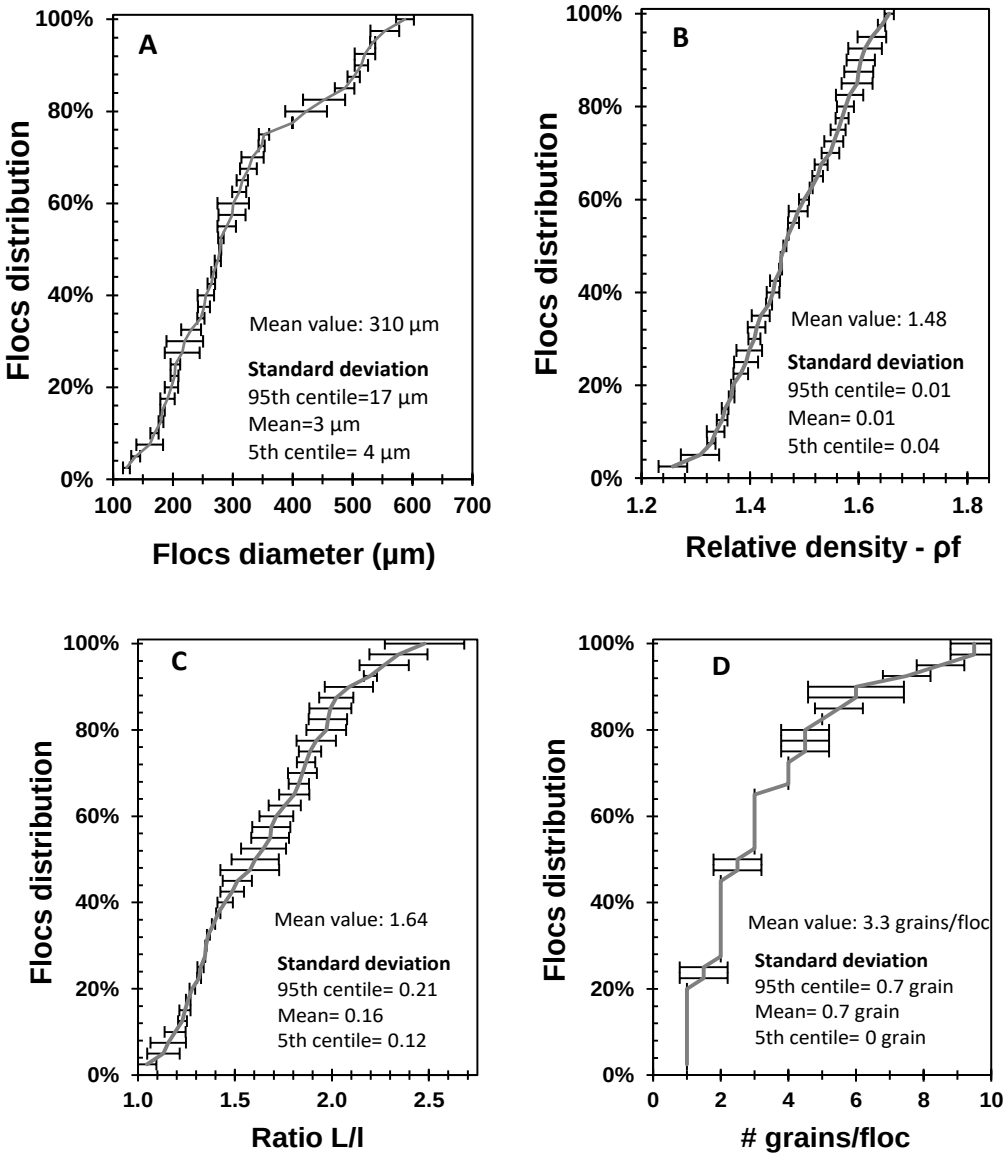

Figure 4.2: Repeatability of the microscopy method measuring floc diameter, density, L/l ratio and the number of media grains per floc. Flocculation conditions: velocity gradient G=165 s^{-1}, polymer=0.4 mg PAM/L, microsand=4 g/L and flocculation time=1 min.

The floc diameters, density and L/l ratio distributions were best fitted as a log-normal distribution ($p = 0.61$), normal distribution ($p = 0.57$) and gamma distribution ($p = 0.51$), respectively. These three floc characteristics were shown to be poorly correlated according to the Pearson coefficient:

floc size vs. floc density (r = -0.10), floc size vs. L/l ratio (r = -0.13) and floc density vs. L/l ratio (r = -0.08).

4.3.2 Calculation of settling velocities based on floc characteristics

An optimized jar test condition was used to produce flocculated waters using Ste Rose River water. Flocs were characterized, and Figure 4.3 summarizes the relative impact of the floc shape, density and diameter on the predicted settling velocity. Settling velocities were calculated by considering combinations of the 5th percentile, mean and 95th percentile floc diameters, density and shape factor.

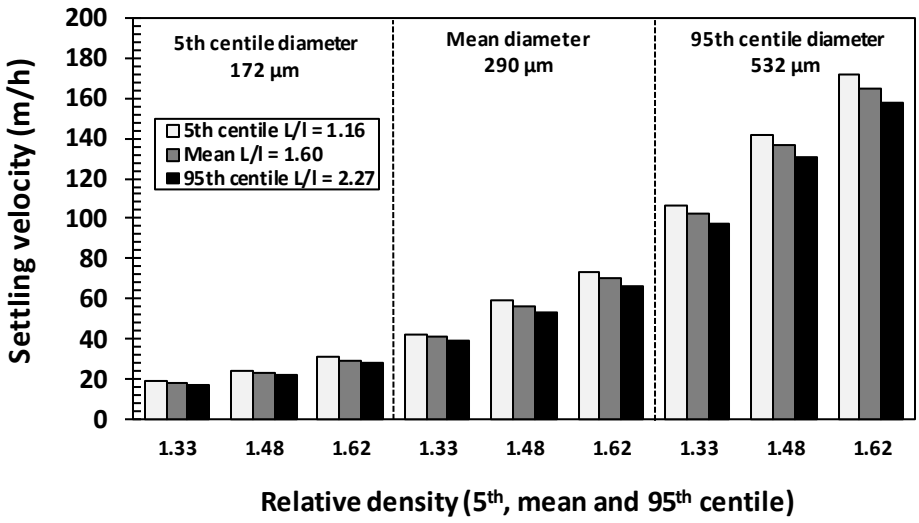

Figure 4.3: Impact of form, density and floc diameter on the settling velocity, considering the 5th percentile, mean and 95th percentile values of each parameter for the source water. Flocculation conditions: velocity gradient G=165 s^{-1}, polymer=0.4 mg PAM/L, microsand=4 g/L and flocculation time=1 min.

For the measured range of values and considering the 5th percentile to the 95th percentile, the floc size is the parameter that has the predominant impact on the settling velocity. A gain of 210% is predicted as the diameter is increased from 172 to 532 µm. The density also significantly increased the calculated settling velocity (a maximal gain of 55% is predicted for the 5th percentile to the 95th percentile, i.e., from 1330 to 1620 kg/m^3). Finally, the shape factor for the observed range (L/l:

1.16-2.27) had a negligible impact since, as a reduction in the settling velocity of only 12% was predicted as the ratio increased from the 5th percentile to the 95th percentile.

As shown in Figure 4.4, the settling velocities calculated from the floc size, density and shape obtained by microscopy were found to be adequately characterized by a log-normal distribution (p=0.76). As a point of comparison, the settling velocity of the un-ballasted flocs is also represented in Figure 4.4.

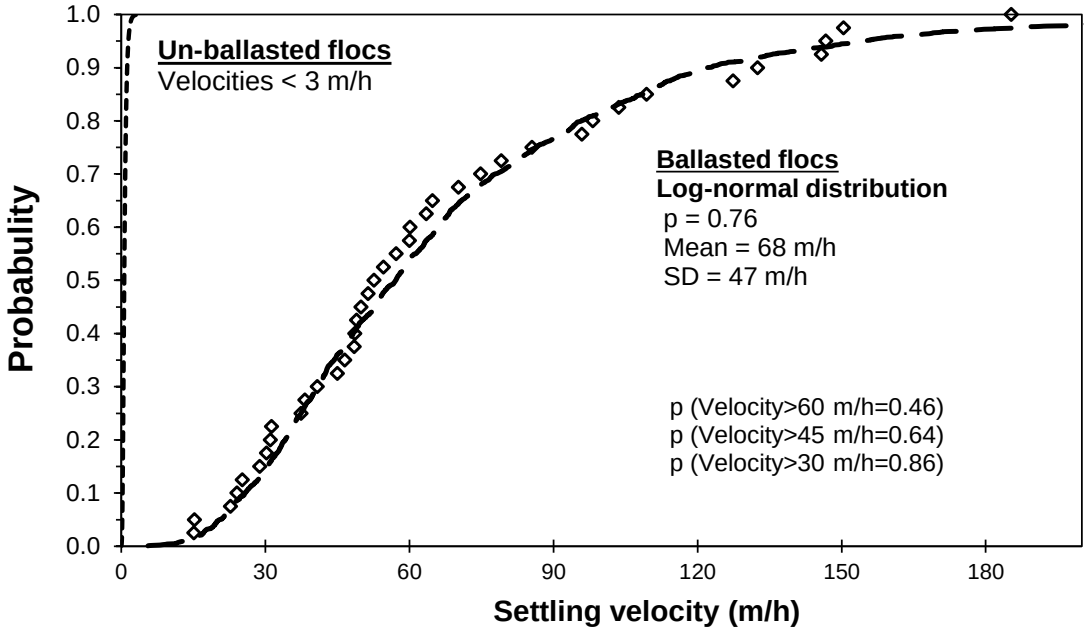

Figure 4.4: Cumulative distribution function describing the probability of the settling velocity for the source water. Flocculation conditions: velocity gradient G=165 s^{-1}, polymer=0.4 mg PAM/L, microsand=4 g/L and flocculation time=1 min.

To better discriminate between the influences of specific floc characteristics on the settling velocity, each floc characteristic was independently correlated with the flocs settling velocity (Figure 4.5). The apparent density and the L/l ratio were not strongly correlated to the settling velocity. The settling velocity was dominated by the influence of the floc equivalent diameter (r = 0.94). Two factors can explain this conclusion. First, the theoretical settling velocity indicates that the settling velocity is proportional to d^2. Second, of the three characteristics evaluated by

microscopy, floc diameter was found to have the largest variation, which is reflected in the fact that the data were best fitted with a log-normal distribution.

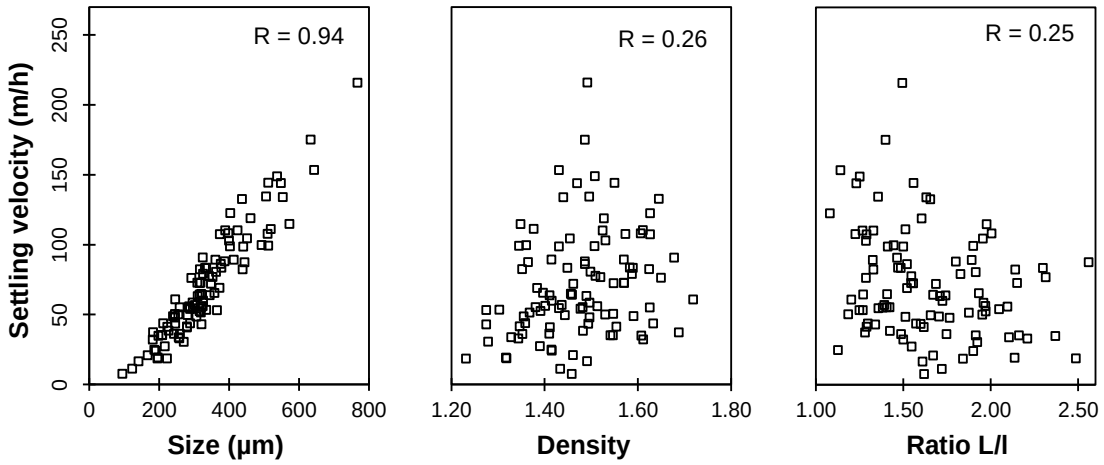

Figure 4.5: Impact of measured morphological flocs characteristics on predicted settling velocity in Ste Rose waters. Flocculation conditions: velocity gradient G=165 s^{-1}, polymer=0.4 mg PAM/L, microsand = 4 g/L and flocculation time = 1 min.

4.3.3 Identification of optimal floc flocculation conditions

1) Adequate mixing intensity

The impact of increasing the flocculation velocity gradient (G) on the ballasted floc size characteristics was evaluated by microscopy (Figure 4.7A). The observations showed an important adverse impact of increasing *G* from 165 s^{-1} (the usual flocculation conditions for ballasted flocculation) to 300 s^{-1}, as the mean ballasted floc diameter was reduced from 310 ± 8 µm to 200 ± 6 µm. A decrease in the floc mean relative density from 1.53 ± 0.02 to 1.39 ± 0.03 (data not shown) was also observed when high shearing (300 s^{-1}) is induced during the flocculation stage.

2) Optimal flocculation time

Microscopic observations also provided information related to the aggregation kinetics. The floc size distributions were assessed after 0.5, 1 and 4 minutes of flocculation (Figure 4.7B). The mean floc diameters after 0.5, 1 and 4 minutes of flocculation were 183 ± 6 µm, 290 ± 9 µm and 275 ± 7 µm, respectively. The difference in diameter between 1 and 4 minutes of flocculation was

statistically significant ($p < 0.01$, paired *t-test*). For this specific water, a maturation time of 1 minute at 21˚C is sufficient to form proper ballasted flocs under lab-scale conditions (i.e., ideal hydrodynamic conditions). Figure 4.6C provides direct visual evidence that the flocculation was complete after 1 min. For the wastewater tested, 30-40 seconds was enough to complete the aggregation and to remove 99 % of the turbidity (data not shown).

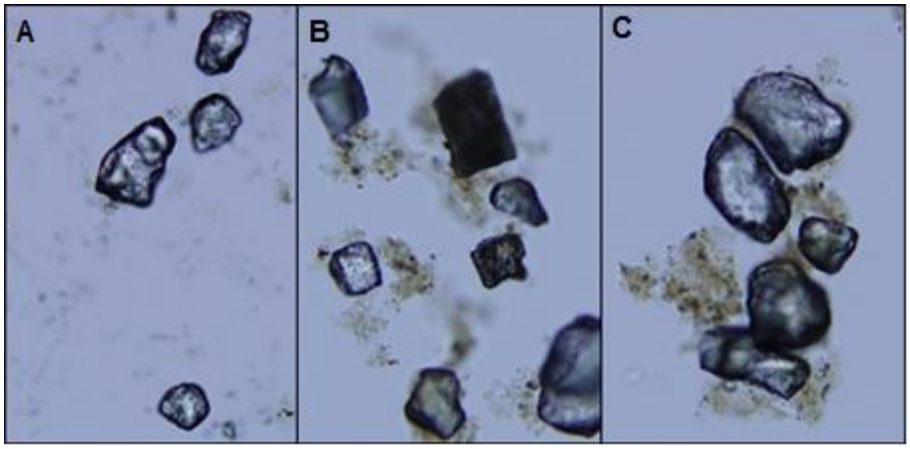

Figure 4.6: Evolution of floc size A) before flocculation, B) after 0.5 minute C) and after 1 minute of flocculation of the source water. Flocculation conditions: velocity gradient G=165 s^{-1}, polymer=0.4 PAM mg/L and microsand=4 g/L.

3) Effect of polyelectrolyte properties

Synthetic PAM and starch-based polymers were compared under identical flocculation conditions (1 min at G = 165 s^{-1}). Figure 4.7C indicates that PAM (mean floc diameter = 310 ± 8 µm) formed significantly larger flocs ($p < 0.01$) compared with those formed with the starch polymer (mean floc diameter = 203 ± 5 µm). However, the relative densities were not significantly different (mean densities: 1.53 ± .02 for PAM vs 1.55 ± 0.04 for starch, p=0.43).

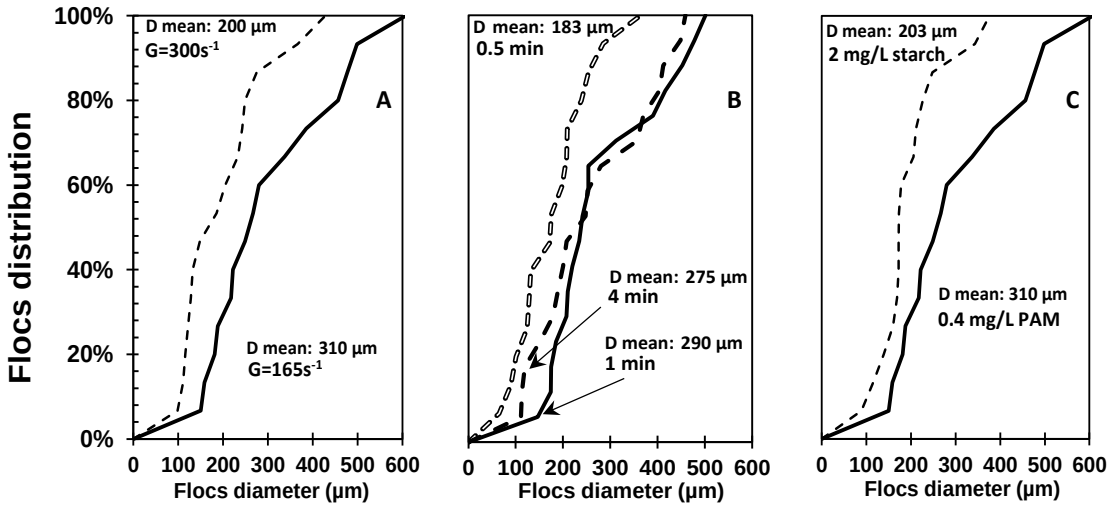

Figure 4.7: A) Velocity gradient, B) maturation time and C) polymer type effect on the floc size distribution for the source water. Flocculation conditions: velocity gradient G=165 or 300 s^{-1}, Polymer: 0.4 mg PAM/L or 2 mg starch/L, microsand=4 g/L and flocculation time=0.5, 1 or 4 minutes.

4) Impact of microsand size

Floc characteristics were assessed under varying flocculation scenarios (polymer type, G and water source) for two microsand distributions. The first microsand had a mean diameter of 140 µm (45-300 µm). The second one was produced by sieving and had a mean diameter of 80 µm (45-140 µm). This comparison was performed to evaluate if the larger sand fraction (140-300 µm) was efficiently incorporated into the ballasted flocs. Figure 4.8 illustrates the largest microsand grain size that was incorporated into a ballasted floc depending on its mean diameter. It is shown that larger ballasted flocs have the capacity to embed larger grains of microsand. For example, when flocculation was conducted with an activated starch polymer, approximately 27 % of the sand distribution (on a weight basis) was not embeddable into the flocs. Under this scenario, the largest grain identified in all flocs had a diameter of 183 µm, while the available grain size distribution was larger (45-300 µm). Similar observations were made under high shearing conditions during flocculation (G = 300 s^{-1}). For a wastewater application that requires high PAM dosages, larger flocs were produced. Under that scenario, the entire microsand distribution was embeddable in the ballasted floc structure.

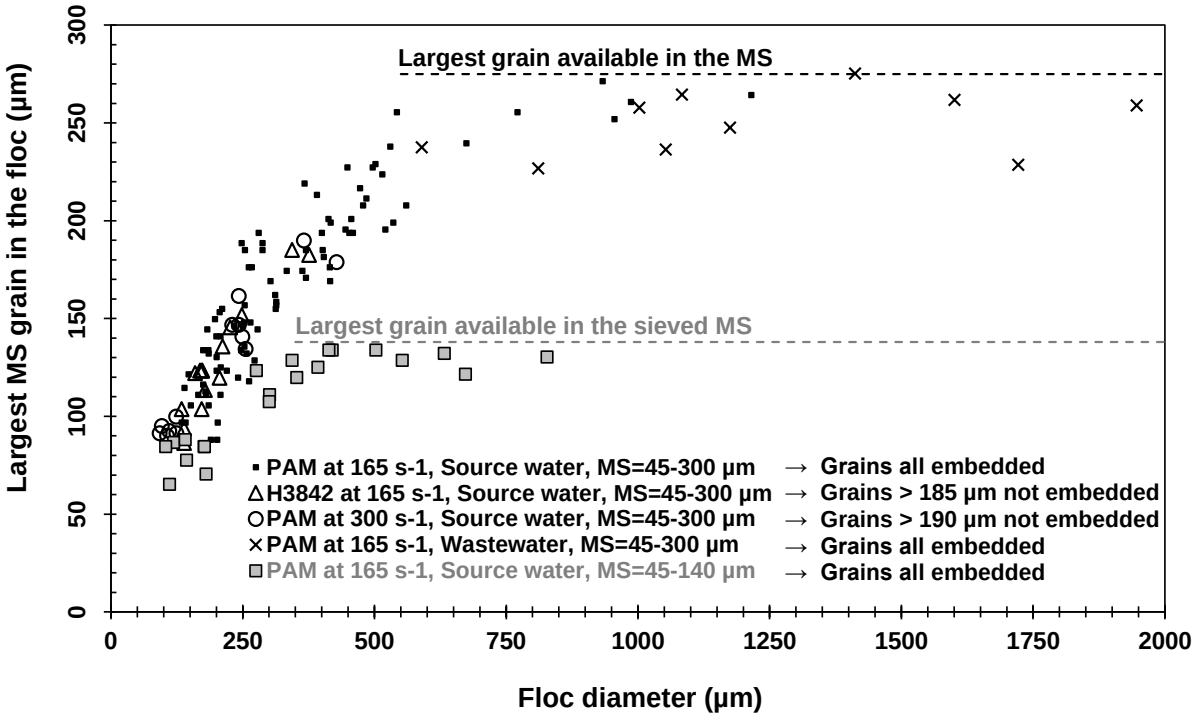

Figure 4.8: Impact of microsand size on its incorporation in the floc. Flocculation conditions: velocity gradient G=165 or 300 s^{-1}, Polymer: 0.4 mg PAM/L (Source water), 0.5 mg PAM/L (Wastewater) or 2 mg starch/L (Source water), microsand=4 g/L and flocculation time=1 minute.

4.3.4 Turbidity removal related to floc settling velocity

In this study, turbidity removal was always measured after settling. The turbidity removal (expressed in log) was correlated to the predicted settling velocity based on the measured floc size, density and shape factor. Many flocculation scenarios and two source waters (surface and wastewater) were considered for this analysis. Figure 4.9 indicates that, independent of the mixing conditions, polymer type, polymer dosage and source water, there is a clear relation between the mean settling velocity and the separation process performance in terms of turbidity removal.

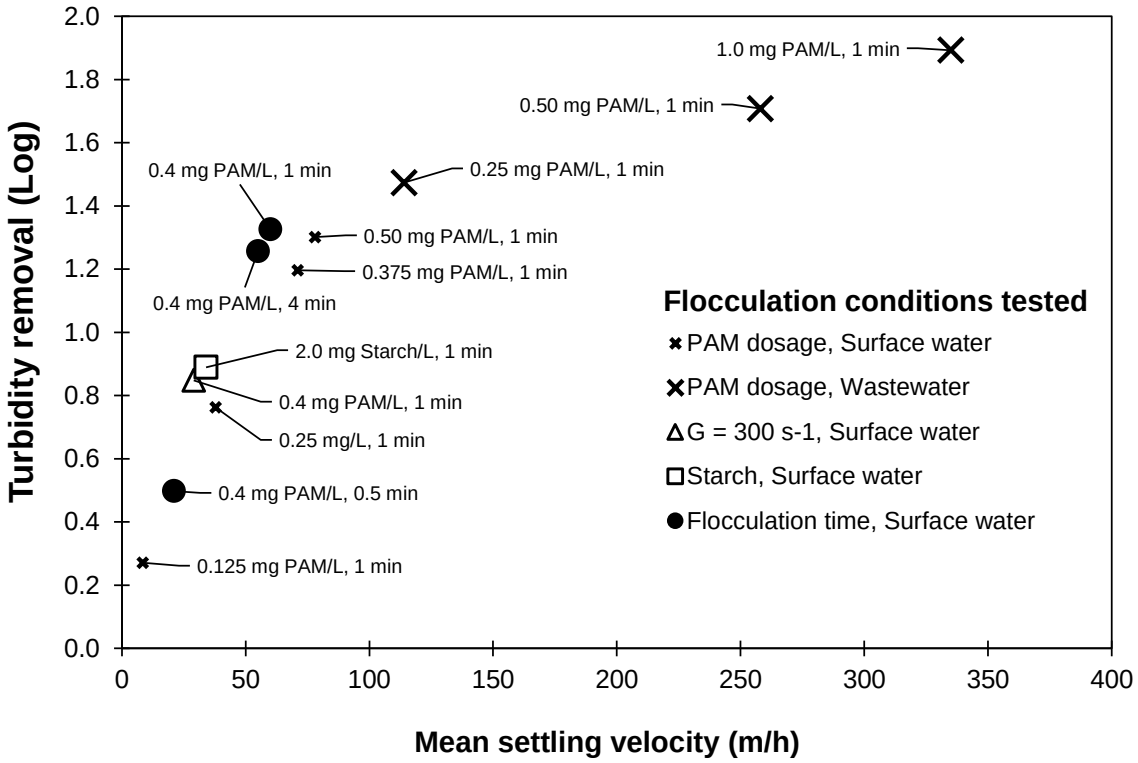

Figure 4.9: Impact of settling velocity calculated from floc size, density and shape factor on turbidity removal for varying flocculation conditions. Flocculation conditions: velocity gradient G=165 or 300 s^{-1}, Polymer: 0.125, 0.25, 0.375, 0.4, 0.5 or 1.0 mg PAM/L or 2 mg starch/L, microsand=4 g/L and flocculation time=0.5, 1 or 4 minutes.

4.4 Discussion

4.4.1 Parameters controlling the floc settling velocity

The floc settling velocity is dominated by the floc equivalent diameter (section *Calculation of settling velocities based on floc characteristics*). This is attributable to the small variation in density observed (1.25-1.70) in comparison to the variation in diameter (95 - 790 µm) as well as the fact that the settling velocity is proportional to d^2. In the case of the shape factor θ, a small impact on settling velocity was observed, even if a wide range of L/l ratio was established by microscopic observation (1.0-2.5). This is attributable to the fact that θ (derived from the ratio L/l, section *Floc shape factor*) is under a square root in the settling velocity equation (Johnson, C. et al., 1996). The high correlation between the floc diameter and settling velocity (r = 0.94, Figure 4.5) suggests that a good description of the floc size distribution would be sufficient to properly size a ballasted

settler. The on-line measurement of the floc distribution in flocculated waters could also be a valuable tool for process control. The determination of an acceptable applied surface load on the settling tanks could be estimated from a cumulative settling velocity probability distribution function, such as the one presented in Figure 4.4. For an applied settling velocity smaller than 15 m/h, all of the ballasted flocs are theoretically removed. Hence, there is no considerable gain to operating between 3 and 15 m/h because, for this settling velocity range, all of the un-ballasted flocs would still be refractory to settling.

4.4.2 Floc characteristics

The floc sizes and densities obtained in this study reveal the importance of a ballast media, as a considerably larger equivalent diameter and apparent density were measured compared with those obtained under a conventional coagulation-flocculation process. The flocs obtained under optimal polymer and mixing intensity conditions were 46% denser (increase from 1.05 to 1.53) compared with flocs formed with iron salts (Larue & Vorobiev, 2003). The floc diameters (log-normal distribution, considered typical for particles and flocs (Gregory, 1997; Lartiges et al., 2001)) were not correlated with the floc densities (best fitted with a normal distribution) or L/l ratios (best fitted with a gamma distribution).

1) Polymer impact on particle removal and floc size

A starch-based polymer was tested in this study because of increasing concerns related to PAM toxicity and residual acrylamide monomer in the final treated water (Bolto & Gregory, 2007). The lower particle removal when starch polymer is used as an alternative in ballasted flocculation appears to be explained by the presence of smaller polymer chains compared with those offered by synthetic PAM (Gaid & Sauvignet, 2011). This study also indicated that the flocs formed during the maturation process are significantly smaller (mean diameter = 203 µm) than those formed with PAM (mean diameter = 310 µm) (Figure 4.7C), which is known to be detrimental to the aggregate settling velocity. This leads to other recommendations related to the MS size to be injected when a polymer having a smaller molecular weight is used as a flocculant (discussed in section 4.4.3).

2) Mixing intensity influence on floc structure

The mixing intensity during flocculation is already known to be an important parameter for successful aggregation. Many studies have mentioned the limited resistance of flocs and the

importance of controlling the shear on the floc surface (Jarvis, Jefferson, Gregory, & Parsons, 2005; Yu, Wen, Gregory, Campos, & Li, 2011). Even using high molecular weight PAM with an appropriate low anionic charge density leading to a full polymer chain expansion, which is able to adsorb on many sites of the particle, thereby creating strong aggregation, an inadequate shear can easily rupture the bridges formed by the polymer chain (Owen, A., Fawell, & Swift, 2007). G values for conventional flocculation that are proposed as optimal can vary from 20 s^{-1} (Biggs & Lant, 2000) to 50 s^{-1} (Spicer, Patrick T. et al., 1998). For ballasted flocculation, a minimal *G* has to be induced to maintain the ballasting agent in suspension. For MS having a relative density of 2.65, a range of 160 to 200 s^{-1} has been proposed as optimal (Desjardins et al., 2002). De Dianous et Dernaucourt (1991) showed that *G* values as high as 700 s^{-1} can be tolerated by a floc structure formed from polyacrylamide polymer and silica sand. The polymer properties (molecular weight and charge density) controlling the number of points of attachment on the floc surface greatly influence the maximum *G* value that can be withstood before the flocs break up. For this study and for the specific PAM employed, 300 s^{-1} was detrimental for the ballasted aggregates, as a significant reduction of floc size (30-40%) and density (10-15%) was observed. For these inadequate mixing conditions, many aggregates were identified as non-ballasted flocs (no MS grain was attached to the floc structure). G values lower than 165 s^{-1} were not proposed as optimal because the suspension of MS was incomplete under these low mixing intensities. In other words, the minimum mixing is controlled by the ballasting agent density.

3) Evaluation of the optimal flocculation time

The adsorption kinetics related to the interactions between the polymer chains, the MS and the particles to be removed are discussed in this section. For particles destabilized by alum without PAM injection as a coagulant aid, extended flocculation time under low G values are ideal conditions to allow floc growth (Yukselen & Gregory, 2004). For ballasted flocculation, high molecular weight polymer (up to 10^7 g/mol) is needed to bridge small particles to the MS. Hence, the maturation step is controlled by different mechanisms, such as polymer particle bridging and an electrostatic patch effect (Yoon & Deng, 2004), than those controlling conventional flocculation without the use of a coagulant aid. The minimum time to complete aggregation is generally inversely proportional to the particle concentration and related to the polymer chain length and charge density (Gregory & Barany, 2011). However, long polymer chains may undergo a reconfiguration after extended flocculation (Enarsson & Wågberg, 2008). Hence, the available

contact time during the flocculation (after the MS and polymer injection) has to be sufficient to permit the polyelectrolyte chain to adsorb on the particles but less than the critical time that allows chain reconfiguration. The optimal flocculation time is hard to predict because many factors, aside from the polymer characteristics, will influence the affinity between the particles, the MS and the polymer chain. For the surface water investigated, a flocculation of 1 minute is optimal. However, for the municipal wastewater, a flocculation time lower than 40 seconds is sufficient to complete the MS incorporation in the flocs and to achieve 99% particle removal. This high kinetics of aggregation is most likely explained by the high particle concentration present in the municipal wastewater combined with the high concentration of PAM injected (0.5-1.0 mg/L for wastewater applications rather than 0.2-0.4 mg/L for drinking water applications). Provisions for a longer contact time are used for industrial applications to account for the impact of water temperature and hydrodynamic effects.

4.4.3 Selection of ballasting agent properties

The MS size is an important factor to consider in ballasted flocculation. Large grains of high density are known to generate an important hydrodynamic repulsion on the smaller particles in suspension (Thomas et al., 1999). Moreover, large MS grains are hard to maintain in suspension due to their high settling velocities. This is of concern because higher energies (G) will cause floc fragmentation as well as an increase in the total energy consumption of the plant. This study presents a new understanding of the behavior of MS for drinking and wastewater applications. Synthetized data derived from floc observations showed a correlation between the largest MS grain embedded in the floc and the floc size. Independent of the polymer choice, G value during flocculation and water source, it was observed that larger flocs were able to incorporate larger MS grains. Similar incorporation mechanisms were reported by Young et Edwards (2000). Flocs produced under optimal conditions with a high polymer dosage (*i.e.*, 0.5 mg/L of PAM for wastewater applications having high turbidity) incorporated all of the available grains of the MS distribution. Hence, for wastewater applications, larger grains (> 300 µm) could be injected to ballast the aggregates. However, the opposite conclusion should be reached for the smaller flocs produced in certain drinking water applications (e.g., operated under low coagulant/polymer dosages, with polymers having small molecular weights or under unsuitable mixing conditions). Under these conditions, a significant portion of the MS distribution is not incorporable into the floc

structure. This observation leads to specific recommendations for wastewater or drinking water applications because the correlation established could predict the appropriate grain size, *i.e.*, the largest grain embeddable in the floc.

4.5 Conclusions

The microscopy method provides new information regarding the characteristics of ballasted flocs: density, media ballast incorporation, shape and diameter. The method offers a high repeatability. The information derived by microscopy was used to predict floc settling velocities. Based on a series of controlled assays at the lab scale, the following conclusions can be drawn:

- Settling floc velocities follow a log-normal distribution.
- The optimal ballast media size is correlated with the floc equivalent diameter, *i.e.*, larger flocs can incorporate larger microsand.
- The floc diameter has a higher impact on the settling velocity than floc density or shape. Process control techniques should therefore target this parameter.
- Optimal polymer and microsand dosages are better identified with the microscopy technique compared with an analysis based on turbidity removal, as it is possible with microscopy to differentiate the roles of flocculation and settling.
- At the bench scale and room temperature, a flocculation time of 1 min and a mixing intensity of 165 s^{-1} were determined to be optimal conditions when microsand is employed as the ballasting agent.
- Starch polymer forms smaller flocs than polyacrylamide polymer and does not significantly embed microsand larger than 190 µm.
- Unsuitable shearing during flocculation is detrimental as it reduces the aggregate size and density by leading to microsand disincorporation.
- The assessed floc parameters could facilitate settler sizing and design based on floc settling velocity prediction and also permit the particle removal estimation of existing settler units for a specific applied surface load.

More research is recommended to compare the floc characteristics of full-scale ballasted processes with equivalent lab-scale conditions. Experimental measurements of ballasted floc settling

velocities and comparison with theoretical predictions would also be of value for improved modelling of the settling process.

Acknowledgments

These experiments were conducted as part of the Industrial-NSERC Chair in Drinking Water (Polytechnique Montreal) research program, which benefits from the financial support of Veolia Water Technologies Canada, Inc., the City of Montreal, the City of Laval and the City of Repentigny

CHAPITRE 5 ARTICLE 3 - EVALUATION OF ACTIVATED STARCH AS AN ALTERNATIVE TO POLYACRYLAMIDE POLYMERS FOR DRINKING WATER FLOCCULATION

Cette section compare les performances de l'amidon par rapport à celles du PAM lors de la floculation lestée. On y constate entre autres les limitations des polymères à base d'amidon: réduction de l'abattement de turbidité, flocs moins résistants au cisaillement, concentrations requises plus élevées, *etc*. Il est démontré dans cet article (publié: *Journal of Water Supply: Research and Technology-Aqua*) que les concentrations requises des polymères à base d'amidon sont de 4 à 5 plus élevées que celles du PAM. En complément à ce chapitre, les chapitres 6 et 7 se consacrent quant à eux davantage à l'optimisation de l'amidon lors de la floculation lestée. Toutefois, des pistes d'optimisation sont déjà mentionnées dans ce chapitre, notamment en lien avec la taille du média lestant et l'intensité de mélange (*G*) lors de la floculation. Il a aussi été détecté que les polymères à base d'amidon pouvaient relarguer du CODb, plus particulièrement lors d'une coagulation sous-optimale. Ce CODb n'avait cependant pas d'impact notable sur la formation de THM et de AHA.

Evaluation of activated starch as an alternative to polyacrylamide polymers for drinking water flocculation

Mathieu Lapointe[1] and Benoit Barbeau[1]*

[1] Industrial NSERC Chair on Drinking Water, Department of Civil, Geological and Mining Engineering, Polytechnique Montreal, Montreal, Quebec H3C 3A7, Canada

*Corresponding author e-mail: mathieu.lapointe@polymtl.ca

Abstract

Polyacrylamide polymers are one of the most common water treatment chemicals used in clarification processes. Concerns have been raised with regards to the aquatic and human toxicity of acrylamide monomer. Greener polymers, produced using potato starch, were investigated at lab-scale as a potential non-toxic alternative to the use of PAM within a ballasted flocculation process (Actiflo®). Even under extreme temperature (1°C), starch and PAM showed comparable turbidity removal performances, although higher starch dosages (4-5 times) were needed to achieve such result. Compared to PAM, activated starch polymers also benefited from the use of lower mixing energy and smaller microsand. A slight BDOC release (≈ 0.15 mg C/L) was also measured while using starch polymer but this did not impact THM and HAA formation. These results indicate that activated starch polymers represent a promising alternative to the use of PAM polymers in a ballasted flocculation process.

Keywords: *Polyacrylamide; Starch; Ballasted flocculation; Turbidity; Microsand; BDOC; THM; HAA*

5.1 Introduction

Amongst alternative coagulation-flocculation-settling processes, ballasted flocculation is an economical technology for surface water clarification due to the possibility to operate at high superficial velocity (40-85 m/h). The process involves the injection of microsand during flocculation in order to increase settling velocity (Plum et al., 1998). Polymers, once attached to microsand, provide high flocs settling velocity and turbidity removal. Typically, polyacrylamide-based polymers (PAM) are used for ballasted flocculation as they improve flocs strength and compactness (Jin et al., 2013). However, recent studies have highlighted concerns related to the toxicity for humans and aquatic organisms of residual acrylamide monomer which may escape in

finished water or be discharged in the aquatic ecosystem (Bolto & Gregory, 2007; Rice, 2005). Other studies have also linked the use of synthetic polyelectrolytes to the formation of disinfection by-products (DBPs) (Bolto, 2005; Fielding, 1999). As a result, some countries have restricted (France, Germany) or abolished (Spain, Japan, Switzerland) the use of PAM in water treatment for drinking water production. The maximum value recommended by NSF/ANSI-60 certification is typically 1-3.5 mg/L, depending on the residual acrylamide monomer content. Commercially available PAM typically contains a maximum of 0.05% acrylamide monomer. For a dosage of 1 mg/L, the maximum possible concentration in treated water is therefore 0.5 µg/L. However, a typical conventional treatment process does not remove the residual acrylamide monomer (WHO, 2004). Consequently, limiting acrylamide monomer in finished water implies either (i) a reduction of the applied dosage, (ii) the use of a high purity PAM (lower acrylamide content) or (iii) the use of an alternative polymer than PAM.

Greener polymers manufactured from starch potatoes, recognized to be biodegradable and non-toxic, offer an economical potential alternative to replace PAM in conventional treatment processes. The general aim of this paper is to evaluate the performances of starch-based polymers for ballasted flocculation. Polymers are used within this process, commercialized as the Actiflo® process, in order to attach the flocs to the microsand. The performance of PAM and starch polymers were compared under a challenging temperature condition (1˚C) waters using a modified jar test procedure. This work provides strong evidence that specific starch-based polymers can be used as an alternative to PAM within a ballasted flocculation process. As example, 5 plants are running in France/Spain with such product and the drinking water produced is in accordance with industrial standard.

5.2 Materials and methods

5.2.1 Ballasted flocculation: jar test simulation methodology

All assays were conducted using surface waters from the St. Lambert water treatment plant which is fed by the St. Lawrence River (Quebec, Canada). This source water exhibits a moderate alkalinity (80 mg $CaCO_3$/L), a relatively high pH (≈ 8.0), a low TOC (< 3 mg C/L) and a fairly low turbidity

(2.5 - 3.5 NTU). Ballasted flocculation using alum and the Superfloc A-100 PAM (from Kemira) is in operation at this facility.

Source waters were sampled and characterized upon reception at the laboratory. Two liters square beakers (B-Kers^{TM}, Phipps & Bird) were used to conduct the jar tests. Alum ($(Al_2SO_4)_3.14H_2O$) and ferric chloride ($FeCl_3.6H_2O$) were used as coagulants. Assays with alum were conducted at 1°C and 21°C while assays with ferric chloride were only conducted at 21°C. Cold water assays were conducted in a thermostated cold room. Following coagulant injection, the flocculant and microsand were injected according to the sequence described in Figure 5.1. Either the Superfloc A-100 (a low anionic and high molecular weight PAM) or the Hydrex 3841 (a low anionic and low molecular weight starch polymer) were injected as flocculant. The Superfloc A-100 was selected as it was the optimal polymer found by the St. Lambert water facility operators. The Hydrex 3841 (H3841) was selected following pre-tests that identified it as optimal amongst a group of three candidate starch-based polymers from Hydrex.

Figure 5.1 summarizes the sequential procedure used to simulate a ballasted flocculation in jar test. Briefly, raw waters are flash-mixed during 2 minutes at 400 s^{-1}. After flash-mix, 50 % of the polymer dosage and the entire dosage of microsand are injected and mixed at 165 s^{-1}. The remaining polymer dosage is introduced after 5 minutes of flocculation to allow flocs growth. After flocculation, the process requires 3 minutes of settling (equivalent to an overflow velocity of 40 m/h) to ensure turbidity removal. Samples were collected 10 cm under the water surface. This simulation was established to replicate a full scale ballasted treatment (Desjardins et al., 2002).

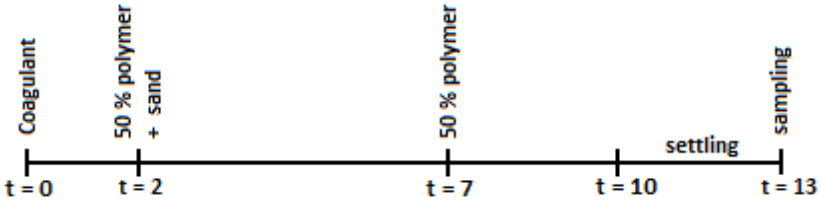

Figure 5.1 : Conventional ballasted flocculation procedure.

5.2.2 Modifications to the conventional ballasted flocculation procedure

The jar test procedure described previously was originally developed for PAM. Compared to PAM, starch-based polymers differ significantly in terms of their chemical properties. Therefore, a four step experimental design was developed to evaluate if ballasted flocculation conditions should be

revisited while using starch polymers. Firstly, triplicate assays were conducted in order to evaluate the reproducibility of the jar test procedure. Secondly, optimal polymer dosages were identified using the conventional (Desjardins et al., 2002) procedure for both polymers. Thirdly, the impact of microsand diameter (63-80 µm vs. 100-160 µm) was tested. Finally, variable flocculation velocity gradients (*G* values from 60 to 540 s^{-1}) were also tested. In all cases, settled water (SW) turbidities were used as an indicator of process performance. For the study on the impact of G, particle concentration in SW were firstly evaluated by turbidity measurements and secondly evaluated by micro flow imaging using a particle analyzer (Brightwell Technologies, DPA-4100).

5.2.3 Impacts of using a starch polymer on filtered water quality

SW, produced under optimal conditions using both types of polymers, were microfiltered (0.45 µm, Pall Supor-450, CA28147-640) to remove residual microflocs. Filtered waters (FW) were then characterized for DOC, BDOC, trihalomethanes (THM) and haloacetic acids (HAA) using uniform formation conditions (UFC) (according to the analytical methods summarized in Table 5.1).

Table 5.1: Analytical methods summary

Parameters	**Methods (Equipment)**
Turbidity	Standard Method, 2130B (Hach 2100N turbidimeter)
DOC	Standard Method, 5310C (Sievers 5310c total organic carbon analyzer, GE Water)
BDOC	Suspended growth method form Servais et al. (1989), (Sievers 5310c total organic carbon analyzer, GE Water)
THM-UFC, HAA-UFC	Method: Summers et al. (1996). Incubation for 24h at pH 8.0 and 20ºC with Cl_2 dosage sufficient to maintain 1.0 mg Cl_2/L after 24h (Uniform formation conditions)

Statistical comparisons were made using paired Student's *t*-tests at the usual 5% significance level.

5.3 Results

5.3.1 Reproducibility of the jar test procedure

Turbidity measurements performed was one of the main criteria to establish comparatives differences between PAM and starch-based polymers. The reproducibility of the procedure was first evaluated by comparing SW turbidities from triplicate jar tests. Figure 5.2 indicates the precision obtained at 1˚C with alum and a starch polymer. The 95th centile confidence intervals indicate that the procedure was highly reproducible as turbidities varied less than ± 0.05 NTU for adequate polymer dosage (> 0.2 mg/L).

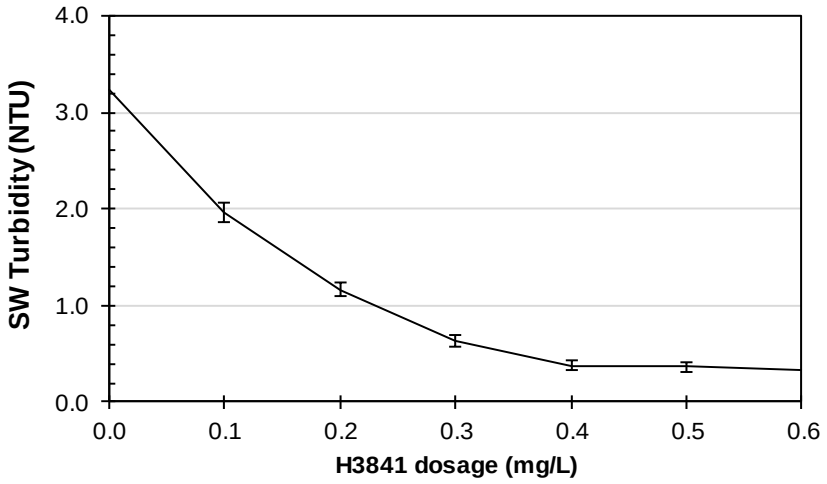

Figure 5.2: Reproducibility of SW turbidity following a jar test conducted in triplicate. Conditions: Alum dosage=0.13 meq./L, temperature=1˚C, microsand=4 g/L, *G* during flocculation=165 s^{-1}, 3 minutes of settling.

5.3.2 Optimized jar test procedure

Polymer dosage selection

Starch polymers and PAM used in this study have different molecular weight (MW), spatial conformation and charge density (CD) which led to differences in optimal flocculation conditions. To assess the performance of each polymer, their optimal dosages were first evaluated with the

conventional jar test procedure detailed in Figure 5.1. Alum or ferric chloride (0.13 meq./L) were used as coagulants while PAM and H3841 were used as flocculants. Figure 5.3 indicates the optimal dosage of each polymer used in conjunction with 4 g/L of microsand while Table 5.2 summarizes the optimal conditions identified. Optimal dosages were selected in order to minimize SW turbidities (*i.e.* under 0.8 NTU) while minimize polymer dosages. The performance of PAM was found to be independent of coagulant type and water temperature. An optimal dosage of 0.075 mg/L was identified. In the case of H3841, slight differences were observed with alum at 21°C performing the best while ferric at 21°C had the lowest performance. However, for all three conditions, it was found that a H3841 dosage of 0.3 mg/L to reduce turbidity in a close range (0.39 - 0.72 NTU). Therefore, the starch polymer dosage was found to be roughly equivalent to 4 to 5 times the PAM dosage needed. The return of experience on Actiflo® drinking water plants already operated by Veolia using starch-based polymer in France reported a ratio of 3 to 4 times compare to the PAM dosage (Gaid & Sauvignet, 2011).

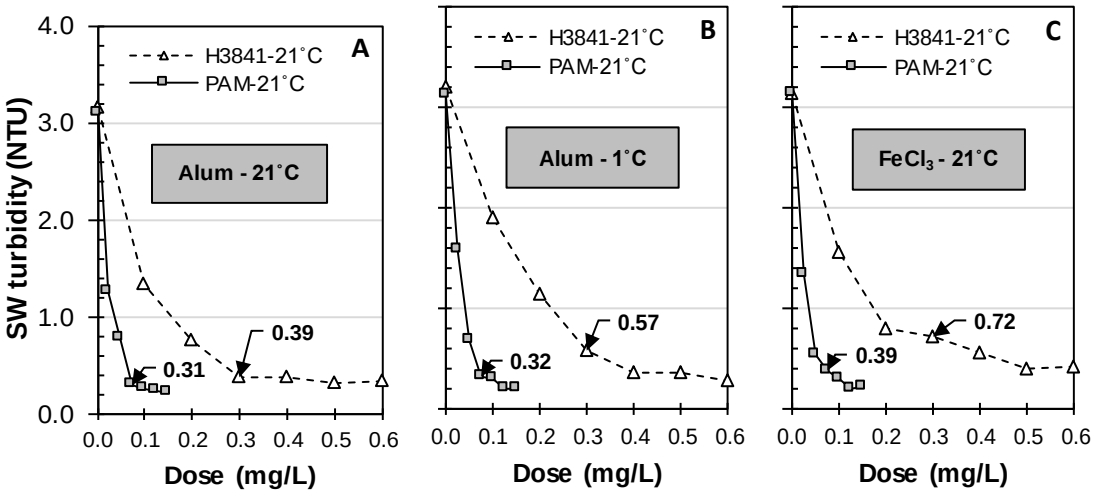

Figure 5.3: SW turbidity in relation with polymers dosage during conventional ballasted jar test procedure. Conditions: Coagulant dosage=0.13 meq./L, microsand=4 g/L, G during flocculation =165 s^{-1}, settling: 3 minutes.

Table 5.2: Optimal dosage of polymers and associated SW turbidity obtained from Figure 5.3.

	PAM		H3841		Dose ratio from Figure 5.3A (H3841/PAM)
	Dose (mg/L)	SW turbidity (NTU)	Dose (mg/L)	SW turbidity (NTU)	
Alum - 21˚C		0.31		0.39	
Alum - 1˚C	0.075	0.32	0.3	0.57	**4.0**
$FeCl_3$ - 21˚C		0.39		0.72	

Alum & $FeCl_3$ dosages = 0.13 meq./L

Microsand dosage selection

To allow the formation of a denser floc, microsand is added during flocculation. The optimal concentrations of microsand (expressed in g/L) were determined while using the optimal polymer dosages identified in Figure 5.3A (with alum at 21˚C). The microsand selected for this test had an average diameter of 137 µm as shown in Figure 5.4A. Figure 5.4B suggests that a microsand concentration of 2 g/L was sufficient to remove turbidity for both polymers. Again, PAM provided slightly lower SW turbidity (0.19 NTU) than H3841 (0.26 NTU).

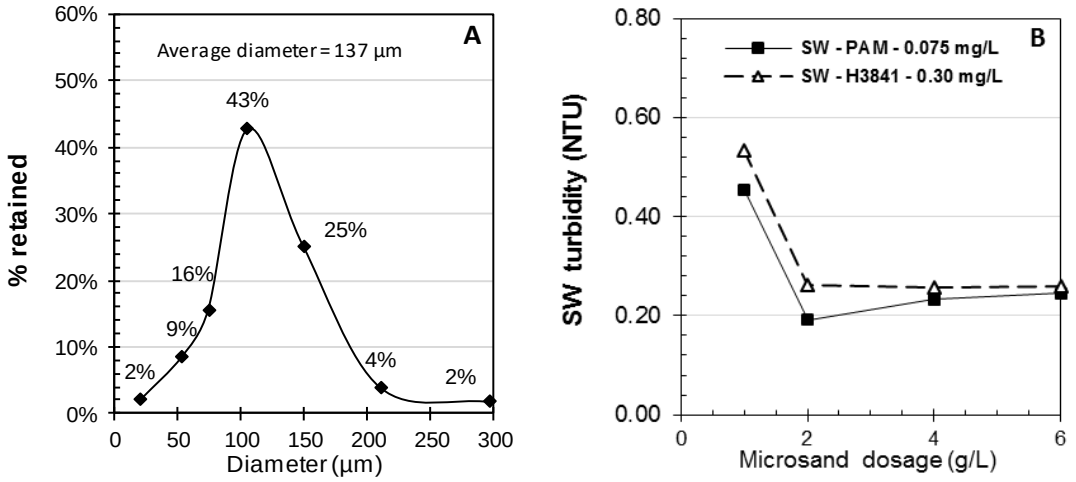

Figure 5.4: (A) Microsand grain size distribution (B) SW and FW turbidity for increased microsand dosage for jar testing under optimal PAM or H3841 polymer dosages. Conditions: Alum dose=0.13 meq./L, temperature=21˚C, G during flocculation =165 s^{-1}, 3 minutes of settling.

Selection of an optimal velocity gradient for flocculation (*G*)

Jar tests were conducted under increased velocity gradients in order to identify the optimal flocculation conditions. In order to achieve Camp numbers (i.e. *G* values) higher than 300 s^{-1}, volumes were reduced down to 1000 ml. The concentrations of non-settleable particles (Figure 5.5A) and SW turbidities (Figure 5.5B) both indicate that the adequate velocity gradient for H3841 is lower than for the PAM polymer. Achieving a turbidity lower than 0.5 NTU in SW required using *G* values below 400 s^{-1} for PAM as opposed to less than 250 s^{-1} for H3841. Consequently, a higher shear stress was more deleterious to H3841 than PAM. However, for a *G* close to 140 s^{-1}, both flocculants had similar performances considering non-settleable particles and SW turbidities. Figure 5.5A also showed that PAM needed a minimal energy gradient during flocculation (>60 s^{-1}) in order to reduce particles after settling.

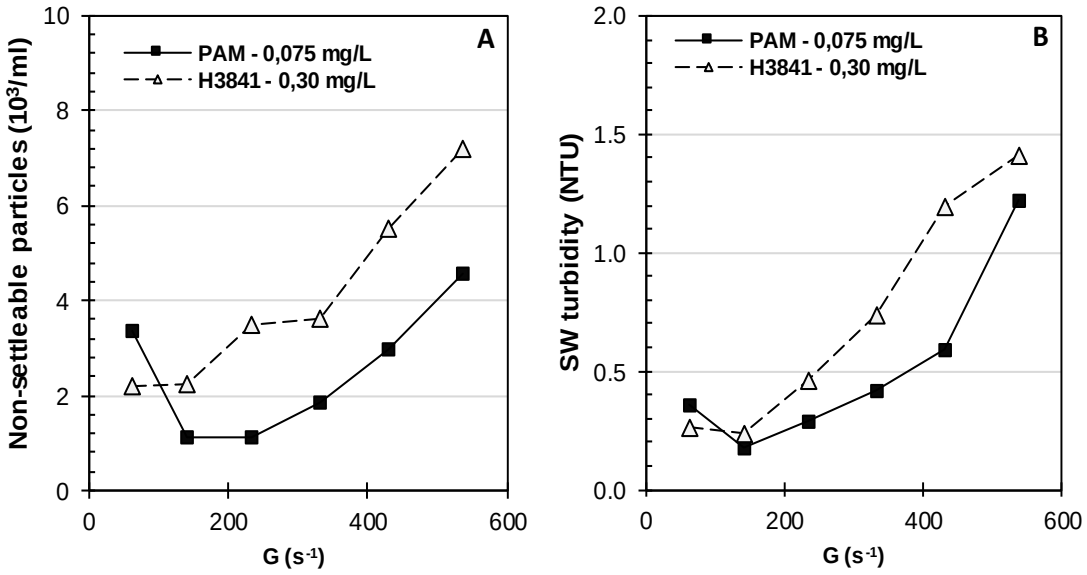

Figure 5.5: Non-settleable particles concentration and SW turbidity obtained with different velocity gradient during flocculation. Conditions: Alum dose=0.13 meq./L, temperature=21˚C, microsand= 4 g/L, 3 minutes of settling.

Effect of microsand size distribution on turbidity removal

The original microsand was sieved in order to produce two microsand size fractions and compare their effects on flocculation performance. The smaller fraction included microsand with size

ranging from 60 to 83 µm while the larger fraction included particle size ranging from 100 to 160 µm. These fractions represented respectively 7% and 50% (by weight) of the original microsand distribution. Figure 5.6A demonstrates that a sand diameter between 63-80 µm produced comparable SW turbidities, independently of the polymer selected. Using this size fraction, it was also possible to largely reduce the dosage of microsand required and previously obtained in Figure 5.4B. For example, a 0.2 g/L dosage of microsand, PAM and H3841 respectively yielded SW turbidities of 0.28 and 0.43 NTU. However, Figure 5.6B illustrates that using the larger microsand (100-160 µm) negatively impacted both polymers. As opposed to the optimal microsand dosage (2 g/L) found in Figure 5.4B, Figure 5.6A reveals that an optimal microsand dosage approximately 10 times smaller (0.2 g/L) is found when a 63-80 µm microsand is employed during flocculation. In addition, Figure 5.6B shows that H3841 did not bridge stable particles with the microsand larger than 100 µm. The SW turbidity achieved with this larger microsand (1.25 NTU) is equivalent to the results obtained without sand (data not shown). Similar results were also observed with waters from the Mille-Îles River (Quebec, Canada). A favorable effect of using smaller microsand for turbidity removal was also noted for this very turbid raw water (75 NTU). With 0.3 mg/L of PAM, SW turbidities produced from microsand respectively having diameters in the range for 63-80, 80-100 and 100-160 µm, were 0.28, 0.37 and 0.45 NTU. This impact was more significant when starch polymers were used.

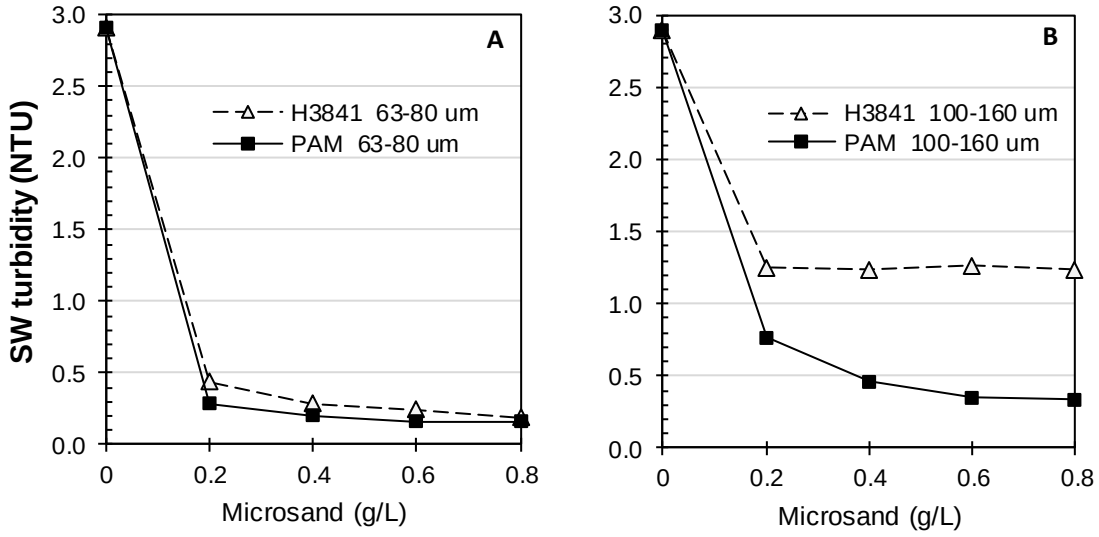

Figure 5.6: Grain size effect on turbidity removal. Conditions: Alum dose=0.13 meq./L, temperature=21˚C, G during flocculation =165 s^{-1}, 3 minutes of settling.

Temperature effect on turbidity removal

Both polymers were tested at 1˚C and 21˚C to observe the global impact of temperature on the clarification process. PAM was not impacted by cold temperature (p-value = 0.43) and the previous optimal dosage (0.075 mg/L) was identical for both temperatures (Figure 5.7A). On the other hand, H3841 was shown to be impacted by lower water temperature (p=0.04). Nevertheless, under optimal polymer dosages (0.4-0.6 mg/L) presented in Figure 5.7B, the differences were not statistically significant (p-value: 0.61).

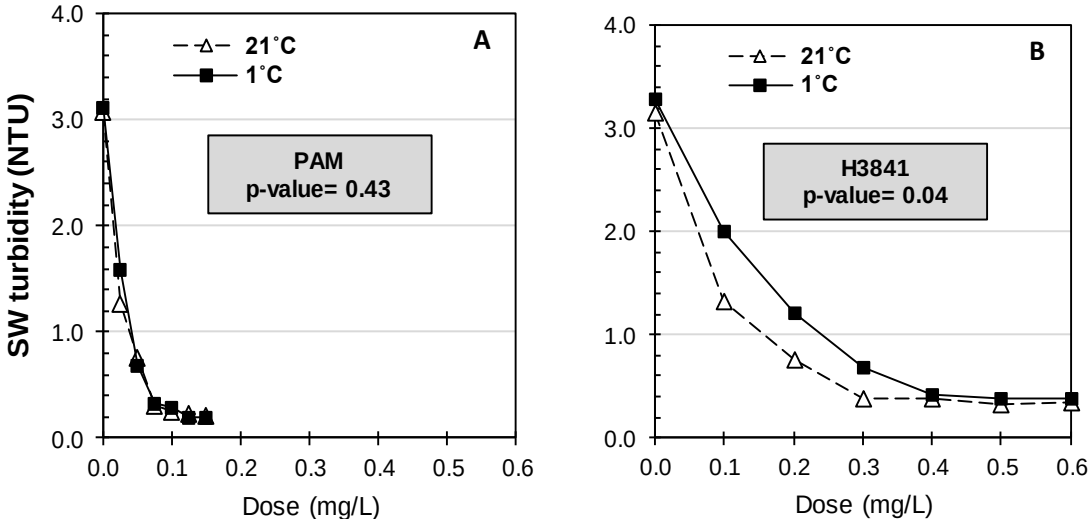

Figure 5.7: Temperature effect on turbidity removal with (A) PAM or (B) H3841 polymers. Conditions: Alum dose=0.13 meq./L, microsand=4 g/L, G during flocculation=165 s^{-1}, 3 minutes of settling.

5.3.3 Impact of polymer dosage on filtered water quality

DOC and BDOC removal

DOC and BDOC removals from raw to coagulated/settled/microfiltered waters were measured in order to assess if the treated waters were impacted by the polymer type. Several assays were performed using alum or ferric chloride (as coagulants) in conjunction with PAM or H3841 (as flocculants). The experimentations using alum coagulant were realized at 1˚C and 21˚C while ferric chloride was solely tested at 21˚C. For all coagulation conditions, Figure 5.8A revealed a slightly better DOC removal with PAM than H3841. Differences in DOC removal between both polymers were statistically significant (p-value: 0.02). Alum performance was not significantly altered by

cold water temperature and exhibited a similar residual DOC after filtration (p-value: 0.11). In Figure 5.8B, ferric chloride (21-23%) offered better DOC removal than alum (8-21%), mainly when H3841 was used as flocculant (p-value: 0.01). In the case of BDOC, Figure 5.9 reveals that the starch-based polymer was responsible for a small BDOC release compare to what it should be expected from biodegradable molecule (≈ 0.15 mg C/L, detection limit: 0.11 mg C/L) in filtered water. However, as shown in Figure 5.9A, the release was more pronounced for alum in cold water while ferric chloride provided equivalent final BDOC (H3841 = 0.37 mg C/L vs. PAM = 0.33 mg C/L).

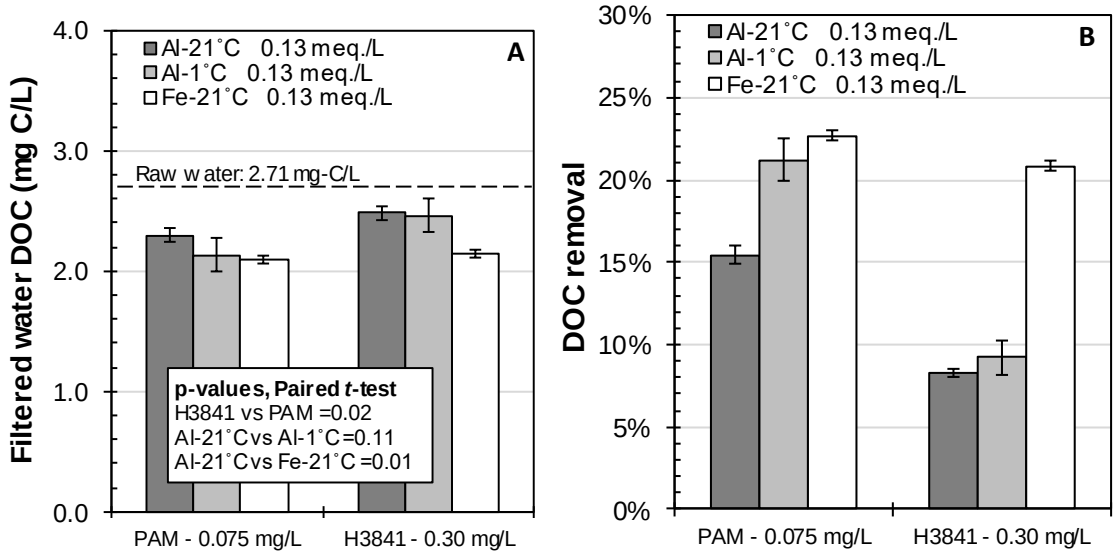

Figure 5.8: (A) Residual DOC and (B) DOC removal in filtered waters according to different coagulant-polymer combinations. Conditions: Microsand=4 g/L, *G* during flocculation =165 s^{-1}, filtered on 0.45 µm membrane. Error bars indicate the 95th centile confidence intervals.

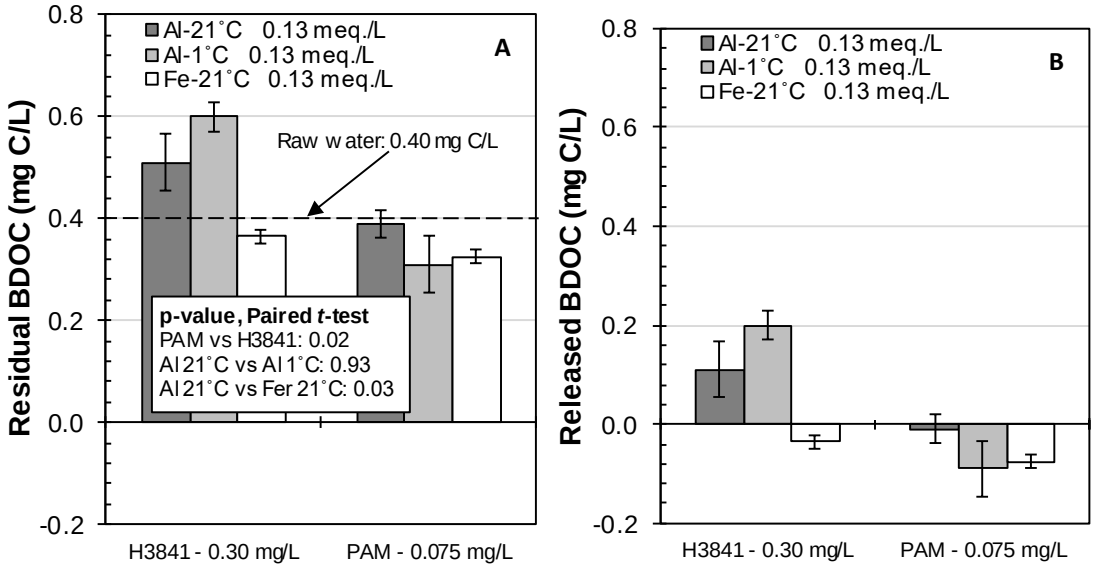

Figure 5.9: (A) Residual BDOC in filtered waters according to different coagulant-polymer combinations (B) BDOC release considering initial BDOC in raw water. Conditions: Microsand=4 g/L, G during flocculation =165 s^{-1}, filtered on 0.45 µm membrane. Error bars indicate the 95th centile confidence intervals.

Removal of THM-UFC and HAA-UFC precursors

Filtered waters were chlorinated under uniform formation conditions to evaluate the removal of THM and HAA precursors (Figure 5.10). THM-UFC and HAA formations were shown to be statistically independent of the polymer selection (p=0.42 and 0.35, respectively). No significant impacts of water temperature (p=0.96) and coagulant type (p=0.14) on THM-CFU removals were noted while it was the opposite for HAA-UFC which were observed to be better removed under warm than cold water temperatures (p=0.02) and using alum as opposed to ferric chloride (0.03).

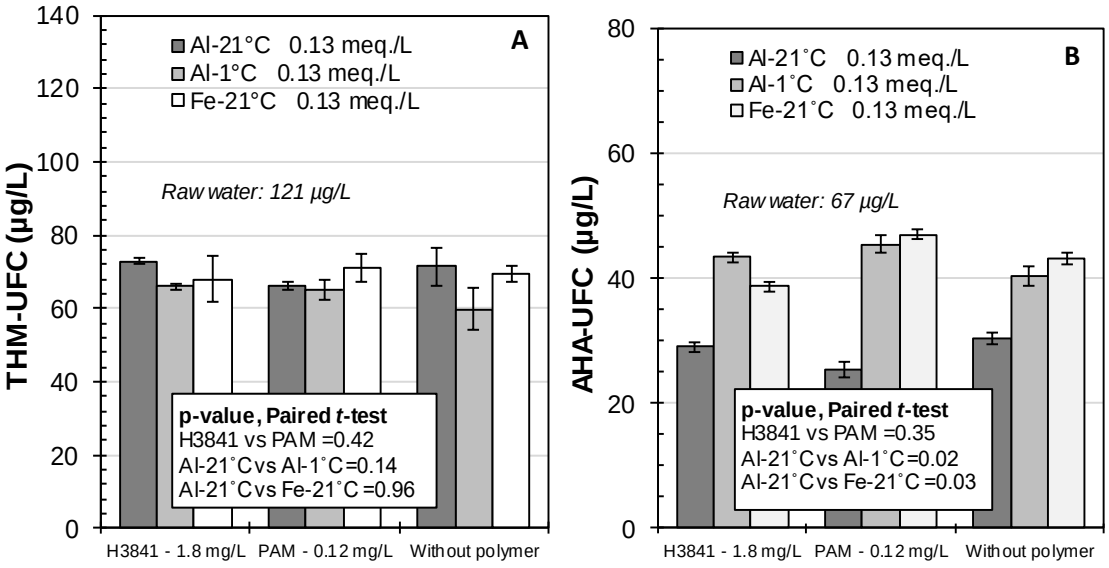

Figure 5.10: (A) THM-UFC (B) and HAA-UFC formation in filtered waters using different coagulant/polymer combinations. Conditions: Microsand=4 g/L, *G* during flocculation =165 s^{-1}, filtered on 0.45 µm membrane. Error bars indicate the 95th centile confidence intervals.

5.4 Discussion

5.4.1 Optimal polymers dosage and properties

During coagulation-flocculation, particles are generally removed by two main mechanisms: charge neutralization and inter-particle bridging. With anionic high molecular weight polymers, bridging is potentially the principal mechanism for particles trapping . Bolto et Gregory (2007) demonstrated the importance of selecting the appropriate MW and CD polymer to optimize flocculation kinetics and particle trapping. As coagulant aids or flocculants, polymers with high MW and low CD offer better performance. A low negative CD assures the expansion of polymer chain and gives an opened structure considered ideal for flocculation using the bridging mechanism (Somasundaran & Moudgill, 1988). Contrary to a high negative CD, using a low CD does not create significant repulsion between polymer chain and negative particles. This theory suggests that there is an optimal CD for each type of water, depending of the specific charge of residual particles after coagulation and the ionic strength.

PAM, having a tendency to be polymerized in a more linear structure than starch, leads to longer polymer chains and higher MW up to several million (Caskey & Primus, 1986). For flocculation

using principally bridging mechanism, the length of chain is an important factor (Bolto & Gregory, 2007) and could explain the need for using higher dosage of starch polymer. Replacing PAM with H3841 will have probably no significant impact on the global costs since the costs of polymer applied during flocculation are less than 1% of the total chemicals costs typically observed in conventional plant (i.e. including coagulation, flocculation, settling, filtration and chlorine disinfection). Despite the differences in dosage, H3841 and PAM showed similar and adequate SW turbidities. Performances were better with alum than ferric chloride. This outcome may have resulted from the lower amount of microflocs formed with alum compared to ferric salts. Lower performances of $FeCl_3$ concerning turbidity removal were also detailed by Matilainen et al., (2010)

5.4.2 Optimal microsand dosage, ballast media size and velocity gradient

Young et Edwards (2000) showed that microsand is not part of a chemical reaction and is rather included in the floc by contact and differential momentum during flocculation. Therefore, the optimal sand dosage is strongly related to raw water turbidity, coagulant dosage and polymer dosage which will all influence the final amount of flocs formed. This study highlighted the importance of microsand concentration and notably the importance of microsand size distribution. Young et Edwards (2000) have also noted that an over dosage of microsand may lead to a slightly increased SW turbidity. Starch polymers performance was improved by the use of a microsand smaller than 100 µm; otherwise incorporation of microsand in the floc structure was problematic. This conclusion is similar to the work published by Sibony (1981) who recommended the use of microsand with a diameter between 20 µm and 100 µm. For low turbidity waters such as the one tested in this study, this author recommends using a range of 40 µm to 80 µm for particles removal. Others authors have also suggested a grain diameter smaller than 160 µm to optimize the supernatant quality (De Dianous & Dernaucourt, 1991). In the review of Thomas et al. (1999) on flocculation, these authors highlighted that hydrodynamic repulsion between large and small particles reduces collision efficiencies. Over a certain particle diameter, more specifically expressed as the ratio of $R/\sqrt{k}$ (R: aggregate radius and k: aggregate permeability), the collision efficiency is close to zero . Furthermore, large microsand may generate substantial shear leading to floc breakage. Consequently, the present study indicates that reduced microsand dosages up to 75% (i.e. entirely eliminating the microsand bigger than 100 µm) might be achieved by using a smaller microsand, a benefit that would especially advantage the starch-based polymer.

Another advantage related to the use of a smaller microsand relates to the reduced power needed during flocculation. The ballasting agent, in this case the microsand, is heavier than flocs and is enmeshed into the floc by inertial forces . The power induced during ballasted flocculation must be greater than for conventional flocculation in order to maintain the sand in suspension. Therefore, the resistance of polymers to shear is important to prevent aggregates' rupture. Starch polymers were shown to be less resistant to shearing than PAM, probably due to the higher molecular weight of PAM which favors inter-particle bridging. Reducing the microsand diameter improved the performance of the starch-based polymer and also allowed operating at a lower mixing energy. It is therefore advisable to revisit ballasted flocculation conditions while operating with activated starch polymers.

5.4.3 Temperature effect

It is well known that alum hydrolysis can be significantly slowed down at low water temperatures (Duan, Jinming & Gregory, 2003). The latter also give rise to an irregular floc structure reducing potentially its shear strength. However, it was shown that PAM compensated the poor turbidity removal from alum at 1˚C and the global clarification process was not impacted by these extreme conditions. It was also the case when starch polymer was employed as flocculant. However, H3841 needed a slightly higher dosage (0.4 instead of 0.3 mg/L) in cold water to compensate for non-settleable particles left from alum and to achieve a good SW turbidity (0.4 NTU).

Alum performance for DOC removal was improved under low temperature. The minimal point of solubility for Al species is increased by one pH unit when temperature drops from 25˚C to 5˚C (Driscoll & Letterman, 1988; Duan, Jinming & Gregory, 2003). For the coagulation conditions in this study (initial pH of 8.0), an increased presence of positive alum hydrolysis products would be expected at low temperature, a benefit that favored the higher DOC removal observed.

5.4.4 Impacts on filtered water quality

Activated starch polymers were responsible for a slight release of BDOC in filtered waters. This carbon release explained the small gap of performances between PAM and starch polymer concerning the overall DOC removals. The current assays did not include the use of biological filters. BDOC from starch polymers could potentially have a beneficial side effect for plant using biological filtration. Yavich et al. (2004) described the benefits of bio-stimulants like acetate or

others simple carbon chain for biomass fixed on a media. This may have a significant impact for carbon removal specifically for raw water having initially low content of easily assimilable carbon. More studies are needed to evaluate the removal of residual starch by heterotrophic biomass present in a granular biofiltration.

Although slight differences in DOC removals were observed between both polymer types, this result did not translate into differences in THM or HAA formation. Chlorinated disinfection by-product formation was only dependent on the coagulation conditions (especially for HAA precursor removals). Some authors already indicated that starch is not considered to be a significant THM precursor (Crane, Kovacic, & Kovacic, 1980; Hong, Mazumder, Wong, & Liang, 2008)

5.5 Conclusion

The general aim of this paper was to evaluate the potential of starch-based polymers to replace PAM in flocculation process. This study revealed that this specific activated starch polymers offer a good alternative to polyacrylamide. However, its integration in a ballasted flocculation is subjected to new design considerations and previous typical procedure should be revised to enhance the process performance and account for the specific properties of these polymers. Lower velocity gradient (<250 s^{-1}) and smaller microsand (< 100) µm are considered to be the key elements to consider for the design of improved ballasted flocculation involving starch polymers. Future work should evaluate the fate of residual starch-based polymers in granular media and membrane filtration.

Acknowledgments

The authors acknowledge Veolia, especially Edith Laflamme and Gilles Delaisse, who provided the activated starch polymers developed by Veolia and valuable technical information concerning them. These experiments were conducted as part of the Industrial-NSERC Chair in Drinking Water (Polytechnique Montreal) research program which benefits from the financial support from the City of Montreal, John Meunier Inc. and the City of Laval.

CHAPITRE 6 ARTICLE 4 - DUAL STARCH–POLYACRYLAMIDE POLYMER SYSTEM FOR IMPROVED FLOCCULATION

Au chapitre précédent, il a été mentionné que des concentrations relativement élevées de polymère d'amidon étaient nécessaires afin d'égaler les enlèvements de turdidé obtenus par l'entremise du PAM. Dans le but de réduire les doses requises d'amidon, mais sans toutefois affecter la taille des flocs et l'abattement de turbidité, cet article, publié dans *Water Research*, propose une combinaison synergique amidon-PAM. Cette synergie s'appuie sur le principe à partir duquel les polymères de plus faibles poids moléculaires, tels que l'amidon, sont en mesure d'amorcer l'agrégation et qu'une très faible dose de PAM à haut poids moléculaire est nécessaire afin de compléter la maturation des flocs. Toutefois, dans ce genre de système, le PAM n'est que partiellement remplacé par l'amidon; des monomères d'acrylamide, certaines impuretés issues de la fabrication de ces produits et divers sous-produits (provenant de l'interaction avec un oxydant *e.g.,* le chlore ou l'ozone) peuvent donc persister dans les eaux traitées. Néanmoins, leur concentration en est considérablement réduite puisque pour certains systèmes, il a été possible de remplacer près 70 % du PAM par de l'amidon.

Dual starch–polyacrylamide polymer system for improved flocculation

Mathieu Lapointe[1]* *and Benoit Barbeau*[1]

[1] Industrial NSERC Chair on Drinking Water, Department of Civil, Geological and Mining Engineering, Polytechnique Montreal, Montreal, Quebec H3C 3A7, Canada

*Corresponding author e-mail: mathieu.lapointe@polymtl.ca

Abstract

Organic polyelectrolytes such as polyacrylamide (PAM) are commonly used in the water industry to improve flocculation. However, potential adverse health effects may arise from the use of PAM owing to the presence of trace acrylamide monomers in commercial products. Hence, there is growing interest in replacing synthetic polyelectrolytes with natural and sustainable alternatives, which would eliminate risks related to the presence of toxic monomers/impurities and oxidation by-products from the interaction of polymers and common disinfectants such chlorine and ozone. Starch-based flocculants are recognized to offer fairly good flocculation performance, but require higher polymer dosages than conventional high-molecular-weight PAM. To reduce exposure to acrylamide monomers, this study examined the combination of an activated starch-based polymer with PAM to determine whether synergistic effects can be achieved using a dual polymer system. Flocculation performance (floc size, density and rate of aggregation) was monitored using jar tests. Turbidity removal was also assessed to confirm settling performance. Single PAM/starch mixture injection and sequential dual polymer injection were compared in order to simplify practical industrial applications. For the tested samples of surface water and wastewater, jar tests showed that the PAM dosage can be significantly reduced (50–70% for surface water) for both conventional and ballasted flocculation if a dual starch–PAM polymer system is used.

Keywords: *Dual flocculation; polyacrylamide; starch, turbidity removal; acrylamide toxicity; floc size*

6.1 Introduction

Organic polyelectrolytes are commonly used in the water industry to improve the performance of gravitational separation processes (Aguilar et al., 2005; Gregory & Barany, 2011). However, potential adverse health effects may arise from the use of polyacrylamide (PAM) or acrylamide sodium acrylate owing to the presence of trace acrylamide monomers in commercial products

(Bolto & Gregory, 2007; Fielding, 1999; Mallevialle, Bruchet, & Fiessinger, 1984), which are considered potentially toxic and carcinogenic (Johnson, K. A. et al., 1986; Rice, 2005). Japan, Switzerland, Spain, the USA, the UK, Germany, and France have already forbidden or restricted the use of some polyelectrolytes, including PAM, for drinking water applications. According to the NSF/ANSI 60 standard, PAM concentrations are limited to 1 mg/L based on a lifetime cancer risk of 10^{-5} for PAM with an acrylamide concentration of 0.05%. Under such a scenario, the theoretical concentration of injected acrylamide monomers would be equivalent to 0.5 µg/L (USEPA, 2009), assuming that acrylamide is not removed during conventional treatment. On the other hand, the European standard authorizes a maximal acrylamide concentration of 0.1 µg/L (EN-1407), limiting the dosage to 0.5 mg/L for PAM with an acrylamide concentration of 0.02%. Polymer restrictions have also been put in place because of their ecotoxicity. For example, cationic PAM tends to sorb on fish gills (*Pimephales promelas*), causing suffocation (Biesinger & Stokes, 1986). Finally, polyacrylic acids, polystyrene sulfonic acids, and PAM are synthetized from nonrenewable oil-based materials and are considered hardly biodegradable (Xing et al., 2010).

Considering the numerous limitations listed above, there is growing interest in replacing synthetic polyelectrolytes with natural and sustainable alternatives, which would eliminate the risks related to the presence of toxic monomers/impurities (*e.g.* acrylamide, acrylic acid, hydroxypropionitrile and isobutyronitrile, Mallevialle et al. (1984)) and oxidation by-products from polymers interacting with disinfectants (e.g. formaldehyde (< 50 ug/L) from the interaction of PAM and ozone; chloroform (< 2 ug/L) or formaldehyde (< 40 ug/L) from the interaction of PAM and chlorine (Fielding, 1999)). Such products have already been proposed in the early 1990s (Kawamura, 1991) and demonstrated to be viable substitutes to synthetic products. Among the frequently mentioned substitutes, starch-based (Xing et al., 2010) or chitosan-based flocculants (Lu, Y. et al., 2011) are recognized to offer fairly good flocculation performance. However, the use of activated starch in flocculation systems requires higher polymer dosages than the use of conventional high-molecular-weight (MW) PAM (3–5 times higher) (Gaid & Sauvignet, 2011; Lapointe & Barbeau, 2015). Starch-based polymers have a more branched structure than the linear PAM configuration and hence have smaller chain lengths that reduce aggregation via interparticle bridging. Moreover, activated starch flocs have been shown to be more sensitive to shear than flocs produced with PAM (Lapointe & Barbeau, 2015).

To reduce exposure to acrylamide monomers, it is possible to use high-purity PAM products with lower acrylamide monomer contents. Another option is to replace PAM using an alternative flocculant. A third option, which has received minimal attention, is to use lower PAM dosages in combination with an alternative flocculant. For example, some utilities have successfully used activated silica in combination with PAM. However, to the best of our knowledge, no studies have tested the combination of PAM with activated starch. This study examines the combination of an activated starch-based polymer with PAM to determine whether a synergistic effect can be achieved using a dual polymer system. It is hypothesized that activated starch can be first injected to initiate aggregation, leading to small flocs. In a second step, floc maturation could be completed with very low PAM dosages to form large aggregates. This strategy would limit acrylamide monomer concentrations in treated water. In addition, the option of injecting both polymers simultaneously was investigated. This scenario is of interest, as it would simplify full-scale process operations (only one injection point would be needed) as well as polymer preparation (only one polymer preparation system could be used). To investigate flocculation performance, jar tests were used to monitor floc size, density and rate of aggregation. Turbidity removal was also examined to confirm settling performance.

6.2 Materials and methods

6.2.1 Water characteristics

All experiments were conducted at the lab-scale using either (i) surface water (SW) from the Pont-Viau water treatment plant (21 NTU, pH 7.0), which is fed by the Des Prairies River (Quebec, Canada) or (ii) municipal wastewater (WW) from the Repentigny (Quebec, Canada) water resource recovery facility (81 NTU, pH 8.4; collected after the 6 mm influent bar screens). Floc size and density were characterized during flocculation by direct microscopic observation (Olympus DP70 camera connected to an Olympus BX51 optical microscope for measurements of a counting cell with a depth of 2 mm) as described by Lapointe et Barbeau (2016). This method enables to evaluate the floc fraction composed of ballast media. A camera (time exposure: 1/1000 s, FlocCAM^{TM}) was installed on a square jar test beaker (2 L, Phipps and Bird^{TM}) to evaluate the rate of floc aggregation. Finally, turbidity measurements were carried out on raw and settled water samples at various settling times (Turbidimeter, Hach 2100N, SM 2130 B) (APHA et al., 2012).

6.2.2 Jar test procedure

Water samples were flash mixed (velocity gradient (G) = 300 s^{-1}) for 2 min at 21°C with alum. Alum dosages of 3.64 mg Al/L (0.40 mEq/L) and 12.73 mg Al/L (1.41 mEq/L) were identified as optimal (based on settled water turbidities) for SW and WW, respectively. The respective pH values after settling of SW and WW were 6.2 ± 0.1 and 8.0 ± 0.1. As illustrated in Figure 6.1, two flocculation strategies were tested, referred to hereafter as split injection and simultaneous injection. In the split injection procedure (Figure 6.1A), preflocculation was initiated by dosing with a starch polymer (Hydrex 3842, a moderate-high-MW (< 10^6) polymer with low anionic charge density (2.40 meq/g) over 2 min (G = 165 s^{-1}). The starch dosage was equally divided: 50% at the onset of preflocculation and 50% after 1 min. Silica sand with d_{50} of 160 µm was also injected at time 0 during this preflocculation phase as a weighting agent to increase floc size and density. A mixing intensity of 165 s^{-1} has previously been established by Lapointe et Barbeau (2015) as the optimal mixing intensity for silica sand with d_{50} of 160 µm. The second step, termed maturation, was initiated by injecting PAM at t = 2 min (Hydrex 3551, a very-high-MW (10^6-10^7) polymer with low anionic charge density (2.52 meq/g)) while maintaining agitation for an additional 2 min (end of preflocculation; G = 165 s^{-1}). Similar to the procedure used during preflocculation, PAM was also dosed in two steps (50% at the onset of maturation (t = 2 min) and 50% at mid-maturation (t = 3 min)). In the simultaneous treatment strategy (Figure 6.1B), 50 % of PAM and starch dosages were simply injected at 0 min and 1 min of flocculation, which was conducted for a total duration of 4 min at 165 s^{-1} (i.e., identical mixing conditions as for the split treatment). Settling was performed for only 1 min, which is sufficient to remove ballasted flocs. Optimal polymer dosages were established based on the targeted residual turbidity in settled water: <1 NTU for drinking water and <3 NTU for WW. If these objectives were not achieved, the optimal dosage was established by identifying the point of diminishing return in the turbidity vs dosage curves.

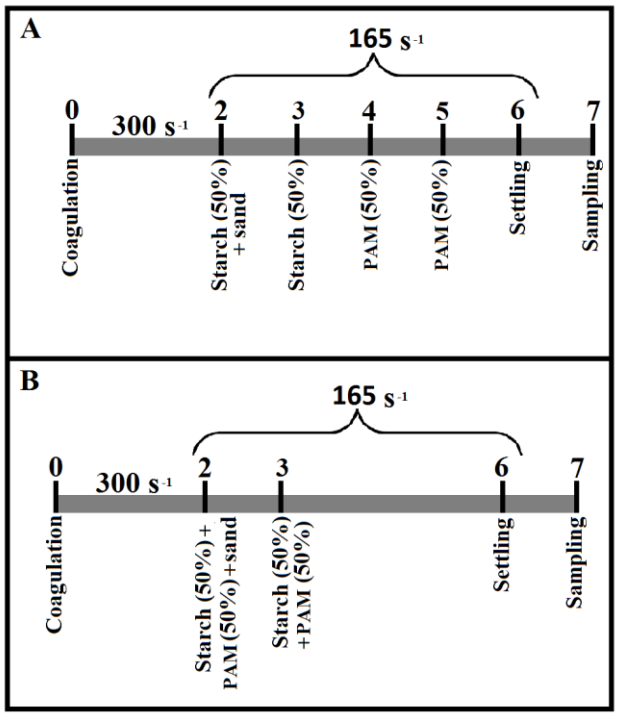

Figure 6.1: Jar test sequence for coagulation, flocculation, and settling. (A) Split polymer injection and (B) simultaneous polymer injection.

6.3 Results

6.3.1 Polymer efficiency for particulate matter removal

The individual performances of PAM and starch are compared in Figure 6.2 for a flocculation time of 4 min. For SW (Figure 6.2A), the starch dosage required to obtain a suitable settled water turbidity was 14 times higher than that of PAM (4.46 mg starch/L vs 0.32 mg PAM/L). For WW (Figure 6.2B), the starch/PAM ratio was approximately 66 (18.36 mg starch/L vs 0.28 mg PAM/L). All optimal polymer dosages were established based on the criteria mentioned in section 6.2.2. The observed starch/PAM ratios are significantly higher than the typical ratios of 3:1 to 5:1, which is partially caused by the aggressive flocculation conditions tested (4 min flocculation + 1 min settling).

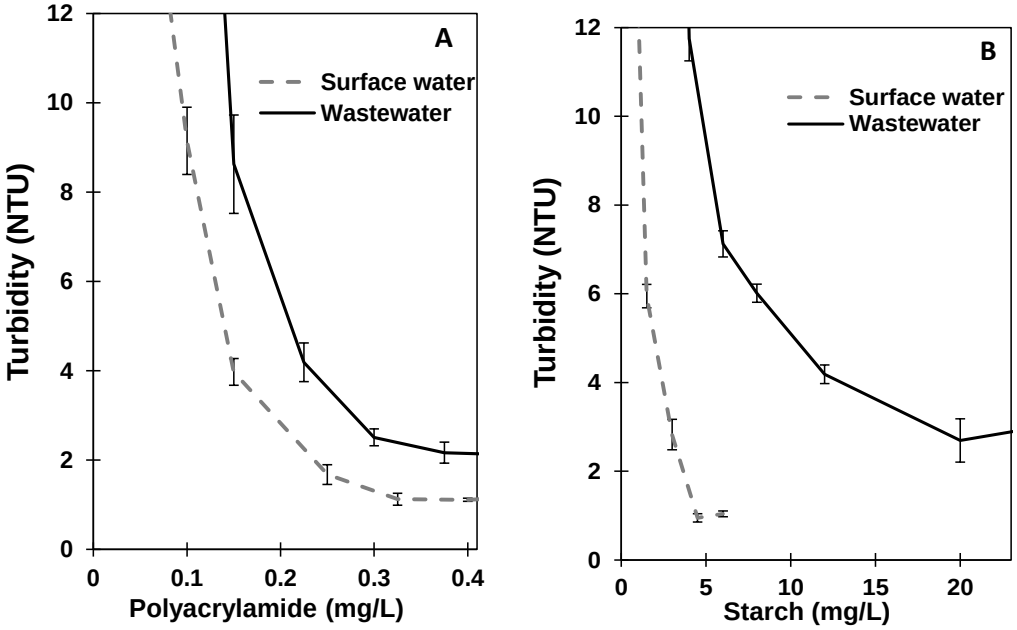

Figure 6.2: Optimal polyacrylamide (A) and starch (B) dosages at 21°C. Surface water flocculation: 4 min at 165 s^{-1} with 3 g silica sand/L. Wastewater flocculation: 4 min at 165 s^{-1} with 5 g silica sand/L. Error bars correspond to the standard deviation (2 replicates).

6.3.2 Impact of dual polymer split injection on turbidity removal

The performance of split injection of PAM/starch is presented in Figure 6.3. A synergistic effect was observed for both water types (SW and WW). Using a relatively low starch concentration (0.40 mg/L) permitted reduction of the PAM dosage by more than three times for SW (from 0.32 to 0.10 mg PAM/L) and by almost two times for WW (from 0.28 to 0.15 mg PAM/L). Under these split injection conditions, the targeted turbidity removals were achieved (<1 NTU for SW and <3 NTU for WW). For dosages of starch above 0.4 mg/L, no additional gain was observed upon dosing PAM. For example, increasing the starch dosage from 0.4 to 2.0 mg/L did not significantly improve the performance of the dual polymer split injection strategy.

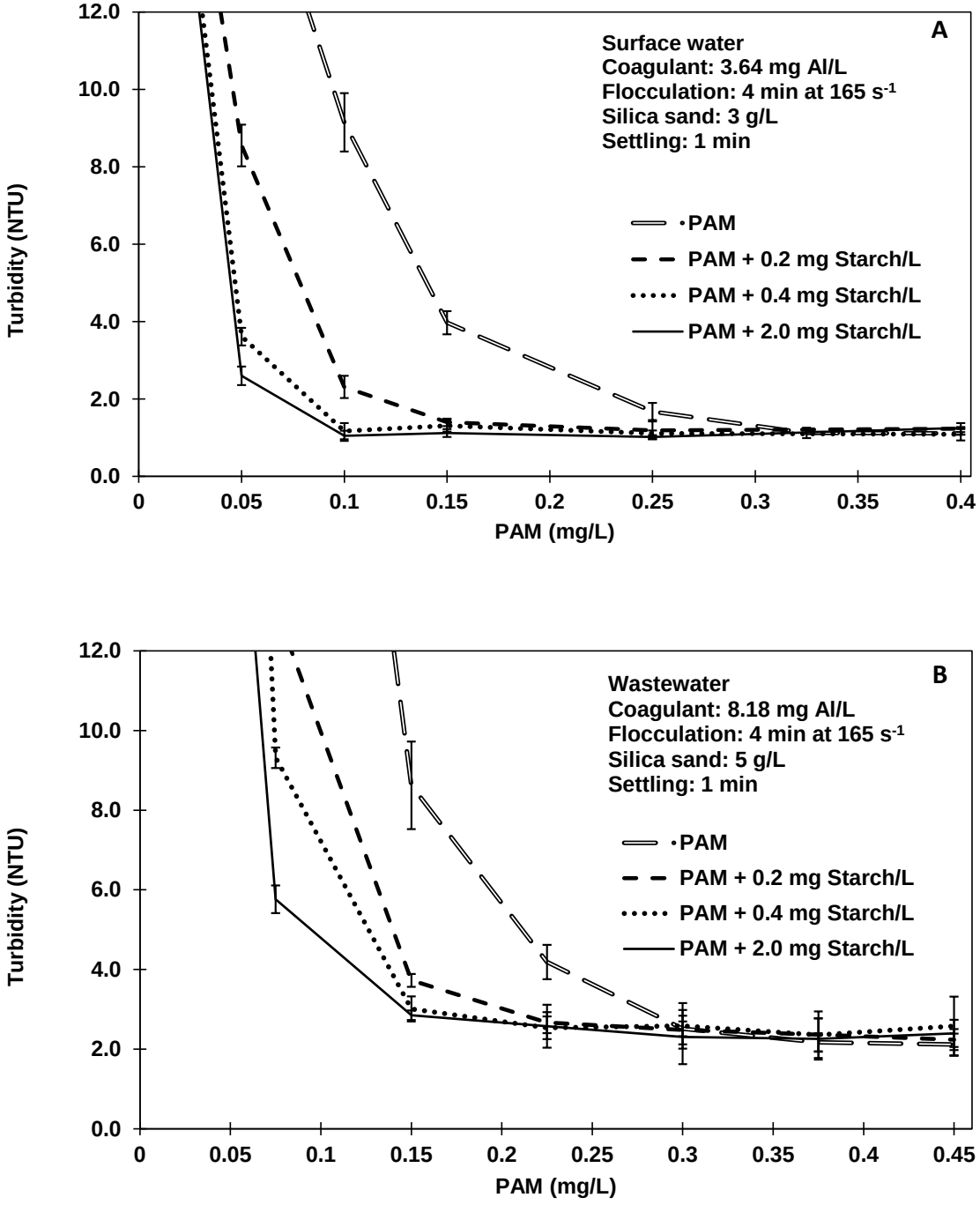

Figure 6.3: Reduction of polyacrylamide (PAM) dosage compensated for by increasing starch dosages during ballasted flocculation/settling of surface water (A) or wastewater (B) at 21°C. Error bars correspond to the standard deviation (2 replicates).

6.3.3 Preflocculation with starch during split injection: Impact on floc size

The floc size distribution was measured during preflocculation with starch. As a reference, the floc size distribution obtained with alum used alone is presented. Under these conditions of high shear ($G= 165\ s^{-1}$), small flocs are produced since no polymer is used to connect the microfloc structure by interparticle bridging mechanisms. Figure 6.4 demonstrates the impact of starch dosage on floc size. Images obtained with a camera (FlocCAM^{TM}) and visual inspection revealed that although floc growth was noticeable, silica sand was not incorporated adequately into the floc structure, especially at the lowest starch dosages (0.2 mg starch/L). The offset between the 0.4 and 2.0 mg starch/L curves in Figure 6.4 is attributable to initiation of silica sand aggregation onto/into the floc matrix at 2.0 mg starch/L. Despite the low aggregation of starch and silica sand at low starch dosages, its use as a preflocculant proved to be beneficial for reducing PAM dosages during maturation, as has been shown previously. The best synergy between the polymers was observed when adding only 0.2–0.4 mg starch/L. For these starch dosages, PAM reductions of approximately 53–69% for SW and 22–47% for WW were achieved.

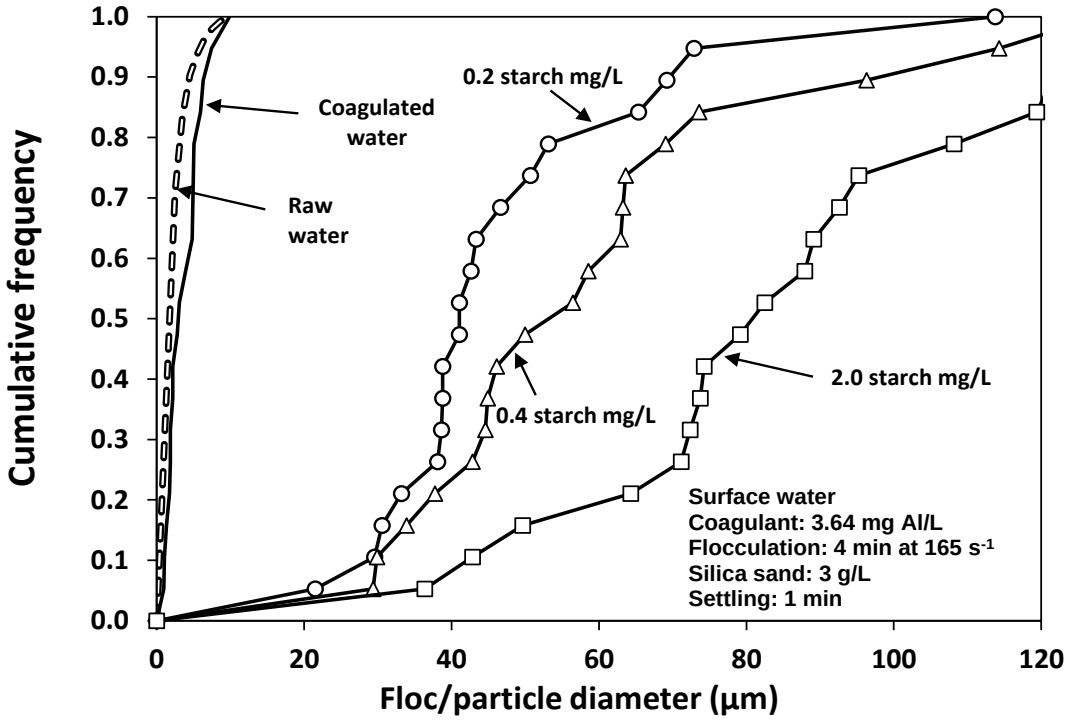

Figure 6.4: Impact of starch dosage on floc size distribution after 2 min of preflocculation of surface water at 21°C.

6.3.4 Impact of dual polymer split injection on aggregation kinetics

The aggregation kinetics for various polymer dosages are presented in

Figure 6.5A. To compare the rate of ballasted floc formation, the floc size was monitored during preflocculation (0–2 min) and during floc maturation (i.e., after PAM injection, 2–4 min). A reference condition was also tested with PAM used as a unique flocculant. When PAM was used alone and injected at time 0, a plateau proportional to the PAM dosage was reached after 4 min of maturation. The obtained mean floc diameters were 257 ± 9 µm (0.05 mg/L), 395 ± 25 µm (0.15 mg/L), 497 ± 34 µm (0.25 mg/L) and 539 ± 21 µm (0.40 mg/L). In comparison, the dual polymer split injection strategy (0.30 mg starch/L + 0.05 mg PAM/L) generated flocs with a mean diameter of 510 ± 17 µm. By interpolation, this result corresponds to a unique dosage of 0.30 mg PAM/L. An assay with a dosage of 0.30 mg starch/L as a unique flocculant is also illustrated in

Figure 6.5A as a reference. The dosage of PAM, although very low (0.05 mg/L), was essential to flocculate properly when a dual system was used.

Figure 6.5B compares the performance of dual polymer injection (0.05 mg/L PAM + 0.30 mg/L starch) for conventional (i.e., without silica sand injection) and ballasted flocculation. As a reference, performance of 0.05 mg/L of PAM as a unique flocculant is also provided. In this example, the combined starch–PAM system increased the mean floc size by 28% (from 231 µm to 295 µm) and 99% (from 257 µm to 510 µm) for conventional and ballasted flocculation, respectively. The higher synergistic effect observed for ballasted flocculation is attributable to the incorporation/adsorption of silica sand into the floc structure. Finally, a comparable mean ballasted floc specific gravity was measured for PAM (1.32 ± 0.11) and the dual system (1.28 ± 0.08).

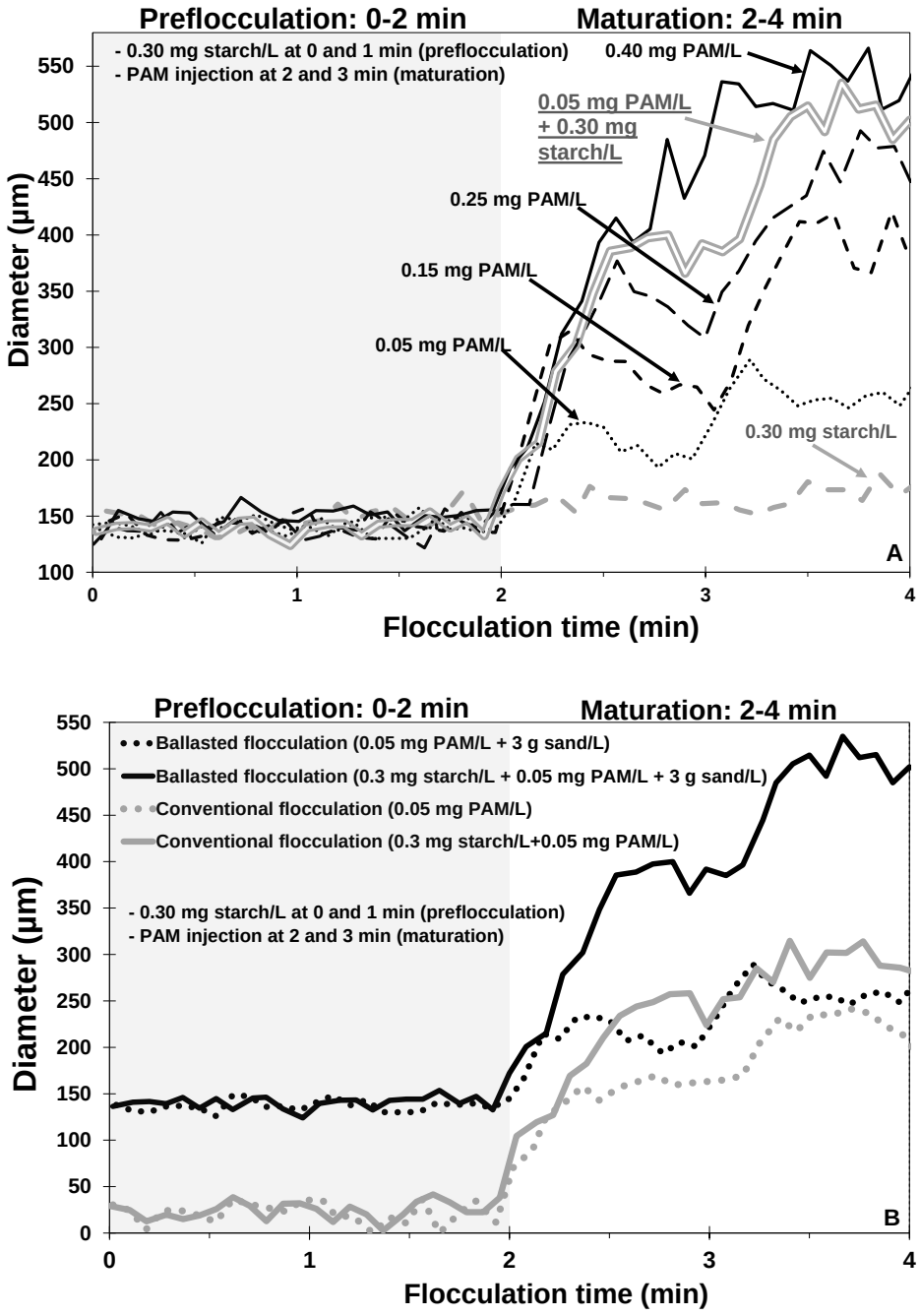

Figure 6.5: Impact of dual polymer split injection and polyacrylamide as a unique flocculant on aggregation kinetics and floc size at 21°C (A). Impact of the dual polymer split injection system on ballasted and conventional flocculation (B). Conditions for surface water: ballast media: 3 g/L and flocculation = 4 min at 165 s^{-1}.

6.3.5 Floc resistance to shearing

To quantify floc resistance under higher shear conditions, turbidity removal in settled water was evaluated under optimal coagulant/polymer dosages for *G* values from 100 to 400 s^{-1} (165 s^{-1} having been established as optimal for ballasted flocculation using silica sand (160 µm)) (Figure 6.6). Overall, the dual polymer split injection strategy (0.4 mg starch + 0.1 mg PAM/L; this starch/PAM ratio of 4 was selected from Figure 6.3A to minimize the PAM dosage) and PAM alone achieved similar resistances. For the range of *G* values evaluated, the difference between the two polymer dosing strategies was not statistically significant (p-value = 0.12, paired *t*-test).

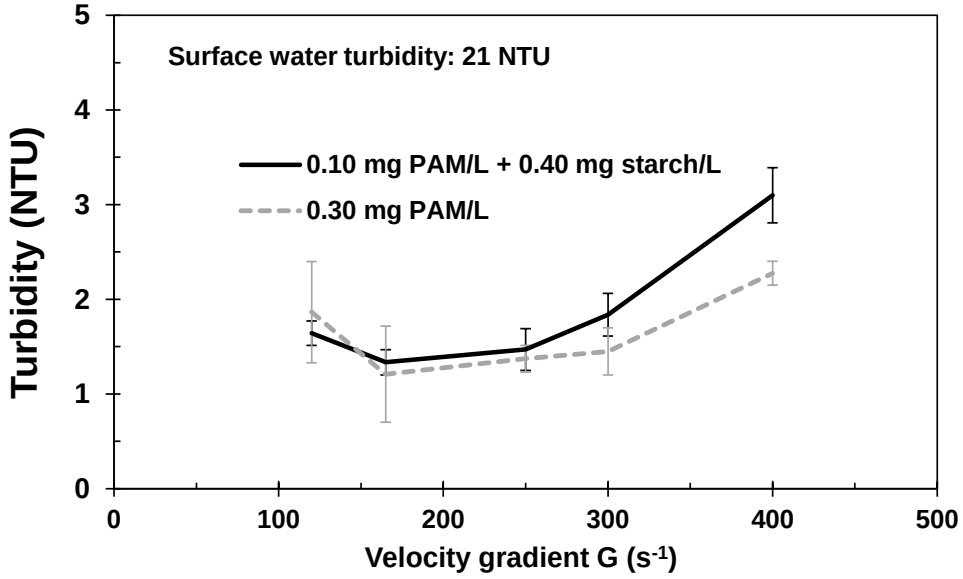

Figure 6.6: Floc resistance for ballasted flocculation with polyacrylamide and the dual polymer split injection strategy. Conditions for surface water: coagulant = 3.64 mg Al/L, temperature = 21°C, and flocculation = 4 min. Error bars correspond to the standard deviation (2 replicates).

6.3.6 Impact of settling time on particulate matter removal

Settling rates were compared by measuring turbidity vs time profiles under various polymer injection strategies for ballasted flocculation (Figure 6.7A) and conventional flocculation (Figure 6.7B). Single injections of 0.3 mg/L of starch resulted in low settling rates and low doses of PAM were also suboptimal. However, the combination of 0.05 mg/L of PAM with 0.30 mg/L of starch provided a performance equivalent to a dosage of 0.30 mg/L of PAM alone (p-value = 0.16). Similar trends were observed for conventional flocculation (Figure 6.7B), with the main difference

being that lower settling rates were achieved in the absence of silica sand. For conventional flocculation, there was also no difference between 0.30 mg PAM/L and 0.05 mg PAM/L + 0.30 mg starch/L (p-value = 0.35).

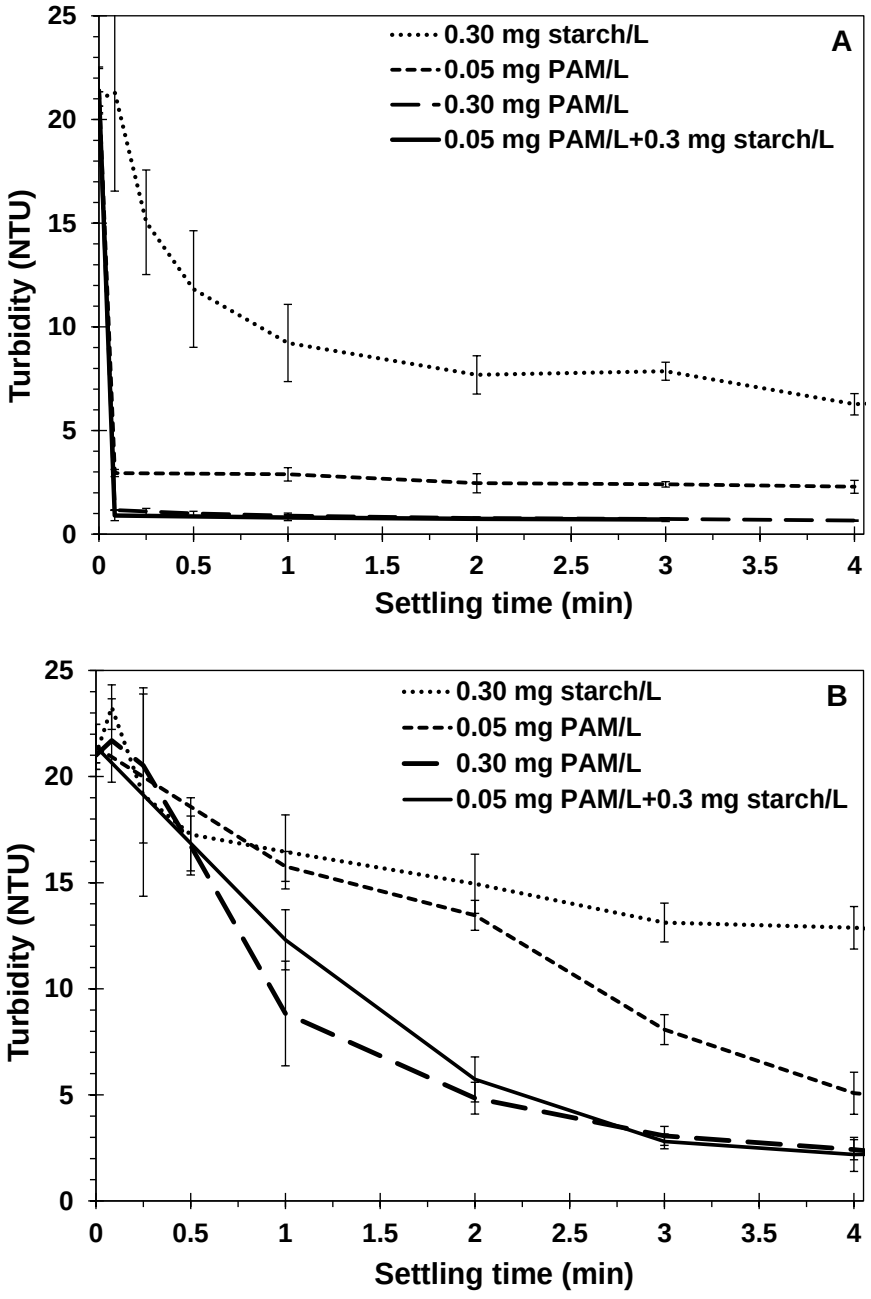

Figure 6.7: Turbidity removal during settling for (A) ballasted flocculation and (B) conventional flocculation with polyacrylamide or the dual polymer split injection strategy. Conditions for surface water: coagulant = 3.64 mg Al/L, temperature = 21°C, and flocculation = 4 min at 165 s^{-1}. Error bars correspond to the standard deviation (2 replicates).

6.3.7 Comparison of dual polymer split injection and single injection strategies

The dual polymer split injection strategy was useful for identifying the role of both flocculants in the overall process performance. For practical industrial applications, a single injection point to inject a mixture of PAM/starch would be the simplest option to implement. To ensure complete reaction between polymers and particles and to limit competition between starch and PAM chains during flocculation, the polymers were sequentially injected, i.e., starch before PAM. This injection method allowed independent evaluation of the contribution of each polymer during aggregation. However, the settled water turbidities were similar for both split and simultaneous polymer injection: 1) PAM injected before starch (0.71 ± 0.08 NTU), 2) PAM and starch injected simultaneously (0.74 ± 0.09 NTU), and 3) starch injected before PAM (0.62 ± 0.06 NTU).

6.4 Discussion

The MW and polymer charge density are known to be factors that control the performance of flocculation (Bolto & Gregory, 2007). Longer polymer chains lead to better interparticle bridging, which explains why, at equivalent dosages, PAM was more efficient than starch for turbidity removal and floc growth. However, the preaggregation phase with starch allowed the required PAM dosage to be greatly reduced. At low dosages, starch was not able to bridge precoagulated microflocs (<20 µm) with silica sand (d_{50} = 160 µm). However, starch produced intermediate unballasted flocs (20–120 µm), hence initiating the aggregation process. This process could explain why a reduced PAM dosage was sufficient to complete aggregation. Such complimentary effects between two flocculants have been observed previously (Aguilar et al., 2005; Fan, A. et al., 2000; Yu, X. & Somasundaran, 1996). By using a low-MW polymer (polyacrylic acid) followed by a high-MW cationic copolymer (PAM and a quaternary acrylate salt), Fan, A. et al. (2000) showed the importance of the floc size formed during preaggregation. Flocs previously formed during this phase reduced the total particles surface to destabilize, thereby reducing the dosage of PAM required to complete aggregation via bridging mechanisms. Alternatively, starch used during preflocculation could also act as a site blocking agent, allowing increased availability of PAM chains for interparticle bridging (Gregory & Barany, 2011).

The synergy between starch and PAM allowed starch to partially replace PAM. However, a minimal PAM dosage significantly improved the overall process performance. In this study,

maximal PAM dosage fractions of 69% and 45% were substituted by starch for the tested SW and WW samples, respectively. This substitution did not affect the turbidity removal and floc size. To reduce the PAM dosage further, the MW of the starch polymer used during preflocculation could be increased, as proposed by Fan, A. et al. (2000).

The starch/PAM ratio and minimal PAM dosage were more important factors for obtaining proper flocculation than the timing of polymer injection, as no significant difference was observed between polymer coaddition and sequential addition. Others studies have also noted the marginal role of the polymer injection sequence (Fan, A. et al., 2000; Lemanowicz, Gierczycki, & Al-Rashed, 2011). To minimize the number of injection points, both polymers should ideally be mixed together, with a suitable starch/PAM ratio for simultaneous injection. This option is estimated to be more expensive than the use of PAM alone, but the cost of polymers dedicated to flocculation is typically less than 1% of the total chemical cost for conventional treatment processes. Hence, considerable reduction of PAM could be accomplished at a low cost. This study also demonstrated the possibility of PAM dosage reduction for ballasted or conventional flocculation and for SW or WW applications without impacting floc size, settling kinetics, or turbidity removal. The ballasted floc specific gravities (with silica sand) were also similar for both strategies (1.28 ± 0.08 in this study and 1.29 ± 0.06 in Lapointe et al. (2017)).

The floc resistance to shear is of concern for full-scale applications where nonhomogeneous shearing is observable in the flocculation tank. However, under a wide range of *G* values, the dual polymer system produced equivalent settled water turbidity, suggesting that the floc structure was sufficiently resistant despite the considerable reduction of PAM. The lower floc resistance of the dual polymer system was noticeable when *G* was higher than 300 s^{-1}, which could be explained by the weaker bonds between particles achieved by starch in comparison with those achieved by PAM alone. Nevertheless, for the typical mixing conditions applied for ballasted flocculation (165 s^{-1} in Lapointe et Barbeau (2016)), both strategies exhibited similar particle removal performances. However, such a polymer combination could be problematic for systems requiring higher mixing intensities, e.g., during ballasted flocculation with magnetite sand, which requires a *G* of 255 s^{-1} (Lapointe et al., 2017).

6.5 Conclusion

The tested starch polymer was less efficient than PAM for turbidity removal while operating under aggressive flocculation (4 min)/settling (1 min) conditions. However, dual injection of PAM and starch permitted important reductions in PAM dosage without impacting flocculation kinetics, floc size and specific gravity, settling rate, turbidity removal or floc resistance to shearing. More specifically:

- The PAM dosage was reduced by 53% (SW) or 22% (WW) when 0.2 mg starch/L was injected. The PAM dosage was reduced by 69% (SW) or 45% (WW) when 0.4 mg starch/L was injected.
- The floc resistance was not impacted by the use of the dual polymer system for the typical G values (165–200 s^{-1}) used in ballasted flocculation with silica sand.
- PAM usage can be significantly reduced for both conventional and ballasted flocculation if a dual polymer system is used owing to synergy between PAM and starch.
- The injection sequence is not a critical parameter. Therefore, a starch–PAM blend solution could be used for polymer coaddition to simplify the preparation and injection of the polymers.

Further work on the influence of pH on aluminum hydroxide–starch complexes should be carried out in order to achieve further reductions or complete replacement of PAM, as it has been shown that starch can also replace PAM, albeit at higher dosages. Additionally, the impact of using a starch–PAM blend on membrane fouling and granular filter head loss should be investigated. A dual polymer system could also be used to reduce PAM usage in sludge thickening/dewatering processes.

Acknowledgements

These experiments were conducted as part of the Industrial NSERC Chair in Drinking Water (Polytechnique Montreal) research program, which benefits from the financial support of Veolia Water Technologies Canada, Inc., the City of Montreal, the City of Laval, the City of Repentigny, and the City of Longueuil. Experiments were conducted at CREDEAU, a research infrastructure supported by the Canadian Foundation for Innovation and the Ministry of Education of Quebec.

CHAPITRE 7 ARTICLE 5 - SUBSTITUTING POLYACRYLAMIDE WITH AN ACTIVATED STARCH POLYMER DURING BALLASTED FLOCCULATION

Dans le chapitre précédent, les désavantages liés à l'utilisation du PAM n'étaient que partiellement contournés; entre 20-70 % du PAM étant remplacé par l'amidon. Dans ce présent chapitre, le PAM est entièrement remplacé par un polymère anionique à base d'amidon activé. Afin de réduire l'écart de performance entre les polymères synthétiques et naturels, les conditions d'opérations ainsi que les propriétés optimales du média lestant ont été identifiées. Un pH entre 6 et 6,5, un sable de petite taille (<100 µm) composé majoritairement de SiO^2 ainsi qu'une intensité de mélange optimale font partie des principaux éléments permettant la réduction des doses de floculants. L'effet de ces conditions optimales combinées était toutefois encore plus exacerbé sur les polymères à base d'amidon. L'article 5 a été soumis dans *Journal – American Water Works Association.*

Substituting polyacrylamide with an activated starch polymer during ballasted flocculation

Mathieu Lapointe[1] and Benoit Barbeau[1]*

[1] Industrial NSERC Chair on Drinking Water, Department of Civil, Geological and Mining Engineering, Polytechnique Montreal, Montreal, Quebec H3C 3A7, Canada

*Corresponding author e-mail: mathieu.lapointe@polymtl.ca

Abstract

Synthetic polymers, mostly polyacrylamides (PAM), are frequently used in the water industry to improve the performance of clarification. However, synthetic polymers may increase headloss in granular media filters, biodegrade slowly, and are potentially toxic. Alternatively, bio-sourced starch-based polymers may eliminate the drawbacks of synthetic flocculants. It is already known that starch, like many other polysaccharide flocculants, is required in higher dosages for its performance to be comparable to PAM. This study identified all of the conditions favorable to the use of an activated starch polymer as an alternative to PAM during ballasted flocculation: mixing intensity and time, coagulation pH, ballast size and chemical composition, and polymer charge density. Ultimately, under optimal conditions, only 0.66 mg of activated starch/L was required to reach the settled water turbidity objective of 1 NTU.

***Keywords**: starch, polyacrylamide, ballasted flocculation, turbidity removal, acrylamide toxicity, floc size*

7.1 Introduction

Synthetic polymers, mostly polyacrylamides (PAM), are frequently used in the water industry to improve the performance of conventional clarification (Aguilar et al., 2005; Gregory & Barany, 2011), ballasted flocculation (Lapointe & Barbeau, 2015, 2016), upflow sludge blanket clarifiers (Mouchet & Bonnelye, 1998), and sludge dewatering (Chen, Y., Yang, & Gu, 2001). However, synthetic polymers may increase headloss in granular media filters (Zhu, H. et al., 1996). These phenomena result from the presence of unsettled microflocs that contain high molecular weight polymer chains. For over twenty-five years, many polysaccharide-based polymers were suggested as being economical, efficient, and eco-friendly flocculants, including corn or potato starch, guar gum, cellulose, sodium alginate, and tannin (Kawamura, 1991; Lee, C. S., Robinson, & Chong, 2014; Sharma et al., 2006). Moreover, bio-sourced polymers may eliminate some of the drawbacks

associated with synthetic polymers frequently used in the water industry: 1) the risk related to the presence of residual toxic monomers of acrylamide from PAM (Bolto & Gregory, 2007; Mallevialle et al., 1984; Rice, 2005), 2) the formation of oxidation by-products from the interactions between monomers and polymers and impurities in the manufactured products and various oxidants (Fielding, 1999), 3) the low biodegradability of synthetic petroleum-based polymers (Xing et al., 2010), and 4) the ecotoxicity of many cationic polyelectrolytes (Biesinger & Stokes, 1986). As a consequence, many countries, particularly in Europe, have forbidden or restricted the use of synthetic polyelectrolytes such as PAM for drinking water applications (Letterman & Pero, 1990). In the case of PAM, maximal dosages are governed by American and European standards that allow a maximal acrylamide monomer concentration of 0.5 µg/L (NSF/ANSI 60) and 0.1 µg/L (EN-1407) in treated water, respectively. Therefore, maximal dosages are product-specific as they depend on the purity of the commercial PAM.

Due to the aforementioned constraints, there is a growing interest in eliminating or drastically reducing the use of synthetic polyelectrolytes. Although polysaccharides-based flocculants have been recognized to offer fairly good flocculation performance (Kawamura, 1991), the dosages required for starch (Lu, Y. et al., 2011) or chitosan (Xing et al., 2010) were higher than for PAM. In ballasted flocculation applications, the required starch dosages were also shown to be higher in comparison to synthetic PAM polymers: 3–5 times higher (Gaid & Sauvignet, 2011; Lapointe & Barbeau, 2015), 2–10 times higher (Wang, D., 2018), and more than 10 times higher under more aggressive flocculation conditions (Lapointe & Barbeau, 2017). Starch-based polymers chains are shorter and have a more branched structure compared to the linear PAM configuration, which reduces their ability to aggregate particles via interparticle bridging. Additionally, flocs produced with activated starch polymers are more fragile and more sensitive to shearing compared to flocs produced with PAM (Lapointe & Barbeau, 2015). Consequently, starch polymers are more efficient when smaller ballast media (BM) are used due to the lower mixing intensity required to keep them in suspension (Lapointe & Barbeau, 2015; Lapointe et al., 2017). There is also an interest in identifying alternative polymers that are able to improve solid settling and retention in the filter media while simultaneously limiting headloss in the granular media filters.

The general objective of this study was to identify all of the conditions favorable to the use of an activated starch polymer as an alternative to PAM during ballasted flocculation. It is known that activated starch flocculation benefits from a lower shear mixing to reduce floc breakage. As mixing

conditions during ballasted flocculation are intimately linked with the BM characteristics (size and density), we investigated the interdependence of these two factors with regard to ballasted flocculation and settling performance. More specifically, assays were conducted under variable mixing conditions using various BM sizes and chemical compositions (*i.e.* the different oxide groups at the BM surface). The influence of coagulation pH, flocculation time, and polymer charge density was also investigated. Assays with PAM were always performed as a reference condition. Hence, this study hypothesized that starch dosages under such optimal mixing conditions could be notably lowered without impacting turbidity. To compare flocculation performance with both polymers, jar tests and microscopic flocs analysis were used to monitor floc size and the rate of aggregation. Turbidity measurements were also assessed to confirm the settling performance before and after the flocculation optimization.

7.2 Material and methods

7.2.1 Waters characteristics and analytical methods

All jar tests experiments were performed at the laboratory scale (21±1°C) using surface water from the Pont-Viau drinking water treatment plant (turbidity of 6 ± 1 NTU; pH of 7.0 ± 0.1; UV absorbance at 254 nm of 0.25 ± 0.1 cm^{-1}), which is fed by the Prairies River (Quebec, Canada). The tested surface water exhibited a relatively low alkalinity (36 ± 3 mg $CaCO_3$/L) and a high dissolved organic carbon (DOC) concentration (7.1 ± 0.5 mg C/L). The raw water was refrigerated at 4°C prior to its use. The temperature was equilibrated to 21°C before the start of the experiments. The analytical methods used to characterize the water samples and flocs are presented in Table 7.1.

Table 7.1: Monitored parameters and associated analytical methods

Parameters	*Units*	*Methods*
Alkalinity	mg $CaCO_3$/L	SM 2320 B. (APHA et al., 2012), Mettler Toledo DL28 Electrometric Titrator
Turbidity	NTU	Turbidimeter, Hach 2100N, SM 2130 B. (APHA et al., 2012)
UVA_{254}	cm^{-1}	Settled waters filtered on a pre-washed 0.45 µm PES Supor®-450 membrane (Pall) (APHA et al., 2012)
DOC	mg C/L	Sievers 5310c total organic carbon analyzer, GE Water, SM 5310 C. (APHA et al., 2012)
Floc size	µm	1) Modified 2 mm depth counting cell (Sedgwick Rafter # 1801-G20) Camera (Olympus DP70) Optical microscope (Olympus BX51) Equivalent diameter method, Lapointe et Barbeau (2016) 2) FlocCam™ camera, described in Lapointe et Barbeau (2017)

7.2.2 Jar test procedure

Water samples were first flash-mixed (*G* of 300 s^{-1}) for 2 min at room temperature (21 ± 1°C). To assess the influence of coagulation (*i.e.* suboptimal vs. sweep coagulation) on PAM and starch performance, two very different coagulation scenarios were tested in this study: 1) alum: 2.7 mg Al/L (0.30 meq/L; pH = 5–8) and ferric sulfate: 12.5 mg Fe/L (0.67 meq/L; pH = 5–8). The jar test sequence and sampling protocol are presented in Table 7.2. Jar tests were performed in the Phipps & Bird™ apparatus (Richmond, VA) equipped with six square B-Kers™ jars of 2 L, with each possessing a sampling port located 10 cm from the top. The BM was entirely injected at the onset of flocculation (*i.e.*, after the 2-min flash-mix). Flocculation times varying from 10 s to 8 min were tested. The flocculant dosage was equally divided into 50% at the onset of flocculation and 50% at mid-flocculation. This injection sequence is typically used to improve floc size at the end of flocculation since it allows for floc regrowth at mid-flocculation. Turbidity measurements were assessed on settled waters after 180 s of settling. The range of *G* tested (135–195 s^{-1}) was selected based on typical conditions induced during a full-scale ballasted flocculation with silica sand (Lapointe & Barbeau, 2016).

Hydrex^{TM} 3511, 3551, 3553 (anionic), and Hydrex^{TM} 3613 (cationic) polymers (Veolia Water Technologies Canada), very high molecular weight PAM (~ 10^7), were compared to Hydrex^{TM} 3841, 3842 (anionic), and Hydrex^{TM} 3807 (cationic) (Veolia Water Technologies Canada), high molecular weight activated starch polymers (~ 10^6). In terms of molecular structure, starch-based polymers are known to adopt a ramified structure (Bratskaya, Svetlana et al., 2005). In contrast, acrylamide monomers are typically polymerized as linear structures.

Table 7.2: Jar test procedure simulating ballasted flocculation with silica sand

Conditions	***Coagulation***	***Flocculation***	***Settling***
Time	2 min	10 s–8 min	3 min
Velocity gradient	300 s^{-1}	135–195 s^{-1}	-
Coagulant	Alum or Ferric sulfate	-	-
Flocculant	-	Polyacrylamide or Starch	-
Ballast media	-	Silica sand	-
pH	5–8		

Both polymers were subjected to comparative jar tests to determine their capacity to form ballasted floc and remove turbidity. Among the critical factors for the coagulation-flocculation process, the following were separately tested: pH, coagulant types (aluminum or ferric based coagulant), polymer charge density, flocculation time, mixing intensity, mineral composition of the BM, the BM adsorption surface (expressed as m^2 of BM/L), and the BM size. The BM adsorption surface was determined by the BM total external surface injected during the flocculation (Lapointe & Barbeau, 2018a). Optimal polymer dosages were established through interpolation of the turbidity vs. polymer dosage curves to reach 1 NTU after settling, a value that reflects strong performance according to water treatment plants using ballasted flocculation.

7.2.3 Ballast media characterization

Two different types of silica sand with a specific gravity between 2.60–2.67 were tested in this study. To avoid the effect of size during the media comparison, both media grain size distributions were adjusted to obtain a d_{50} of 143 ± 4 µm and a uniformity coefficient (UC) of 1.9. The impact

of three BM d_{50} on turbidity removal was found to be 72, 90, and 143 µm. BM composition was analyzed to identify the different oxides (SiO_2, Al_2O_3, CaO, MgO, Fe_2O_3, Na_2O, K_2O, and MnO) by means of a lithium metaborate ($LiBO_2$) fusion (6 g $LiBO_2$/g of oxide, fused at 1000°C during 15 min; Ingamells (1970)) or by hydrofluoric acid (HF) dissolution (0.87 g HF/g silica oxide; Potts (2012)) and then quantified by atomic absorption (Perkin Elmer; AAnalyst^{TM} 200). The mineral compositions are presented in Table 7.3.

Table 7.3: Element weight percentage for sand 1 and sand 2

Elements (wt %)	*Sand 1*	*Sand 2*
SiO_2 [1]	93.6	98.7
Al_2O_3	2.3	0.3
CaO	0.9	1.0
MgO	0.1	0.1
FeO	0.1	0.1
Na_2O	0.1	0.1
K_2O	2.1	0.3
MnO	0.0	0.0
Total	**99.2%**	**100.5%**

[1] Dissolved in hydrofluoric acid

7.2.4 Floc monitoring

A non-intrusive camera (FlocCAM^{TM}; time exposure: 1/500 s) was directly installed on a jar test beaker to measure the floc size growth and breakage during flocculation (Lapointe & Barbeau, 2017). Floc size and rate of aggregation were also confirmed through optical microscopy (Olympus DP70 camera connected to an Olympus BX51 optical microscope; 100X) with a counting cell depth of 2 mm, as described in Lapointe et Barbeau (2016).

7.3 Results and discussion

7.3.1 Impact of pH on floc size and turbidity removal

The current knowledge about organic polyelectrolytes suggests that the aggregation kinetic is primarily controlled by the polymer molecular weight and its charge density (Bolto & Gregory, 2007; Gregory & Barany, 2011; Laskowski et al., 2007). However, the influence of pH on metal hydroxides species has been documented (Duan, Jinming & Gregory, 2003; Wesolowski & Palmer, 1994) and, because hydrogen bonding is involved, it is anticipated that coagulated particles and the polymer chain interactions and adsorption affinities will also be controlled by the nature of these metal hydroxides ($Me(OH)_{+2}$, $Me(OH)^{2}_{+}$, $Me(OH)^{3}_{(s)}$, and $Me(OH)^{4-}$) and by polynuclear species (Liu, Q., Zhang, & Laskowski, 2000).

When a ferric coagulant is used, both polymers were optimized for a pH between 6.0–6.5 (

Figure 7.1). For both polymers, more alkaline conditions (pH > 7.5) were considered to be detrimental as they drastically reduced both the floc diameter and turbidity removal. For a dosage of 1.5 mg starch/L, the settled water turbidity was 0.9 NTU and 2.9 NTU for a pH of 6.4 and 6.9, respectively. A similar pH impact was noted for PAM, although to a lesser extent since settled water turbidity increased from 0.2 NTU to 1.5 NTU for a pH increase from 6.4 to 6.9. Similar conclusions were made when considerably different coagulation conditions were tested using only 2.7 mg Al/L (data not shown). In such case, the optimal pH range was narrower (5.7–5.9) and the settled water turbidity (2.5 NTU) was higher when starch was used in suboptimal coagulation conditions. The largest floc sizes were achieved with the ferric coagulant in the pH range of 6.0–6.5 (

Figure 7.1A). However, the ferric flocs formed with starch were significantly smaller in comparison with PAM, despite dosages that were tenfold higher: 246 µm with 2 mg starch/L vs. 477 µm with 0.2 mg PAM/L (pH: 6.5), respectively. The results concerning the floc size are partly attributable to the polymer molecular weight, which is discussed in the following section.

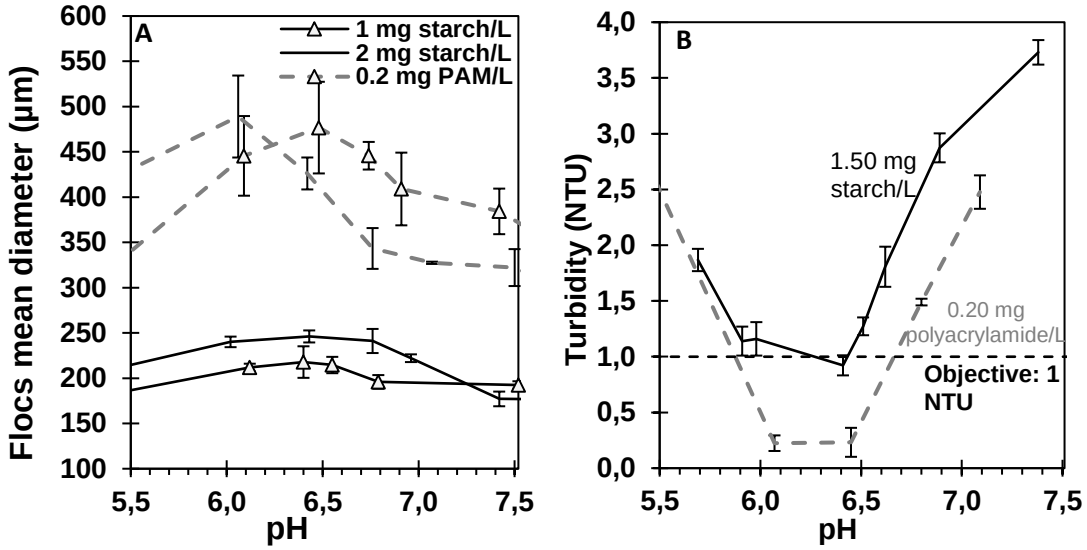

Figure 7.1: Impact of coagulation pH on floc size (A) and the settled water turbidity (B). Coagulation: 12.5 mg Fe/L at 300 s^{1}. Flocculation: 1 min with 5 g sand 1/L at 165 s^{-1}. Settling: 3 min. The error bars correspond to the standard deviation.

7.3.2 Impact of the polymer charge density and molecular weight

The difference in turbidity removal between activated starch and PAM is likely attributable primarily to the polymer molecular weight. Previous studies have reported the importance of this factor on the aggregation kinetic, floc size, floc stability, and resistance to shearing (Bolto & Gregory, 2007; Fan, A. et al., 2000; Mabire, Audebert, & Quivoron, 1984). The polymer molecular configuration has also been reported to have an impact on the effective length of polymer chains that are able to connect particles through interparticle bridging (Lapointe & Barbeau, 2017). Starch is known to be less effective for such reasons. However, no study has evaluated the impact of the starch charge density during ballasted flocculation. The impact of the polymer charge density on turbidity removal for both types of polymers is presented in this section. As shown in Figure 7.2, a slightly anionic charge density between 2.4 and 0.4 mEq/g (corresponding to approximately 18% to 3% of the negatively charged monomers) in the case of PAM and around 1.9 mEq/g in the case of starch were established as optimal. In comparison, when a low cationic polymer was used rather than a low anionic polymer, the settled water turbidity was negatively affected as it increased by 30% for starch (from 1.04 NTU to 1.35 NTU) and 105% for PAM (from 0.19 NTU to 0.39 NTU).

In the case of PAM, it could be argued that any of the tested polymers could be selected by the water utility as they all met the target of 1 NTU in settled waters. Such observations and behavior, where an inadequate charge density caused an unfavorable polymer chain reconfiguration leading to the reduction of polymer chain bridging capacity, were also reported by Gregory et Barany (2011) and Bolto et Gregory (2007). Nevertheless, the studies confirmed that there is an optimal charge density for each polymer type that is influenced by the coagulant type, the pH, and the water characteristics, among other factors (Bolto & Gregory, 2007; Nasser & James, 2006).

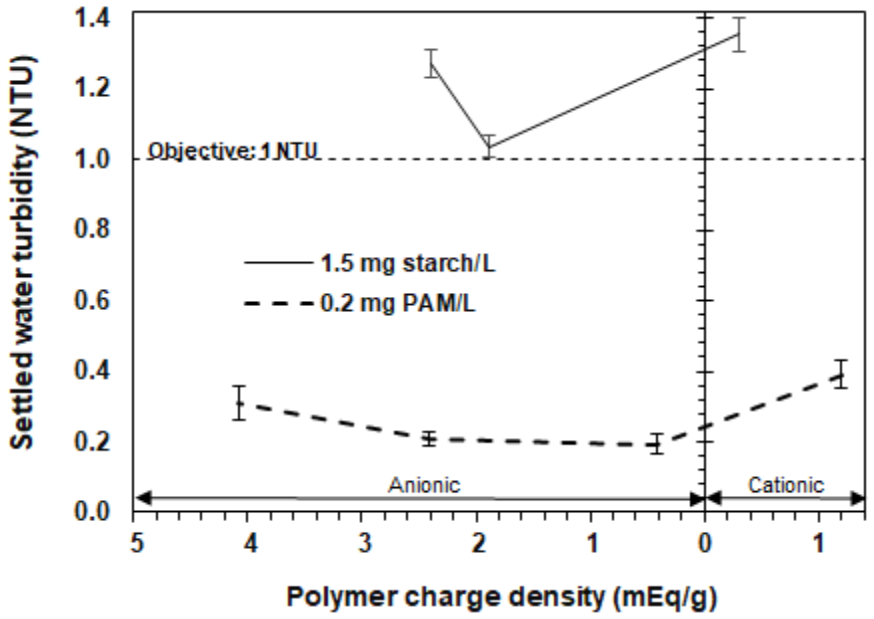

Figure 7.2: Impact of polymer charge density on settled water turbidity. Coagulation: 12.5 mg Fe/L (pH: 6.5) at 300 s^{-1}. Flocculation: 8 min with 5 g sand 1/L at 165 s^{-1}. Settling: 3 min. The error bars correspond to the standard deviation.

7.3.3 Impact of flocculation time on turbidity removal and floc size

The aggregation kinetic between the polymer chain and a given particle can be expressed as a second-order reaction (*i.e.* higher particle and polymer concentrations will lead to a higher aggregation rate) (Gregory & Barany, 2011). Gregory (1988) states that the required time to adsorb a particle onto a polymer chain is inversely proportional to the effective size of the polymer. The starch polymer required approximately 5 min to reach 1 NTU while the PAM needed less than 2

min (Figure 7.3B). Nonetheless, both polymers benefited from a longer flocculation time (8 min) as the settled water turbidity was 0.80 and 0.21 NTU for starch and PAM, respectively. The mean floc diameter was simultaneously measured during these experiments (Figure 7.3A). It is clearly evident that the maximal floc size for both polymers was reached after only 4 min of flocculation (364 µm for starch and 580 µm for PAM). Moreover, a longer flocculation time of 8 min caused a floc size reduction for both polymers (342 µm for starch and 552 µm for PAM). This could be associated with the extended shearing of the floc structure or unfavorable chain reconfiguration as both phenomena lead to floc restructuration or disaggregation (Bolto & Gregory, 2007). This observation indicates that floc size may not be the best parameter, when used individually, to predict clarification performance as better turbidity removal was observed at 8 min even though smaller flocs were formed under these conditions. It is hypothesized that the better turbidity removal at 8 min can be explained by the aggregation of smaller particles or microflocs either onto or into the existing ballasted floc. These microflocs would not impact the average diameter but would be observable during a turbidity analysis.

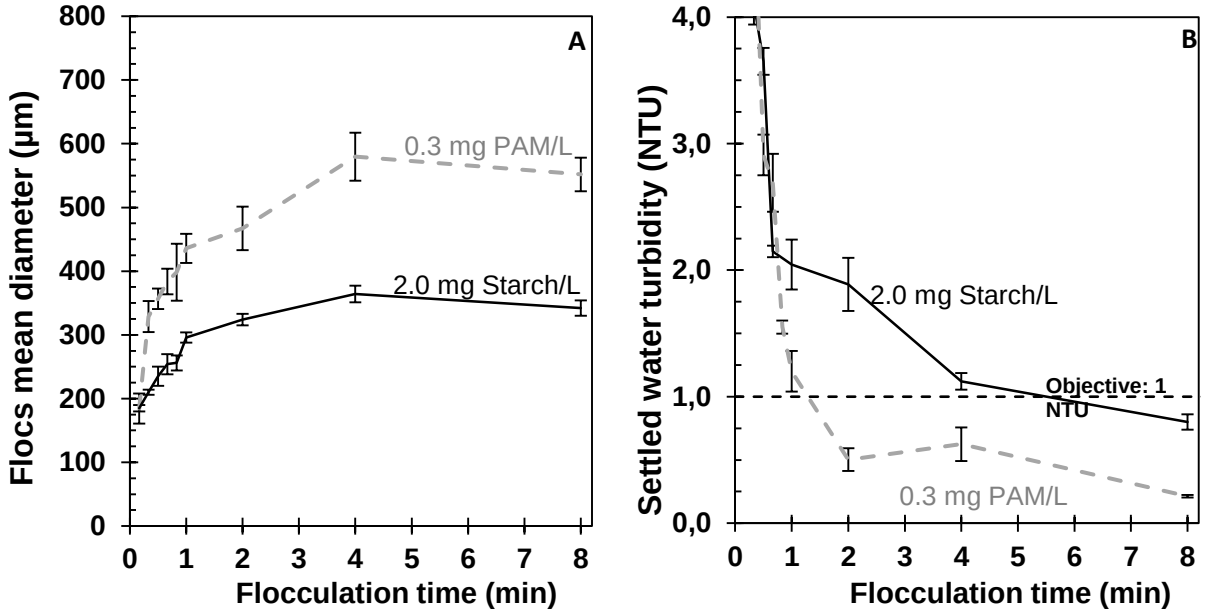

Figure 7.3: Impact of flocculation time on (A) mean floc size and (B) settled water turbidity. Coagulation: 12.5 mg Fe/L (pH: 6.5) at 300 s^{-1}. Flocculation: 10 s to 8 min with 5 g sand No1/L at 165 s^{-1}. Settling: 3 min. The error bars correspond to the standard deviation.

7.3.4 Floc resistance to shearing

In this section, the impact of velocity gradient on turbidity removal was evaluated to confirm the optimal mixing conditions (Figure 7.4). In the case of starch, the optimal value was 165 s^{-1} (0.65 NTU). In Lapointe et Barbeau (2016) the higher settled water turbidity values under non-optimal *G* were attributable to ballasted floc disaggregation. In the current study, PAM was less sensitive to shearing for the *G* range tested (135–195 s^{-1}), a conclusion similar to that observed in our previous study (Lapointe & Barbeau, 2015) where PAM was only impacted at a mixing intensity higher than 300 s^{-1}. Generally, for ballasted flocculation, the optimal mixing conditions are determined by two factors: the need to maintain the BM in suspension and limit the floc disaggregation that occurs due to shearing forces (Lapointe et al., 2017).

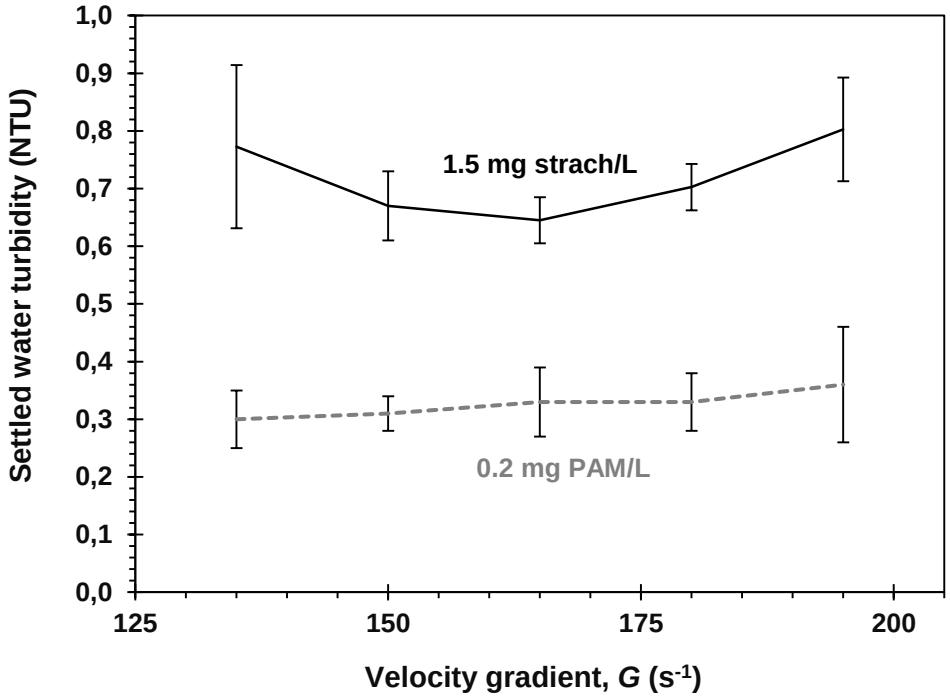

Figure 7.4: Velocity gradient (*G*) impact on settled water turbidity. Coagulation: 12.5 mg Fe/L (pH: 6.5) at 300 s^{-1}. Flocculation: 8 min with 5 g sand 2/L and *G* between 135–195 s^{-1}. Settling: 3 min. The error bars correspond to the standard deviation.

7.3.5 Impact of sand mineral composition on turbidity removal and floc size

Besides the previously mentioned factors, the BM mineral composition may have an impact on the floc-BM interactions and adsorption affinities. To evaluate this effect, the performance of ballasted flocculation was assessed for two types of sand with different origins but identical size distribution (d_{50} = 143 µm; UC of 1.9). By using sand No 1 (wt%: 93.6% of SiO_2; see section 7.2.3), the dosages required for the polymer to reach 1 NTU (determined by interpolation and extracted from Figure 7.5) were found to be 1.86 mg for activated starch/L vs. 0.068 mg PAM/L (ratio starch/PAM = 27). With sand No 2, the latter being almost exclusively composed of SiO_2 (wt%: 98.7%), the required dosages for both polymers were considerably reduced, but more notably for starch (0.66 mg of starch/L vs. 0.047 mg PAM/L (ratio starch/PAM = 14). By using sand No 2 as an alternative to sand No 1, the starch and PAM dosages required to reach 1 NTU after settling were reduced by 64% and 31%, respectively. Moreover, the mean floc diameter after 8 min of flocculation, using 2.0 mg/L starch, was increased by 16% (342 ± 10 µm with sand No 1 vs. 396 ± 12 µm with sand

No 2 (*t*-test; p=0.002)). In neutral pH, it was reported that polysaccharide-based polymers and PAM have a higher affinity (expressed in mg of polymer/m^2 of oxide) with aluminum or ferric oxides compared to silica oxides (Lee, L. T. et Somasundaran (1989); Liu, Q. et al. (2000)). The higher polymer adsorption on aluminum oxides covering sand No 1 could influence the chain configuration onto the oxides surface, thus reducing the length of the effective polymer chain responsible for the interparticle bridging.

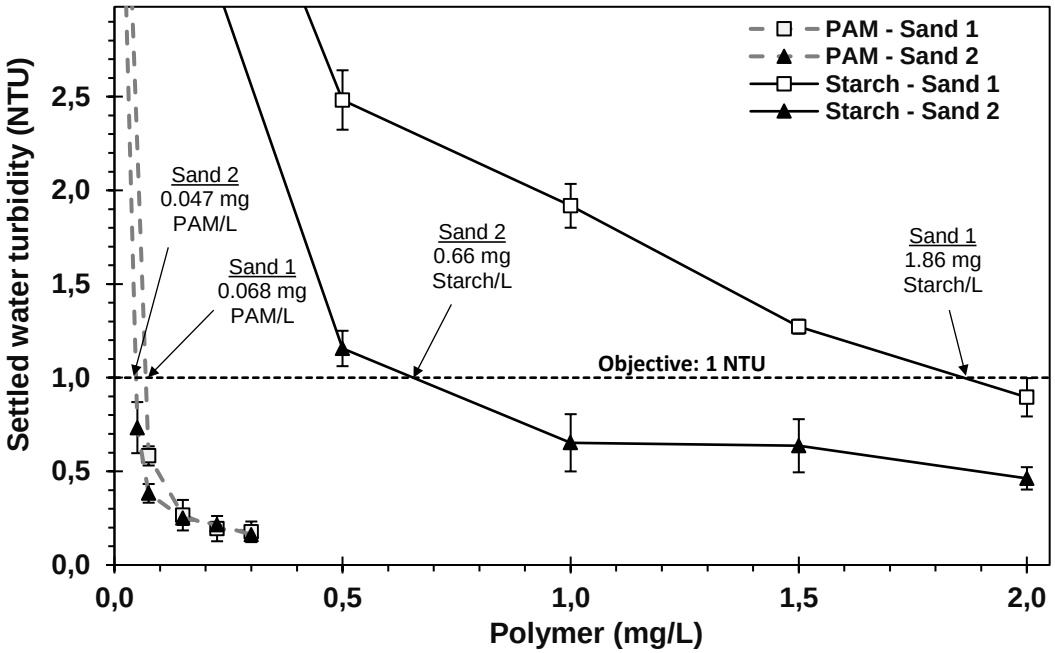

Figure 7.5: Impact of sand 1 vs. sand 2 on settled water turbidity. Coagulation: 12.5 mg Fe/L (pH: 6.5) at 300 s^{-1}. Flocculation: 8 min with 5 g sand/L at 165 s^{-1}. Settling: 3 min. The error bars correspond to the standard deviation.

7.3.6 Impact of ballast media size on turbidity removal

The influence of the BM size on turbidity removal using starch is examined in this section. The initial raw media material was sieved to collect three different sizes with mean diameters of 72, 90, and 143 µm. For both types of sand, a smaller BM achieved lower settled turbidity, the latter being inversely proportional to the grain size. When sand No 2 was used as BM (shown in Figure 7.5), lower turbidity values (*t*-test; p=0.04) were observed (0.49, 0.52, and 0.77 NTU; Figure 7.6) compared to those measured with sand No 1 (0.69, 0.78, and 1.31 NTU; Figure 7.6) for the respective BM diameters mentioned above. A higher solid removal with a smaller BM is explained

by two phenomena: a smaller BM 1) is easily embeddable into the floc structure (Lapointe & Barbeau, 2016) and 2) offers a higher BM adsorption surface for an equivalent BM mass concentration (Lapointe & Barbeau, 2018a).

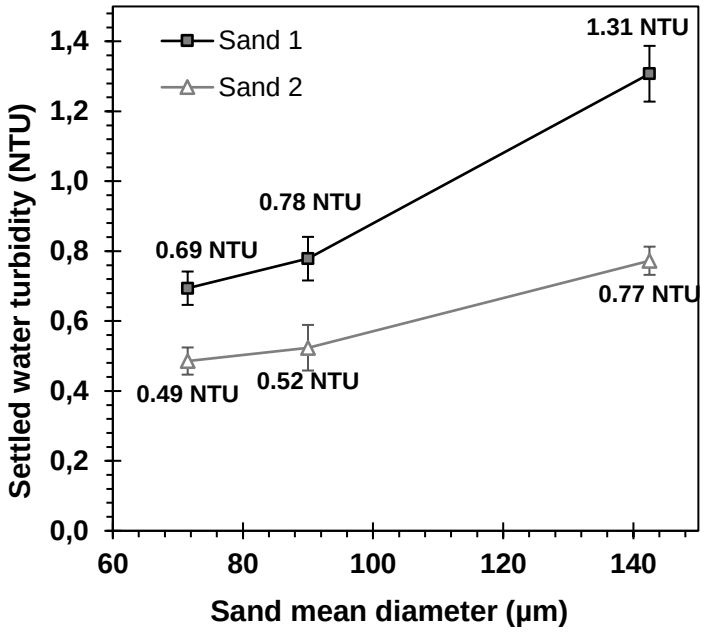

Figure 7.6: Impact of ballast media size on settled water turbidity. Coagulation: 12.5 mg Fe/L (pH: 6.5) at 300 s^{-1}. Flocculation: 8 min with 1.5 mg starch/L and 5 g sand/L at 165 s^{-1}. Settling: 3 min. The error bars correspond to the standard deviation.

7.4 Conclusion

This study addressed the impact of coagulation-flocculation conditions on the optimization of starch-based polymers. By combining the appropriate coagulation pH, flocculation time and mixing intensity, ballast size and surface properties, and polymer charge density, starch is proposed as an effective potential alternative to the use of PAM in ballasted flocculation processes. This alternative would eliminate many of the drawbacks related to the use of PAM including toxicity and carcinogenicity, the clogging effect on the media filter, non-biodegradability, and its production from non-renewable, oil-based materials, etc. In this study, the following observations about starch polymers were considered to be of importance to water treatment specialists aiming to improve process performance:

- A coagulation pH above 6.5 was detrimental for both polymers, but more drastically for starch polymers. Therefore, optimizing coagulation is the first step needed prior to optimizing flocculation.
- A slightly anionic charge density between 2.4 and 0.4 mEq/g was established as optimal for coagulation at a pH of 6.5. The optimal charge density, which is anticipated to be water-specific, was not found to be the most important variable for optimization.
- With a similar anionic charge density, starch required longer flocculation time to complete aggregation and to reach 1 NTU after settling. This is probably attributable to the effective length of the polymer chain. Nevertheless, the flocculation time was short and compatible with a ballasted flocculation process.
- The optimal velocity gradient for starch polymers was fixed at 165 s^{-1}. Starch was more sensitive to shearing compared to PAM, the latter being able to tolerate values higher than 195 s^{1} without it impacting turbidity removal.
- The BM characteristics were shown to have an important impact on floc size and turbidity removal. In the case of starch, smaller BM containing almost exclusively SiO_2 were established as ideal.

More work will be needed to elucidate the interactions between metal hydroxide complexes, polymers, and inorganic oxide-based BM. Finally, a full-scale comparison between starch and PAM should also consider the benefits of using starch for other downstream processes such as membrane granular media filters.

Acknowledgment

These experiments were conducted as part of the Industrial-NSERC Chair in Drinking Water (Polytechnique Montreal) research program, which benefits from the financial support of the City of Montreal, Veolia Water Technologies Canada, Inc., the City of Laval, the City of Longueuil, and the City of Repentigny.

CHAPITRE 8 ARTICLE 6 - ASSESSING ALTERNATIVE MEDIA FOR BALLASTED FLOCCULATION

Les chapitres 5, 6 et 7 étaient consacrés à l'intégration d'un nouveau polymère en floculation lestée : l'amidon activé. Cette seconde section de la thèse (chapitres 8 et 9) explore les impacts de la densité, de la taille et de la concentration de média lestant (exprimée en g/L ou en m^2 de surface externe de média/L). Ce présent article (publié dans *Journal of Environmental Engineering*) compare divers médias lestants exclusivement sur la base de leur densité, et ce, à taille équivalente. Par l'entremise de la méthode en microscopie optique présentée au chapitre 4, il a été possible d'évaluer la taille ainsi que la densité des flocs en fonction du pourcentage volumique du floc occupé par un média ayant une densité connue. Il a notamment été démontré qu'un média plus lourd requerrait une intensité de mélange plus élevée pour sa mise en suspension. Due à l'érosion et à la fragmentation probable des flocs, il a été en plus observé que la taille des flocs lestés était inversement proportionnelle à la densité du média testé, qui est elle-même dépendante de l'intensité de mélange. Par contre, étant donné une densité moyenne plus élevée des flocs, l'emploi d'un média lestant plus dense a globalement un impact bénéfique sur la vitesse de chute, et conséquemment, sur la charge superficielle maximale potentiellement applicable).

Assessing Alternative Media for Ballasted Flocculation

Mathieu Lapointe[1], Catherine Brosseau[1], Yves Comeau[1] and Benoit Barbeau[1]*

[1] Department of Civil, Geological and Mining Engineering, Polytechnique Montreal, Montreal, Quebec, Canada H3C 3A7

*Corresponding author e-mail: mathieu.lapointe@polymtl.ca

Abstract

Most current commercial applications of ballasted flocculation use silica sand to increase floc size and density. Other ballast media with different specific gravity may offer advantages such as increased applicable superficial velocity or increased particulate matter removal. This study assessed the relative impact of five ballast media on ballasted flocculation/settling performance: anthracite, recycled crushed glass, conventional silica sand, garnet sand and magnetite sand, with a common d_{50} of 150 µm but variable specific densities of 1.45, 2.58, 2.62, 3.93 and 5.08, respectively. Based on microscopic observations and assuming discrete particle removal in an ideal settler, mean superficial media settling velocities were respectively calculated as 35, 73, 74, 122 and 137 m/h. These values do not account for the impact of lamella or other specific geometries of different patented clarifiers (*e.g.* CoMag®, Densadeg®, Sirofloc® and Actiflo®). Although the use of magnetite sand allows the total suspended solids load to increase by more than twofold compared to silica sand, the residual turbidity increased after settling as the mixing intensity needed to maintain denser media in suspension was augmented. Consequently, the lowest residual turbidity (0.78 NTU for surface water and 1.38 NTU for wastewater) was observed when anthracite was used as the ballast medium. The ballast media geometry did not significantly impact turbidity removal and settling velocity. Hence, recycled crushed glass was identified as a potential alternative to conventional silica sand despite its higher angularity.

Keywords: *Ballast media; Floc specific gravity; Floc size, Particles removal, critical settling velocity*

8.1 Introduction

Settling is one of the most common water treatment processes. Reducing particle loading before filtration or recovering suspended solids after an activated sludge treatment are common gravity separation applications. The pulp and paper and mining industries also use clarifiers to remove organics and/or particulate matters. One of the main drawbacks of conventional settling lies in its

significant footprint. Increasing settling velocities by incorporating a ballast medium (BM) (typically sand) within flocs was proposed in the 1980s (Sibony, 1981) as an effective method for reducing the process footprint. For example, the Actiflo® process has been validated in Quebec (Canada) for settling rates up to 85 m/h for drinking water applications (MDDELCC, 2018). Even under high superficial velocities, ballasted flocculation/settling may provide good removal of total suspended solids (TSS) and turbidity (>85 % and > 90 %, respectively, according to Plum et al. (1998)).

Compared with conventional flocculation systems, ballasted flocculation is operated under high mean velocity gradients (G) because a minimal mixing intensity must be induced in the water to maintain the BM in suspension (G=160-200 s^{-1}) (Desjardins et al., 1999). The minimal G value is controlled by the media specific gravity and size, *i.e.*, denser and larger BM require higher mixing. The specific gravity of ballasted flocs is mainly dependent on the specific gravity of the BM and its degree of incorporation into the floc structure (Lapointe & Barbeau, 2016). Most ballasted flocculation studies have been conducted with silica sand (SS) (De Dianous & Dernaucourt, 1991; Desjardins et al., 2002; Lapointe & Barbeau, 2015; Young & Edwards, 2000). However, an alternative BM could have important advantages over SS in some applications: 1) a denser BM increases the specific gravity and settling velocity of flocs for high-rate clarification, 2) BM with sorbing-desorbing properties could simultaneously ballast flocs and adsorb contaminants; magnetite sand could possibly ballast flocs and remove arsenic, 3) other materials such as dolomite can be used to simultaneously increase alkalinity (Piirtola et al., 1999) and 4) a lighter BM could be used to reduce the mixing intensity, which limits the shear on sensitive floc structure. BM with higher densities than SS, such as magnetite and apatite (Piirtola et al., 1999), have been tested in the past, but no study has yet assessed the fundamental impacts of variable BM specific gravity on floc morphology (density, size and aspect ratio) and the resulting settling velocity distributions. Such information is critical for identifying the optimal settler design, *i.e.*, the settling velocity needed to remove all ballasted flocs.

This study presents a comprehensive evaluation of ballasted floc characteristics (settling velocity, specific gravity, size and shape) produced from five alternative media: anthracite (ANT), silica sand (SS), crushed glass (CG), garnet sand (GS) and magnetite sand (MS). The BM were tested both for drinking and municipal wastewater applications. We propose that an improved insight into ballasted floc characteristics will help in selection of the appropriate medium for a given settling

application. Considering that many factors impact the ballast flocculation procedure, this study presents a method to assess objectively the particulate matter removal efficiency and the floc settling velocity distribution for various BM. More specifically, the objectives were to 1) evaluate optimal flocculation conditions for each BM (chemical dosages, BM concentration and mixing intensity), 2) assess the impact of the BM specific gravity on floc settling velocity distributions under optimal flocculation conditions (established in 1), 3) determine the role of BM shape on settling performance by comparing BM of variable angularity but identical density and size, and 4) identify the optimal BM for a given design criterion based either on a targeted turbidity removal or a designed superficial velocity.

8.2 Material and methods

8.2.1 Water characteristics

All experiments were conducted at laboratory scale using either 1) surface water (SW) from the Sainte-Rose drinking water treatment plant, which is fed by the Mille-Îles River (Quebec, Canada), or 2) municipal wastewater (WW) from the Repentigny (Quebec, Canada) water resource recovery facility (collected after the 6 mm influent bar screens). The water characteristics assessed before coagulation and after flocculation and settling (and the associated analytical methods) are presented in following two tables.

Table 8.1: Monitored parameters and associated analytical methods

Parameters	*Units*	*Methods*
Total COD [1]	Mg O^2/L	Dichromate Reactor Digestion Method, Hach® Method 8000 High-range 20-1500 mg COD/L (Hach Company, 2014, Method 8000 DOC316.53.01099.) Potassium hydrogen phtalate standard solution, SM 5220 B. APHA et al., 2012)
$CBOD_5$ [2]	mg/L	SM 5210 B. (APHA et al., 2012)
TSS [3]	mg/L	SM 2540 D. (APHA et al., 2012)
VSS [4]	mg/L	SM 2540 E. (APHA et al., 2012)
Alkalinity	mg $CaCO_3$/L	SM 2320 B. (APHA et al., 2012), Mettler Toledo DL28 Electrometric Titrator

Table 8.1: Monitored parameters and associated analytical methods (suite)

Total Phosphorus	mg P/L	In-line UV/Persulfate Digestion Method and Flow Injection Analysis, Lachat QuikChem® Method 10-115-01-3-A Range 0.10 to 10.0 mg P/L (Lachat-Instruments, 2001) SM 4500-P I. (APHA et al., 2012)
Soluble phosphorus (S_P)	mg P/L	Flow Injection Analysis, Lachat QuikChem® Method 10-115-01-1-A Range 0.01 to 2.00 mg P/L (Lachat-Instruments, 2001) SM 4500-P G.; (APHA et al., 2012) S_{PO4} was determined on the filtrate of 1.2 µm glass microfiber Grade 934-AH™ filter (Whatman™) and 0.45 µm cellulose membrane filter (EMD Millipore) superimposed
Turbidity	NTU	Turbidimeter, Hach 2100N, SM 2130 B. (APHA et al., 2012)
SCV[5]	-	Chemtrac® Systems, Inc. (ECA-2100 charge analyzer)
UVA_{254}	cm^{-1}	Settled waters filtered on a pre-washed 0.45 µm PES Supor®-450 membrane (Pall), (APHA et al., 2012)
Particle counts	# part./mL	Particles analyzer, Brightwell Technologies, DPA-4100
DOC	mg C/L	Sievers 5310c total organic carbon analyzer, GE Water, SM 5310 C. (APHA et al., 2012)
Floc size	µm	Counting cell (2 mm depth, Model # 1801-G20) Camera (Olympus DP70) Optical microscope (Olympus BX51) Equivalent diameter method (Lapointe & Barbeau, 2016)
Floc specific gravity	-	Counting cell (2 mm depth, Model # 1801-G20) Camera (Olympus DP70) Optical microscope (Olympus BX51) Ballast media incorporation method (Lapointe & Barbeau, 2016)

1: chemical oxygen demand, 2: 5-day carbonaceous biochemical oxygen demand, 3: total suspended solids, 4: volatile suspended solids, 5: streaming current value

Table 8.2: Water characteristics and chemical dosages used during jar tests

Parameters	*Units*	*Surface water (SW)*	*Wastewater (WW)*
Coagulation-flocculation conditions			
Alum dosage	mEq/L	0.40 (3.64 mg Al/L) [3]	1.41 (12.73 mg Al/L) [3]
PAM dosage	mg/L	0.375 [1]	0.5 [1]
BM concentration	g/L	2.0[1]	3.0 [1]
Raw water characteristics (unless specified otherwise)			
Turbidity	NTU	12.0 after settling: < 2.0 [4] (> 83% removal)	130 after settling: < 4 [4] (> 97% removal)
Particles concentration	#/mL	250 000 after settling: < 10 000 [4] (> 96% removal)	-
COD	mg/L	-	613 (> 60% removal, after settling)
$CBOD_5$	mg/L	-	215 (> 55% removal, after settling)
DOC	mg C/L	raw: 6.9 after settling: 3.1 [2] (55% removal)	-
TSS	mg/L	24 after settling: < 5 [4] (> 80% removal)	266 after settling: < 8 [4] (> 97% removal)
VSS	mg/L	-	229
pH	-	raw: 7.5 after settling 6.4 [2]	raw: 7.8 after settling: 7.4 [2]
Alkalinity	mg $CaCO_3$/L	raw: 35 (consumed: 57%) after settling: 15 [2]	raw: 305 (consumed: 23%) after settling: 235 [2]

Table 8.2: Water characteristics and chemical dosages used during jar tests (suite)

UVA_{254}	cm^{-1}	raw: 0.244 after settling:0.049 [2] (80 % removal)	-
Total Phosphorus	mg P/L	-	raw: 7.70 after settling: < 0.17 [2] (98% removal)
Soluble Phosphorus (S_P)	mg P/L	-	raw: 4.60 after settling: < 0.06 [2] (99% removal)

[1] Optimal dosage retained for comparison (PAM: Polyacrylamide)

[2] Similar observations for all BM and independent of PAM dosage

[3] See section *Identification of optimal coagulation conditions*

[4] Removals obtained with optimal PAM dosage and BM concentration

8.2.2 Ballast media characteristics

To avoid the potential confounding effect of ballast media size distribution on performance (Lapointe & Barbeau, 2015), an identical media size distribution was generated for all BM by sieving. The d_{10}, d_{50}, d_{60} and the uniformity coefficient were 98 μm, 150 μm, 162 μm and 1.65, respectively. The main BM physical properties anticipated to have an impact on settling velocity once integrated into a floc structure are listed in the following table. The *G* numbers correspond to the minimum values needed to maintain the grains in suspension during a jar test, hence allowing each grain to potentially contribute to the ballasted flocculation.

Table 8.3: Ballast media physical properties and minimum mean velocity gradient needed to maintain the media in suspension during flocculation

Ballast media	*Specific gravity*	*Mean ratio L/l* [1]	*Hardness*	*Minimum G (s^{-1})*	*Point of zero charge (PZC)*[2]
Anthracite (ANT)	1.45	1.61	2.2 - 3.0	100	7
Silica sand (SS)	2.62	1.44	6.0 - 7.0	165	< 3.0 (Kim & Lawler, 2005; Kosmulski, 2011)
Crushed glass (CG)	2.58	2.05	5.5 - 7.0	165	< 3.0 (Kosmulski, 2011)
Garnet sand (GS)	3.93	1.93	7.5 - 8.0	215	3.5 – 4.0 (Kosmulski, 2011)
Magnetite sand (MS)	5.08	1.36	5.5 - 6.5	255	6.5 – 6.7 (Kosmulski, 2011)

[1] Floc and BM shapes are characterized as an ellipse (*L* and *l* represent the longest and the shortest ellipse dimensions, respectively)

[2] Between 20-25 °C

8.2.3 Identification of optimal coagulation conditions

Bench-scale test experiments were conducted in 2-L square B-KER[2] jars (Phipps & Bird). The water was first coagulated by flash-mixing for 2 minutes with alum ($G=300\ s^{-1}$). The coagulation mechanisms expected for both waters tested were charge neutralization and sweep coagulation (mostly sweep coagulation in the case of the wastewater tested). Flocculation was then initiated by the simultaneous injection of a BM and polymer. Optimal alum dosages for both water types (0.40 mEq/L for SW and 1.41 mEq/L for WW) were determined based on turbidity removal (*i.e.*, when an asymptote was observed on the turbidity versus coagulant curve). For the SW, the optimal coagulation dosage was also established based on UVA_{254} (80 % removal), dissolved organic carbon (DOC; 55% removal), pH of coagulated water (6.4), residual alkalinity after coagulation (15 mg $CaCO_3$/L) and the streaming current value (SCV) as an indicator of particle residual charge (SCV = 0 for a coagulant dosage of 0.38 mEq./L). The SCV was not a good indicator for the WW tested because it overestimated the coagulant dosage needed (SCV=0 at 4.65 mEq/L, which was 3.3 times the dose required to obtain the minimal turbidity). This overestimation can be explained

by the high concentration of particles, which led to important sweep coagulation, interception and enmeshment mechanisms. Therefore, the optimal alum dosage that was needed to coagulate the wastewater was determined by relying on the removal efficiency of TSS, turbidity, total phosphorus and soluble phosphate.

8.2.4 Laboratory scale ballasted flocculation

Different *G* values (from 100 to 300 s^{-1}) were tested during flocculation to account for the differing BM densities. The Superfloc® A-100 polymer, an anionic high molecular weight polyacrylamide (PAM) from Kemira, was used to bridge BM with the microflocs. After floc maturation (1 min was sufficient to complete floc formation for all media) and settling (3 min), the settled waters were characterized by particle count, residual TSS and turbidity measurements. Settling times longer than 3 min did not provide significant improvements in settling performance. Optimal *G* values were established from turbidity measurements in settled waters.

8.2.5 Ballasted flocculation performance

Ballasted flocculation performance was assessed in terms of 1) turbidity removal after settling and 2) calculation of theoretical floc settling velocity distributions based on floc characteristics derived from microscopy analysis. This twofold approach offers the ability to distinguish between the performance of flocculation (*i.e.*, quality of flocs formed leading to high settling velocity) versus the performance of settling (*i.e.*, particle removal for a specific settling time or simulated settler superficial velocity). Turbidity was the preferred option for estimating particle removal due to its simplicity and the high correlation observed between turbidity and TSS removal during preliminary assays. Theoretical floc settling velocity distributions were calculated according to the method described in Lapointe et Barbeau (2016). In this procedure, forty individual ballasted flocs are characterized for their shape, diameter and density using microscopic analysis. The Stokes' equation (for $Re < 1$) and Newton's equations (for $1 < Re < 1000$), as proposed by Johnson, C. et al. (1996), are then used to predict floc settling velocity distributions (assuming discrete settling).

8.3 Results

8.3.1 Impact of PAM dosage and BM concentration on settling performances

Dosages of 0.375 mg PAM/L for SW and 0.5 mg PAM/L for WW were selected as sufficient to provide an acceptably low settled water turbidity (Figure 8.1A, B and F). ANT, SS and CG had similar requirements for PAM dosage, while GS and MS needed more PAM to achieve the minimum settled turbidity. BM concentrations of 2 and 3 g/L were defined as appropriate for SW and WW, respectively (Figure 8.1C and D). Conclusions were identical whether particle counts or turbidity was used to evaluate performance (data not shown). For full-scale ballasted flocculation processes, BM concentrations in the range of 3 to 5 g/L for SW and 4-6 g/L for WW are commonly used. For a full-scale application, the BM concentration is generally above the optimal concentration as raw water turbidity fluctuations and BM export in settled water have to be considered in the design.

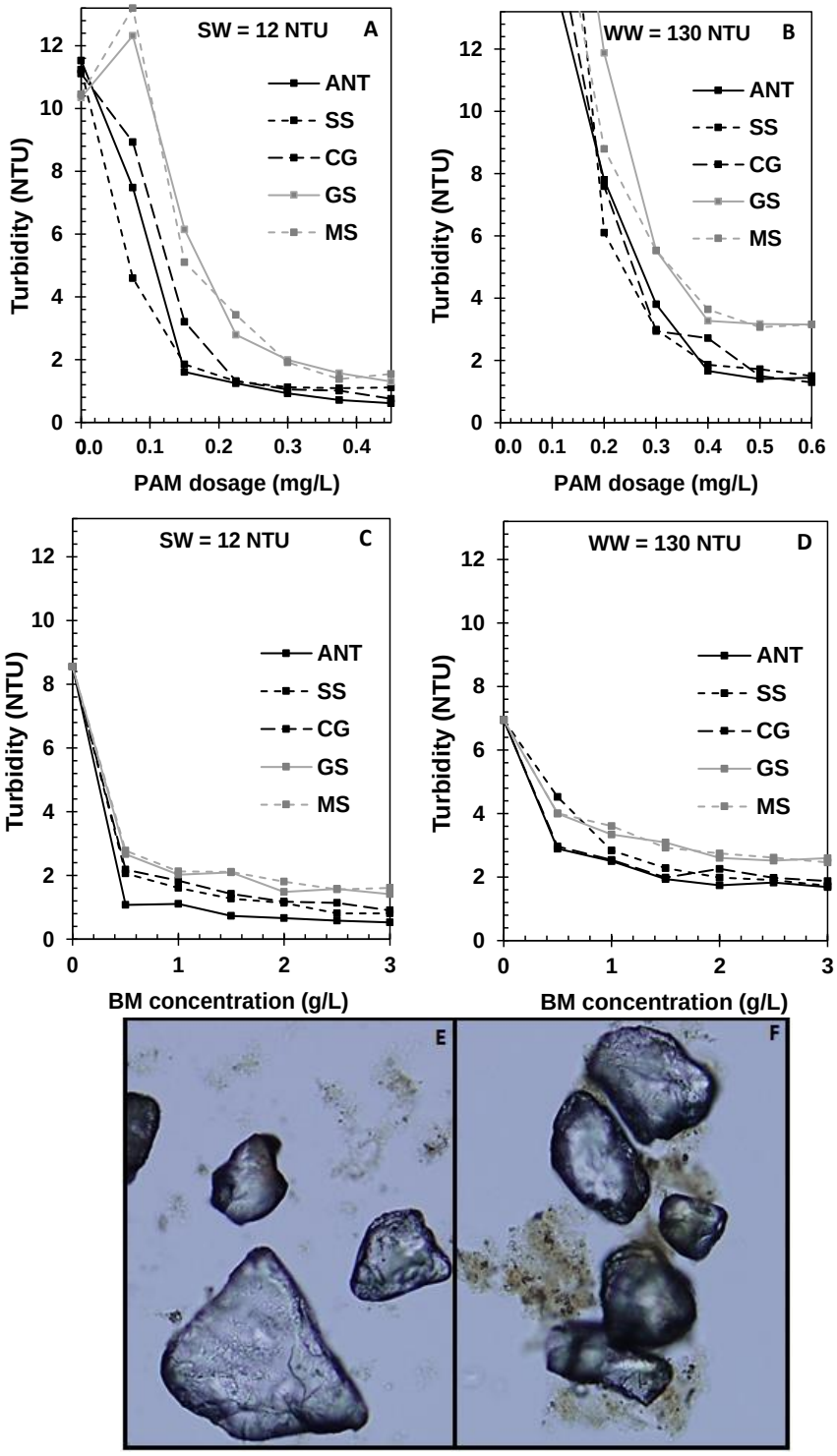

Figure 8.1: Settled water turbidity for variable PAM dosages for A) SW and B) WW (Conditions: BM = 4 g/L, flocculation time = 1 min at optimal *G*, settling time = 3 min) or variable BM dosages for C) SW and D) WW (Conditions: PAM = 0.375 mg/L (SW) and 0.5 mg/L (WW). Images in E) and F) illustrate the impact of low (0.10 mg/L) and optimal (0.375 mg/L) polyacrylamide dosage on sand aggregation, respectively.

8.3.2 Particulate matter removal under optimal conditions

Figure 8.2 presents the settled water turbidities achieved under optimal coagulation/flocculation conditions. Good turbidity removals of 80-90 % and 97-99 %, depending on the BM, were achieved in SW and WW, respectively. Residual turbidity after settling increased as the mixing intensity needed to maintain denser BM in suspension was augmented. Consequently, the lowest residual turbidity was observed when ANT was used as the BM, even though it was the lightest medium tested. For both water sources, ANT produced the lowest residual particle concentration (0.78 nephelometric turbidity unit (NTU) in SW and 1.38 NTU for WW). The better performance of ANT is explained by the lower shear required in the tank (G = 100 s^{-1}) to maintain the medium in suspension. Nevertheless, for all BM and water types, a turbidity removal higher than 80% was always attained.

The impact of BM angularity can be assessed by comparing the performances of silica sand and crushed glass (Figure 8.2). Both media have similar specific gravity but considerably different geometry (L/l ratios of 1.44 and 2.05, respectively; Table 8.3). Both media produced equivalent settled water turbidity, which suggests a negligible impact of the BM aspect ratio on process performance.

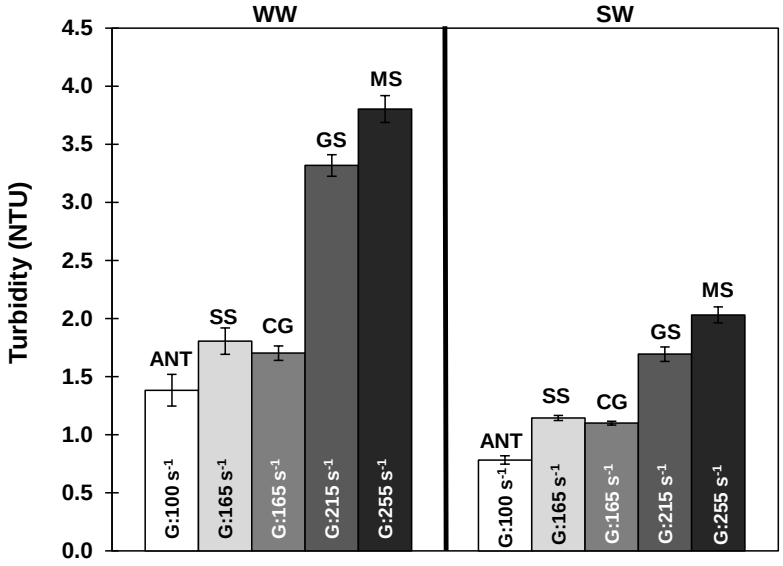

Figure 8.2: Settled water turbidity achieved under optimal coagulation/flocculation conditions. Conditions: PAM = 0.375 mg/L (SW) and 0.5 mg/L (WW), BM dosage: 2 g/L (SW) and 3 g/L (WW), flocculation time = 1 min, settling time = 3 min. Error bars correspond to the standard deviation. Temperature: 21°C.

8.3.3 Impact of mixing intensity on particle removal and energy consumption

For each BM investigated, optimal *G* values were identified to minimize settled water turbidity. The optimal *G* was always the minimum value needed to maintain the BM in suspension (data not shown). Too low of a *G* value reduces the concentration of BM available for ballasting. A higher *G* value increases floc breakage. For both source water types, Figure 8.3 indicates that the residual turbidity after settling (3 min) was inversely correlated to the *G* value employed during flocculation. The residual turbidity was confirmed microscopically to be caused by un-ballasted microflocs. The energy consumption for each BM was calculated using the optimal *G* value. Considering that all of the BM had identical grain size distributions, MS and GS consumed 2.4 and 1.7 times more energy, respectively, compared to SS. The required energy for ANT corresponded to only 37% of the energy needed for SS. A similar energy consumption was estimated for SS and CG, as comparable optimal *G* values had been identified for both media.

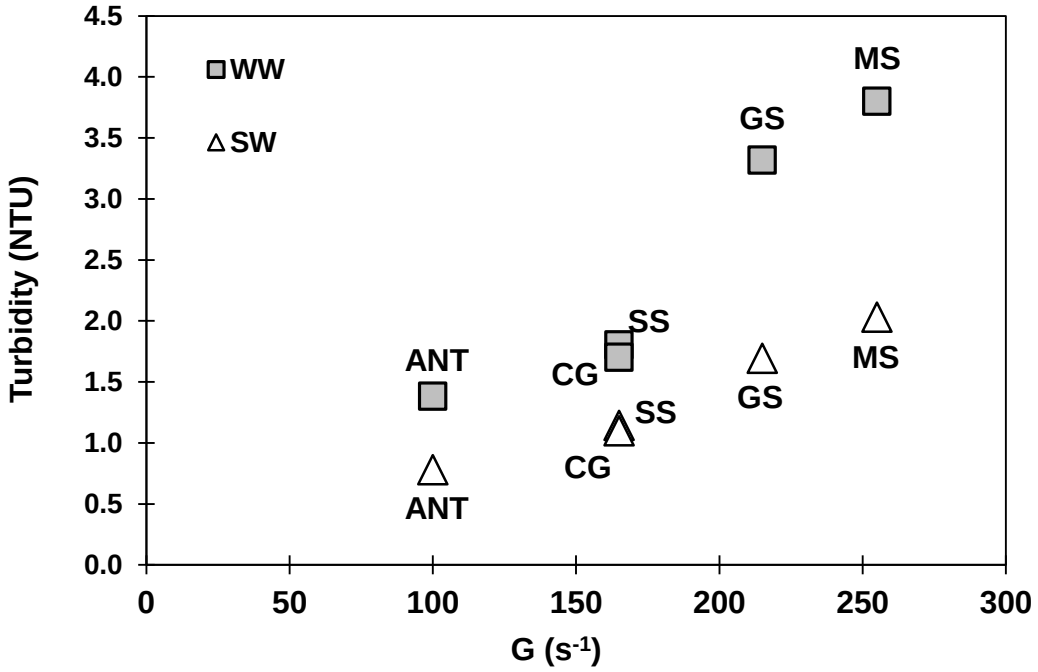

Figure 8.3: Settled water turbidities achieved under optimal *G* for each ballasting medium. Conditions: PAM = 0.375 mg/L (SW) and 0.5 mg/L (WW), BM: 2 g/L (SW) and 3 g/L (WW), flocculation time = 1 min, settling time = 3 min. Maximal standard deviation observed = 0.14 NTU. Maximal standard deviation for any media: 0.14 NTU. Temperature: 21°C.

8.3.4 Predicted floc settling velocity based on microscopic observation

Floc size and specific gravity

Floc size and specific gravity characterization through microscopic observation permitted calculation of floc settling velocity distributions. The mean floc diameter, BM incorporation (i.e., the percentage of the volume of the floc made up of BM), the aspect ratio and the specific gravity for each tested medium are listed in Table 8.4. Under optimal mixing conditions, ANT produced the largest ballasted flocs (553 µm, 22 % larger than by conventional SS, *t*-test, $p < 0.05$), but the lowest BM incorporation ($p < 0.05$) and hence, the lowest floc specific gravity (1.09, 16 % lower than SS, $p < 0.05$). In contrast, MS produced the smallest flocs (390 µm, 14 % smaller than by SS, $p < 0.05$). However, a relatively high BM incorporation (20.1%, a proportion 22 % higher than SS) and specific gravity (1.84, 43 % denser than SS, $p = 0.07$) were achieved when MS was employed as the BM. Similar floc characteristics were observed between GS and SS. BM incorporation and floc size were proportional and inversely proportional, respectively, to the mixing intensity (expressed in terms of *G*).

Table 8.4: Floc diameter, BM incorporation and specific gravity obtained under optimal conditions.

BM	Floc mean diameter (µm)	Mean BM incorporation (%)	Floc mean specific gravity	Floc mean aspect ratio (L/l)
ANT	553 ± 16	13.2 ± 0.3	1.09 ± 0.03	1.80 ± 0.06
SS	454 ± 18	16.5 ± 1.6	1.29 ± 0.06	1.74 ± 0.11
CG	465 ± 17	16.6 ± 0.8	1.29 ± 0.05	1.88 ± 0.23
GS	403 ± 13	22.7 ± 0.4	1.69 ± 0.04	1.80 ± 0.09
MS	390 ± 10	20.1 ± 0.1	1.84 ± 0.02	1.74 ± 0.09

Errors correspond to standard deviations

Mean BM incorporation: volume fraction of the floc composed of BM

Predicted settling velocities

Settling velocity is controlled by ballasted floc density, size and, to a lesser extent, shape. Settling velocity distributions were predicted based on the individual assessment of 40 flocs produced in SW with various BM (Figure 8.4). Mean settling velocities varied from 35 m/h (ANT) to 137 m/h (MS). GS and MS exhibited similar settling velocity distribution profiles, even though their specific gravities were considerably different (3.93 for GS vs. 5.08 for MS). The lower density of the flocs ballasted with GS was partially compensated by the formation of larger aggregates compared to those formed with MS. CG and SS produced nearly identical settling velocity distributions despite their different geometries.

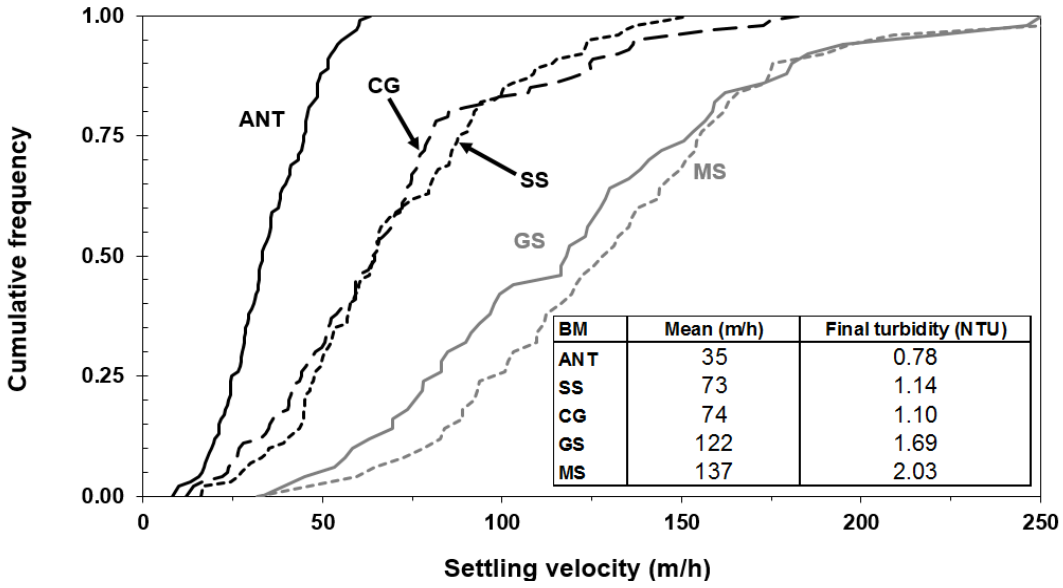

Figure 8.4: Cumulative frequency distributions of predicted floc settling velocity for 5 BM tested in surface waters. Conditions: PAM = 0.375 mg/L, BM: 2 g/L, flocculation time = 1 min, settling time = 3 min. Temperature: 21°C.

Critical superficial velocity for TSS removal

For some applications, the criterion of settling performance is TSS removal (expressed in flux of solids removed, kg of TSS removed h^{-1} m^{-2}) rather than residual turbidity in the settled water. For SW prior to settling, the TSS in the jar test was estimated at 2,040 mg/L, which was calculated by the sum of the BM concentration (2,000 mg/L), the alum precipitate (10.5 mg/L of precipitate), the PAM added (0.3 mg/L), the DOC removed (3.8 mg C/L) and the initial TSS (24 mg/L). The TSS

are mostly composed of BM (98.1% in this example). With the use of the floc characteristics (size, density shape and settling velocity) obtained by microscopy, TSS removal can be predicted for various superficial velocities. For this calculation, it was assumed that flocs having a settling velocity higher than the settler velocity were entirely removed, whereas flocs with a lower settling velocity remained in the supernatant. Figure 8.5 presents the predicted residual TSS in settled waters for increased settling velocities and variable BM. A critical superficial velocity, *i.e.,* the maximal velocity not to be exceeded to remove all ballasted flocs, can be identified for each BM. For superficial velocities under the critical velocity, only un-ballasted flocs will be found in settled waters. Critical velocities at 22°C (identified as empty squares on the inset of Figure 8.5) varied between 10 m/h for ANT to 40 m h^{-1} for MS. It is important to point out that the procedure does not precisely predict the full-scale performance of ballasted technologies (e.g. CoMag® and Sirofloc® with magnetite or Actiflo® with silica sand). Full-scale clarifiers performance also depends on the hydrodynamic and other phenomena such as flocs aggregation into the lamella and energy gradient distribution inside the process. For example, full-scale Actiflo® settlers with silica sand are commonly designed at velocities of 60 m/h, which is a value higher the critical value of 17.5 m/h calculated for SS in this study.

The plateaus of TSS observed below critical velocities are explained by un-ballasted flocs, which are not removed if the superficial velocity is above 1 m/h. Using these critical velocities, TSS loadings (excluding BM) were calculated at 22°C and expressed as kg of TSS removed h^{-1} m^{-2}. These values were 0.37, 0.54, 0.64, 1.23 and 1.38 kg of TSS h^{-1} m^{-2} for ANT, CG, SS, GS and MS, respectively. Consequently, the use of MS increases the TSS load by almost fourfold compared to ANT. The costs for this improved settling are: (i) higher mixing energy and (ii) higher final TSS concentration due to floc breakage.

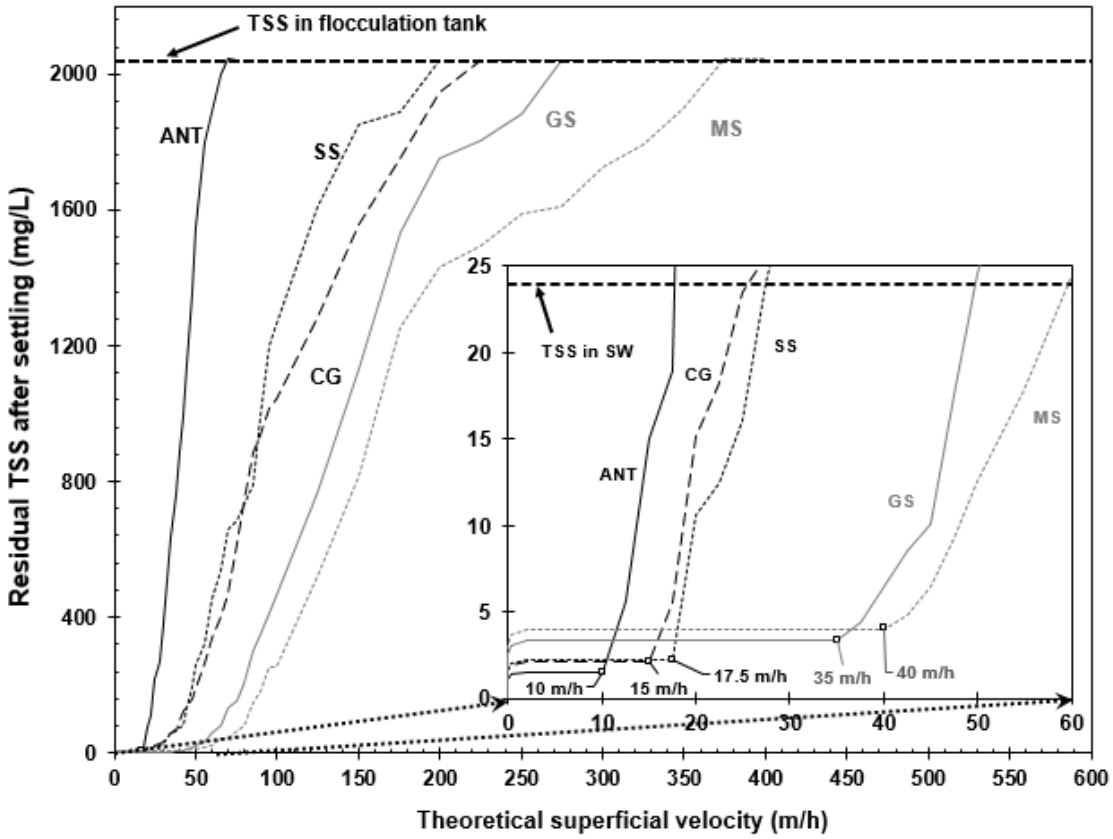

Figure 8.5: Predicted residual TSS in settled water for increasing superficial velocities at 21°C. Inset: Empty squares = Maximal superficial velocities needed to remove all ballasted flocs i.e., to obtain the ultimate residual TSS. Conditions: PAM = 0.375 mg/L, BM: 2 g/L, flocculation time = 1 min, settling time = 3 min.

Figure 8.6A presents the raw water TSS removals for the five tested BM and identifies the maximal applicable superficial velocity for 100% removal of ballasted flocs (i.e., only un-ballasted flocs remain). This figure enables prediction of intermediate TSS removal performance (between 60% and the maximal value observed for each BM). The overall performance of the process results from two distinct mechanisms: the removal of ballasted and un-ballasted flocs. The data obtained in Figure 8.6B were compared with values collected from the scientific literature for laboratory scale jar tests using SS as the BM. The variability in these data is explained by the fact that the studies were conducted with different coagulant-polymer dosages, BM concentrations and size, water temperature and types.

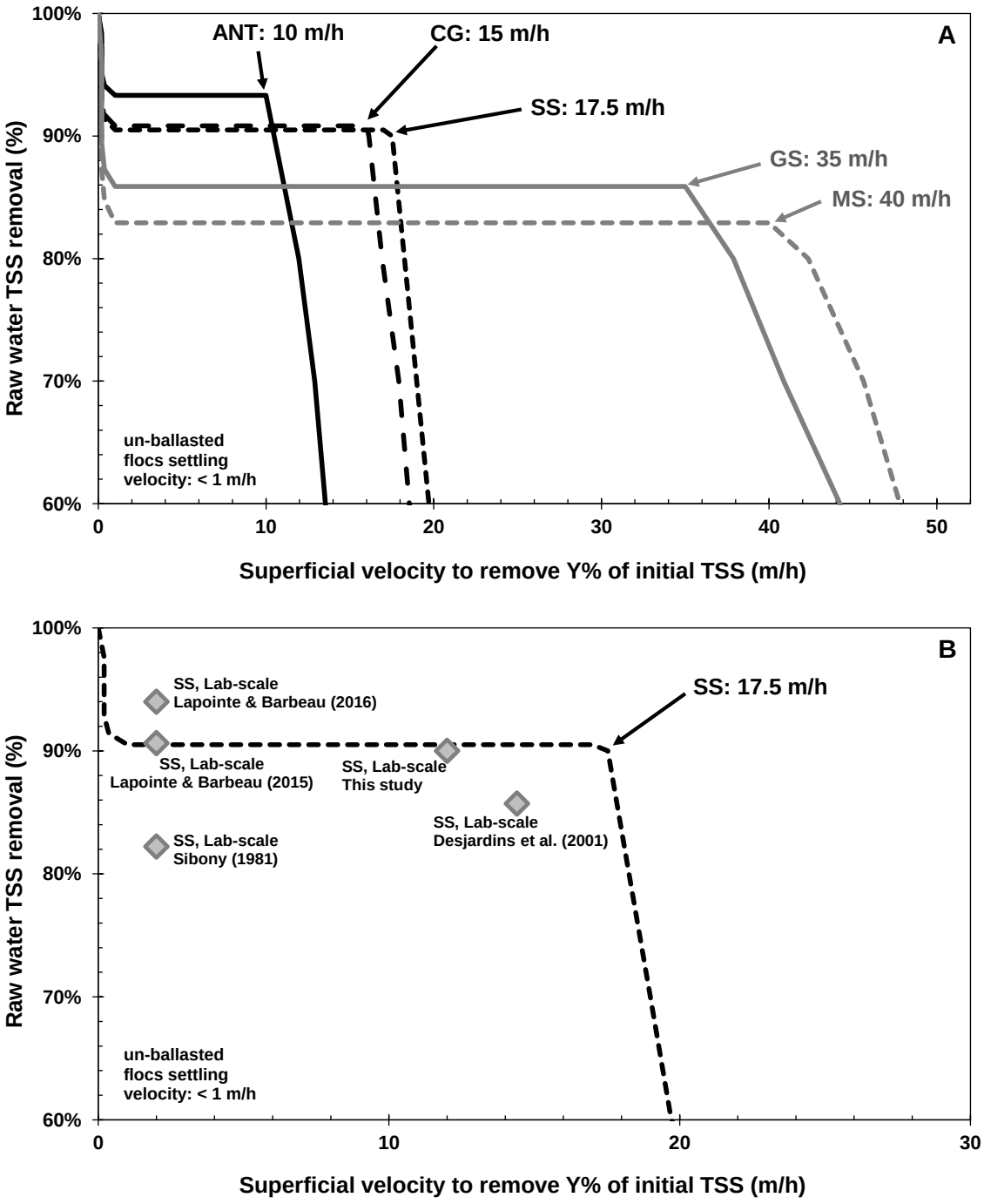

Figure 8.6: A) Relation between the raw water TSS removal and superficial velocity. B) TSS removals compared with values from the scientific literature (lab-scale). Conditions for this study: PAM = 0.375 mg/L, BM: 2 g/L, flocculation time = 1 min, settling time = 3 min. Temperature: 20-23°C.

8.4 Discussion

8.4.1 Effect of PAM dosage and BM concentration

In this study, identical BM concentrations (in terms of w/v) were used. However, because the five tested BM had different specific gravities, variable amounts of BM grains were injected and the numbers were inversely proportional to the BM specific gravity. Thus, ANT offered more than 12 times the surface area than did MS. Consequently, it was observed that a higher concentration of MS (on a w/v basis) was needed compared to SS (15 g MS/L vs. 5-8 g SS/L) to achieve a turbidity removal above 85% (Imasuen et al., 2004). During this study, we identified an optimal concentration of approximately 1-2 g SS/L for a SW application. This range corresponds closely to those observed by Sibony (1981) (0.8-1.8 g/L), Young et Edwards (2003) (1.25 g SS/L) and Desjardins et al. (2002) (1-2 g SS/L, turbidity < 0.25 NTU). However, Ghanem et al. (2007) observed an optimal density for ballasted flocs when higher SS concentrations were used (5-7 g SS/L).

The polymer molecular weight, which is more than several millions daltons in the case of PAM (Gaid & Sauvignet, 2011), largely influences the bridging mechanism during flocculation (Caskey & Primus, 1986). In theory, the PAM dosage needed to form proper aggregates (see Figure 8.1E and F) is proportional to the cumulative surface of all coagulated particles (Gregory & Barany, 2011). MS should have required the smallest PAM dosages because it offered the smallest total surface available for polymer chain adsorption. However, higher PAM dosages were required for optimal TSS removal by GS and MS. These increased flocculant demands are most likely explained by the higher shear forces on the floc structure (G value of 255 s^{-1} for MS) which were applied to maintain the BM in suspension. In this case, an increased PAM dosage could have compensated the negative impact of shear on floc size and BM incorporation into the floc. Additional visual information of the impact of mixing conditions on floc morphology can be found in (Lapointe & Barbeau, 2015, 2016).

8.4.2 Floc characteristics and particles refractory to settling

This study focused on the characteristics that flocs must have to be properly removed during settling. Floc size, density and shape mainly control the settling rate (Johnson et al., 1996; Tambo & Watanabe, 1979). The floc shape was shown to be a minor parameter by Lapointe et Barbeau (2016). The comparison between SS and CG confirmed the negligible impact of the BM shape. Hence, the main objective of ballasted flocculation is to produce the largest and densest flocs. Ballasted flocs have considerably higher specific gravity (1.1-2.0, depending on the BM used in this study and 1.2-2.0 in Young et Edwards (2000)) compared to conventional flocs (1.03-1.05, Larue et Vorobiev (2003)). However, this study revealed an inverse relation between the floc size and the BM specific gravity. Moreover, a direct relation was observed between the BM specific gravity and the non-settleable particle concentration. The increased *G* value, required to maintain a denser BM in suspension, augments the disaggregation of microflocs from the main floc structure. For each tested BM, two distinct floc size distributions were observed: ballasted flocs and un-ballasted flocs (Lapointe et al., 2017). The concentration of small un-ballasted aggregates (with settling velocity < 1 m/h) dictated the final settled water turbidity. Thus this study highlights the importance of limiting the mixing intensity during ballasted flocculation to reduce the concentration of non-settleable particles. For WW, higher settling turbidity was observed compared to SW applications. The higher turbidity that is produced in settled WW is likely attributable to a less compact floc structure associated with a higher drag coefficient. For porous aggregates, shear forces are heterogeneously distributed into the structure (i.e., shearing planes are obtained when flocs have an expanded structure).

Floc size is related to numerous factors, including water type, coagulant/flocculant dosage, polymer type, size and density of BM used, and mixing intensity. For this reason, comparisons with other studies are difficult. As an example, while we measured ballasted floc sizes of 300-800 µm (polymer dosage: 0.375 mg/L, SS concentration: 2 g/L), Young et Edwards (2003) observed SS ballasted flocs having diameters ranging from 500 to 7,000 µm (polymer dosage: up to 10 mg/L and SS concentration: up to 10 g/L).

8.4.3 Ballast medium selection

The critical superficial velocity to remove 100% of ballasted flocs is an important reference, as with higher superficial velocities TSS removal decreases rapidly (11% removal decrease for each additional m/h in the case of ANT). This sharp increase of TSS concentration in settled water is attributable to exportable BM in settled waters (either incorporated or not into the floc). Denser BM, such as MS and GS, exhibit higher critical velocities. Using denser BM offers the ability to operate at higher velocities (and reduce footprint) as long as the residual turbidity in settled waters is acceptable. During this study, the turbidity of 1.7-2.0 NTU achieved with GS and MS in surface waters is relatively high and would therefore not be considered optimal for a drinking water application. On the other hand, for some other industrial applications in which higher settled water turbidity is acceptable and a small footprint is desirable (e.g., settling of combined sewer overflows), using a denser BM such as MS may prove a useful alternative to SS.

Independent of the BM used, a significant increase of the solid flux removal (kg of TSS m^{-2} h^{-1}) was observed compared to conventional flocculation (10-24 times when SS was used as BM and considering a superficial velocity between 0.71 – 3.3 m/h for conventional flocculation (Kawamura, 2000). Other parameters must be considered for the final comparison of all existing BM: costs material, geographic availability, stability, hydrocyclone separation effectiveness (directly proportional to BM specific gravity), energy costs to maintain particles in suspension and the impact of BM angularity on abrasion of the recirculation piping.

8.5 Conclusion

This study reports tests conducted with ballasted flocculation media as alternatives to SS. The final BM selection is a compromise between settled water quality and the highest applicable superficial velocity, the latter having a direct impact on capital and operational expenditures. This study revealed the advantages of operating ballasted flocculation with a BM having a relatively low specific gravity: lower *G* led to a reduction in energy consumption, lower shearing induced on floc structure and improved turbidity removal. However, certain industrial applications could benefit from the higher solids flux removal offered by denser BM. More specifically, this study concluded that:

- The critical theoretical superficial velocity can be calculated based on microscopic observations of ballasted flocs.
- ANT produced the best settled water quality while MS ballasted flocs had the highest mean superficial velocity.
- The BM angularity did not significantly impact turbidity removal. Hence, CG was established as a potential alternative to the conventionally used SS, especially for wastewater applications where the contamination of the BM is not an issue.
- SS is a good compromise for providing simultaneously low settled water turbidity and high solids flux removal.

Acknowledgements

These experiments were conducted as part of the Industrial-NSERC Chair in Drinking Water (Polytechnique Montreal) research program, which benefits from the financial support of Veolia Water Technologies Canada, Inc., the City of Montreal, the City of Laval and the City of Repentigny. The authors are grateful for the technical support of Professor Félix Gervais (Polytechnique Montreal).

CHAPITRE 9 ARTICLE 7 - SELECTION OF MEDIA FOR THE DESIGN OF BALLASTED FLOCCULATION PROCESSES

En complément au chapitre précédent, cette section propose une approche systématique pour la sélection de la taille et de la densité du média lestant en fonction des abattements de turbidité attendus par rapport à la charge superficielle souhaitée. Pour un Actiflo® opéré à forte charge (65 m/h; capacité de 90 000 m^3/jour), il a été observé qu'une portion granulométrique du sable (<100 µm) pouvait être exportée vers les goulottes. Or, à masse équivalente, un plus petit média lestant offre une surface de réaction plus grande. L'article présenté dans ce chapitre (publié dans *Water Research*) démontre que cette surface de média lestant (exprimée en m^2/L) est un facteur important dictant la performance de la floculation lestée. Cependant, pour des charges superficielles plus élevées, la taille et la densité du média lestant ont un impact aussi considérable sur l'enlèvement de particules.

Selection of media for the design of ballasted flocculation processes

Mathieu Lapointe[1] *and Benoit Barbeau*[1]

[1]Department of Civil, Geological and Mining Engineering, Polytechnique Montreal, Quebec, Canada, H3C 3A7

E-mail: mathieu.lapointe@polymtl.ca

Abstract

Conventional clarification processes imply specific facility footprints that translate into important capital costs. Ballasted flocculation, consisting of injecting ballast medium to increase floc specific gravity and size, is being increasingly used in the water industry owing to its potential for design with very high superficial velocities. However, no systematic approach has yet been proposed to compare and select an appropriate ballast medium with respect to its specific gravity and size. In order to facilitate this procedure, this research project explores the hypothesis that flocculation performance is controlled by the surface area of the medium available for ballasted flocculation. This hypothesis was tested at laboratory scale by evaluating five ballast media with differing specific gravity and size: granular activated carbon, anthracite, silica sand, ilmenite, and magnetite sand having specific gravities of 1.24, 1.45, 2.62, 3.70, and 5.08, respectively. Flocculation kinetics were monitored by measuring floc size through microscopy and with a camera installed directly on the jar-test beaker. Settling performance was monitored using turbidity measurements. This study shows that all ballast media, when expressed as total surface available during flocculation, required similar surface concentrations to achieve settled water turbidity near 1 NTU and lower. In addition, the effects from the ballast media size and specific gravity were lowered for settling time longer than 3 min. Inversely, for settling time of 12 s, larger and denser media produced lower settled water turbidity. For certain applications, lighter ballast media may be more economical because they offer more available surface area for a given mass concentration, hence reducing the amount of ballast media required in the flocculation tank. Finally, the ballast media point of zero charge and shape were not identified as key criteria for ballasted flocculation.

Keywords*: flocculation key criteria, specific gravity, surface concentration, turbidity removal, floc size*

9.1 Introduction

Clarification processes require specific footprints that translate into important capital costs, especially in the Nordic climate where settling basins must be located inside heated buildings. Ballasted flocculation, consisting of injecting micron-sized granular media to increase the specific gravity (SG) and size of flocs, is being used increasingly in the water industry owing to its potential for achieving very high superficial design velocities (as high as 85 m/h; MDDELCC (2018)). This advantage offers a more compact process (i.e., smaller footprint), stable suspended solids removal performance, faster start-up, and important savings compared to conventional flocculation (Desjardins et al., 2002; Guibelin, Delsalle, & Binot, 1994). In earlier studies, we showed that the floc SG and size were two important factors for predicting settling performance (Lapointe et al., 2017). The final SG of flocs depends on the SG of the medium: a denser ballast medium (BM) leading to denser flocs. However, a denser medium requires a higher velocity gradient (*i.e.*, *G* value in s^{-1}) to maintain it in suspension. This leads to lower average floc diameters owing to floc break-up, and to higher fraction of un-ballasted flocs. Therefore, with reference to the design criteria (minimizing footprint or minimizing settled water turbidity); an optimal BM can be selected for a given application.

The concentration of BM inside the flocculation tank (typically referred to as the maturation tank) is very high, in the range of 4–10 g silica sand (SS)/L for industrial applications. The BM concentration depends on the particle concentration in the flocculated waters (which is linked to the coagulant dosage and the source-water particle concentration). For example, in jar testing, a higher BM concentration was necessary for a wastewater application compared to a drinking water application (2 g of SS/L for surface water of 12 NTU and 3 g of SS/L for municipal wastewater of 130 NTU (Lapointe & Barbeau, 2017; Lapointe et al., 2017)). Apart from the BM concentration, its particle size distribution is also expected to impact ballasted media performance. A medium of smaller particles translates into a higher number of available BM particles for a given mass concentration. Flocculation performance is known to be a function of $G \times t \times N_o$, where G is the mean velocity gradient, t the flocculation time, and No, the initial number of particles to flocculate. However, large BM media can produce larger flocs, which settle more rapidly. Consequently, similar to the selection of a BM SG, there is an optimum selection of the medium size to achieve the best overall flocculation/settling performance.

In summary, the selection of an appropriate BM medium is dictated by its SG, size, and the need to minimize un-ballasted flocs. This is because the latter are not well removed during settling at high superficial velocity. In addition, BM availability and cost, its resistance to abrasion, and the effectiveness of its recovery by hydrocyclone are important criteria to consider (Desjardins et al., 2002; Sibony, 1981; Young & Edwards, 2003). However, no systematic approach has yet been proposed to compare and select an appropriate BM with respect to its SG and size for a given application. In order to facilitate this procedure, this research project explored the hypothesis that flocculation performance is controlled by the surface area of BM available for ballasted flocculation, expressed as m^2 of surface per L of water. We hypothesized that differing media density and particle size distributions impact ballast media performance by increasing/reducing the reaction surface. This hypothesis was tested at laboratory scale by evaluating five ballast media with differing SG, all of which were sieved to produce three different particle size distributions. Flocculation kinetics were monitored by measuring floc size by microscopy and with a camera installed directly on the jar-test beaker. Settling performance was monitored using turbidity measurements. Recommendations are made for guiding the selection of an adequate BM to achieve turbidity removal for a specific design superficial velocity.

9.2 Material and methods

9.2.1 Water characteristics

All experiments were conducted at laboratory scale at 21±1 °C using surface water from the Sainte-Rose drinking water treatment plant (10±2 NTU; pH 6.9), which is fed by the Mille-Îles River (Quebec, Canada). The tested surface water exhibits a relatively low alkalinity (30 mg $CaCO_3$/L) and a significant dissolved organic carbon (DOC) concentration (6.9 mg C/L). The raw water was collected just past the 10 mm influent bar screens and refrigerated at 4°C during the experiments (2 weeks).

9.2.2 Jar test procedure

The jar test sequence and protocol sampling are presented in Figure 9.1. Jar tests were performed in Phipps & Bird equipment (Richmond, VA) equipped with six square *B-Kers*^{TM} jars of 2 L, each having a sampling port 10 cm from the top. Water samples were first flash mixed (G = 300 s^{-1})

during 2 min at 21°C with a simultaneous injection of alum (2.73 mg Al/L = 30 mg dry alum/L) and a pre-hydrolyzed coagulant (polyaluminum chloride PAX XL6 with a 56 % basicity; 0.40 mg Al/L). Optimal coagulant conditions were chosen based on settled water turbidity, pH, and streaming current value (SCV; Chemtrac® Systems, Inc.; ECA-2100 charge analyzer). This dual injection strategy is currently used at the full-scale plant to improve coagulation/flocculation performance, especially under cold water conditions. The pH targeted after coagulation was 6.15±0.05. Hydrex 3551 polymer (Veolia Water Technologies Canada), an anionic and high molecular weight polyacrylamide (PAM), was used to bridge BM with coagulated microflocs (mean diameter < 10 µm). The optimal PAM dosage selected was 0.4 mg/L because this provided the lowest settled water turbidity for all BM without causing floc restabilization. The BM was entirely injected at the onset of flocculation (i.e., after the 2-min flash-mix). The PAM dosage was equally divided: 50% at the onset of flocculation and 50% after 30 s (Figure 9.1 ; expressed in min). After additional floc maturation of 30 s, turbidity measurements were assessed on settled waters after 12, 60, and 180 s of settling (Turbidimeter, Hach 2100N, SM 2130 B (APHA et al., 2012)). Approximately 12 s corresponds to a typical superficial velocity of 40 m/h as used for industrial application. In this case, 60 and 180 s were selected to simulate intermediate and lower superficial velocity (Desjardins et al., 2002). BM dosages spanning from 0.2 to 7.0 g/L were tested.

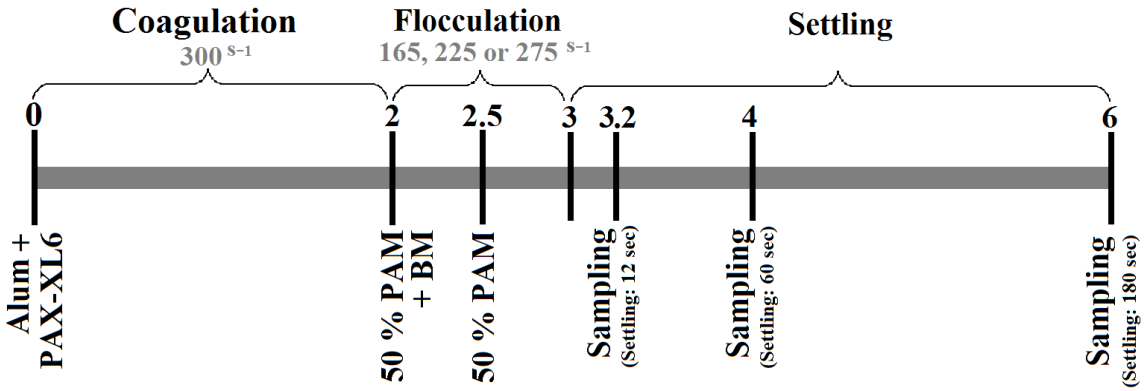

Figure 9.1: Jar test and sampling sequence.

9.2.3 Floc analysis

Flocs size and SG were characterized during flocculation by optical microscopy with a counting cell of 2 mm depth, as described in Lapointe et Barbeau (2016). To evaluate the floc rate of aggregation, a camera (FlocCAM^{TM}; time exposure: 1/1000 s) was also installed on the jar-test beaker. This equipment measured the mean floc equivalent diameter as function of time (Lapointe & Barbeau, 2017). Because the floc properties impact this analysis, the equipment was first calibrated using optical microscopy measurements as a benchmark.

9.2.4 Media properties

The media characteristics are presented in Table 9.1. Five different BM with SG ranging from 1.24 to 5.08 were evaluated: granular activated carbon (GAC), anthracite (ANT), silica sand (SS), ilmenite (IL), and magnetite sand (MS) (Table 9.1). All five media were sieved to generate three particle size distributions: 80–125 µm (*D*: 103 µm), 125–160 µm (*D*: 143 µm), and 160–212 µm (*D*: 186 µm). Because the suspension of larger/denser BM requires higher mixing intensity (Lapointe et al., 2017), the *G* value was augmented as a function of BM size. The optimal velocity gradients for those three categories were 165, 220 and 275 s^{-1}, respectively. The latter were selected based on the more restrictive of two criteria: the minimal value needed to maintain the BM in suspension and the settled water turbidity after 3 min of settling.

The optimal BM concentration (expressed in surface concentration: m^2 of BM/L) rather than mass concentration (g BM/L)) were established based on a targeted residual turbidity of 1 NTU in settled water. When this objective could not be achieved, the optimal surface concentration was identified using the point of diminishing return in the turbidity vs concentration curves (fixed at -0.5 NTU/10^{-2} m^2/L). Assuming spherical particles, the BM surface concentration was calculated as follows:

$$1)\ M_1 = V_1 \times SG$$

$$2)\ M_T = N_0 \times M_1 = N_0 \times V_1 \times SG \text{ , using eq. 1}$$

$$3)\ N_0 = \frac{M_T}{V_1 \times SG} \text{ , from eq. 2}$$

$$4)\ V_1 = \frac{\pi D^3}{6}$$

$$5)\ S_1 = \pi D^2$$

$$6)\ S_T = N_0 \times S_1$$

$$7)\ S_T = \frac{M_T}{V_1 \times SG} \times \pi D^2 \text{ , using eq. 3, 5 and 6}$$

$$8)\ S_T = \frac{M_T}{\frac{\pi D^3}{6} \times SG} \times \pi D^2 \text{ , using eq. 4 and 7}$$

$$9)\ S_T = \frac{6M_T}{SG \times D} \text{ , from eq. 8}$$

M_1: mass per grain of ballast medium (kg)

V_1: volume per grain of ballast medium (m^3)

SG: ballast medium specific gravity (kg/m^3)

M_T: total mass of ballast media (kg)

N_0: number of grain (-)

D: ballast medium mean diameter for the tested particle size distribution (m)

S_1: surface per grain of ballast medium (m^2)

S_T: total surface of ballast media (m^2)

Table 9.1: Ballast media physical properties

Ballast media	*Specific gravity*	*Aspect ratio L/l* [1]	*Hardness*	*Point of zero charge (PZC)*[2]
Granular activated carbon (GAC)	1.24	1.72	2.0 - 3.0	2.5 -12.1 (from Norit ®) (Kosmulski, 2011)
Anthracite (ANT)	1.45	1.61	2.2 - 3.0	7 (Tillman Jr et al., 2005)
Silica sand (SS)	2.62	1.44	6.0 - 7.0	< 3 (Kim & Lawler, 2005; Kosmulski, 2011)
Ilmenite (IL)	3.70	1.41	5.0 - 6.0	4.5-7.2 (Kosmulski, 2006)
Magnetite sand (MS)	5.08	1.36	5.5 - 6.5	6.5-6.7 (Kosmulski, 2011; Milonjić, Kopečni, & Ilić, 1983)

[1] BM shapes are characterized as an ellipse (*L* and *l* represent the longest and the shortest ellipse dimensions, respectively).

[2] Value for a temperature of 20–25 °C

9.3 Results and discussion

9.3.1 Selection of the optimal ballast medium concentration

In past research efforts, BM optimal dosages were selected on the basis of mass base concentration (expressed in g/L). However, identical mass base concentration BM media with differing average diameters or densities will generate different particle concentration and surface area. Figure 9.2

compares the impact of the BM media (expressed in g/L in Figure 9.2A and m^2/L in Figure 9.2B) on settled water turbidities. To prepare this figure, the smallest/lightest GAC (80–125 µm) and largest/densest MS medium (160–212 µm) were selected because they provided the most different conditions evaluated in our experimental design. In Figure 9.2A, the optimal BM concentration for GAC and MS to achieve a settled water turbidity of 1 NTU (after 3 min of settling) were very different: respectively, 0.57 g/L and 4.22 g/L for the GAC and the MS (a MS/GAC ratio of 7.4). However, when expressed as total surface available during flocculation (m^2 of BM/L; Figure 9.2B), GAC and MS required a similar BM surface concentration (0.027 m^2/L) to achieve settled water turbidity near 1 NTU, even though MS was flocculated with a higher *G* (275 s^{-1} for MS vs 165 s^{-1} for GAC). The difference between the media was not statistically different (p = 0.33). Therefore, the BM concentration will be presented throughout this paper as surface concentration (expressed as m^2 of BM/L).

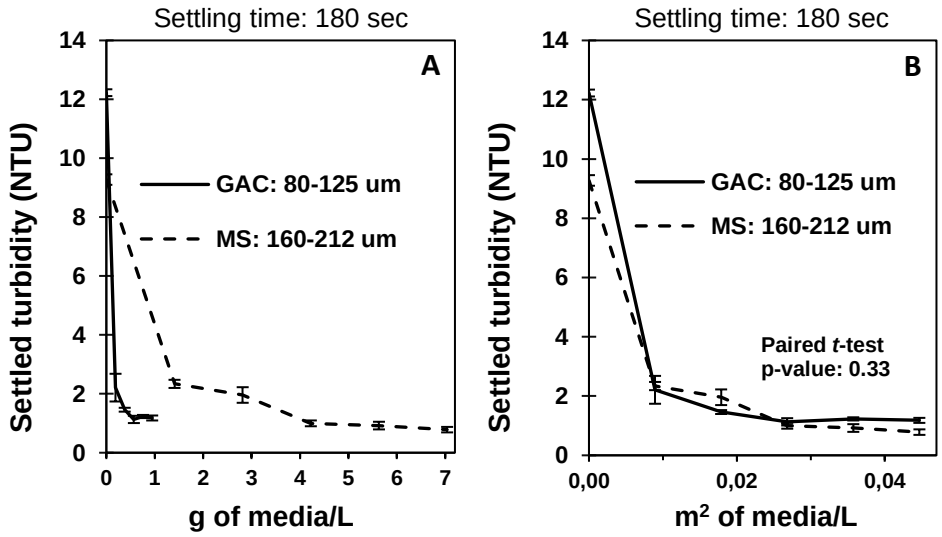

Figure 9.2: Optimal ballast medium concentration expressed as A) g/L and B) m^2/L. Flocculation conditions: 1 min at 165 s^{-1} for GAC and 1 min at 275 s^{-1} for magnetite (MS). Settling time: 180s.

9.3.2 Ballast media size, point of zero charge, and shape impacts on turbidity removal

For each medium tested, the settled water turbidities were measured after 12, 60, and 180 s of settling time (reflecting indirectly the superficial velocity of the clarifier) for three different grain size distributions. As presented in Figure 9.3, for settling time of 60 and 180 s (approximately

corresponding to superficial velocity of 6 and 2 m/h on an ideal settler without lamella), the BM size distribution (comparing 80–125 vs 160–212 µm) has no effect on settled water turbidity when normalized as m^2/L ($p = 0.65$ at 60 s and $p = 0.68$ at 180 s). For a settling time of 12 s (corresponding to 30 m/h), the BM size and type did effect the clarification performance (see Figures 9.3 A and B). The latter observation is explained by the presence of smaller/less dense flocs. For GAC and ANT, when the smallest grain size distribution (80–125 µm; 0.036 m^2 of BM/L) was used with 12 s of settling, the water turbidities were 6.4 and 7.1 NTU, respectively, compared to 3.0 and 4.0 NTU when the largest BM (160–212 µm) was used. On the other hand, the effect of BM size with 12 s of settling was lower when denser media such as SS and MS were used (Figure 9.3C and D). For a high-rate clarifier (simulated with 12 s and 0.045 m^2 of BM/L), it was demonstrated that the settled water turbidity is inversely proportional to the BM mean equivalent diameter (Figure 9.4A). However, for a settling time of 180 s, the BM size distribution and density had no significant impact ($p = 0.50$, comparing GAC and MS with respective SG of 1.24 and 5.08) on the final turbidity; so long as the BM surface concentration was kept constant amongst the different media/size distributions (Figure 9.4B). As opposed to the key role of the BM size and SG, no apparent relation was identified between turbidity removal and BM shape or point of zero charge (PZC) (cf. Table 9.1). Those conclusions were also reported in Lapointe et Barbeau (2016) and (Lapointe et al., 2017). Lee, L. T. et Somasundaran (1989) mentioned the important role of mineral oxides PZC on PAM adsorption density (i.e. PAM direct adsorption onto mineral oxides without the injection of a metal salt as coagulant). However, the current study evaluated the interactions of different BM with coagulated and flocculated waters. In other words, the impact of aluminum hydroxide/cationic monomers/polymers (from alum) and aluminum polymers (from polyaluminum chloride) greatly modified the particle charge density and adsorption affinities/mechanisms between PAM and BM. Once adsorbed onto or enmeshed into a metal hydroxide-based floc, it is expected that all BM should have similar charge densities despite their initially differing PZC. Figure 9.4B suggests that the settled water turbidity was not influenced by G (from 165 to 275 s^{-1} and proportional to the BM size). However, our study revealed the sensitivity of flocs to shearing, especially when high SG BM were used (MS was flocculated at 255 s^{-1}; (Lapointe et al., 2017)). The floc resistance to shearing and the optimal G are multifactorial and largely dependent on the PAM charge density and molecular weight, the coagulation dosage, the BM size and SG, the pH, and the temperature (Bolto & Gregory, 2007; Gregory & Barany, 2011;

Lapointe & Barbeau, 2015, 2016). Nevertheless, some researchers mentioned that ballasted flocculation could be operated under a wide range of mixing conditions without causing considerable floc breakage: 150–200 s^{-1} (150 rpm in a 2 L beaker; (Desjardins et al., 2002)), 200 s^{-1} (Ghanem, A. et al., 2007), ~ 400 s^{-1} (200 rpm in a 0.5 L beaker) (Imasuen et al., 2004), from 200 s^{-1} to 1200 s^{-1} (Young & Edwards, 2000) and 700 s^{-1} (De Dianous & Dernaucourt, 1991).

1

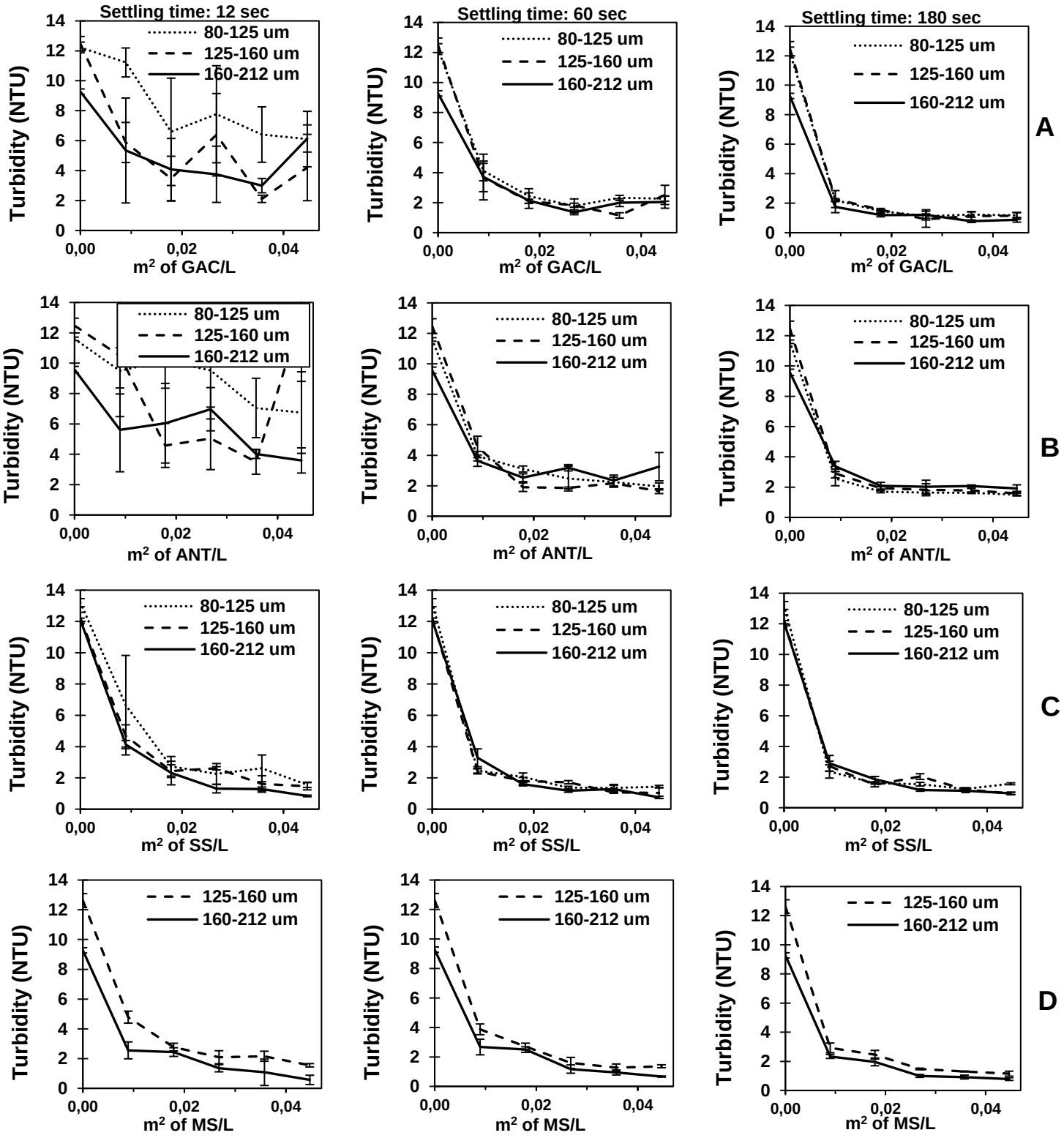

Figure 9.3: Impact of medium size and specific gravity, and settling time on turbidity removal for granular activated carbon (A), anthracite (B), silica sand (C), and magnetic sand (D). Initial turbidity = 10 ± 2 NTU.

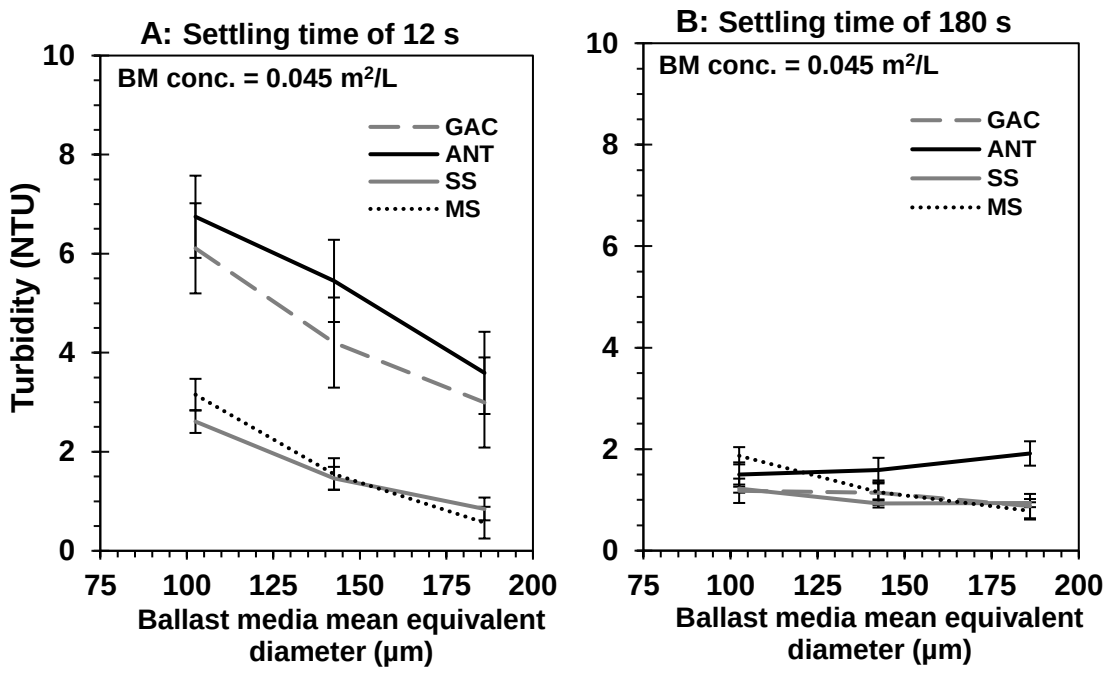

Figure 9.4: Impact of the ballast medium equivalent mean diameter on the settled water turbidity after 12 s (A) or 180 s (B) of settling. Flocculation conditions: 1 min at 165 s^{-1}, 225 s^{-1}, and 275 s^{-1} for (80–125, 125–160, and 160–212) µm, respectively.

9.3.3 Impact of ballast media specific gravity on turbidity removal

Small and light BM produced the highest settled water turbidities at high settling rates (Figure 9.4A at 12 s). For such a challenging settling time, SS, IL, and MS were all found to be suitable options (Figure 9.5A) to maximize turbidity removal independent of the particle size distributions, as long as the BM surface concentration was adjusted accordingly with the BM size distribution. Hence, denser and larger BM were best indicated to increase the design settling velocity. However, this goal is achieved at the expense of producing higher settled water turbidities, which is caused by un-ballasted flocs generated by the high-shear conditions required to maintain large/dense BM in suspension.

The higher settled water turbidity after 12 s, achieved using GAC and ANT, can be explained by the presence of unsettled ballasted flocs. For example, at 21 °C, a spherical GAC and ANT grain of 80 µm requires ballasted jar-test settling times of approximately 116 and 62 s. For a longer settling time of 180 s (Figure 9.5B), turbidity removal was not influenced by the BM SG ($p = 0.50$;

comparing GAC vs MS). For this settling condition, it was observed that the BM available surface (m^2 of BM/L) was the most influential factor (cf. Figure 9.3). Consequently, for settling times longer than 180 s, a lighter BM might be more economical because it offers more available surface per mass concentration; hence the amount of BM required in the flocculation tank is reduced. However, BM exportation to settled water and the difficulty of recovering a lighter medium via hydrocyclone might place practical constraints on selection of very light media such as GAC (which is also very brittle). On the other hand, by using smaller and lighter BM, a considerably lower mass concentration can be used, which would translate into the design of smaller hydrocyclones and pumps on the sludge recycle line.

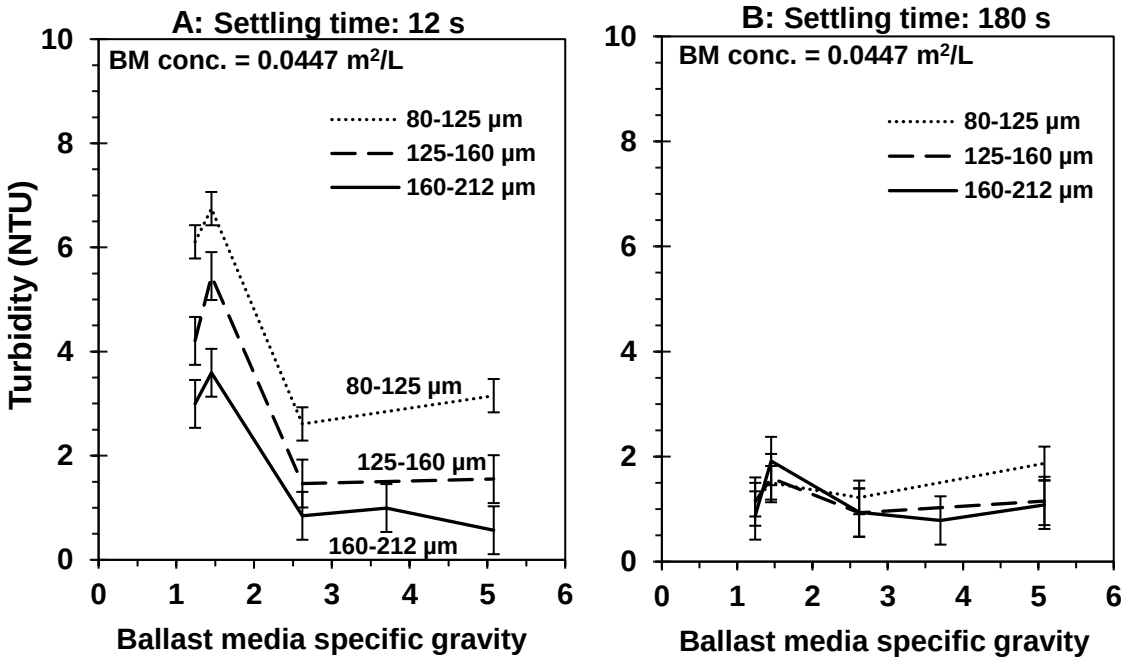

Figure 9.5: Ballast media specific gravity and grain size distribution impacts on turbidity removal. Flocculation conditions: 1 min at 165, 225 and 275 s^{-1} for 80–125, 125–160, and 160–212 µm, respectively.

9.3.4 Role of BM size distribution on floc growth kinetic

Floc growth kinetics was measured during jar tests using a camera for three conditions of BM size distributions and two surface concentrations (m^2/L) (Figure 9.6). All tests were performed with SS as BM. Floc growth was observed to increase fairly linearly with time during the 1 min flocculation

procedure. While using 0.045 m^2 of SS/L, the final floc sizes were 425, 454, and 478 µm for size ranges of 80–125 µm (flocculated at 165 s^{-1}), 125–160 µm (220 s^{-1}), and 160–212 µm (275 s^{-1}), respectively. In comparison, the final floc diameters, when 0.0089 m^2 of SS/L was used, were 389, 379, and 366 µm for the same respective size ranges ($p < 0.05$). In summary, the growth rate was mainly influenced by the SS surface concentration rather than the SS size or *G* value, the latter being proportional to the BM size. After 3 min of settling, the impact of SS surface concentration was clearly discernable as 0.0089 m^2 of SS/L led to settled water turbidities of 2.66±0.27 NTU vs. 1.14±0.36 NTU for 0.045 m^2 SS/L (Figure 9.6). It is important to point out that the floc diameters measured during settling (i.e., after 1 min) are not biased because the camera (brightness and time exposure) was calibrated to measure ballasted flocs (i.e., before 1 min), which are considerably larger than unsettleable particles.

The theoretical orthokinetic flocculation model for predicting the rate of successful collisions between particles, proposes that collision rates are linearly proportional to *G* (Smoluchowski, 1917). Later, Camp et Stein (1943) proposed that flocculation was dependent on the product $G \times N_o \times t$ where *No* is the initial number of particles in suspension. In this study, the rates of aggregation in Figure 9.6 were similar for the three *G* tested: 165, 225, and 275) s^{-1}. In theory, the net rate of aggregation depends on the floc rate of aggregation vs disaggregation, the latter being negatively impacted by higher shear (Thomas et al., 1999).

However, for a given surface concentration, Figure 9.6 indicates no clear relation between the mixing intensity and the rate of aggregation. The floc resistance, when flocculation involved very high molecular weight polymers, was frequently reported to be considerably higher (see Section 9.3.2). Hence, the aggregation kinetics was rather influenced by the available BM surface, and independent of the grain size. Figure 9.6 indicates that the number of BM grains (about 3.7 times higher with BM of 80–125 vs 160–212 µm) does not impact the rate of aggregation during ballasted flocculation.

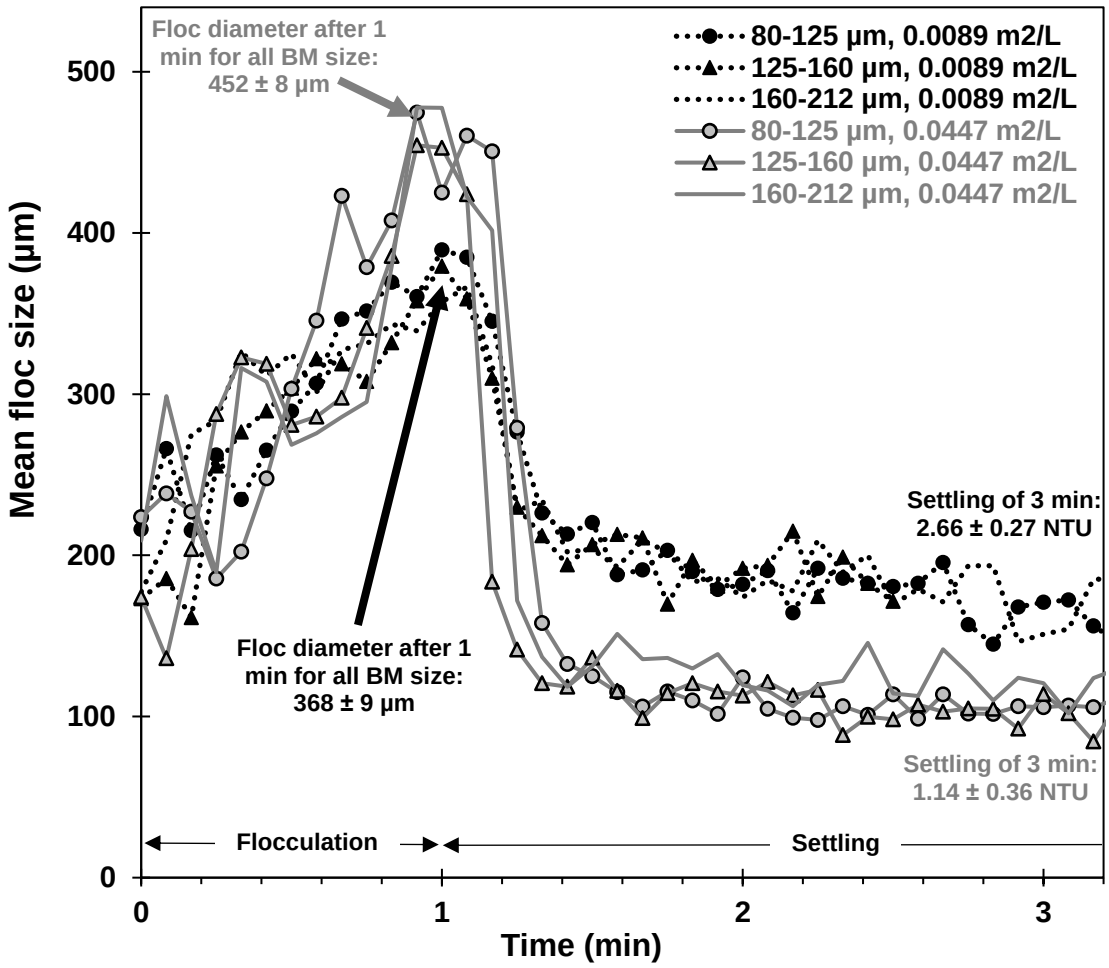

Figure 9.6: Evaluation of variable silica sand concentration and impact of the ballast size on floc formation rate, floc size, and settled water turbidity. Flocculation conditions: 1 min at 165, 225, and 275 s^{-1} for 80–125, 125–160, and 160–212 µm, respectively. Error corresponds to the standard deviation.

9.4 Conclusion

This study demonstrated that ballasted flocculation is best described as contact between surfaces (microflocs and BM). Consequently, the BM concentrations should be normalized with respect to surface in order to select an optimal and appropriate BM. For very high settling rates, the BM surface concentration, SG, and size had important effects on turbidity removal. On the other hand, as the superficial velocity applied in the clarifier decreased, it was shown that the BM SG and size were less significant, compared to the BM surface concentration. More specifically, for certain applications, a lighter BM might be more economical because it offers more available surface for

a given mass concentration, hence reducing the amount of BM required in the flocculation tank. For all tested conditions, the BM shape and PZC were not correlated with turbidity removal.

The impact of hydrodynamic repulsion caused by the use of larger BM still requires deeper evaluation because it is expected to lead to particle disaggregation. In addition, the weathering of BM caused by repeated passage through a hydrocyclone should be quantified to guide the final selection of the BM.

Acknowledgments

These experiments were conducted as part of the Industrial-NSERC Chair in Drinking Water (Polytechnique Montreal) research program, which benefits from the financial support of Veolia Water Technologies Canada, Inc., the City of Montreal, the City of Laval, the City of Repentigny and the City of Longueuil. Experiments were conducted at the CREDEAU, a research infrastructure supported by the Canadian Foundation for Innovation and the Ministry of Education of Quebec.

CHAPITRE 10 DISCUSSION GÉNÉRALE

Dans le cadre de cette thèse, les performances de la floculation liées aux caractéristiques du floculant ainsi qu'à celles du média lestant sont détaillées et décrites par l'entremise d'indicateurs de performance, tels que l'abattement de turbidité et la taille des flocs. En complément, les interactions de surface entre le coagulant, le polymère et le média lestant sont abordées à la section 10.1. Certaines limitations des modèles actuels prédisant la cinétique d'agrégation sont également soulevées à la section 10.2. Finalement, les principales conclusions tirées des chapitres 2 à 9 sont revisitées à la section 10.3 en considérant la réalité d'une filière de floculation exploitée à pleine échelle.

10.1 Interactions coagulant-polymère-média lestant

Le processus global de lestage est régi par l'efficacité de 1) la coagulation primaire et 2) de la liaison entre des microflocs coagulés et un média lestant (aidé d'un floculant). Il est à cet effet mentionné au chapitre 2 (section 2.5.1 sur le PAM) que les hydroxydes métalliques ($Me(OH)_x$) issus des coagulants métalliques ont un impact notable lors de l'adsorption du PAM sur une surface majoritairement constituée d'oxyde de silice (sable de silice, lequel contient aussi des oxydes d'aluminium, de calcium, de magnésium de potassium et de fer (cf. Tableau 7.3)). Comme la densité d'adsorption du PAM sur le sable sera influencée par la présence de $Me(OH)_x$ (Lee, L. T. & Somasundaran, 1989), la dose et le pH de coagulation joueront donc un rôle de premier plan lors du pontage interparticulaire (Duan, Jinming & Gregory, 2003; Lapointe & Barbeau, 2018b). La performance de la floculation lestée est donc dans un premier temps tributaire des conditions de la coagulation. Il serait par la suite possible, une fois la chaîne de PAM adsorbée sur le média lestant via les hydroxydes métalliques, d'appliquer les modèles prédisant la cinétique d'agrégation basés sur le taux de collisions efficaces entre les microflocs coagulés et le média lestant (ou entre deux grains de sable). Plusieurs limitations quant à l'utilisation de ces modèles en floculation lestée sont discutées à la section 10.2.

Il est probable qu'une coagulation à pH élevé avec un faible COD (*e.g.*, Fleuve St-Laurent: COD de 3 mg C/L et une coagulation avec 1,8 mg Al/L à pH 7,8) comparée à une coagulation en conditions plus acides avec un COD élevé (*e.g.*, Riv.-des-Prairies: COD de 6 mg C/L et une coagulation avec 4,5 mg Al/L à pH 6) requiert un floculant qui diffère en termes de densité de

charge. De plus, la densité de charge du polymère peut parfois compenser une coagulation non optimale. Par exemple, un PAM cationique peut améliorer la liaison entre la MON et certains oxydes présents à la surface des particules (selon leur PZC; Lee, L. T. et Somasundaran (1989)) lorsqu'une dose insuffisante d'alun est utilisée (Bolto et al., 2001). Dans ce cas précis, le PAM cationique agit comme agent de pontage par l'entremise d'interactions de type électrostatique (sur divers oxydes et sur la MON tous deux chargés négativement) plutôt que par des liaisons hydrogène entre les $Me(OH)_x$ et les groupes amides du PAM.

Dans un contexte nord-américain, certaines villes sélectionnent les conditions de coagulation de sorte à maximiser l'abattement de COD et minimiser les précurseurs de SPO. Inversement, certaines installations pour lesquelles les eaux de surface sont peu enclines à la formation de SPO auront tendance à limiter les doses de coagulant, réduisant ainsi les coûts d'opération. Plusieurs autres installations ajustent la dose de coagulant pour optimiser l'abattement de turbidité et laissent plutôt à d'autres procédés (e.g. O_3) le soin de contrôler la formation de SPO. La variabilité des conditions de coagulation d'une installation à l'autre ne permet donc pas l'utilisation d'une approche systématique et prédéterminée d'optimisation de la floculation par l'entremise d'un polymère unique. De ce fait, plusieurs villes bénéficieraient d'essais de traitabilité démontrant l'évolution (et la stabilité) de la taille des flocs en fonction du temps de floculation, et ce, en fonction des conditions de coagulation propres à leur installation. Les résultats présentés à l'Annexe B montrent d'ailleurs la possible décroissance des flocs en fonction du temps de contact, laquelle est accentuée lors de l'utilisation d'un floculant inadéquat (*Hydrex* 3511). Ces essais ont démontré que malgré des poids moléculaires très similaires (1,2–1,4 x 10^7 g/mol), deux PAM avec des densités de charge distinctes (*Hydrex* 3511 (anionique : 3%) vs *Hydrex* 3613 (cationique: 10%)) génèrent des flocs de taille significativement différente (*t*-test pairé; p-value < 0,05) : diamètres moyens respectifs de 536 et 695 µm à la fin de la floculation. Considérant une densité de l'ordre de 1400–1500 kg/m^3, cette augmentation de la taille moyenne des flocs (30%) avec l'utilisation d'*Hydrex* 3613 se traduit par une augmentation de la vitesse de chute de 38% (à 21°C et lorsque 1 < Nr < 1000). Il est donc clair que la performance de la décantation, et plus particulièrement la charge superficielle pouvant être appliquée, est intimement liée au choix du floculant.

10.2 Cinétique de la floculation lestée

En excluant la coagulation, il est possible de scinder la cinétique de floculation en 2 phases : 1) la phase latente d'agrégation liée au temps minimal requis pour l'adsorption du PAM sur des surfaces et 2) la phase d'agrégation contrôlée par le taux de collisions efficaces par rapport au bris des flocs. Les résultats présentés dans cette thèse démontrent que la taille des flocs et la cinétique d'agrégation sont notamment influencées par l'intensité de mélange, la dose et le type de polymère, la taille du média lestant ainsi que sa surface disponible. Or, les modèles classiques, tel que celui de Smoluchowski (1917) et les modèles plus récents (Biggs & Lant, 2002; Hogg, 1984; Thomas et al., 1999) s'y référant ne considèrent pas la présence d'un média lestant. Une des hypothèses posées par certains modèles mentionnés plus haut est celle de la distribution unique des particules. Par contre, en ce qui concerne la floculation lestée, deux distributions de taille sont en jeu lors de l'amorce de la floculation : les particules constituant la turbidité (typiquement 0,01–10 µm) et le média lestant (50-300 µm; *d50* de 130–160 µm). Le média lestant augmente considérablement le volume et la surface des particules présentes dans le système (cf. section 9.3). Or, aucune étude ne s'est consacrée au développement d'équations prédisant la cinétique d'agrégation en présence d'un média lestant. Les sous-sections suivantes marquent les hypothèses émises par les modèles actuels pour lesquelles des discordances sont anticipées lorsqu'un média lestant est en jeu.

10.2.1 Impact du média lestant sur les modèles d'agrégation-désagrégation classiques

Selon la littérature scientifique, la croissance des flocs est contrôlée par le nombre de collisions et par le facteur d'efficacité de collisions (α). La probabilité que deux particules entrent en contact, quant à elle, est plus spécifiquement influencée par le volume des particules et par le gradient de vitesse (*G*) (Camp & Stein, 1943). Comme la floculation lestée implique un média lestant de taille considérablement plus élevée que les particules initialement présentes dans les eaux brutes, il est clair que le taux de collisions réussies et la désagrégation ne peuvent être prédits par les modèles classiques. Deux mécanismes pourraient influencer le taux de collisions réussies et la cinétique de désagrégation dans ce contexte : A) les effets de poussée/répulsion hydrodynamique générés par un média lestant et B) les forces de compression et de cisaillement causées par les collisions de ce même média sur la structure existante d'un floc.

Dans le cas du mécanisme A), il a été démontré par Thomas et al. (1999) qu'une collision entre deux particules pouvait être évitée due à la zone d'influence hydrodynamique autour de certaines particules; une compression de la couche du fluide entre celles-ci étant la source de cette répulsion menant à la réduction du taux de collisions (et par le fait même, du taux de collisions réussies). Ce concept propose donc que des particules puissent adopter une trajectoire curviligne alors que la plupart des modèles font assise sur l'hypothèse d'une trajectoire rectiligne. Plus particulièrement en lien avec la floculation orthocinétique durant laquelle les forces de mélange supplantent celles induites par le mouvement *Brownien,* Han et Lawler (1992) mentionnent que le taux de collisions peut être passablement surestimé pour certaines distributions de particules lorsque l'hypothèse de la trajectoire rectiligne est implantée dans un modèle. Ces mêmes auteurs dénotent que cette surestimation est davantage marquée pour des particules de distributions de taille considérablement différentes (1 vs 1000 µm), ce qui est d'ailleurs le cas de la floculation lestée (Lapointe et al., 2017). Chellam et Wiesner (1993) ont d'ailleurs démontré que la trajectoire d'un floc était influencée par sa porosité. Des flocs très denses, donc peu poreux, adopteraient une trajectoire plus curviligne alors que des flocs très poreux, donc moins influencés par les zones d'influence hydrodynamique, adopteraient une trajectoire semi-curviligne. Il est conséquemment à prévoir qu'un floc lesté ou un grain de sable (densité respective d'environ 1400 et 2650 kg/m^3) soit davantage soumis aux forces de répulsion hydrodynamique par rapport à un floc conventionnel (typiquement : 1030−1050 kg/m^3; Larue et Vorobiev (2003)).

En ce qui concerne le mécanisme B), il est aussi envisageable que certaines collisions mènent au bris des flocs : la force d'impact générée par une particule en mouvement étant proportionnelle à sa taille et à sa vitesse. Ce phénomène n'a cependant pas été couvert par la littérature scientifique. Des résultats partiels issus d'expérimentations faites au cours de cette thèse soutiennent cette hypothèse. À surface externe équivalente (exprimée en m^2 de média lestant/L), les turbidités de l'eau décantée lors de l'utilisation d'un média lestant de 143 µm (20 g/L = 0,063 m^2/L) et de 72 µm (5 g/L = 0,063 m^2/L) ont été respectivement de 1,87 et 0,69 UTN. Pour ces deux essais, il a été considéré que le floculant (amidon) et le coagulant n'étaient pas limitants. À la lumière ces observations, similairement à ce qui est mentionné à la section 4.4.3, les phénomènes d'incorporation de média lestant en fonction de sa taille doivent également être considérés. Il est toutefois difficile de différencier les effets intriqués de la répulsion hydrodynamique, du bris des

flocs et de l'incorporation du média selon sa taille. Cette thèse a évalué seulement les impacts confondus de ces divers phénomènes.

Peu d'auteurs dans la littérature actuelle ont tenté d'expliquer l'effet d'une double distribution de taille et de l'effet de particules de forte dimensions sur la cinétique d'agrégation et d'érosion. En adaptant les modèles de Spicer, Patrick T et Pratsinis (1996) et de Serra et Casamitjana (1998), les travaux de Biggs et Lant (2002) prévoit l'ajustement de l'érosion des flocs en fonction de leur taille lors de la floculation de boues activées (sans agent lestant). Ce facteur pénalisant proposé par ces auteurs est toutefois associé à la fragilité croissante des flocs en fonction de leur taille, ce qui diffère de ce qui est mentionné plus haut.

10.2.2 Efficacité des collisions

Le facteur d'efficacité de collisions α des propriétés surfaciques des particules (*e.g.*, le potentiel zêta, présence de $Me(OH)_x$) (Hogg, 1984). Tel que discuté au chapitre 2 (Lapointe & Barbeau, 2019), le pH, le type de coagulant et le type de floculant jouent chacun un rôle majeur sur α. Ce dernier paramètre est cependant inconstant durant la floculation. Il tend parfois à diminuer lors de la floculation lorsque les sites d'ancrage du floculant deviennent limitants ou lorsque le floculant adopte une configuration moins optimale (aplatie) pour le pontage (cf. section 2.2). Le facteur d'efficacité de collisions est aussi latent en début de floculation lorsque la surface des particules est dénuée de PAM. Le temps minimal requis afin de lié un segment du floculant sur une surface est inversement proportionnel à son poids moléculaire, au gradient de vitesse et la taille des particules impliquées (Gregory & Barany, 2011). Selon les modèles de Gregory (1988) et Gregory et Barany (2011), considérant une concentration de particules de 0,02 % et un G de 165 s^{-1}, le temps d'adsorption d'un PAM (10^7 g/mol) sur la surface d'un microfloc de 1 µm sera de l'ordre de 8 s alors qu'il serait de l'ordre de 10^{-6} s sur un média lestant de 300 µm. Ces auteurs mentionnent que l'adhésion d'un polymère sur des particules est régie par une réaction d'ordre 2, c'est-à-dire, en fonction de la concentration de floculant et celle des particules.

10.2.3 Modélisation adaptée à la floculation lestée

Tel que mentionné à la section précédente et au chapitre 2, le PAM et les conditions de coagulation sont considérés comme des intrants importants à l'optimisation de α (Hogg, 1984). Selon les modèles classiques et ceux plus récents, le volume des particules et le gradient de vitesse sont aussi

influents en ce qui concerne la cinétique d'agrégation. Tout particulièrement pour la floculation lestée, indépendamment de cette cinétique, le *G* est au préalable fixé en fonction de la résistance des flocs au cisaillement (afin de maximiser l'abattement de turbidité) et afin de maintenir le média lestant en suspension (cf. section 8.3.3). De plus, le volume (ou la concentration) des particules dans un système influence largement la cinétique d'agrégation (Camp & Stein, 1943; Han & Lawler, 1992; Smoluchowski, 1917; Thomas et al., 1999). En considérant les données présentées à la Figure 9.6, il est constaté que cette cinétique est influencée par la surface disponible de média lestant plutôt que par sa taille ou sa concentration exprimée en g/L. En augmentant cette surface de 0,0089 m^2/L à 0,0447 m^2/L (augmentation de 400 %), la croissance de la taille des flocs ont évolué de 227 µm/min à 310 µm/min (augmentation de 37 %). Selon les conclusions du chapitre 8 et considérant ce qui est mentionné précédemment, la cinétique d'agrégation pourrait être simplifiée et prédite selon une réaction d'ordre 1, soit en fonction de la surface disponible de média lestant. Toutefois, Fadda, Cincotti, Concas, Pisu et Cao (2009) mentionnent qu'une réaction d'ordre 2 serait plus appropriée, notamment lorsque des particules ont des distributions de taille considérablement différentes (*e.g.*, des microflocs coagulés de 10 µm par rapport à un média lestant de 140 µm). En s'appuyant sur l'étude Fadda et al. (2009), la formation de flocs lestés serait régie par une réaction d'ordre 2 en fonction des concentrations exprimées en unité de surface de microflocs coagulés et du média lestant. L'érosion des flocs serait pour sa part régie par une réaction d'ordre 1, soit en fonction de la concentration des flocs lestés seulement. Une approche similaire est proposée dans Lu, C. F. et Spielman (1985), où le bris de flocs est fonction du produit entre le volume des flocs formés et la contrainte de cisaillement induite.

En termes cinétiques, il faut toutefois distinguer la croissance des flocs par rapport au taux de disparition des microflocs. Les résultats présentés à la Figure 7.3 ont montré que le diamètre des flocs n'était pas toujours un bon indicateur de l'abattement de turbidité. Pour certains systèmes avec des temps de floculation écourtés (30–60 s), des flocs de taille appréciable pouvaient être formés tandis que plusieurs particules demeuraient non agrégées. Pour cette étude (chapitre 6), les tailles moyennes des flocs lestés après 1 min et 2 min de floculation ont été respectivement de 436 µm et de 467 µm (augmentation de seulement 7 %) alors que les turbidités respectives à l'eau décantée ont diminué considérablement, soit de 1,2 UTN à 0,5 UTN (réduction de 58 %). Ces observations suggèrent donc que deux systèmes d'équations soient nécessaires afin d'optimiser la floculation lestée : un dédié à l'augmentation des flocs en fonction du temps et l'autre quantifiant

la concentration de particules non agrégées (Parker, Kaufman, & Jenkins, 1972; Watanabe, 2017). Le suivi simultané de la taille des flocs et des particules réfractaires à l'agrégation est d'ailleurs justifié par les tavaux de Thomas et al. (1999). Ces travaux stipulent qu'une collision entre deux grosses particules *j* (floc lesté) est beaucoup plus probable qu'une collision entre une petite particule *i* (microfloc) et une particule *j*. Similairement au COD réfractaire en *enhanced coagulation*, la notion de particules réfractaires définirait la performance réelle de la floculation lestée, sachant que ces particules non agrégées peuvent résulter du bris de micro-flocs. À l'heure actuelle, il n'est toujours pas clair dans quelle proportion la turbidité résiduelle après décantation résulte de particules qui n'ont pas été correctement floculées ou de microparticules résultant du bris de flocs induits par le brassage requis pendant la floculation.

10.3 Échelle laboratoire vs échelle réelle

Cette section traite des écarts de performances parfois observables entre la floculation en bécher et celle à échelle réelle. Les enjeux liés à la répartition de la puissance dissipée, au court-circuitage hydraulique et à la dispersion du floculant expliquent majoritairement ces écarts.

10.3.1 Répartition de la puissance dissipée

Dans un floculateur à échelle réelle, le mélange induit est réparti de manière plus hétérogène que dans un réacteur contrôlé en laboratoire. En station, la hauteur et le type de mélangeur ont un impact important sur la répartition de la puissance (Myers, Ward, & Bakker, 1997). Un ratio plus élevé du diamètre de l'agitateur par rapport à l'aire de la section du floculateur explique aussi la meilleure répartition de la puissance dissipée en laboratoire (Alexopoulos, Maggioris, & Kiparissides, 2002). Le *G* maximal local auquel les flocs seront soumis dans un floculateur à échelle réelle sera donc plus élevé que celui en laboratoire. Le diamètre moyen des flocs est principalement limité par ce *G* maximal (près du mélangeur) plutôt que par le *G* moyen (puissance dissipée en W/volume total du réacteur en m^3) (Biggs & Lant, 2000; Lapointe & Barbeau, 2015; Yukselen & Gregory, 2004). Cette observation a aussi été reportée par Ducoste et Clark (1998). À puissance dissipée équivalente, ces derniers auteurs mentionnent que la taille des flocs est inversement proportionnelle à la taille du bassin de mélange. Il a aussi été démontré par Hopkins et Ducoste (2003) qu'une mauvaise dispersion de l'intensité de mélange menait à une distribution de taille des flocs plus étalée causée par l'apparition de flocs de faible taille. Cet aspect concernant la puissance mal

répartie explique partiellement les meilleures performances d'abattement de turbidité souvent observées en laboratoire.

Contrairement à l'agrégation due aux interactions électrostatiques, le bris des flocs formés au préalable par l'entremise du pontage interparticulaire via un floculant organique à haut poids moléculaire est considéré comme partiellement irréversible (Yoon & Deng, 2004), notamment en raison d'une reconfiguration moins favorable et définitive de la chaîne de polymère sur une surface (Bolto & Gregory, 2007). Ce dernier aspect marque d'autant plus l'importance de limiter le bris de flocs.

10.3.2 Temps de contact et court-circuitage

La configuration d'un floculateur opéré en continu (réacteur en continu parfaitement mélangé) a un impact sur les phénomènes de court-circuitage, lesquels mènent à une distribution du temps de résidence (Cholette & Cloutier, 1959; Rebhun & Argaman, 1965). Contrairement aux essais effectués en laboratoire (cuvée), certains flocs auront un temps de contact faible ou élevé menant respectivement à une agrégation insuffisante (Gregory, 1988; Lapointe & Barbeau, 2016) ou à une surexposition au cisaillement causant le bris des flocs et la reconfiguration moins avantageuse du polymère à la surface des particules (Caskey & Primus, 1986; Gregory & Barany, 2011). Si le PAM requiert un temps minimal afin de s'adsorber sur une particule et qu'il peut également subir une reconfiguration en fonction du temps, il est donc essentiel de contrôler la distribution des temps de résidence au sein du floculateur. Cet objectif peut être atteint par une conception portant attention à la géométrie des bassins ainsi qu'aux conditions d'entrée/sortie de chacune des cuves. Il demeure malgré tout très difficile de concevoir un procédé avec un comportement hydraulique idéal pour tous les débits d'opération anticipés, lesquels peuvent varier dans un ratio de 4 pour 1.

10.3.3 Dispersion des produits chimiques et âge de la solution mère

Une dispersion homogène du coagulant et du floculant est essentielle lors de l'optimisation du traitement conventionnel (Kawamura, 2000), mais également lors de la floculation lestée. Tel que mentionné par Owen, A. T. et al. (2002), une mauvaise dispersion du PAM mène à 1) à la présence insuffisante de chaine polymérisée à la surface des particules et 2) à une densité d'adsorption trop élevée sur d'autres particules menant à un reversement de charge. Ces derniers auteurs notent également l'importance de l'âge de la solution de PAM, la viscosité (lié au poids moléculaire)

ayant tendance à réduire en fonction du temps. Dans le cadre de ces présents travaux, un âge de moins de 5 h de la solution de polymère a permis de maintenir la viscosité du PAM (poids moléculaire de 10^7 g/mol; solution mère de 400 mg/L). Cette potentielle réduction de viscosité est la plupart du temps associée soit 1) à la reconfiguration de la chaine polymérisée due à l'influence des molécules d'eau sur les liaisons hydrogène (Klein & Westerkamp, 1981; Kulicke, W. M., 1986), 2) à une oxydation causée par certains radicaux libres résiduels venant du catalyseur lors de la polymérisation ou 3), pour des temps de stockage plus élevés, à la biodégradation lorsque la température est adaptée à la croissance microbiologique (poids moléculaire de 10^6 g/mol; solution mère de 200 mg/L; Chmelir, Künschner et Barthell (1980)). Étant plus rapidement biodégradables que les PAM, les polymères à base d'amidon sont plus susceptibles à une biodégradation.

10.4 Effet des floculant à base d'amidon sur les filières en aval

En considérant le risque toxicologique en lien avec l'acrylamide provenant de l'alimentation, il n'apparait pas prioritaire de mettre en place des mesures plus coercitives que celles actuellement en vigueur en Amérique du Nord par rapport à l'utilisation du PAM en traitement de l'eau potable. Toutefois, une approche plus globale considérant l'impact du floculant sur les filières de traitement en aval de la décantation doit être considérée. Il a été démontré que certains floculants à base d'amidon comme alternative au PAM pouvaient réduire les pertes de charge lors de la filtration granulaire (à concentrations équivalentes de particules; Ouellet (2017b)), ces dernières étant causées par l'exportation de particules non décantables vers les filtres. Certains enjeux liés à la capacité de production et à l'économie d'eau pourraient donc bénéficier de floculants alternatifs tels que les polymères à base d'amidon. Le floculant utilisé, lequel se retrouve dans les boues de traitements, a également un impact sur la déshydratation des boues.

10.5 Coût environnemental du polyacrylamide vs celui du polymère d'amidon

Outre l'impact d'un polymère sur la performance de la floculation, ou encore sur les filières en aval, son coût énergétique de production et son empreinte environnementale doivent aussi être considérés lors de la sélection de produits. Une analyse de cycle de vie comparant le PAM et l'amidon pourrait être complétée en considérant que les concentrations requises d'amidon sont typiquement 4−14 fois plus élevées que celles du PAM. Toutefois, le PAM est synthétisé à partir

de produits issus de la pétrochimie (Xing et al., 2010) alors que l'amidon (patate, riz, maïs, etc.) est un polysaccharide d'origine naturelle et davantage biodégradable que le PAM (Lapointe & Barbeau, 2019). L'aspect plus biodégradable d'un polymère peut lui conférer un net avantage en ce qui concerne la gestion et l'épandage de boues en tant que fertilisant agricole.

CHAPITRE 11 CONCLUSIONS ET RECOMMANDATIONS

Les résultats ont montré que le type de polymère et de média lestant avaient tous deux une importance cruciale sur la taille et la densité des flocs ainsi que sur l'abattement de turbidité. Cette thèse fait la démonstration que des floculants à base d'amidon peuvent être utilisés comme alternative au PAM. Les chapitres 4, 5 et 6 proposent des recommandations quant au mode opératoire approprié lors de l'utilisation de ces polymères alternatifs. Ils pourraient être utilisés à échelle réelle, en eau froide comme en eau chaude, par des installations de traitement souhaitant 1) réduire les pertes de charge lors de la filtration granulaire, 2) limiter l'exposition au monomère d'acrylamide ainsi que divers sous-produits présents dans les polymères synthétiques, ou 3) augmenter la biodégradabilité des boues de traitement.

Outre le PAM et les floculants à base d'amidon, le chapitre 1 classifie les propriétés de plus de vingt floculants synthétiques, naturels ou naturels-*g*-synthétiques. En énumérant leurs divers avantages et inconvénients, cette revue de littérature facilite dorénavant la sélection d'un floculant en fonction d'une application donnée.

Les résultats obtenus aux chapitres 7 et 8 ont montré que le choix de la densité du média lestant s'établissait sur un compromis entre la charge superficielle souhaitée et l'abattement de turbidité. L'utilisation d'un média plus dense a nécessité une énergie de mélange plus élevée, réduit la taille des flocs et impacté négativement l'abattement de turbidité. Toutefois, dû à la densité plus élevée des flocs lestés formés par ce genre de média (*e.g.*, la magnétite), la vitesse de chute calculée a été conséquemment plus élevée.

Ces divers diagnostics mentionnés plus haut sur la morphologie des flocs lestés ont pu être posés grâce à la méthode développée, décrite au chapitre 4, sans laquelle il n'était auparavant pas possible de mesurer la densité des flocs lestés. En utilisant les équations de vitesses de chute déjà développées dans la littérature ou par l'entremise de méthodes par éléments finis, la densité mesurée permettrait dorénavant de modéliser et de prédire la performance d'abattement dans un décanteur lamellaire. Cette méthode a aussi démontré, lors de conditions de lestage adéquates, que la vitesse de chute était davantage corrélée avec la taille des flocs plutôt qu'avec leur densité. La forme de ceux-ci a eu peu d'impact sur la vitesse de chute calculée par rapport à l'influence combinée de la taille et de la densité.

Plus spécifiquement, en lien avec les polymères d'amidon utilisés comme alternative au PAM, il a été possible d'améliorer considérablement leur performance d'abattement de turbidité; la turbidité à l'eau décantée était sous la valeur cible de 1 UTN. Les conditions d'opération suivantes avaient un impact marqué sur l'enlèvement de turbidité.

- Sur la base d'une étude comparée, il a été démontré que la composition du média lestant avait un impact important sur l'abattement de turbidité. Dans le cas du PAM et des polymères d'amidon, mais plus particulièrement pour ce dernier, un sable exempt d'oxydes métalliques (99% de SiO_2) permettait de réduire les doses requises de floculant.
- La taille du média lestant avait également un impact significatif sur l'abattement de turbidité, l'amidon bénéficiant de la présence d'un média lestant plus petit.
- Un *G* d'environ 165 s^{-1} permettait de maintenir le sable de silice en suspension sans toutefois soumettre la structure des flocs à un cisaillement excessif. Ce *G* optimal n'était valide que pour les granulométries étudiées.
- La taille des flocs et l'enlèvement de turbidité ont été influencés par le temps de floculation. Pour des essais en laboratoire permettant d'atteindre 1 UTN, le polymère d'amidon a nécessité un temps de floculation de 4 à 8 min comparativement à 1 à 2 min pour la PAM.
- Il est connu qu'un floculant interagit avec les hydroxydes métalliques provenant du coagulant afin de lier les particules à divers oxydes, tels que le sable de silice. Les présents travaux ont confirmé que les polymères d'amidon étaient sensibles au pH. La plage optimale de pH était entre 6,0 et 6,5 pour un polymère d'amidon anionique ayant une densité de charge entre 1,8 et 2,4 meq/g.
- La densité de charge des polymères d'amidon peuvent également être optimisée. Par exemple, une faible densité de charge anionique (environ 2 meq/g) est optimale pour les conditions de coagulation spécifique à la station de production d'eau potable de Chomedey (Laval).
- La combinaison de l'amidon et du PAM a eu des effets synergiques sur l'abattement de turbidité et sur la taille des flocs. Près de 70 % du PAM peut être remplacé par l'amidon, et ce, sans affecter la taille, la résistance au cisaillement et la densité de flocs. La cinétique d'agrégation ainsi que l'abattement de turbidité avait demeuré aussi inchangés. Comme

l'amidon est moins colmatant que le PAM, il est donc anticipé qu'un système amidon-PAM puisse réduire le développement de perte de charge lors de la filtration granulaire.

Dans le deuxième volet de cette thèse en lien avec l'impact des propriétés du média lestant sur l'enlèvement des particules, les résultats ont démontré que l'utilisation d'un média plus dense et plus volumineux comportait simultanément et indissociablement certains avantages et inconvénients, notamment l'abattement de turbidité au détriment de la charge superficielle.

- Divers scénarios de granulométrie et de densité d'un média ont permis de comprendre le mode de fonctionnement lors du lestage. Pour un temps de décantation supérieur à 1 min, la surface de média lestant a ainsi contrôlé la performance de la floculation.
- La vitesse de chute calculée des flocs a été proportionnelle à la densité du média. En contrepartie, pour des temps de décantation plus longs, l'abattement de turbidité s'est avéré inversement proportionnel à la densité du média. Ce phénomène est attribuable au bris de flocs lorsqu'un gradient de vitesse plus élevé était induit. Globalement, cette thèse décrit et démontre la potentielle flexibilité de la floculation lestée en fonction de la taille et de la densité d'un média lestant.
- Lors des études sur l'effet de la taille, il a été constaté que des médias lestants plus petits ont parfois offert des abattements de turbidité plus élevés, et ce, même à surface de média équivalente. Plus spécifiquement, la taille appropriée d'un média (*i.e.*, la taille maximale incorporée dans la structure d'un floc) a été proportionnelle à la taille des flocs formés. Cette relation entre la taille d'un floc et la taille du média est valide indépendamment du polymère utilisé et du mode opératoire (*e.g.*, *G* et temps de mélange). Toutefois, pour des applications à pleine échelle, la notion de perte de média lestant à l'eau décantée est un enjeu, cette perte étant justement inversement proportionnelle à la taille du média.

Les recommandations suivantes sont issues des observations et des contraintes mentionnées précédemment, mais aussi modulées en fonction d'une campagne d'échantillonnage effectuée lors de ces présents travaux sur des décanteurs lamellaires et des connaissances actuelles de secteur de l'eau.

- La densité de charge que doit avoir un polymère ainsi que la concentration optimale de ce dernier sont influencées par les conditions de coagulation ainsi que par les caractéristiques

de l'eau, lesquelles sont spécifiques à chaque installation. Des essais de traitabilité affinant le choix du floculant doivent donc être effectués afin d'optimiser l'abattement de turbidité et d'améliorer la robustesse des installations de traitement de l'eau. La présélection d'un floculant devrait idéalement être basée sur l'évolution de la taille des flocs et sur la concentration de particules non agrégées en fonction du temps mélange. À cet effet, la possibilité d'avoir deux polymères disponibles en station doit être envisagée, plus particulièrement si une installation modifie considérablement ses conditions de coagulation durant une période prolongée.

- Similairement à la recommandation précédente, le suivi de la taille des flocs des installations de traitement permettrait non seulement de poser un diagnostic sur le choix des produits chimiques et celui de l'intensité de mélange, mais également de faire un pronostic de la filtration granulaire. Le risque microbiologique est basé sur des mesures de turbidité en aval de la filtration et calculé indépendamment de la performance de la décantation. Or, il n'est pas garanti qu'une eau décantée de meilleure qualité mène nécessairement à une amélioration de celle filtrée.

- Les résultats obtenus ont également montré que la surface de média lestant avait un impact important. Cependant, des incertitudes demeurent présentes en lien avec la portion granulométrique contribuant réellement au lestage par rapport à celle générant des forces hydrodynamiques et des collisions menant à l'érosion et à la fragmentation des flocs. En testant différentes tailles d'un média monodispersé, il seait aussi possible de distinguer l'impact des collisions émises par de gros grains sur le bris de flocs par rapport à l'impact de l'augmentation de la surface provenant de ces grains sur la cinétique d'agrégation.

- Afin de prédire les performances de la floculation lestée, un modèle cinétique simplifié pourrait être développé selon une réaction d'ordre 1 (ou de pseudo-premier ordre) en fonction du volume ou de la surface du média lestant. Pour ce genre de système simplifié, les Me(OH)x et le floculant ne doivent pas être limitants. Tel que mentionné au point précédent, l'utilisation d'un média lestant avec un faible coefficient d'uniformité (monodispersé) faciliterait la mise en place de ce modèle basé sur une cinétique d'ordre 1.

- En ce qui concerne la carboxyméthylation de l'amidon, il serait possible d'adapter le ratio NaOH/amidon afin d'optimiser le poids moléculaire et simultanément sacrifier la densité

de charge. La carboxyméthylation, dictant la densité de charge anionique d'un polymère en fonction du degré de substitution, peut être la cause d'une réduction marquée du poids moléculaire de plusieurs polysaccharides. Or, pour la floculation lestée, le poids moléculaire plus faible de l'amidon semble être la limitation principale à son déploiement à l'échelle industrielle. D'autres conditions pourraient être revues lors de la carboxyméthylation afin de maximiser le poids moléculaire (type de solvant, température, temps et concentration de l'amidon).

- Une analyse coût-bénéfice de l'amidon-*g*-PAM ou du CMC-*g*-PAM utilisé en floculation lestée pourrait être effectuée afin d'estimer leur potentiel par rapport au PAM.

Dans le but d'améliorer l'enlèvement des particules, d'augmenter la robustesse du procédé, d'élargir les applications possibles, d'accélérer la liaison des microflocs sur le média lestant ou d'augmenter les charges superficielles admissibles sur un décanteur lamellaire :

- Grâce à la méthode en microscopie développée lors des présents travaux permettant de calculer la vitesse de chute d'un floc lesté, il est désormais possible de prédire l'enlèvement de ces flocs au sein de décanteurs lamellaires en fonction du régime d'écoulement entre les lamelles (la charge superficielle). La densité des flocs était auparavant l'information *sine qua non* mais manquante pour ce genre de modélisation.
- Considérant que l'enlèvement des particules au sein d'un décanteur lamellaire est aussi dicté par la concentration de flocs de faible taille et densité, il serait pertinent d'évaluer l'impact d'un troisième point d'injection de PAM au sein du maturateur afin d'en évaluer l'influence sur la distribution de taille des flocs lestés par rapport celle des flocs non-lestées.

Plus globalement, les performances d'abattement de turbidité sont influencées par l'étroite collaboration entre la floculation et la décantation. La configuration d'un séparateur gravitaire doit considérer la distribution de vitesse de chute des agrégats formés en amont, mais aussi le régime d'écoulement au sein des lamelles. Plusieurs modèles prédisant le taux de capture d'un décanteur supposent que les particules ne peuvent être remises en suspension une fois déposées sur la structure lamellaire. Or, plus particulièrement lors de la floculation lestée, où les charges superficielles et la vitesse d'écoulement entre les lamelles sont plus élevées, la remise en suspension des particules au sein de lamelles n'est probablement pas négligeable. Peu d'études

modélisent la balance du taux de capture par rapport au taux de soulèvement en fonction de la morphologie des lamelles et du régime d'écoulement. Si la remise en suspension peut s'avérer considérable pour certains systèmes, il serait alors pertinent de comprendre et considérer les affinités d'adsorption entre les microflocs et le matériau des lamelles. Ces affinités peuvent entre autres limiter la remise en suspension. Ce concept d'interactions surfaciques entre les flocs et les lamelles est semblable à celui évoqué lors de la floculation : le taux de collisions efficaces contrôlé par α est tributaire des conditions de coagulation-floculation. Ce concept suggère également que la surface projetée de lamelles ne serait pas le seul paramètre important pour la rétention des microflocs.

BIBLIOGRAPHIE

Adachi, Y., & Wada, T. (2000). Initial stage dynamics of bridging flocculation of polystyrene latex spheres with polyethylene oxide. *Journal of Colloid and Interface Science, 229*(1), 148-154.

Adhikary, P., & Singh, R. (2004). Synthesis, characterization, and flocculation characteristics of hydrolyzed and unhydrolyzed polyacrylamide grafted xanthan gum. *Journal of applied polymer science, 94*(4), 1411-1419.

Agarwal, S., Gupta, R. K., & Doraiswamy, D. (2009). A model for the collision efficiency of shear-induced agglomeration involving polymer bridging. *Colloids and Surfaces A: Physicochemical and Engineering Aspects, 345*(1), 224-230.

Aguilar, M. I., Sáez, J., Lloréns, M., Soler, A., & Ortuño, J. F. (2003). Microscopic observation of particle reduction in slaughterhouse wastewater by coagulation–flocculation using ferric sulphate as coagulant and different coagulant aids. *Water Research, 37*(9), 2233-2241.

Aguilar, M. I., Sáez, J., Lloréns, M., Soler, A., Ortuño, J. F., Meseguer, V., & Fuentes, A. (2005). Improvement of coagulation–flocculation process using anionic polyacrylamide as coagulant aid. *Chemosphere, 58*(1), 47-56.

Ahmad, A. L., Wong, S. S., Teng, T. T., & Zuhairi, A. (2008). Improvement of alum and PACl coagulation by polyacrylamides (PAMs) for the treatment of pulp and paper mill wastewater. *Chemical Engineering Journal, 137*(3), 510-517.

Alexopoulos, A. H., Maggioris, D., & Kiparissides, C. (2002). CFD analysis of turbulence non-homogeneity in mixing vessels: A two-compartment model. *Chemical Engineering Science, 57*(10), 1735-1752.

Amal, R., Gazeau, D., & Waite, T. D. (1994). Small angle X-ray scattering of hematite aggregates. *Particle & Particle Systems Characterization, 11*(4), 315-319.

Andersson, M., Wittgren, B., & Wahlund, K.-G. (2003). Accuracy in multiangle light scattering measurements for molar mass and radius estimations. Model calculations and experiments. *Analytical Chemistry, 75*(16), 4279-4291.

Anthony, A. J., King, P. H., & Randall, C. W. (1975). The effects of branching and other physical properties of anionic polyacrylamides on the flocculation of domestic sewage. *Journal of Applied Polymer Science, 19*(1), 37-48.

APHA, AWWA, & WEF. (2012). WEF Standard methods for the examination of water and wastewater 22nd ed. *American Public Health Association, Washington*.

Arimitu, H., Ikebukuro, H., & Seto, I. (1975). The biological degradability of acrylamide monomer. *Journal of the Japan Water Works Association, 487*, 31-39.

Athawale, V., & Rathi, S. (1999). Graft polymerization: starch as a model substrate. *Journal of Macromolecular Science, Part C, 39*(3), 445-480.

Avadiar, L., Leong, Y.-K., & Fourie, A. (2014). Effects of polyethylenimine dosages and molecular weights on flocculation, rheology and consolidation behaviors of kaolin slurries. *Powder Technology, 254*, 364-372.

Baade, W., Hunkeler, D., & Hamielec, A. (1989). Copolymerization of acrylamide with cationic monomers in solution and inverse-microsuspension. *Journal of applied polymer science, 38*(1), 185-201.

Baar, A., Kulicke, W. M., Szablikowski, K., & Kiesewetter, R. (1994). Nuclear magnetic resonance spectroscopic characterization of carboxymethylcellulose. *Macromolecular Chemistry and Physics, 195*(5), 1483-1492.

Bagheri-Khoulenjani, S., Taghizadeh, S. M., & Mirzadeh, H. (2009). An investigation on the short-term biodegradability of chitosan with various molecular weights and degrees of deacetylation. *Carbohydrate Polymers, 78*(4), 773-778.

Ball, T., Carriere, A., & Barbeau, B. (2011). Comparison of two online flocculation monitoring techniques for predicting turbidity removal by granular media filtration. *Environmental technology, 32*(10), 1095-1105.

Barba, C., Montané, D., Rinaudo, M., & Farriol, X. (2002). Synthesis and characterization of carboxymethylcelluloses (CMC) from non-wood fibers I. Accessibility of cellulose fibers and CMC synthesis. *Cellulose, 9*(3-4), 319-326.

Barbusiński, K., & Kościelniak, H. (1995). Influence of substrate loading intensity on floc size in activated sludge process. *Water Research, 29*(7), 1703-1710.

Bassi, R., Prasher, S. O., & Simpson, B. (2000). Removal of selected metal ions from aqueous solutions using chitosan flakes. *Separation Science and Technology, 35*(4), 547-560.

Berg, J. M., Claesson, P. M., & Neuman, R. D. (1993). Interactions between mica surfaces in sodium polyacrylate solutions containing calcium ions. *Journal of colloid and interface science, 161*(1), 182-189.

Besra, L., Sengupta, D., Roy, S., & Ay, P. (2003). Influence of surfactants on flocculation and dewatering of kaolin suspensions by cationic polyacrylamide (PAM-C) flocculant. *Separation and Purification Technology, 30*(3), 251-264.

Biesinger, K. E., & Stokes, G. N. (1986). Effects of synthetic polyelectrolytes on selected aquatic organisms. *Journal of Water Pollution Control Federation*, 207-213.

Biggs, C. A., & Lant, P. A. (2000). Activated sludge flocculation: on-line determination of floc size and the effect of shear. *Water Research, 34*(9), 2542-2550.

Biggs, C. A., & Lant, P. A. (2002). Modelling activated sludge flocculation using population balances. *Powder Technology, 124*(3), 201-211.

Bingöl, B., Meyer, W.H., Wagner, M., Wegner, G. (2006). Synthesis, microstructure, and acidity of poly(vinylphosphonic acid). *Macromolecular Rapid Communications, 27*(20), 1719-1724.

Biswal, D. R., & Singh, R. P. (2004). Characterisation of carboxymethyl cellulose and polyacrylamide graft copolymer. *Carbohydrate Polymers, 57*(4), 379-387.

Biswal, D. R., & Singh, R. P. (2006). Flocculation studies based on water-soluble polymers of grafted carboxymethyl cellulose and polyacrylamide. *Journal of applied polymer science, 102*(2), 1000-1007.

Bolto, B. (1995). Soluble polymers in water purification. *Progress in Polymer Science, 20*(6), 987-1041.

Bolto, B. (2005). Reaction of chlorine with organic polyelectrolytes in water treatment: A review. *Journal of Water Supply: Research & Technology-AQUA, 54*(8).

Bolto, B., Dixon, D., Eldridge, R., & King, S. (2001). Cationic polymer and clay or metal oxide combinations for natural organic matter removal. *Water Research, 35*(11), 2669-2676.

Bolto, B., & Gregory, J. (2007). Organic polyelectrolytes in water treatment. *Water Research, 41*(11), 2301-2324.

Booker, N., Öcal, G., & Priestley, A. (1996). Novel high-rate processes for sewer overflow treatment. *Water Science and Technology, 34*(3), 103-109.

Botha, L., Davey, S., Nguyen, B., Swarnakar, A. K., Rivard, E., & Soares, J. B. P. (2017). Flocculation of oil sands tailings by hyperbranched functionalized polyethylenes (HBfPE). *Minerals Engineering, 108*, 71-82.

Bouyer, D., Coufort, C., Liné, A., & Do-Quang, Z. (2005). Experimental analysis of floc size distributions in a 1-L jar under different hydrodynamics and physicochemical conditions. *Journal of Colloid and Interface Science, 292*(2), 413-428.

Bratskaya, S., Golikov, A., Lutsenko, T., Nesterova, O., & Dudarchik, V. (2008). Charge characteristics of humic and fulvic acids: Comparative analysis by colloid titration and potentiometric titration with continuous pK-distribution function model. *Chemosphere, 73*(4), 557-563.

Bratskaya, S., Schwarz, S., Laube, J., Liebert, T., Heinze, T., Krentz, O., . . . Kulicke, W. M. (2005). Effect of polyelectrolyte structural features on flocculation behavior: cationic polysaccharides vs. synthetic polycations. *Macromolecular Materials and Engineering, 290*(8), 778-785.

Bratskaya, S. Y., Avramenko, V., Sukhoverkhov, S., & Schwarz, S. (2002). Flocculation of humic substances and their derivatives with chitosan. *Colloid Journal, 64*(6), 681-686.

Buléon, A., Colonna, P., Planchot, V., & Ball, S. (1998). Starch granules: structure and biosynthesis. *International journal of biological macromolecules, 23*(2), 85-112.

Burek, J., Albee, R., Beyer, J., Bell, T., Carreon, R., Morden, D., . . . Gorzinski, S. (1980). Subchronic toxicity of acrylamide administered to rats in the drinking water followed by up to 144 days of recovery. *Journal of environmental pathology and toxicology, 4*(5-6), 157-182.

Bushell, G. C., Yan, Y. D., Woodfield, D., Raper, J., & Amal, R. (2002). On techniques for the measurement of the mass fractal dimension of aggregates. *Advances in Colloid and Interface Science, 95*(1), 1-50.

Butler, G. B., Hogen-Esch, T. E., Meister, J. J., & Pledger Jr, H. (1983). *Brevet américain n^{o} US06188999*. University of Florida, FL: I. C. P. Services.

Cadotte, M., Tellier, M. E., Blanco, A., Fuente, E., Van De Ven, T. G., & Paris, J. (2007). Flocculation, retention and drainage in papermaking: a comparative study of polymeric additives. *The Canadian Journal of Chemical Engineering, 85*(2), 240-248.

Camp, T. R., & Stein, P. C. (1943). Velocity gradients and internal work in fluid motion. *Journal of the Boston Society of Civil Engineers, 85*, 219-237.

Cao, J., Zhang, S., Han, B., Feng, Q., & Guo, L. f. (2012). Characterization of cationic polyacrylamide-grafted starch flocculant synthesized by one-step reaction. *Journal of Applied Polymer Science, 123*(2), 1261-1266.

Carter, O. C., & Scheiner, B. (1991). Removal of toxic metals from an industrial wastewater using flocculants. *Fluid Particle Separation Journal, 4*, 193-196.

Caskey, J., & Primus, R. (1986). The effect of anionic polyacrylamide molecular conformation and configuration on flocculation effectiveness. *Environmental progress, 5*(2), 98-103.

Chakraborti, R. K., Atkinson, J. F., & Van Benschoten, J. E. (2000). Characterization of alum floc by image analysis. *Environmental science & technology, 34*(18), 3969-3976.

Chang, S., Gupta, R., & Ryan, M. (1992). Effect of the adsorption of polyvinyl alcohol on the rheology and stability of clay suspensions. *Journal of Rheology, 36*(2), 273-287.

Chellam, S., & Wiesner, M. R. (1993). Fluid mechanics and fractal aggregates. *Water Research, 27*(9), 1493-1496.

Chen, J., Heitmann, J. A., & Hubbe, M. A. (2003). Dependency of polyelectrolyte complex stoichiometry on the order of addition. 1. Effect of salt concentration during streaming current titrations with strong poly-acid and poly-base. *Colloids and Surfaces A: Physicochemical and Engineering Aspects, 223*(1), 215-230.

Chen, M. H., & Wyatt, P. J. (1999). *The measurement of mass and size distributions, conformation, and branching of important food polymers by MALS following sample fractionation.* Communication présentée à Macromolecular Symposia (vol. 140, p. 155-163).

Chen, Q., Yu, H., Wang, L., Abdin, Z.-u., Yang, X., Wang, J., . . . Chen, X. (2016). Synthesis and characterization of amylose grafted poly(acrylic acid) and its application in ammonia adsorption. *Carbohydrate Polymers, 153*, 429-434.

Chen, Y., Yang, H., & Gu, G. (2001). Effect of acid and surfactant treatment on activated sludge dewatering and settling. *Water Research, 35*(11), 2615-2620.

Cheng, K.-C., Demirci, A., & Catchmark, J. M. (2011). Pullulan: biosynthesis, production, and applications. *Applied microbiology and biotechnology, 92*(1), 29.

Cheng, W. P., Kao, Y. P., & Yu, R. F. (2008). A novel method for on-line evaluation of floc size in coagulation process. *Water Research, 42*(10), 2691-2697.

Chi, F. H., & Cheng, W. P. (2006). Use of chitosan as coagulant to treat wastewater from milk processing plant. *Journal of Polymers and the Environment, 14*(4), 411-417.

Chibowski, S., Paszkiewicz, M., & Krupa, M. (2000). Investigation of the influence of the polyvinyl alcohol adsorption on the electrical properties of Al2O3–solution interface, thickness of the adsorption layers of PVA. *Powder Technology, 107*(3), 251-255.

Chmelir, M., Künschner, A., & Barthell, E. (1980). Water soluble acrylamide polymers, 2. Aging and viscous flow of aqueous solutions of polyacrylamide and hydrolyzed polyacrylamide. *Die Angewandte Makromolekulare Chemie: Applied Macromolecular Chemistry and Physics, 89*(1), 145-165.

Choi, H. W., Lee, H. J., Kim, K. J., Kim, H.-M., & Lee, S. C. (2006). Surface modification of hydroxyapatite nanocrystals by grafting polymers containing phosphonic acid groups. *Journal of Colloid and Interface Science, 304*(1), 277-281.

Cholette, A., & Cloutier, L. (1959). Mixing efficiency determinations for continuous flow systems. *The Canadian Journal of Chemical Engineering, 37*(3), 105-112.

Claesson, P. M., Paulson, O. E. H., Blomberg, E., & Burns, N. L. (1997). Surface properties of poly(ethylene imine)-coated mica surfaces—salt and pH effects. *Colloids and Surfaces A: Physicochemical and Engineering Aspects, 123-124*, 341-353.

Contado, C., & Wahlund, K. G. (2006). High-speed separation and size characterization of wheat and barley starch granules by lift-hyperlayer asymmetrical flow field-flow fractionation in synergy with SPLITT fractionation. *Starch-Stärke, 58*(3-4), 140-154.

Crane, A. M., Kovacic, P., & Kovacic, E. D. (1980). Volatile halocarbon production from the chlorination of marine algal byproducts, including D-mannitol. *Environmental Science & Technology, 14*(11), 1371-1374.

Das, K. K., & Somasundaran, P. (2003). Flocculation-dispersion characteristics of alumina using a wide molecular weight range of polyacrylic acids. *Colloids and Surfaces A: Physicochemical and Engineering Aspects, 223*(1), 17-25.

Das, K. K., & Somasundaran, P. (2004). A kinetic investigation of the flocculation of alumina with polyacrylic acid. *Journal of Colloid and Interface Science, 271*(1), 102-109.

De Dianous, F., & Dernaucourt, J. (1991). Advantages of weighted flocculation in water treatment. *Water Supply, 9*, 43-46.

Del Blanco, L., Rodriguez, M., Schulz, P., & Agullo, E. (1999). Influence of the deacetylation degree on chitosan emulsification properties. *Colloid and Polymer Science, 277*(11), 1087-1092.

Deshmukh, S., Sudhakar, K., & Singh, R. (1991). Drag-reduction efficiency, shear stability, and biodegradation resistance of carboxymethyl cellulose-based and starch-based graft copolymers. *Journal of applied polymer science, 43*(6), 1091-1101.

Desjardins, C., Koudjonou, B., & Desjardins, R. (2002). Laboratory study of ballasted flocculation. *Water Research, 36*(3), 744-754.

Dintzis, F. R., & Fanta, G. F. (1996). Effects of jet-cooking conditions upon intrinsic viscosity and flow properties of starches. *Journal of applied polymer science, 62*(5), 749-753.

Divakaran, R., & Pillai, V. S. (2001). Flocculation of kaolinite suspensions in water by chitosan. *Water Research, 35*(16), 3904-3908.

Domard, A., & Rinaudo, M. (1983). Preparation and characterization of fully deacetylated chitosan. *International Journal of Biological Macromolecules, 5*(1), 49-52.

Dongowski, G. (1990). Chitin sourcebook: A guide to the research literature. *Food/Nahrung, 34*(3), 300-300.

Driscoll, C., & Letterman, R. (1988). Chemistry and fate of Al(III) in treated drinking water. *Journal of Environmental Engineering, 114*(1), 21-37.

Du, B., Li, J., Zhang, H., Huang, L., Chen, P., & Zhou, J. (2009). Influence of molecular weight and degree of substitution of carboxymethylcellulose on the stability of acidified milk drinks. *Food Hydrocolloids, 23*(5), 1420-1426.

Du, Q., Wang, Y., Li, A., & Yang, H. (2018). Scale-inhibition and flocculation dual-functionality of poly(acrylic acid) grafted starch. *Journal of Environmental Management, 210*, 273-279.

Duan, J., & Gregory, J. (2003). Coagulation by hydrolysing metal salts. *Advances in Colloid and Interface Science, 100–102*(0), 475-502.

Duan, J., Lu, Q., Chen, R., Duan, Y., Wang, L., Gao, L., & Pan, S. (2010). Synthesis of a novel flocculant on the basis of crosslinked Konjac glucomannan-graft-polyacrylamide-co-sodium xanthate and its application in removal of Cu2+ ion. *Carbohydrate Polymers, 80*(2), 436-441.

Ducoste, J. J., & Clark, M. M. (1998). The influence of tank size and impeller geometry on turbulent flocculation: I. Experimental. *Environmental Engineering Science, 15*(3), 215-224.

Duman, O., Tunç, S., & Çetinkaya, A. (2012). Electrokinetic and rheological properties of kaolinite in poly(diallyldimethylammonium chloride), poly(sodium 4-styrene sulfonate) and poly(vinyl alcohol) solutions. *Colloids and Surfaces A: Physicochemical and Engineering Aspects, 394*, 23-32.

Durmus, Z., Erdemi, H., Aslan, A., Toprak, M. S., Sozeri, H., & Baykal, A. (2011). Synthesis and characterization of poly(vinyl phosphonic acid) (PVPA)–Fe3O4 nanocomposite. *Polyhedron, 30*(2), 419-426.

Dyer, K. R., & Manning, A. J. (1999). Observation of the size, settling velocity and effective density of flocs, and their fractal dimensions. *Journal of Sea Research, 41*(1), 87-95.

Eaton, A. D., & Franson, M. A. H. (2005). *Standard methods for the examination of water & wastewater*.

El Halal, S. L. M., Colussi, R., Pinto, V. Z., Bartz, J., Radunz, M., Carreño, N. L. V., . . . da Rosa Zavareze, E. (2015). Structure, morphology and functionality of acetylated and oxidised barley starches. *Food chemistry, 168*, 247-256.

Enarsson, L.-E., & Wågberg, L. (2008). Polyelectrolyte adsorption on thin cellulose films studied with reflectometry and quartz crystal microgravimetry with dissipation. *Biomacromolecules, 10*(1), 134-141.

Fadda, S., Cincotti, A., Concas, A., Pisu, M., & Cao, G. (2009). Modelling breakage and reagglomeration during fine dry grinding in ball milling devices. *Powder Technology, 194*(3), 207-216.

Fan, A., Turro, N. J., & Somasundaran, P. (2000). A study of dual polymer flocculation. *Colloids and Surfaces A: Physicochemical and Engineering Aspects, 162*(1–3), 141-148.

Fan, W., Yan, W., Xu, Z., & Ni, H. (2012). Formation mechanism of monodisperse, low molecular weight chitosan nanoparticles by ionic gelation technique. *Colloids and Surfaces B: Biointerfaces, 90*, 21-27.

Fevola, M. J., Hester, R. D., & McCormick, C. L. (2003). Molecular weight control of polyacrylamide with sodium formate as a chain-transfer agent: Characterization via size exclusion chromatography/multi-angle laser light scattering and determination of chain-

transfer constant. *Journal of Polymer Science Part A: Polymer Chemistry, 41*(4), 560-568.

Fielding, M. (1999). *Analytical methods for polymers and their oxidative by-products*. Denver, U.S.A: AWWA Research Fondation.

Flory, P., & Fox, T. (1951). Treatment of intrinsic viscosities. *Journal of the American Chemical Society, 73*(5), 1904-1908.

Franz, R. G. (2001). Comparisons of pKa and log P values of some carboxylic and phosphonic acids: synthesis and measurement. *AAPS PharmSci, 3*(2), 1.

Fuente, E., Blanco, A., Negro, C., Pelach, M. A., Mutje, P., & Tijero, J. (2005). Study of filler flocculation mechanisms and floc properties induced by polyethylenimine. *Industrial & engineering chemistry research, 44*(15), 5616-5621.

Gaid, K., & Sauvignet, P. (2011). The flocculants of natural origin: the real alternative. *L'Eau, l'Industrie, les Nuisances*, (345), 83-88.

Gajdziok, J., Holešová, S., Štembírek, J., Pazdziora, E., Landová, H., Doležel, P., & Vetchý, D. (2015). Carmellose mucoadhesive oral films containing vermiculite/chlorhexidine nanocomposites as innovative biomaterials for treatment of oral infections. *BioMed research international, 2015*, 1-16.

García-Ochoa, F., Santos, V. E., Casas, J. A., & Gómez, E. (2000). Xanthan gum: production, recovery, and properties. *Biotechnology Advances, 18*(7), 549-579.

Ghanem, Young, J., & Edwards, F. (2013). Settling velocity models applied to ballasted flocs–A review. *SABER, 25*(3), 247-253.

Ghanem, A., Young, J., & Edwards, F. (2007). Mechanisms of ballasted floc formation. *Journal of Environmental Engineering, 133*(3), 271-277.

Ghorai, S., Sarkar, A., Panda, A. B., & Pal, S. (2013). Evaluation of the flocculation characteristics of polyacrylamide grafted xanthan gum/silica hybrid nanocomposite. *Industrial & Engineering Chemistry Research, 52*(29), 9731-9740.

Gillies, E. R., Dy, E., Fréchet, J. M., & Szoka, F. C. (2005). Biological evaluation of polyester dendrimer: poly (ethylene oxide)“bow-tie” hybrids with tunable molecular weight and architecture. *Molecular pharmaceutics, 2*(2), 129-138.

Gölander, C.-G., & Eriksson, J. C. (1987). ESCA studies of the adsorption of polyethyleneimine and glutaraldehyde-reacted polyethyleneimine on polyethylene and mica surfaces. *Journal of colloid and interface science, 119*(1), 38-48.

Gong, J., Peng, Y., Bouajila, A., Ourriban, M., Yeung, A., & Liu, Q. (2010). Reducing quartz gangue entrainment in sulphide ore flotation by high molecular weight polyethylene oxide. *International Journal of Mineral Processing, 97*(1), 44-51.

Gorczyca, B., & Ganczarczyk, J. (1996). Image analysis of alum coagulated mineral suspensions. *Environmental technology, 17*(12), 1361-1369.

Gregory, J. (1985). Turbidity fluctuations in flowing suspensions. *Journal of colloid and interface science, 105*(2), 357-371.

Gregory, J. (1988). Polymer adsorption and flocculation in sheared suspensions. *Colloids and Surfaces, 31*, 231-253.

Gregory, J. (1997). The density of particle aggregates. *Water Science and Technology, 36*(4), 1-13.

Gregory, J., & Barany, S. (2011). Adsorption and flocculation by polymers and polymer mixtures. *Advances in Colloid and Interface Science, 169*(1), 1-12.

Gregory, J., & Nelson, D. W. (1986). Monitoring of aggregates in flowing suspensions. *Colloids and Surfaces, 18*(2), 175-188.

Grube, M., Leiske, M. N., Schubert, U. S., & Nischang, I. (2018). POx as an alternative to PEG? A hydrodynamic and light scattering study. *Macromolecules, 51*(5), 1905-1916.

Grubisic, Z., Rempp, P., & Benoit, H. (1967). A universal calibration for gel permeation chromatography. *Journal of Polymer Science Part B: Polymer Letters, 5*(9), 753-759.

Güçlü, G., Al, E., Emik, S., İyim, T. B., Özgümüş, S., & Özyürek, M. (2010). Removal of Cu 2+ and Pb 2+ ions from aqueous solutions by starch-graft-acrylic acid/montmorillonite superabsorbent nanocomposite hydrogels. *Polymer Bulletin, 65*(4), 333-346.

Gugliemelli, L. A., Ollidene, W. M., & Russell, C. R. (1968). *Brevet américain n^{o} US3377302A*. Agriculture USA: U. D. o. Agriculture.

Guibal, E., & Roussy, J. (2007). Coagulation and flocculation of dye-containing solutions using a biopolymer (Chitosan). *Reactive and functional polymers, 67*(1), 33-42.

Guibelin, E., Delsalle, F., & Binot, P. (1994). The Actiflo® process: A highly compact and efficient process to prevent water pollution by stormwater flows. *Water Science and Technology, 30*(1), 87-96.

Han, M., Kim, T.-i., & Kim, J. (2006). Application of image analysis to evaluate the flocculation process. *Journal of Water Supply: Research and Technology-AQUA, 55*(7-8), 453-459.

Han, M., & Lawler, D. F. (1992). The (relative) insignificance of G in flocculation. *Journal-American Water Works Association, 84*(10), 79-91.

Heinze, T. (1998). New ionic polymers by cellulose functionalization. *Macromolecular Chemistry and Physics, 199*(11), 2341-2364.

Henderson, J., & Wheatley, A. (1987). Factors effecting a loss of flocculation activity of polyacrylamide solutions: Shear degradation, cation complexation, and solution aging. *Journal of applied polymer science, 33*(2), 669-684.

Herrington, T. M., & Midmore, B. R. (1993). Investigation of scaling effects in the aggregation of dilute kaolinite suspensions by quasi-elastic light scattering. *Colloids and Surfaces A: Physicochemical and Engineering Aspects, 70*(2), 199-202.

Ho, Y., Norli, I., Alkarkhi, A. F., & Morad, N. (2009). Analysis and optimization of flocculation activity and turbidity reduction in kaolin suspension using pectin as a biopolymer flocculant. *Water Science and Technology, 60*(3), 771-781.

Ho, Y., Norli, I., Alkarkhi, A. F., & Morad, N. (2010). Characterization of biopolymeric flocculant (pectin) and organic synthetic flocculant (PAM): a comparative study on treatment and optimization in kaolin suspension. *Bioresource technology, 101*(4), 1166-1174.

Hogg, R. (1984). Collision efficiency factors for polymer flocculation. *Journal of Colloid and Interface Science, 102*(1), 232-236.

Hong, H. C., Mazumder, A., Wong, M. H., & Liang, Y. (2008). Yield of trihalomethanes and haloacetic acids upon chlorinating algal cells, and its prediction via algal cellular biochemical composition. *Water Research, 42*(20), 4941-4948.

Hoover, M., & Butler, G. (1974). *Recent advances in ion-containing polymers.* Communication présentée à Journal of Polymer Science: Polymer Symposia (vol. 45, p. 1-38).

Hopkins, D. C., & Ducoste, J. J. (2003). Characterizing flocculation under heterogeneous turbulence. *Journal of Colloid and Interface Science, 264*(1), 184-194.

Huang, C., Chen, S., & Ruhsing Pan, J. (2000). Optimal condition for modification of chitosan: a biopolymer for coagulation of colloidal particles. *Water Research, 34*(3), 1057-1062.

Huang, M., Wang, Y., Cai, J., Bai, J., Yang, H., & Li, A. (2016). Preparation of dual-function starch-based flocculants for the simultaneous removal of turbidity and inhibition of Escherichia coli in water. *Water Research, 98*, 128-137.

Imasuen, E., Judd, S., & Sauvignet, P. (2004). High-rate clarification of municipal wastewaters: a brief appraisal. *Journal of Chemical Technology and Biotechnology, 79*(8), 914-917.

Ingamells, C. (1970). Lithium metaborate flux in silicate analysis. *Analytica Chimica Acta, 52*(2), 323-334.

Jaafari, K., Ruiz, T., Elmaleh, S., Coma, J., & Benkhouja, K. (2004). Simulation of a fixed bed adsorber packed with protonated cross-linked chitosan gel beads to remove nitrate from contaminated water. *Chemical Engineering Journal, 99*(2), 153-160.

Jain, V., Tammishetti, V., Joshi, K., Kumar, D., & Rai, B. (2017). Guar gum as a selective flocculant for the beneficiation of alumina rich iron ore slimes: Density functional theory and experimental studies. *Minerals Engineering, 109*, 144-152.

Järnström, L., Lason, L., & Rigdahl, M. (1995). Flocculation in kaolin suspensions induced by modified starches 1. Cationically modified starch—effects of temperature and ionic strength. *Colloids and Surfaces A: Physicochemical and Engineering Aspects, 104*(2), 191-205.

Jarvis, P., Jefferson, B., Gregory, J., & Parsons, S. A. (2005). A review of floc strength and breakage. *Water Research, 39*(14), 3121-3137.

Jin, P., Feng, Y., Xu, J., & Wang, X. (2013). *The effect of polyacrylamide on floc structure of typical systems.* Communication présentée à 2012 Asian Pacific Conference on Energy, Environment and Sustainable Development, APEESD 2012, November 12, 2012 - November 13, 2012, Kuala Lumpur, Malaysia (vol. 261-262, p. 887-890).

Jiraprasertkul, W., Nuisin, R., Jinsart, W., & Kiatkamjornwong, S. (2006). Synthesis and characterization of cassava starch graft poly (acrylic acid) and poly [(acrylic acid)-co-acrylamide] and polymer flocculants for wastewater treatment. *Journal of applied polymer science, 102*(3), 2915-2928.

Johnson, C., Li, X., & Logan, B. E. (1996). Settling velocities of fractal aggregates. *Environmental science & technology, 30*(6), 1911-1918.

Johnson, K. A., Gorzinski, S. J., Bodner, K. M., Campbell, R. A., Wolf, C. H., Friedman, M. A., & Mast, R. W. (1986). Chronic toxicity and oncogenicity study on acrylamide incorporated in the drinking water of Fischer 344 rats. *Toxicology and Applied Pharmacology, 85*(2), 154-168.

Jung, S. J., Amal, R., & Raper, J. A. (1995). The use of small angle light scattering to study structure of flocs. *Particle & particle systems characterization, 12*(6), 274-278.

Kam, S.-k., & Gregory, J. (1999). Charge determination of synthetic cationic polyelectrolytes by colloid titration. *Colloids and Surfaces A: Physicochemical and Engineering Aspects, 159*(1), 165-179.

Kamburova, K., Milkova, V., Petkanchin, I., & Radeva, T. (2008). Effect of Pectin Charge Density on Formation of Multilayer Films with Chitosan. *Biomacromolecules, 9*(4), 1242-1247.

Karizmeh, M. S., Delatolla, R., & Narbaitz, R. M. (2014). Investigation of settleability of biologically produced solids and biofilm morphology in moving bed bioreactors (MBBRs). *Bioprocess and biosystems engineering, 37*(9), 1839-1848.

Kasaai, M. R., Arul, J., & Charlet, G. (2000). Intrinsic viscosity–molecular weight relationship for chitosan. *Journal of Polymer Science Part B: Polymer Physics, 38*(19), 2591-2598.

Kawamura, S. (1991). Effectiveness of natural polyelectrolytes in water treatment. *Journal (American Water Works Association), 83*(10), 88-91.

Kawamura, S. (2000). *Integrated design and operation of water treatment facilities* (2nd^{e} éd.). New York ; Toronto: John Wiley & Sons.

Keleş, S., & Güçlü, G. (2006). Competitive removal of heavy metal ions by starch-graft-acrylic acid copolymers. *Polymer-Plastics Technology and Engineering, 45*(3), 365-371.

Khalil, M. I., & Aly, A. A. (2002). Preparation and evaluation of some anionic starch derivatives as flocculants. *Starch-Stärke, 54*(3-4), 132-139.

Kilander, J., Blomström, S., & Rasmuson, A. (2006). Spatial and temporal evolution of floc size distribution in a stirred square tank investigated using PIV and image analysis. *Chemical Engineering Science, 61*(23), 7651-7667.

Kim, J.-K., & Lawler, D. F. (2005). Characteristics of zeta potential distribution in silica particles. *Bulletin of the Korean Chemical Society, 26*(7), 1083-1089.

Klein, J., & Westerkamp, A. (1981). Peculiarities of polyacrylamide analysis by aqueous GPC. *Journal of Polymer Science: Polymer Chemistry Edition, 19*(3), 707-718.

Knox, J., & Wan, Q.-H. (1996). Surface modification of porous graphite for ion exchange chromatography. *Chromatographia, 42*(1-2), 83-88.

Koksal, E., Ramachandran, R., Somasundaran, P., & Maltesh, C. (1990). Flocculation of oxides using polyethylene oxide. *Powder Technology, 62*(3), 253-259.

Kosmulski, M. (2006). pH-dependent surface charging and points of zero charge: III. Update. *Journal of Colloid and Interface Science, 298*(2), 730-741.

Kosmulski, M. (2011). The pH-dependent surface charging and points of zero charge: V. Update. *Journal of colloid and interface science, 353*(1), 1-15.

Krentz, D. O., Lohmann, C., Schwarz, S., Bratskaya, S., Liebert, T., Laube, J., . . . Kulicke, W. M. (2006). Properties and flocculation efficiency of highly cationized starch derivatives. *Starch-Stärke, 58*(3-4), 161-169.

Kuakpetoon, D., & Wang, Y. J. (2001). Characterization of different starches oxidized by hypochlorite. *Starch-Stärke, 53*(5), 211-218.

Kulicke, W.-M., Kull, A. H., Kull, W., Thielking, H., Engelhardt, J., & Pannek, J.-B. (1996). Characterization of aqueous carboxymethyl cellulose solutions in terms of their molecular structure and its influence on rheological behaviour. *Polymer, 37*(13), 2723-2731.

Kulicke, W. M. (1986). *Unusual instability effects observed in ionic and non-ionic water soluble polymers.* Communication présentée à Makromolekulare Chemie. Macromolecular Symposia (vol. 2, p. 137-153).

Kumar, A., Rao, K. M., & Han, S. S. (2018). Application of xanthan gum as polysaccharide in tissue engineering: A review. *Carbohydrate Polymers, 180*, 128-144.

Kumar, D., Jain, V., & Rai, B. (2018). Can carboxymethyl cellulose be used as a selective flocculant for beneficiating alumina-rich iron ore slimes? A density functional theory and experimental study. *Minerals Engineering, 121*, 47-54.

Kurita, K. (2006). Chitin and chitosan: functional biopolymers from marine crustaceans. *Marine Biotechnology, 8*(3), 203.

Kusters, K. A., Wijers, J. G., & Thoenes, D. (1997). Aggregation kinetics of small particles in agitated vessels. *Chemical Engineering Science, 52*(1), 107-121.

Labidi, N., & Djebaili, A. (2008). Studies of the mechanism of polyvinyl alcohol adsorption on the calcite/water interface in the presence of sodium oleate. *Journal of Minerals and Materials Characterization and Engineering, 7*(02), 147.

Lachat-Instruments. (2001). Methods manual for automated ion analyzers. Milwaukee, WI: Hach Company.

Lapcik, L., Alince, B., & Van de Ven, T. (1995). Effect of poly (ethylene oxide) on the stability and flocculation of clay dispersions. *Journal of pulp and paper science, 21*(1), J19-J24.

Lapointe, M., & Barbeau, B. (2015). Evaluation of activated starch as an alternative to polyacrylamide polymers for drinking water flocculation. *Journal of Water Supply: Research and Technology—AQUA, 64*(3), 333-343.

Lapointe, M., & Barbeau, B. (2016). Characterization of ballasted flocs in water treatment using microscopy. *Water Research, 90*, 119-127.

Lapointe, M., & Barbeau, B. (2017). Dual starch–polyacrylamide polymer system for improved flocculation. *Water Research, 124*, 202-209.

Lapointe, M., & Barbeau, B. (2018a). Selection of media for the design of ballasted flocculation processes. *Water Research, 147*, 25-32.

Lapointe, M., & Barbeau, B. (2018b). Substituting polyacrylamide with an activated starch polymer during ballasted flocculation.

Lapointe, M., & Barbeau, B. (2019). Understanding the roles of synthetic vs. natural polymers to improve clarification through interparticle bridging: A review. *Advances in Colloid and Interface Science*.

Lapointe, M., Brosseau, C., Comeau, Y., & Barbeau, B. (2017). Assessing Alternative Media for Ballasted Flocculation. *Journal of Environmental Engineering, 143*(11), 04017071.

Lartiges, B. S., Deneux-Mustin, S., Villemin, G., Mustin, C., Barrès, O., Chamerois, M., . . . Babut, M. (2001). Composition, structure and size distribution of suspended particulates from the Rhine River. *Water Research, 35*(3), 808-816.

Larue, O., & Vorobiev, E. (2003). Floc size estimation in iron induced electrocoagulation and coagulation using sedimentation data. *International Journal of Mineral Processing, 71*(1–4), 1-15.

Laskowski, J., Liu, Q., & O'Connor, C. (2007). Current understanding of the mechanism of polysaccharide adsorption at the mineral/aqueous solution interface. *International Journal of Mineral Processing, 84*(1-4), 59-68.

Laue, C., & Hunkeler, D. (2006). Chitosan-graft-acrylamide polyelectrolytes: Synthesis, flocculation, and modeling. *Journal of applied polymer science, 102*(1), 885-896.

Laurienzo, P., Malinconico, M., Motta, A., & Vicinanza, A. (2005). Synthesis and characterization of a novel alginate–poly(ethylene glycol) graft copolymer. *Carbohydrate Polymers, 62*(3), 274-282.

Lavertu, M., Méthot, S., Tran-Khanh, N., & Buschmann, M. D. (2006). High efficiency gene transfer using chitosan/DNA nanoparticles with specific combinations of molecular weight and degree of deacetylation. *Biomaterials, 27*(27), 4815-4824.

Lawal, O. S., Storz, J., Storz, H., Lohmann, D., Lechner, D., & Kulicke, W.-M. (2009). Hydrogels based on carboxymethyl cassava starch cross-linked with di-or polyfunctional carboxylic acids: Synthesis, water absorbent behavior and rheological characterizations. *European Polymer Journal, 45*(12), 3399-3408.

Lee, C. S., Robinson, J., & Chong, M. F. (2014). A review on application of flocculants in wastewater treatment. *Process Safety and Environmental Protection, 92*(6), 489-508.

Lee, J.-H., Kim, J.-H., Zhu, I.-H., Zhan, X.-B., Lee, J.-W., Shin, D.-H., & Kim, S.-K. (2001). Optimization of conditions for the production of pullulan and high molecular weight pullulan by Aureobasidium pullulans. *Biotechnology Letters, 23*(10), 817-820.

Lee, J. H., Han, J.-A., & Lim, S.-T. (2009). Effect of pH on aqueous structure of maize starches analyzed by HPSEC-MALLS-RI system. *Food Hydrocolloids, 23*(7), 1935-1939.

Lee, K. Y., & Mooney, D. J. (2012). Alginate: properties and biomedical applications. *Progress in polymer science, 37*(1), 106-126.

Lee, L., Rahbari, R., Lecourtier, J., & Chauveteau, G. (1991). Adsorption of polyacrylamides on the different faces of kaolinites. *Journal of colloid and interface science, 147*(2), 351-357.

Lee, L. T., & Somasundaran, P. (1989). Adsorption of polyacrylamide on oxide minerals. *Langmuir, 5*(3), 854-860.

Lee, M., Nah, J.-W., Kwon, Y., Koh, J. J., Ko, K. S., & Kim, S. W. (2001). Water-soluble and low molecular weight chitosan-based plasmid DNA delivery. *Pharmaceutical Research, 18*(4), 427-431.

Leeman, M., Islam, M. T., & Haseltine, W. G. (2007). Asymmetrical flow field-flow fractionation coupled with multi-angle light scattering and refractive index detections for characterization of ultra-high molar mass poly(acrylamide) flocculants. *Journal of Chromatography A, 1172*(2), 194-203.

Lemanowicz, M., Gierczycki, A., & Al-Rashed, M. H. (2011). Dual-polymer flocculation with unmodified and ultrasonically conditioned flocculant. *Chemical Engineering and Processing: Process Intensification, 50*(1), 128-138.

Letterman, R. D., & Pero, R. W. (1990). Contaminants in polyelectrolytes used in water treatment. *Journal / American Water Works Association, 82*(11), 87-97.

Levecq, C., Breda, C., Ursel, V., Marteil, P., & Sauvignet, P. (2007). A new design of flocculation tank: the Turbomix applied to weighted flocculation. *Water Science & Technology, 56*(11).

Levine, N. (1981). Natural Polymer Sources in Polyelectrolytes for Water and Wastewater Treatment: CRC: Boca Raton, FL.

Li, T., Zhu, Z., Wang, D., Yao, C., & Tang, H. (2007). The strength and fractal dimension characteristics of alum–kaolin flocs. *International Journal of Mineral Processing, 82*(1), 23-29.

Li, X.-y., & Yuan, Y. (2002). Collision frequencies of microbial aggregates with small particles by differential sedimentation. *Environmental science & technology, 36*(3), 387-393.

Lindquist, G. M., & Stratton, R. A. (1976). The role of polyelectrolyte charge density and molecular weight on the adsorption and flocculation of colloidal silica with polyethylenimine. *Journal of Colloid and Interface Science, 55*(1), 45-59.

Liu, Q., Zhang, Y., & Laskowski, J. (2000). The adsorption of polysaccharides onto mineral surfaces: an acid/base interaction. *International Journal of Mineral Processing, 60*(3-4), 229-245.

Liu, Z., & Rempel, G. (1997). Preparation of superabsorbent polymers by crosslinking acrylic acid and acrylamide copolymers. *Journal of Applied Polymer Science, 64*(7), 1345-1353.

Lu, C. F., & Spielman, L. A. (1985). Kinetics of floc breakage and aggregation in agitated liquid suspensions. *Journal of Colloid and Interface Science, 103*(1), 95-105.

Lu, Y., Shang, Y., Huang, X., Chen, A., Yang, Z., Jiang, Y., . . . Yang, H. (2011). Preparation of strong cationic chitosan-graft-polyacrylamide flocculants and their flocculating properties. *Industrial & Engineering Chemistry Research, 50*(12), 7141-7149.

Mabire, F., Audebert, R., & Quivoron, C. (1984). Flocculation properties of some water-soluble cationic copolymers toward silica suspensions: a semiquantitative interpretation of the role of molecular weight and cationicity through a "patchwork" model. *Journal of Colloid and Interface Science, 97*(1), 120-136.

Maier, H., Anderson, M., Karl, C., Magnuson, K., & Whistler, R. (1993). Guar, locust bean, tara, and fenugreek gums. Dans *Industrial Gums (Third Edition)* (p. 181-226): Elsevier.

Mallevialle, J., Bruchet, A., & Fiessinger, F. (1984). How safe are organic polymers in water treatment? *Journal (American Water Works Association)*, 87-93.

Mas, S., & Ghommidh, C. (2001). On-line size measurement of yeast aggregates using image analysis. *Biotechnology and bioengineering, 76*(2), 91-98.

Masina, N., Choonara, Y. E., Kumar, P., du Toit, L. C., Govender, M., Indermun, S., & Pillay, V. (2017). A review of the chemical modification techniques of starch. *Carbohydrate Polymers, 157*, 1226-1236.

Mayo, J., Yavuz, C., Yean, S., Tomson, M., & Colvin, V. (2007). The effect of nanocrystalline magnetite size on arsenic removal. *Science and Technology of Advanced Materials, 8*(1), 71-75.

MDDELCC. (2018). *Fiche d'information technique - Technologie Actiflo® + Dusenflo®*. Tiré de http://www.mddelcc.gouv.qc.ca/eau/potable/guide/actiflo.pdf

Meiczinger, M., Dencs, J., Marton, G., & Dencs, B. (2005). Investigation of Reactions Occurring at Starch Phosphorylation. *Industrial & Engineering Chemistry Research, 44*(25), 9581-9585.

Messaud, F. A., Sanderson, R. D., Runyon, J. R., Otte, T., Pasch, H., & Williams, S. K. R. (2009). An overview on field-flow fractionation techniques and their applications in the separation and characterization of polymers. *Progress in Polymer Science, 34*(4), 351-368.

Mészáros, R., Thompson, L., Bos, M., & De Groot, P. (2002). Adsorption and electrokinetic properties of polyethylenimine on silica surfaces. *Langmuir, 18*(16), 6164-6169.

Michaels, A., & Morelos, O. (1955). Polyelectrolyte adsorption by kaolinite. *Industrial & Engineering Chemistry, 47*(9), 1801-1809.

Miguez-Pacheco, V., Misra, S. K., & Boccaccini, A. R. (2014). Biodegradable and bioactive polymer/inorganic phase nanocomposites for bone tissue engineering (BTE). Dans A. R. Boccaccini & P. X. Ma (édit.), *Tissue Engineering Using Ceramics and Polymers (Second Edition)* (2e éd., p. 115-150): Woodhead Publishing.

Milonjić, S., Kopečni, M., & Ilić, Z. (1983). The point of zero charge and adsorption properties of natural magnetite. *Journal of Radioanalytical and Nuclear Chemistry, 78*(1), 15-24.

Mino, G., & Kaizerman, S. (1958). A new method for the preparation of graft copolymers. Polymerization initiated by ceric ion redox systems. *Journal of Polymer Science, 31*(122), 242-243.

Miyata, N., Sakata, I., & Senju, R. (1975). The effects of the properties of trunk polymers on the flocculating action of graft copolymers. *Bulletin of the Chemical Society of Japan, 48*(11), 3367-3371.

Modig, G., Nilsson, P. O., & Wahlund, K. G. (2006). Influence of jet-cooking temperature and ionic strength on size and structure of cationic potato amylopectin starch as measured by asymmetrical flow field-flow fractionation multi-angle light scattering. *Starch-Stärke, 58*(2), 55-65.

Molyneux, P. (2018). *Water-Soluble Synthetic Polymers: Volume II: Properties and Behavior*: CRC press.

Monakhova, Y. B., Diehl, B. W. K., Do, T. X., Schulze, M., & Witzleben, S. (2018). Novel method for the determination of average molecular weight of natural polymers based on 2D DOSY NMR and chemometrics: Example of heparin. *Journal of Pharmaceutical and Biomedical Analysis, 149*, 128-132.

Mouchet, P., & Bonnelye, V. (1998). Solving algae problems: French expertise and world-wide applications. *Journal of water supply: research and technology-AQUA, 47*(3), 125-141.

Mpofu, P., Addai-Mensah, J., & Ralston, J. (2003). Investigation of the effect of polymer structure type on flocculation, rheology and dewatering behaviour of kaolinite dispersions. *International Journal of Mineral Processing, 71*(1–4), 247-268.

Mpofu, P., Addai-Mensah, J., & Ralston, J. (2004). Temperature influence of nonionic polyethylene oxide and anionic polyacrylamide on flocculation and dewatering behavior of kaolinite dispersions. *Journal of Colloid and Interface Science, 271*(1), 145-156.

Myers, K., Ward, R., & Bakker, A. (1997). A digital particle image velocimetry investigation of flow field instabilities of axial-flow impellers. *Journal of fluids engineering, 119*(3), 623-632.

Namazian, M., & Halvani, S. (2006). Calculations of pKa values of carboxylic acids in aqueous solution using density functional theory. *The Journal of Chemical Thermodynamics, 38*(12), 1495-1502.

Napper, D. H. (1983). *Polymeric stabilization of colloidal dispersions* (vol. 7): Academic Press London.

Nasser, M. S., & James, A. E. (2006). The effect of polyacrylamide charge density and molecular weight on the flocculation and sedimentation behaviour of kaolinite suspensions. *Separation and Purification Technology, 52*(2), 241-252.

Neufeld, R., & Stalke, D. (2015). Accurate molecular weight determination of small molecules via DOSY-NMR by using external calibration curves with normalized diffusion coefficients. *Chemical science, 6*(6), 3354-3364.

Nicu, R., Bobu, E., Miranda, R., & Blanco, A. (2012). Flocculation efficiency of chitosan for papermaking applications. *BioResources, 8*(1), 768-784.

Nie, H., Liu, M., Zhan, F., & Guo, M. (2004). Factors on the preparation of carboxymethylcellulose hydrogel and its degradation behavior in soil. *Carbohydrate Polymers, 58*(2), 185-189.

No, H. K., & Meyers, S. P. (2000). Application of chitosan for treatment of wastewaters. Dans *Reviews of environmental contamination and toxicology* (p. 1-27): Springer.

Novak, J. T., Prendeville, J. F., & Sherrard, J. H. (1988). Mixing intensity and polymer performance in sludge dewatering. *Journal of Environmental Engineering, 114*(1), 190-198.

Okieimen, F. (2003). Preparation, characterization, and properties of cellulose–polyacrylamide graft copolymers. *Journal of applied polymer science, 89*(4), 913-923.

Ong, B. C., Leong, Y. K., & Chen, S. B. (2009). Interparticle forces in spherical monodispersed silica dispersions: Effects of branched polyethylenimine and molecular weight. *Journal of Colloid and Interface Science, 337*(1), 24-31.

Ouellet, L.-D. (2017a). *Impact de l'utilisation d'un polymère biosourcé sur la réduction du colmatage en filtration granulaire.* (M.A.Sc., Ecole Polytechnique, Montreal (Canada), Ann Arbor). Accessible par Dissertations & Theses @ Ecole Polytechnique de Montreal; ProQuest Dissertations & Theses Global. Tiré de https://search.proquest.com/docview/2081832701?accountid=40695

Ouellet, L.-D. (2017b). *Impact de l'utilisation d'un polymère biosourcé sur la réduction du colmatage en filtration granulaire.* (École Polytechnique de Montréal).

Ovenden, C., & Xiao, H. (2002). Flocculation behaviour and mechanisms of cationic inorganic microparticle/polymer systems. *Colloids and Surfaces A: Physicochemical and Engineering Aspects, 197*(1), 225-234.

Owen, A., Fawell, P., & Swift, J. (2007). The preparation and ageing of acrylamide/acrylate copolymer flocculant solutions. *International Journal of Mineral Processing, 84*(1), 3-14.

Owen, A. T., Fawell, P. D., Swift, J. D., & Farrow, J. B. (2002). The impact of polyacrylamide flocculant solution age on flocculation performance. *International Journal of Mineral Processing, 67*(1), 123-144.

Öztekin, N., Alemdar, A., Güngör, N., & Erim, F. B. (2002). Adsorption of polyethyleneimine from aqueous solutions on bentonite clays. *Materials Letters, 55*(1), 73-76.

Pal, S., Mal, D., & Singh, R. (2007). Synthesis and characterization of cationic guar gum: A high performance flocculating agent. *Journal of applied polymer Science, 105*(6), 3240-3245.

Pal, S., Mal, D., & Singh, R. P. (2005). Cationic starch: an effective flocculating agent. *Carbohydrate Polymers, 59*(4), 417-423.

Paneva, D., Mespouille, L., Manolova, N., Degée, P., Rashkov, I., & Dubois, P. (2006). Comprehensive study on the formation of polyelectrolyte complexes from (quaternized) poly [2-(dimethylamino) ethyl methacrylate] and poly (2-acrylamido-2-methylpropane sodium sulfonate). *Journal of Polymer Science Part A: Polymer Chemistry, 44*(19), 5468-5479.

Parker, D. S., Kaufman, W. J., & Jenkins, D. (1972). Floc breakup in turbulent flocculation processes. *Journal of the Sanitary Engineering Division, 98*(1), 79-99.

Parovuori, P., Hamunen, A., Forssell, P., Autio, K., & Poutanen, K. (1995). Oxidation of potato starch by hydrogen peroxide. *Starch-Stärke, 47*(1), 19-23.

Parzefall, W. (2008). Minireview on the toxicity of dietary acrylamide. *Food and Chemical Toxicology, 46*(4), 1360-1364.

Pattanayek, S. K., & Juvekar, V. A. (2002). Prediction of adsorption of nonionic polymers from aqueous solutions to solid surfaces. *Macromolecules, 35*(25), 9574-9585.

Pavlova, S., & Dobrevsky, I. (2005). Modified Sirofloc process for natural water treatment. *Desalination, 173*(1), 55-59.

Pefferkorn, E. (1999). Polyacrylamide at solid/liquid interfaces. *Journal of Colloid and Interface Science, 216*(2), 197-220.

Peres, A. E. C., & Correa, M. I. (1996). Depression of iron oxides with corn starches. *Minerals Engineering, 9*(12), 1227-1234.

Pérez, L., Salgueiro, J. L., Maceiras, R., Cancela, Á., & Sánchez, Á. (2016). Study of influence of pH and salinity on combined flocculation of Chaetoceros gracilis microalgae. *Chemical Engineering Journal, 286*, 106-113.

Pérez, S., Baldwin, P. M., & Gallant, D. J. (2009). Structural features of starch granules I. Dans *Starch (Third Edition)* (p. 149-192): Elsevier.

Piirtola, L., Hultman, B., Andersson, C., & Lundeberg, Y. (1999). Activated sludge ballasting in batch tests. *Water Research, 33*(8), 1799-1804.

Piirtola, L., Hultman, B., & Löwén, M. (1999). Activated sludge ballasting in pilot plant operation. *Water Research, 33*(13), 3026-3032.

Plum, V., Dahl, C. P., Bentsen, L., Petersen, C. R., Napstjert, L., & Thomsen, N. (1998). The actiflo method. *Water Science and technology, 37*(1), 269-275.

Podzimek, S. (1994). The use of GPC coupled with a multiangle laser light scattering photometer for the characterization of polymers. On the determination of molecular weight, size and branching. *Journal of applied polymer science, 54*(1), 91-103.

Potts, P. J. (2012). *A handbook of silicate rock analysis* (1e éd.): Springer Science & Business Media.

Praes, P. E., de Albuquerque, R. O., & Luz, A. F. O. (2013). Recovery of iron ore tailings by column flotation. *Journal of Minerals and Materials Characterization and Engineering, 1*, 212-216.

Radhakrishnan, A. N., Marques, M. P., Davies, M. J., O'Sullivan, B., Bracewell, D. G., & Szita, N. (2018). Flocculation on a chip: a novel screening approach to determine floc growth rates and select flocculating agents. *Lab on a Chip, 18*, 585-594.

Rath, S., & Singh, R. (1997). Flocculation characteristics of grafted and ungrafted starch, amylose, and amylopectin. *Journal of Applied Polymer Science, 66*(9), 1721-1729.

Rath, S. K., & Singh, R. P. (1998). Grafted amylopectin: applications in flocculation. *Colloids and Surfaces A: Physicochemical and Engineering Aspects, 139*(2), 129-135.

Rattanakawin, C. (2005). Aggregate size distributions in sweep flocculation. *Journal of Science and Technology, 27*, 1095-1101.

Ravishankar, S. A., Pradip, & Khosla, N. K. (1995). Selective flocculation of iron oxide from its synthetic mixtures with clays: a comparison of polyacrylic acid and starch polymers. *International Journal of Mineral Processing, 43*(3–4), 235-247.

Rebhun, M., & Argaman, Y. (1965). Evaluation of hydraulic efficiency of sedimentation basins. *Journal of the Sanitary Engineering Division, 91*(5), 37-48.

Ren, P., Nan, J., Zhang, X., & Zheng, K. (2017). Analysis of floc morphology in a continuous-flow flocculation and sedimentation reactor. *Journal of Environmental Sciences, 52*, 268-275.

Renault, F., Sancey, B., Badot, P. M., & Crini, G. (2009). Chitosan for coagulation/flocculation processes – An eco-friendly approach. *European Polymer Journal, 45*(5), 1337-1348.

Rice, J. M. (2005). The carcinogenicity of acrylamide. *Mutation Research/Genetic Toxicology and Environmental Mutagenesis, 580*(1–2), 3-20.

Rinaudo, M. (2006). Chitin and chitosan: Properties and applications. *Progress in Polymer Science, 31*(7), 603-632.

Rolland-Sabaté, A., Guilois, S., Jaillais, B., & Colonna, P. (2011). Molecular size and mass distributions of native starches using complementary separation methods: asymmetrical flow field flow fractionation (A4F) and hydrodynamic and size exclusion chromatography (HDC-SEC). *Analytical and bioanalytical chemistry, 399*(4), 1493-1505.

Roussy, J., Van Vooren, M., Dempsey, B. A., & Guibal, E. (2005). Influence of chitosan characteristics on the coagulation and the flocculation of bentonite suspensions. *Water Research, 39*(14), 3247-3258.

Rubio, J., & Kitchener, J. A. (1976). The mechanism of adsorption of poly(ethylene oxide) flocculant on silica. *Journal of Colloid and Interface Science, 57*(1), 132-142.

Ruehrwein, R., & Ward, D. (1952). Mechanism of clay aggregation by polyelectrolytes. *Soil science, 73*(6), 485-492.

Sableviciene, D., Klimaviciute, R., Bendoraitiene, J., & Zemaitaitis, A. (2005). Flocculation properties of high-substituted cationic starches. *Colloids and Surfaces A: Physicochemical and Engineering Aspects, 259*(1), 23-30.

Salehizadeh, H., Yan, N., & Farnood, R. (2018). Recent advances in polysaccharide bio-based flocculants. *Biotechnology Advances, 36*(1), 92-119.

Samoshina, Y., Diaz, A., Becker, Y., Nylander, T., & Lindman, B. (2003). Adsorption of cationic, anionic and hydrophobically modified polyacrylamides on silica surfaces. *Colloids and Surfaces A: Physicochemical and Engineering Aspects, 231*(1), 195-205.

Sánchez-Rivera, M., García-Suárez, F., Del Valle, M. V., Gutierrez-Meraz, F., & Bello-Pérez, L. (2005). Partial characterization of banana starches oxidized by different levels of sodium hypochlorite. *Carbohydrate polymers, 62*(1), 50-56.

Sánchez-Rivera, M. M., Méndez-Montealvo, G., Núñez-Santiago, C., de la Rosa-Millan, J., Wang, Y. J., & Bello-Pérez, L. A. (2009). Physicochemical properties of banana starch oxidized under different conditions. *Starch-Stärke, 61*(3-4), 206-213.

Sanghi, R., Bhattacharya, B., & Singh, V. (2006). Use of Cassia javahikai seed gum and gum-g-polyacrylamide as coagulant aid for the decolorization of textile dye solutions. *Bioresource Technology, 97*(10), 1259-1264.

Sangseethong, K., Lertphanich, S., & Sriroth, K. (2009). Physicochemical properties of oxidized cassava starch prepared under various alkalinity levels. *Starch-Stärke, 61*(2), 92-100.

Santhiya, D., Subramanian, S., Natarajan, K., & Malghan, S. (1999). Surface chemical studies on the competitive adsorption of poly (acrylic acid) and poly (vinyl alcohol) onto alumina. *Journal of colloid and interface science, 216*(1), 143-153.

Satyanarayana, D., & Chatterji, P. (1993). Biodegradable polymers: challenges and strategies. *Journal of Macromolecular Science, Part C: Polymer Reviews, 33*(3), 349-368.

Sen, G., Ghosh, S., Jha, U., & Pal, S. (2011). Hydrolyzed polyacrylamide grafted carboxymethylstarch (Hyd. CMS-g-PAM): An efficient flocculant for the treatment of textile industry wastewater. *Chemical Engineering Journal, 171*(2), 495-501.

Sen, G., Kumar, R., Ghosh, S., & Pal, S. (2009). A novel polymeric flocculant based on polyacrylamide grafted carboxymethylstarch. *Carbohydrate Polymers, 77*(4), 822-831.

Şen, M., Hayrabolulu, H., Taşkın, P., Torun, M., Demeter, M., Cutrubinis, M., & Güven, O. (2016). Radiation induced degradation of xanthan gum in the solid state. *Radiation Physics and Chemistry, 124*, 225-229.

Serra, T., & Casamitjana, X. (1998). Effect of the shear and volume fraction on the aggregation and breakup of particles. *AIChE Journal, 44*(8), 1724-1730.

Servais, P., Anzil, A., & Ventresque, C. (1989). Simple method for determination of biodegradable dissolved organic carbon in water. *Applied and Environmental Microbiology, 55*(10), 2732-2734.

Seyfarth, F., Schliemann, S., Elsner, P., & Hipler, U. C. (2008). Antifungal effect of high- and low-molecular-weight chitosan hydrochloride, carboxymethyl chitosan, chitosan oligosaccharide and N-acetyl-d-glucosamine against Candida albicans, Candida krusei and Candida glabrata. *International Journal of Pharmaceutics, 353*(1), 139-148.

Shahadat, M., Teng, T. T., Rafatullah, M., Shaikh, Z. A., Sreekrishnan, T. R., & Ali, S. W. (2017). Bacterial bioflocculants: A review of recent advances and perspectives. *Chemical Engineering Journal, 328*, 1139-1152.

Shaikh, S., Nasser, M., Magzoub, M., Benamor, A., Hussein, I., El-Naas, M., & Qiblawey, H. (2018). Effect of electrolytes on electrokinetics and flocculation behavior of bentonite-polyacrylamide dispersions. *Applied Clay Science, 158*, 46-54.

Shaikh, S. M. R., Nasser, M. S., Hussein, I., Benamor, A., Onaizi, S. A., & Qiblawey, H. (2017). Influence of polyelectrolytes and other polymer complexes on the flocculation and rheological behaviors of clay minerals: A comprehensive review. *Separation and Purification Technology, 187*, 137-161.

Sharma, B., Dhuldhoya, N., & Merchant, U. (2006). Flocculants—an ecofriendly approach. *Journal of Polymers and the Environment, 14*(2), 195-202.

Shen, X., & Maa, J. P. Y. (2016). A camera and image processing system for floc size distributions of suspended particles. *Marine Geology, 376*, 132-146.

Shingel, K., & Petrov, P. (2002). Behavior of γ-ray-irradiated pullulan in aqueous solutions of cationic (cetyltrimethylammonium hydroxide) and anionic (sodium dodecyl sulfate) surfactants. *Colloid and Polymer Science, 280*(2), 176-182.

Shogren, R. L. (2009). Flocculation of kaolin by waxy maize starch phosphates. *Carbohydrate Polymers, 76*(4), 639-644.

Shogren, R. L., Willett, J. L., & Biswas, A. (2009). HRP-mediated synthesis of starch–polyacrylamide graft copolymers. *Carbohydrate Polymers, 75*(1), 189-191.

Sibony, J. (1981). Clarification with microsand seeding. A state of the art. *Water Research, 15*(11), 1281-1290.

Sillanpää, M., Ncibi, M. C., Matilainen, A., & Vepsäläinen, M. (2018). Removal of natural organic matter in drinking water treatment by coagulation: A comprehensive review. *Chemosphere, 190*, 54-71.

Simsek, S., Ovando-Martínez, M., Whitney, K., & Bello-Pérez, L. A. (2012). Effect of acetylation, oxidation and annealing on physicochemical properties of bean starch. *Food Chemistry, 134*(4), 1796-1803.

Singh, R. P., Karmakar, G., Rath, S., Karmakar, N., Pandey, S., Tripathy, T., . . . Lan, N. (2000). Biodegradable drag reducing agents and flocculants based on polysaccharides: materials and applications. *Polymer Engineering & Science, 40*(1), 46-60.

Singh, R. P., Nayak, B. R., Biswal, D. R., Tripathy, T., & Banik, K. (2003). Biobased polymeric flocculants for industrial effluent treatment. *Materials Research Innovations, 7*(5), 331-340.

Singh, R. P., Pal, S., Rana, V. K., & Ghorai, S. (2013). Amphoteric amylopectin: A novel polymeric flocculant. *Carbohydrate Polymers, 91*(1), 294-299.

Singh, V., Tiwari, A., Tripathi, D. N., & Sanghi, R. (2004). Microwave assisted synthesis of Guar-g-polyacrylamide. *Carbohydrate Polymers, 58*(1), 1-6.

Sjöberg, M., Bergström, L., Larsson, A., & Sjöström, E. (1999). The effect of polymer and surfactant adsorption on the colloidal stability and rheology of kaolin dispersions. *Colloids and Surfaces A: Physicochemical and Engineering Aspects, 159*(1), 197-208.

Smith-Palmer, T., Campbell, N., Bowman, J. L., & Dewar, P. (1994). Flocculation behavior of some cationic polyelectrolytes. *Journal of applied polymer science, 52*(9), 1317-1325.

Smoluchowski, M. v. (1917). Versuch einer mathematischen theorie der koagulationskinetik kolloider lösungen. *Z. phys. Chem, 92*(129-168), 9.

Solberg, D., & Wågberg, L. (2003). Adsorption and flocculation behavior of cationic polyacrylamide and colloidal silica. *Colloids and Surfaces A: Physicochemical and Engineering Aspects, 219*(1), 161-172.

Somasundaran, P., & Moudgill, B. M. (1988). *Reagents in mineral technology* (vol. 27): CRC Press.

Song, H., Wu, D., Zhang, R.-Q., Qiao, L.-Y., Zhang, S.-H., Lin, S., & Ye, J. (2009). Synthesis and application of amphoteric starch graft polymer. *Carbohydrate Polymers, 78*(2), 253-257.

Song, J., Birbach, N. L., & Hinestroza, J. P. (2012). Deposition of silver nanoparticles on cellulosic fibers via stabilization of carboxymethyl groups. *Cellulose, 19*(2), 411-424.

Sperazza, M., Moore, J. N., & Hendrix, M. S. (2004). High-resolution particle size analysis of naturally occurring very fine-grained sediment through laser diffractometry. *Journal of Sedimentary Research, 74*(5), 736-743.

Spicer, P. T., & Pratsinis, S. E. (1996). Coagulation and fragmentation: Universal steady-state particle-size distribution. *AIChE Journal, 42*(6), 1612-1620.

Spicer, P. T., Pratsinis, S. E., Raper, J., Amal, R., Bushell, G., & Meesters, G. (1998). Effect of shear schedule on particle size, density, and structure during flocculation in stirred tanks. *Powder Technology, 97*(1), 26-34.

Suh, J., Paik, H. J., & Hwang, B. K. (1994). Ionization of poly(ethylenimine) and poly(allylamine) at various pH′s. *Bioorganic Chemistry, 22*(3), 318-327.

Sutherland, I. W. (2001). Microbial polysaccharides from Gram-negative bacteria. *International Dairy Journal, 11*(9), 663-674.

Szyguła, A., Guibal, E., Palacín, M. A., Ruiz, M., & Sastre, A. M. (2009). Removal of an anionic dye (Acid Blue 92) by coagulation–flocculation using chitosan. *Journal of Environmental Management, 90*(10), 2979-2986.

Tambo, N., & Watanabe, Y. (1979). Physical characteristics of flocs—I. The floc density function and aluminium floc. *Water Research, 13*(5), 409-419.

Tanaka, R., Ueoka, I., Takaki, Y., Kataoka, K., & Saito, S. (1983). High molecular weight linear polyethylenimine and poly (N-methylethylenimine). *Macromolecules, 16*(6), 849-853.

Terayama, H. (1952). Method of colloid titration (a new titration between polymer ions). *Journal of Polymer Science, 8*(2), 243-253.

Thomas, D., Judd, S., & Fawcett, N. (1999). Flocculation modelling: a review. *Water Research, 33*(7), 1579-1592.

Tillman Jr, F. D., Bartelt-Hunt, S. L., Craver, V. A., Smith, J. A., & Alther, G. R. (2005). Relative metal ion sorption on natural and engineered sorbents: Batch and column studies. *Environmental Engineering Science, 22*(3), 400-410.

Tripathy, T., & De, B. R. (2006). Flocculation: a new way to treat the waste water. *Journal of Physical Science, 10*(2006), 93-127.

Tripathy, T., Karmakar, N. C., & Singh, R. P. (2001). Development of novel polymeric flocculant based on grafted sodium alginate for the treatment of coal mine wastewater. *Journal of applied polymer science, 82*(2), 375-382.

Tripathy, T., Pandey, S. R., Karmakar, N. C., Bhagat, R. P., & Singh, R. P. (1999). Novel flocculating agent based on sodium alginate and acrylamide. *European Polymer Journal, 35*(11), 2057-2072.

Tripathy, T., & Singh, R. P. (2000). High performance flocculating agent based on partially hydrolysed sodium alginate–g–polyacrylamide. *European Polymer Journal, 36*(7), 1471-1476.

Tripathy, T., & Singh, R. P. (2001). Characterization of polyacrylamide-grafted sodium alginate: A novel polymeric flocculant. *Journal of Applied Polymer Science, 81*(13), 3296-3308.

Tyla, R. W., Friedman, M. A., Losco, P. E., Fisher, L. C., Johnson, K. A., Strother, D. E., & Wolf, C. H. (2000). Rat two-generation reproduction and dominant lethal study of acrylamide in drinking water. *Reproductive Toxicology, 14*(5), 385-401.

USEPA. (2009). *Treatment techniques for acrylamide and epichlorohydrin - 40 CFR 141.111*. U.S. Government Publishing Office

Van de Ven, T., Qasaimeh, M. A., & Paris, J. (2004). PEO-induced flocculation of fines: effects of PEO dissolution conditions and shear history. *Colloids and Surfaces A: Physicochemical and Engineering Aspects, 248*(1-3), 151-156.

Vanier, N. L., da Rosa Zavareze, E., Pinto, V. Z., Klein, B., Botelho, F. T., Dias, A. R. G., & Elias, M. C. (2012). Physicochemical, crystallinity, pasting and morphological properties of bean starch oxidised by different concentrations of sodium hypochlorite. *Food chemistry, 131*(4), 1255-1262.

Vanier, N. L., El Halal, S. L. M., Dias, A. R. G., & da Rosa Zavareze, E. (2017). Molecular structure, functionality and applications of oxidized starches: A review. *Food Chemistry, 221*, 1546-1559.

Viebke, C., & Williams, P. A. (2000). Determination of molecular mass distribution of κ-carrageenan and xanthan using asymmetrical flow field-flow fractionation. *Food Hydrocolloids, 14*(3), 265-270.

Volk, C., Bell, K., Ibrahim, E., Verges, D., Amy, G., & LeChevallier, M. (2000). Impact of enhanced and optimized coagulation on removal of organic matter and its biodegradable fraction in drinking water. *Water Research, 34*(12), 3247-3257.

Wan, X., Li, Y., Wang, X., Chen, S., & Gu, X. (2007). Synthesis of cationic guar gum-graft-polyacrylamide at low temperature and its flocculating properties. *European Polymer Journal, 43*(8), 3655-3661.

Wang, D. (2018). Activated starch as an alternative to polyacrylamide-based polymers for in-line filtration of low turbidity source water. *Journal of Water Supply: Research and Technology-Aqua*, jws2018023.

Wang, J.-P., Chen, Y.-Z., Zhang, S.-J., & Yu, H.-Q. (2008). A chitosan-based flocculant prepared with gamma-irradiation-induced grafting. *Bioresource Technology, 99*(9), 3397-3402.

Wang, S., Zhang, L., Yan, B., Xu, H., Liu, Q., & Zeng, H. (2015). Molecular and surface interactions between polymer flocculant chitosan-g-polyacrylamide and kaolinite particles: Impact of salinity. *The Journal of Physical Chemistry C, 119*(13), 7327-7339.

Wassmer, K. H., Schroeder, U., & Horn, D. (1991). Characterization and detection of polyanions by direct polyelectrolyte titration. *Die Makromolekulare Chemie: Macromolecular Chemistry and Physics, 192*(3), 553-565.

Watanabe, Y. (2017). Flocculation and me. *Water Research, 114*, 88-103.

Weissenborn, P. K. (1996). Behaviour of amylopectin and amylose components of starch in the selective flocculation of ultrafine iron ore. *International Journal of Mineral Processing, 47*(3), 197-211.

Wesolowski, D. J., & Palmer, D. A. (1994). Aluminum speciation and equilibria in aqueous solution: V. Gibbsite solubility at 50°C and pH 3–9 in 0.1 molal NaCl solutions (a general model for aluminum speciation; analytical methods). *Geochimica et Cosmochimica Acta, 58*(14), 2947-2969.

WHO. (2002). *Health Implications of Acrylamide in Food: Report of a Joint FAO/WHO Consultation*. Geneva, Switzerland: World Health Organization.

WHO. (2004). *Guidelines for drinking-water quality: recommendations* (3e éd. vol. 1). Geneva, Switzerland: World Health Organization.

Wibowo, S., Velazquez, G., Savant, V., & Torres, J. A. (2007). Effect of chitosan type on protein and water recovery efficiency from surimi wash water treated with chitosan–alginate complexes. *Bioresource Technology, 98*(3), 539-545.

Wiśniewska, M. (2011). The temperature effect on electrokinetic properties of the silica–polyvinyl alcohol (PVA) system. *Colloid and polymer science, 289*(3), 341-344.

Wiśniewska, M., Terpiłowski, K., Chibowski, S., Urban, T., Zarko, V. I., & Gun'ko, V. M. (2013). Effect of polyacrylic acid (PAA) adsorption on stability of mixed alumina-silica oxide suspension. *Powder Technology, 233*, 190-200.

Wittgren, B., & Wahlund, K.-G. (1997). Fast molecular mass and size characterization of polysaccharides using asymmetrical flow field-flow fractionation-multiangle light scattering. *Journal of Chromatography A, 760*(2), 205-218.

Wyatt, P. J. (1997). Multiangle light scattering: The basic tool for macromolecular characterization. *Instrumentation science & technology, 25*(1), 1-18.

Xiao, F., Huang, J.-C. H., Zhang, B.-j., & Cui, C.-w. (2009). Effects of low temperature on coagulation kinetics and floc surface morphology using alum. *Desalination, 237*(1–3), 201-213.

Xiao, F., Lam, K. M., & Li, X.-y. (2013). Investigation and visualization of internal flow through particle aggregates and microbial flocs using particle image velocimetry. *Journal of Colloid and Interface Science, 397*, 163-168.

Xiao, F., Lam, K. M., Li, X. Y., Zhong, R. S., & Zhang, X. H. (2011). PIV characterisation of flocculation dynamics and floc structure in water treatment. *Colloids and Surfaces A: Physicochemical and Engineering Aspects, 379*(1–3), 27-35.

Xing, W., Guo, W., Ngo, H.-H., Cullum, P., & Listowski, A. (2010). Integration of inorganic micronutrients and natural starch based cationic flocculant in primary treated sewage effluent (PTSE) treatment. *Separation Science and Technology, 45*(5), 619-625.

Yang, F., Li, G., He, Y.-G., Ren, F.-X., & Wang, G.-x. (2009). Synthesis, characterization, and applied properties of carboxymethyl cellulose and polyacrylamide graft copolymer. *Carbohydrate Polymers, 78*(1), 95-99.

Yang, J.-S., Xie, Y.-J., & He, W. (2011). Research progress on chemical modification of alginate: A review. *Carbohydrate polymers, 84*(1), 33-39.

Yang, R., Li, H., Huang, M., Yang, H., & Li, A. (2016). A review on chitosan-based flocculants and their applications in water treatment. *Water Research, 95*, 59-89.

Yang, Z., Li, H., Yan, H., Wu, H., Yang, H., Wu, Q., . . . Cheng, R. (2014). Evaluation of a novel chitosan-based flocculant with high flocculation performance, low toxicity and good floc properties. *Journal of hazardous materials, 276*, 480-488.

Yang, Z., Yang, H., Jiang, Z., Cai, T., Li, H., Li, H., . . . Cheng, R. (2013). Flocculation of both anionic and cationic dyes in aqueous solutions by the amphoteric grafting flocculant carboxymethyl chitosan-graft-polyacrylamide. *Journal of Hazardous Materials, 254-255*, 36-45.

Yang, Z., Yang, H., Jiang, Z., Huang, X., Li, H., Li, A., & Cheng, R. (2013). A new method for calculation of flocculation kinetics combining Smoluchowski model with fractal theory. *Colloids and Surfaces A: Physicochemical and Engineering Aspects, 423*, 11-19.

Yang, Z., Yuan, B., Huang, X., Zhou, J., Cai, J., Yang, H., . . . Cheng, R. (2012). Evaluation of the flocculation performance of carboxymethyl chitosan-graft-polyacrylamide, a novel amphoteric chemically bonded composite flocculant. *Water Research, 46*(1), 107-114.

Yavich, A. A., Lee, K.-H., Chen, K.-C., Pape, L., & Masten, S. J. (2004). Evaluation of biodegradability of NOM after ozonation. *Water Research, 38*(12), 2839-2846.

Yoo, S.-H., & Jane, J.-l. (2002). Molecular weights and gyration radii of amylopectins determined by high-performance size-exclusion chromatography equipped with multi-angle laser-light scattering and refractive index detectors. *Carbohydrate Polymers, 49*(3), 307-314.

Yoon, S.-Y., & Deng, Y. (2004). Flocculation and reflocculation of clay suspension by different polymer systems under turbulent conditions. *Journal of colloid and interface science, 278*(1), 139-145.

Young, J. C., & Edwards, F. G. (2000). Fundamentals of ballasted flocculation reactions. *Proceedings of the Water Environment Federation, 2000*(14), 56-80.

Young, J. C., & Edwards, F. G. (2003). Factors affecting ballasted flocculation reactions. *Water environment research, 75*(3), 263-272.

Yu, W., Gregory, J., Campos, L., & Li, G. (2011). The role of mixing conditions on floc growth, breakage and re-growth. *Chemical Engineering Journal, 171*(2), 425-430.

Yu, W., Wang, Y., Li, A., & Yang, H. (2018). Evaluation of the structural morphology of starch-graft-poly(acrylic acid) on its scale-inhibition efficiency. *Water Research, 141*, 86-95.

Yu, X., & Somasundaran, P. (1996). Role of Polymer Conformation in Interparticle-Bridging Dominated Flocculation. *Journal of Colloid and Interface Science, 177*(2), 283-287.

Yukselen, M. A., & Gregory, J. (2004). The reversibility of floc breakage. *International Journal of Mineral Processing, 73*(2-4), 251-259.

Zeng, D., Wu, J., & Kennedy, J. F. (2008). Application of a chitosan flocculant to water treatment. *Carbohydrate Polymers, 71*(1), 135-139.

Zhang, J., Sun, W., Gao, Z., Niu, F., Wang, L., Zhao, Y., & Gao, Y. (2018). Selective Flocculation Separation of Fine Hematite from Quartz Using a Novel Grafted Copolymer Flocculant. *Minerals, 8*(6), 227-238.

Zhong, R., Zhang, X., Xiao, F., Li, X., & Cai, Z. (2011). Effects of humic acid on physical and hydrodynamic properties of kaolin flocs by particle image velocimetry. *Water Research, 45*(13), 3981-3990.

Zhu, G., Liu, J., & Bian, Y. (2018). Evaluation of cationic polyacrylamide-based hybrid coagulation for the removal of dissolved organic nitrogen. *Environmental Science and Pollution Research, 25*(15), 14447–14459.

Zhu, H., Smith, D. W., Zhou, H., & Stanley, S. J. (1996). Improving removal of turbidity causing materials by using polymers as a filter aid. *Water Research, 30*(1), 103-114.

Zhu, Z., Li, M., & Jin, E. (2009). Effect of an allyl pretreatment of starch on the grafting efficiency and properties of allyl starch-g-poly (acrylic acid). *Journal of applied polymer science, 112*(5), 2822-2829.

Zou, W., Yu, L., Liu, X., Chen, L., Zhang, X., Qiao, D., & Zhang, R. (2012). Effects of amylose/amylopectin ratio on starch-based superabsorbent polymers. *Carbohydrate Polymers, 87*(2), 1583-1588.

ANNEXES

ANNEXE A – SITES D'ATTACHEMENT POSSIBLES SUR L'AMIDON ET LE POLYACRYLAMIDE

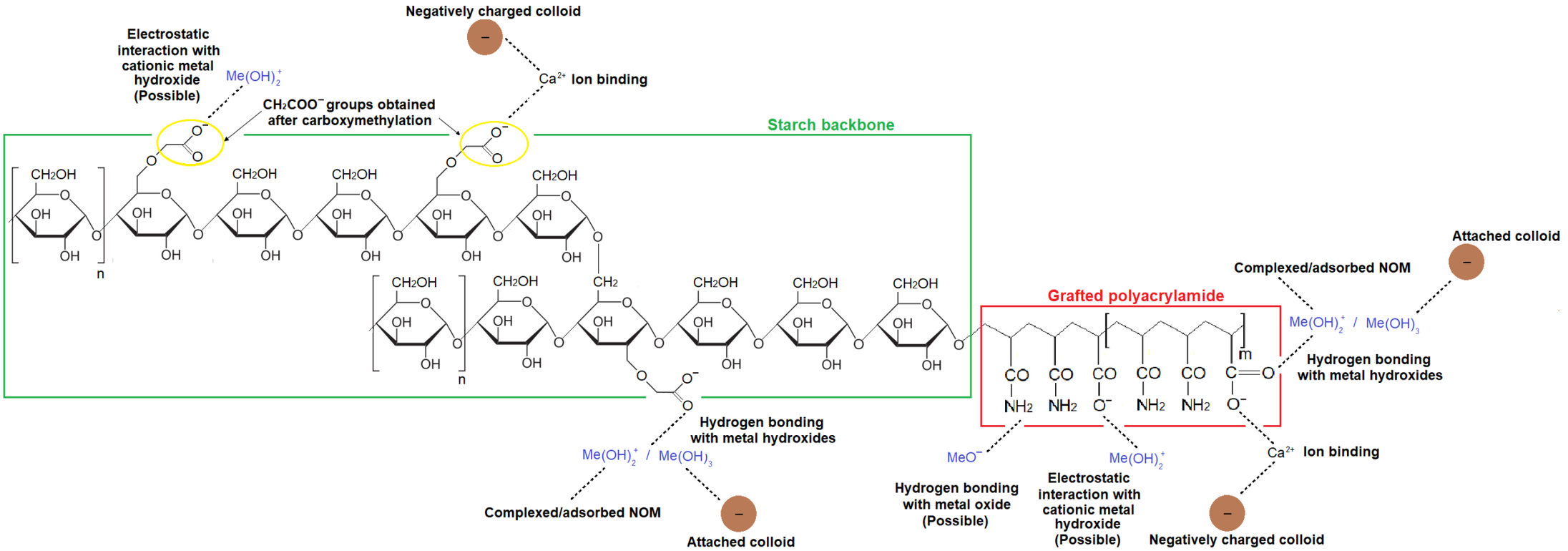

Figure A- 1 : Sites d'adsorption typiques et disponibles pour les hydroxydes métalliques et les colloïdes, tiré de l'article 1 (soumis dans *Advances in Colloid and Interface Science*).

ANNEXE B – ÉVOLUTION DE LA TAILLE MOYENNE DES FLOCS LESTÉS

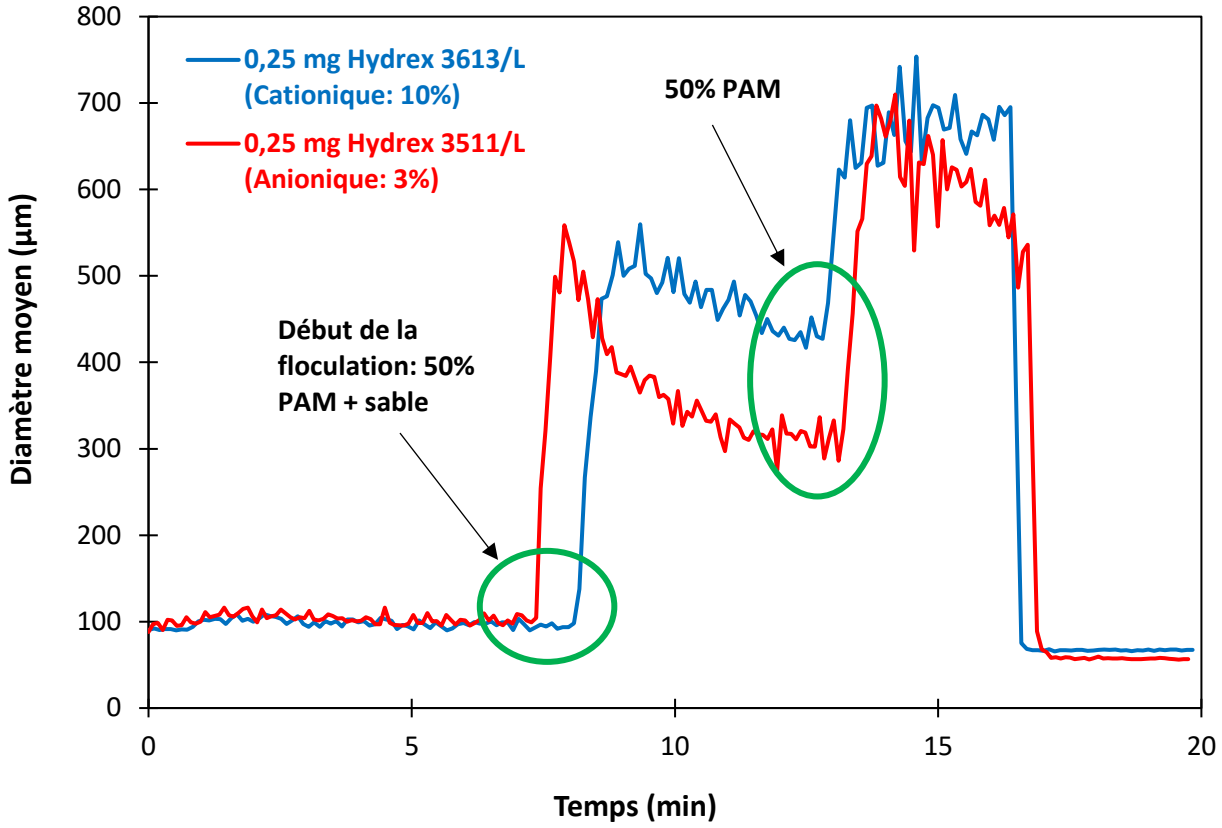

Figure A- 2 : Impact de la séparation du dosage de floculant sur la taille des flocs lestés. Conditions : dose de coagulant de 3,6 mg Al/L à pH 6, température de 22°C, *G* de 165s^{-1} avec 4 g/L de sable de silice et pour un temps de floculation de 8 min.